2017

# Unsupervised monitoring of an elderly person's activities of daily living using Kinect sensors and a power meter

Hossein Pazhoumand-Dar
*Edith Cowan University*

# Edith Cowan University
# Copyright Warning

# Unsupervised Monitoring of An Elderly Person's Activities of Daily Living Using Kinect Sensors and A Power Meter

This thesis is presented for the degree of

**Doctor of Philosophy**

by

**Hossein Pazhoumand-Dar**

**Principal Supervisor**

Dr. Leisa Armstrong
Edith Cowan University
Western Australia

**Associate Supervisor**

Associate Professor Amiya Kumar Tripathy
Don Bosco Institute of Technology
University of Mumbai, Mumbai, India

Edith Cowan University
School of Science
2016

# USE OF THESIS

The Use of Thesis statement is not included in this version of the thesis.

# ABSTRACT

The need for greater independence amongst the growing population of elderly people has made the concept of "ageing in place" an important area of research. Remote home monitoring strategies help the elderly deal with challenges involved in ageing in place and performing the activities of daily living (ADLs) independently. These monitoring approaches typically involve the use of several sensors, attached to the environment or person, in order to acquire data about the ADLs of the occupant being monitored.

Some key drawbacks associated with many of the ADL monitoring approaches proposed for the elderly living alone need to be addressed. These include the need to label a training dataset of activities, use wearable devices or equip the house with many sensors. These approaches are also unable to concurrently monitor physical ADLs to detect emergency situations, such as falls, and instrumental ADLs to detect deviations from the daily routine. These are all indicative of deteriorating health in the elderly.

To address these drawbacks, this research aimed to investigate the feasibility of unsupervised monitoring of both physical and instrumental ADLs of elderly people living alone via inexpensive minimally intrusive sensors. A hybrid framework was presented which combined two approaches for monitoring an elderly occupant's physical and instrumental ADLs. Both approaches were trained based on unlabelled sensor data from the occupant's normal behaviours. The data related to physical ADLs were captured from Kinect sensors and those related to instrumental ADLs were obtained using a combination of Kinect sensors and a power meter. Kinect sensors were employed in functional areas of the monitored environment to capture the occupant's locations and 3D structures of their physical activities. The power meter measured the power consumption of home electrical appliances (HEAs) from the electricity panel.

A novel unsupervised fuzzy approach was presented to monitor physical ADLs based on depth maps obtained from Kinect sensors. Epochs of activities associated with each monitored location were automatically identified, and the occupant's behaviour patterns during each epoch were represented through the combinations of fuzzy attributes. A novel membership function generation technique was presented to elicit membership functions for attributes by analysing the data distribution of attributes while excluding noise and outliers in the data. The

occupant's behaviour patterns during each epoch of activity were then classified into frequent and infrequent categories using a data mining technique. Fuzzy rules were learned to model frequent behaviour patterns. An alarm was raised when the occupant's behaviour in new data was recognised as frequent with a longer than usual duration or infrequent with a duration exceeding a data-driven value.

Another novel unsupervised fuzzy approach to monitor instrumental ADLs took unlabelled training data from Kinect sensors and a power meter to model the key features of instrumental ADLs. Instrumental ADLs in the training dataset were identified based on associating the occupant's locations with specific power signatures on the power line. A set of fuzzy rules was then developed to model the frequency and regularity of the instrumental activities tailored to the occupant. This set was subsequently used to monitor new data and to generate reports on deviations from normal behaviour patterns.

As a proof of concept, the proposed monitoring approaches were evaluated using a dataset collected from a real-life setting. An evaluation of the results verified the high accuracy of the proposed technique to identify the epochs of activities over alternative techniques. The approach adopted for monitoring physical ADLs was found to improve elderly monitoring. It generated fuzzy rules that could represent the person's physical ADLs and exclude noise and outliers in the data more efficiently than alternative approaches. The performance of different membership function generation techniques was compared. The fuzzy rule set obtained from the output of the proposed technique could accurately classify more scenarios of normal and abnormal behaviours.

The approach for monitoring instrumental ADLs was also found to reliably distinguish power signatures generated automatically by self-regulated devices from those generated as a result of an elderly person's instrumental ADLs. The evaluations also showed the effectiveness of the approach in correctly identifying elderly people's interactions with specific HEAs and tracking simulated upward and downward deviations from normal behaviours. The fuzzy inference system in this approach was found to be robust in regards to errors when identifying instrumental ADLs as it could effectively classify normal and abnormal behaviour patterns despite errors in the list of the used HEAs.

# DECLARATION

I certify that this thesis does not, to the best of my knowledge and belief:

i. Incorporate without acknowledgement any material previously submitted for a degree or diploma in any institution of higher education;

ii. Contain any material previously published or written by another person except where due reference is made in the text; or

iii. Contain any defamatory material.

I also grant permission for the library at Edith Cowan University to make duplicate copies of my thesis as required.

……..

Hossein Pazhoumanddar

Date: 20th December, 2016

# ACKNOWLEDGMENTS

I would like to express my deepest gratitude to my Principal Supervisor Dr Leisa Armstrong and Co-supervisor Associate Professor Amiya Kumar Tripathy for their constant guidance and hearted support. You taught me what it means to be a good teacher.

I am also grateful to Arman Abednia whose warm-hearted care, companionship and generous mental support helped me to accomplish this goal.

I owe special thanks to the SOAR Ambassadors at the ECU SOAR Centre, Dr Jacqui Coombes, Dr Helen Renwick, Dr Greg Maguire, Dr John Hall, Dr Martin Masek and Associate Professor C. Peng Lam for their help during the research phase and writing of this thesis.

I wish to thank Samaneh, my wonderful wife, for her extreme patience and understanding. Undoubtedly, without her support I would not have been able to successfully complete this PhD while enjoying every moment of my life.

Finally, I am grateful to my parents who have always encouraged me to do my best but not judge myself.

# DEDICATION

I dedicate this thesis to my grandfather, who passed away a few months after a tragic event in which he fell over in his home. He spent several hours lying on the floor in the dark before he was discovered and taken to hospital.

# TABLE OF CONTENTS

# TABLE OF FIGURES

# LIST OF TABLES

# ABBREVIATIONS

| | |
|---|---|
| ADLs | Activities of Daily Living |
| AIPIA | Approach to Identify the Performance of Instrumental ADLs |
| AMI-ADLs | Approach for Instrumental ADLs |
| AMP-ADLs | Approach for Monitoring Physical ADLs |
| CAV | Circadian Rhythmic Variability |
| FCM | Fuzzy C-Means |
| FIS | Fuzzy Inference System |
| HEAs | House Electrical Appliance |
| MC | medcouple |
| MF | Membership Function |
| MS | Mean Shift |
| MS–RS | Mean Shift Robust Statistics |
| NR | Normal Range |
| PDF | Probability Distribution Function |
| RS | Robust Statistics |
| SAB | Skewness Adjusted Boxplot |
| VBMS | Variable Bandwidth Mean Shift Clustering |

# CHAPTER 1:
# INTRODUCTION

The latest statistics on world population show that population ageing has become a global phenomenon (World Health Organization, 2015). This change has resulted in the demand for aged care services in many countries to go beyond the resources of existing aged care providers (Labonnote & Høyland, 2015). There is a need to find better approaches to allow the elderly to live independently and reduce the demands for aged care services. Automatic well-being monitoring systems may provide one possible solution. This chapter presents a general introduction to key sensory technologies that can be used in these monitoring systems to capture data from elderly people's homes. The chapter also outlines the purpose of the research, its significance, the research questions and the contributions that the research makes to the field of study. The general organisation of this thesis is also presented.

## 1.1 Background to the study

### 1.1.1 The growing elderly population

Today many countries are faced with a growing population of elderly people. Some of the latest statistics and projections on the world population presented by the World Health Organization (2015) show that in 1950 there were nearly 205 million elderly people (aged over 65) across the world with only three countries (i.e. China, India, and the United States of America) having more than ten million elderly people (see Figure 1.1 (a) and b)). By 200 the number of elderly people had triple in population with 5 countries having already having a population more than 20 million older people. China (129 million), India (77 million) and the United States of America (46 million) were found to have the greatest population of elderly people. The number of elderly people is projected to rise dramatically to 974 million by 2030, and subsequently, to nearly 1.5 billion by 2050 worldwide, with 33 countries expected to have more than 10 million people aged 65 or more (World Health Organization, 2015). China (437 million), India (324 million), the United States of America (107 million), Indonesia (70 million), and Brazil (58 million) are five countries that are expected to have more than 50 million elderly people by the year 2050.

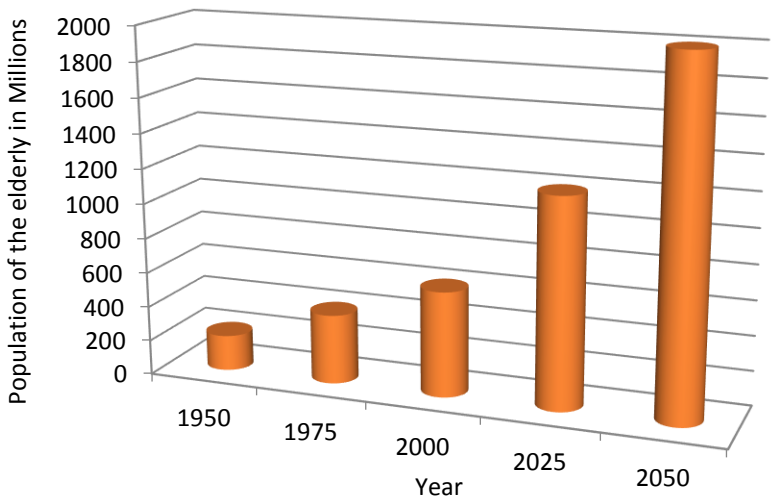


(a)

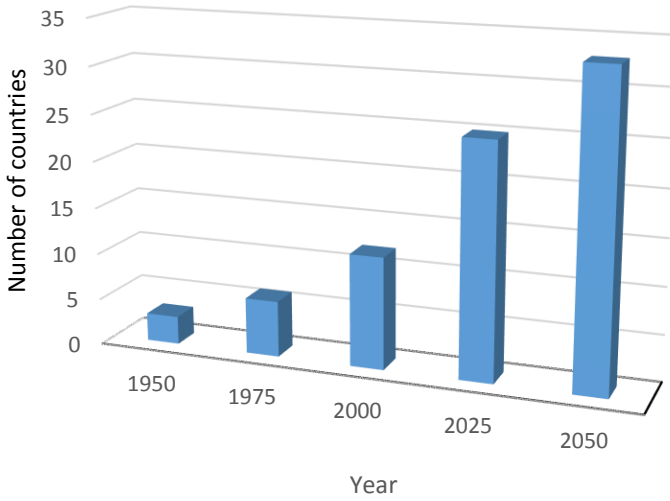


(b)

Figure 1.1. (a) World population aged more than 65, 1950-2050, and (b) the number of countries with the elderly population exceeding 10 million (Harper, 2014).

Estimations also indicate that the older population is growing faster than the total population in both developed and developing countries (Harmankaya et al., 2015). In the 1950s, the average annual rate at which the number of persons aged over 65 increased globally was only slightly higher than that for the whole population. This growth rate is projected to be more than three times the rate of the entire population by the middle of the 21$^{st}$ century.

The proportion of elderly people relative to the rest of the population has increased significantly. One in every 20 individuals were at least 65 years of age in 1950 (see Figure 1.2).

This percentage increased to one in every 10 by the year 2000. By 2050 more than one in every six persons in the world is projected to be aged at least 65, with more developed countries having relatively higher proportions of this age group.

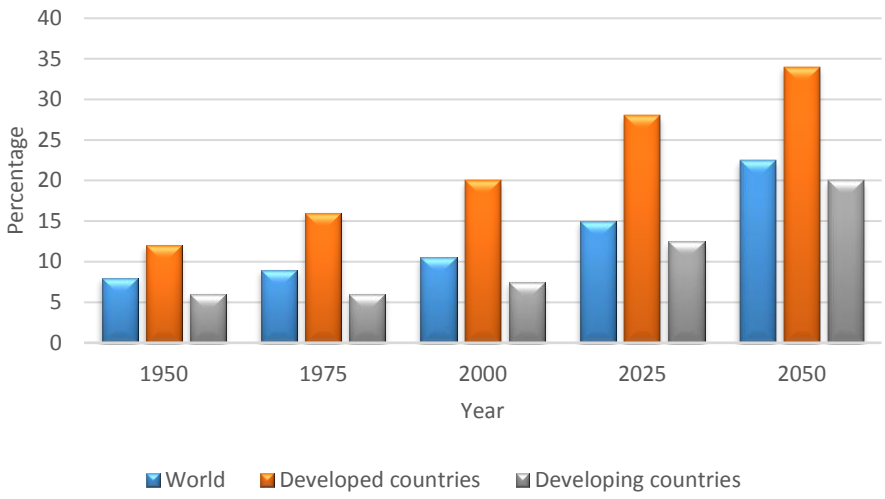


Figure 1.2. Proportion of population aged 65 or over: the world, developing countries and developed countries, 1950-2050 (World Health Organization, 2015).

Older adults have been found to prefer to live independently in their own homes and communities and maintain the control of their lives as long as possible (Claes, Devriendt, Tournoy, & Milisen, 2015). This requires older adults to be functionally stable and capable of independently performing essential daily activities. Those elderly people who do live independently are more prone to high-risk incidents such as falls, collapses or heart attacks, which may result in serious injuries (Bennett, Wu, Kehtarnavaz, & Jafari, 2016; Cohen & Miller, 2000). Even healthy older adults who live independently encounter challenges due to normal age-related changes (Tan, He, Chan, & Vehviläinen-Julkunen, 2015). Tragic deaths amongst the elderly may occur if long delays occur before medical help is made available.

### 1.1.2 Monitoring activities of daily living of elderly people

In order to address the issues that the elderly have in living independently, systems have been devised to monitor their well-being and daily activities. These activities of daily living (ADLs) include self-care activities, such as walking and cooking, that are considered necessary for an individual's daily living (Ravishankar, Burleson, & Mahoney, 2015). These activities can be divided into two categories:

1. Physical ADLs: activities in this category involve the person adopting a certain posture in order to fulfil an activity. Some examples are sitting on a sofa and lying in bed (Mlinac & Feng, 2016).

2. Instrumental ADLs: these activities involve the use of electrical and non-electrical home instruments. Some examples are cooking and watching TV (Debes et al., 2016).

The ageing process is an expected cause of reduced ADL performance. It impacts the performance of both physical and instrumental ADLs (Durant, Leger, Banks, & Miller, 2016). Both types of ADLs are crucial for monitoring the functional abilities of the elderly in order for them to be able to live independently (Bennett et al., 2016). Monitoring physical activities can help identify emergency situations (e.g. falls, collapses or heart attacks), while monitoring instrumental ADLs helps detect deviations from important daily tasks such as cooking and grooming (Riboni, Bettini, Civitarese, Janjua, & Helaoui, 2015). For example, the ADLs of a healthy elderly person for sleeping at night or watching TV in the afternoon typically involve a daily routine. If the person's ADLs register a difference in their daily routine, such as sleeping late in the morning or spending an unusually extended amount of time watching TV, this may indicate a potential change in their well-being. It is important to detect abnormal behaviours in ADLs at an early stage of their occurrence as changes in behaviours are manifestations of changes in the health or the capacity of the elderly to live independently (Fouquet, Franco, Villemazet, Demongeot, & Vuillerme, 2010).

An early study by Barnes, Edwards, Rose, and Garner (1998, p. 1) stated that "*Telecare is the remote or enhanced delivery of health and social care services to people in their own home by means of telecommunications and computer-based systems.*" The study also defined lifestyle monitoring as "*the long-term, continuous gathering and analysis of information about a person's activities and daily routines*," the final goal of which is to notify medical caregivers about the outliers in ADLs including emergencies. Such systems incorporate a range of sensory data that are used to monitor and model ADLs in a way that facilitates the recognition of unusual behaviours and the generation of unique health status reports (Brownsell, Bradley, Blackburn, Cardinaux, & Hawley, 2011). This monitoring can reduce the pressure on caregivers and enable elderly people to live independently in the safety and comfort of their own homes, while ensuring that caregivers are notified of any unexpected event.

### 1.1.3 Sensor technologies for monitoring home environments

A number of practical and affordable sensors have been reported for use in elderly people's houses to provide constant monitoring and detect medical emergencies. (Peetoom, Lexis, Joore, Dirksen, & De Witte, 2015). A wide range of sensor types has already been employed to develop ADL monitoring approaches for home environments. Figure 1.3 depicts the examples of such sensory technology installed in typical locations of a home environment.

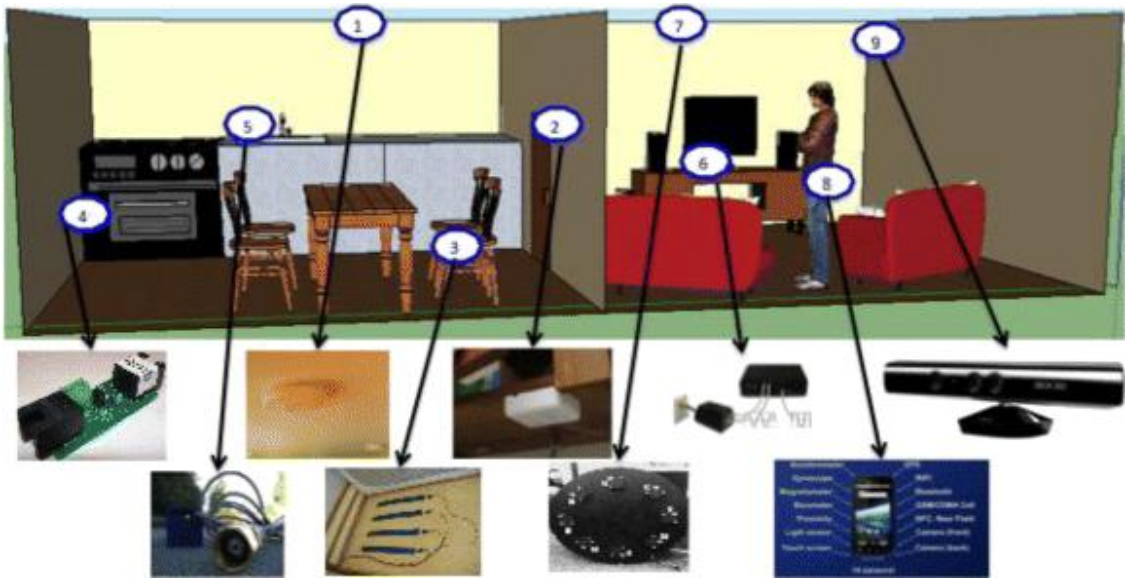


Figure 1.3. Several sensory technologies available for developing ADL monitoring systems, including (1) a passive infrared motion detector (2) a magnetic reed switch door sensor, (3) a pressure sensor to detect if a chair or bed is occupied, (4) a temperature sensor to detect if the stove is being used, (5) a water usage sensor, (6) an electricity consumption sensor to detect appliance power usage, (7) a microphone array, (8) a smart phone equipped with an accelerometer and a gyroscope, and (9) a video/depth camera (image adopted from Cook and Krishnan (2014)).

A study by Akhlaghinia, Lotfi, Langensiepen, and Sherkat (2008) reported that these sensors vary in price, the level of intrusiveness and ease of installation. Various sensors provide complementary information that can be used for monitoring various aspects of behaviour patterns, such as duration and frequency. The following sections outline different sensor technologies employed for ADL monitoring and review relevant studies where a combination of these technologies have been employed to monitor elderly people's ADLs.

#### *1.1.3.1 Wearable sensors*

There are various wearable health monitoring devices equipped with accelerators, gyroscopes and physiological sensors to provide data about an individual's condition. These sensors are

able to measure the orientation of the body using accelerometers and physiological rates (e.g. blood pressure, heart rate, temperature, glucose levels, calories) which are then transferred as raw data to a server (Cook & Holder, 2011). Raw data from these sensors are pre-processed into data segments and features are extracted from segments to characterise ADLs. These features range from spectral to statistical features, such as spectral entropy, dominant frequency components, minimum, mean and variance.

Accelerometers which are used to measure body orientation are considered to be among the most effective and commonly used sensors (Debes et al., 2016). These devices detect activities based on the placement and number of sensors. An individual's waist is the most common place where a single sensor is employed to capture data. A study by Bao and Intille (2004) used waist-worn accelerometers to successfully differentiate 20 different activities related to body movements such as folding laundry and standing still. Waist-worn accelerometers were also used to detect falls, estimate metabolic energy expenditure and monitor functional balance (Bidargaddi & Sarela, 2008; Mathie et al., 2004). Other studies have used ear-worn accelerometer unit to classify the intensity of the level of activities (e.g. very low, low, mid, and high) (Atallah, Lo, Ali, King, & Yang, 2009). Accelerometers have also been attached to belts. Figure 1.4 (a) shows the hardware for an accelerometer used by Putchana, Chivapreecha, and Limpiti (2012) and Figure 1.4 (b) depicts the receiver unit. Data recorded by the device were analysed to identify different movement types including falls.

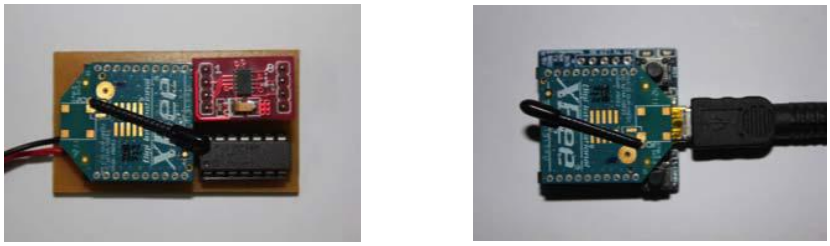

(a) (b)

Figure 1.4. The accelerometer technology used by Putchana et al. (2012) for monitoring body movements. (a) The transmitter unit and (b) the receiver hardware (images adopted from Putchana et al. (2012)).

Wearable physiological sensors have been used to provide information such as blood pressure, heart rate, and respiration for tele-monitoring purposes. This information can be used for early diagnosis of symptoms or monitoring and managing chronic diseases. Caregivers can be notified if abnormal situations occur (Medjahed, Istrate, Boudy, & Dorizzi, 2009).

There are some limitations to the use of wearable sensors. Wearable sensors have been considered to be obstructive since individuals need to constantly carry them. Other disadvantages include short battery life, high cost and the fact that for measurements to be reliable, the sensor has to be worn on specific body parts.

#### *1.1.3.2 Video and audio sensors*

Many studies have reported the use of high-fidelity sensing technologies like video cameras and microphones to monitor people's activities (König et al., 2015; Vuegen, Van Den Broeck, Karsmakers, Van Hamme, & Vanrumste, 2015). The acquired data need to be pre-processed to segment those associated with the monitored person in the environment. For example, a study by Chung and Liu (2008) segmented the image of the person in video frames and then classified their activities by statistically analysing their body posture. A hierarchical method for modelling behaviours was developed when the posture was combined with the location and temporal duration of each activity.

Another study by Nguyen, Phung, Venkatesh, and Bui (2005) mounted four cameras at each corner of the ceiling of an experimental laboratory. The study proposed an algorithm to detect a list of visited cells at specific times based on the partitioning of the scene into cells. A tracking system was then applied to obtain the subject's trajectories and to classify behaviours. Other approaches have estimated features from the silhouette, such as shape, location, aspect ratio of the minimum bounding box and orientation, in order to recognise the ongoing activity (Brulin, Benezeth, & Courtial, 2012; Zhongna et al., 2008).

A study by Jianfeng Chen, Kam, Zhang, Liu, and Shue (2005) used microphones to monitor bathroom activities such as hand washing and showering. The time of occurrence, duration, and sequence of occurrence of each detected activity were reported to the caregiver. Another experimental study by Brdiczka, Langet, Maisonnasse, and Crowley (2009) reported on a role detection approach which combined video with audio information by using a headset to determine the speaking status of the subject. A microphone array was also placed on the wall for noise detection. Video streams were used to track the subject's posture, speed, and interaction with other objects. The data were gathered and integrated as codes to estimate the person's activities.

Video camera images are dependent on appropriate levels of lighting. Any monitored activity is performed in three-dimensional space. The use of 2D video images reduces the discriminative ability to characterise these activities. The use of 3D camera technologies can overcome the drawbacks of these 2D video images. Microsoft recently introduced an inexpensive Kinect sensor ("Kinect v2," 2015) which has a depth camera that captures 3D human motions and an associated software development kit (SDK) which estimates the posture and the location of skeleton joints of the person detected in the scene. The original aim for this technology was to enable users to interact with the Microsoft gaming consoles using gestures. This type of sensor is considered as an improvement on traditional colour cameras as its person detection algorithms operate based on the depth information of the scene rather than colour images, making the algorithms robust to light, colour, and texture variations. Information obtained from Kinect depth maps preserves the privacy of monitored people (Banerjee, Keller, Skubic, & Stone, 2014; Kepski, Kwolek, & Austvoll, 2012).

An example of a person sitting on a sofa in front of a Kinect sensor and the corresponding depth map and the person's silhouette obtained from the Kinect sensor is shown in Figure 1.5. Note that in the depth maps shown in this thesis, the higher depth values are displayed through brighter pixels. Depth measurement errors, which occur because of surface reflections, take the form of black regions.

Many researchers have investigated the use of Kinect sensors for different applications including object recognition (Velayudhan & Gireeshkumar, 2015) and human action classification (Raheja, Minhas, Prashanth, Shah, & Chaudhary, 2015). For monitoring the elderly, Rougier, Auvinet, Rousseau, Mignotte, and Meunier (2011) proposed a technique in which the Kinect depth maps of a subject were used to detect falls. This was achieved by collecting a training dataset of normal activities to establish the thresholds of two types of features, namely the human centroid height relative to the ground and body velocity.

(a)

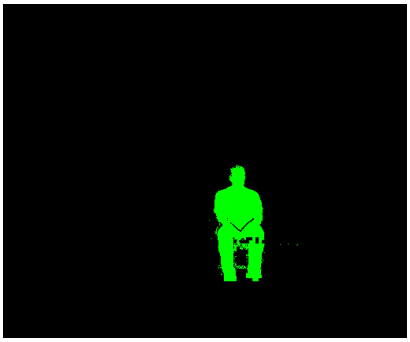

(b) (c)

Figure 1.5. An example of Kinect data: (a) the colour image shows a person sitting in front of the sensor; (b) the corresponding depth map of the scene; and (c) the silhouette of the detected person.

#### *1.1.3.3 Environmental sensors*

Wearable and video-audio sensors are mostly employed to allow the classification of physical activities via individuals' postures and movements. In contrast, environmental sensors are used to detect interactions with domestic objects in the home or the location of the person. Examples include binary switches (door/window contacts), radio frequency identification (RFID) tags, and temperature, light and passive infrared (PIR) sensors. Although these switches are inexpensive and easy to install, a large number is required to distinguish different activities.

**RFID tags and magnetic switches**

RFID tags are postage stamp size and can be attached to everyday objects. The advantages of these tags are that no battery is required and they can withstand day-to-day use for years. A radio frequency pulse is sent to the tag by a tag reader, which then captures a unique identifier based on the tag. Signals from a tag can be picked up in a range of a few centimetres to several metres depending on the power of the reader. This technology has been installed in many types

of home electrical appliances (HEAs) commonly used in ADLs, such as toasters, microwaves, and dishwashers. These tags can be used to estimate ADLs based on recently manipulated objects. For example, Gu, Wu, Tao, Pung, and Lu (2009) asked participants to wear a RFID tag reader on their wrist to identify when the individual was in the vicinity of a key item. Another similar study by Jianxin, Osuntogun, Choudhury, Philipose, and Rehg (2007) described a RFID-based approach for activity recognition. This study used a RFID reader that was attached to the user's wrist to indicate when the hand was near a tagged object.

Another alternative which has been reported is the use of magnetic switches. This type of sensor can be used to monitor old people's activities in their homes by positioning the sensors in different locations (such as on doors, appliances, cabinets, lights and other items in the environment) and detecting any changes to these objects (van Kasteren, Englebienne, & Kröse, 2011).

Other studies have described monitoring specific ADLs by linking spatial locations visited by an elderly person to ADLs. For example, S. Zhang, McCullagh, Nugent, Zheng, and Black (2011) tracked the person's movements by installing RFID readers in various places and identifying the visited locations in the home. The person's position was recorded using a passive tag which was tracked using an antenna. The environment was divided into several functional subareas based on the occupant's likely ADLs. A classifier was then deployed to map the subject's locations to activities.

**PIR and pressure mats**

PIR sensors have been found to be the most commonly used technologies for locating and capturing people's movements (Gokalp & Clarke, 2013). These sensors are widely used to support home alarm systems (Munstermann, Stevens, & Luther, 2012). PIR sensors monitor the infrared (heat) level in the environment and emit a high signal when they detect changes. The sensors are used to record time, location and the frequency of triggering of the sensor. For example, Suryadevara and Mukhopadhyay (2015) developed a ADL tele-monitoring technique that exploited a network of such detectors to locate an elderly resident in a home setting. A similar study by Krishnan and Cook (2014) also employed a wireless network of these sensors in a home environment to obtain the sequences of sensor events resulting from human movement in the house. Those sequences were used to estimate the occupant's appliance usage, activities and mobility (Krishnan & Cook, 2014).

The limitation of the techniques using PIR sensors is that they may not detect emergency situations such as falls. For example, if a person enters a room and does not move (because of an accident such as a fall), the measurements from PIR sensors cannot determine that the person is stationary in the monitored area. The technique cannot provide sufficient information to characterise ADLs as it cannot detect the posture of the person in the house.

Pressure mat sensors have been used in the last decade as another alternative to detect a person's movement and to identify fall incidents and other activities (Hanson, Barth, & Silverman, 2011; Lauterbach, Steinhage, & Techmer, 2012). For example, these mats have been used in a number of studies to measure the position, acceleration as well as the weight of the subject by installing several of these sensors underneath the floor in specific locations (Hamid *et al.*, 2009; Wen-Chih, Wangling, YiLing, & PeiChing, 2007). Pressure mats have also been installed under mattresses to measure rest periods (Fernandez-Luque, Martínez, Domènech, Zapata, & Ruiz, 2013).

**Power sensors**

Power sensors provide another alternative for monitoring elderly people's activities. For example, turning on a hair dryer can imply that the occupant is grooming, or turning on a toaster in the kitchen can indicate a feeding activity. A number of ADL recognition studies have reported the use of power sensors to monitor the status of HEAs via their power signatures and electrical consumption patterns (Noury, Berenguer, Teyssier, Bouzid, & Giordani, 2011; Rahimi, Chan, & Goubran, 2011). Most existing approaches that monitor the usage of HEAs commonly involve installing and maintaining separate sensors for each electrical device (Cho, Yamazaki, & Hahn, 2010; Rowe, Berges, & Rajkumar, 2010). This has been found to be a limitation to the use of these systems as it can increase the cost and complexity of the system.

Studies by Suryadevara, Quazi, and Mukhopadhyay (2012) and Cho et al. (2010) proposed installing separate power sensors for each electrical appliance with data related to the operating status of the appliance transmitted wirelessly to a computer. ADLs were estimated based on the function and location of the appliance connected to the sensor and the time of use.

Another alternative approach for monitoring instrumental ADLs is through nonintrusive load monitoring (NILM) from a centralised location and the identification of the operational state

of HEAs by disaggregating the composite power signal. A power sensor is installed in the electricity box of the house and a training dataset of the power consumption signal is collected in order to identify power signatures associated with the usage of each HEA. A number of studies have used this approach for the classification of instrumental ADLs. For example, Rahimi et al. (2011) demonstrated the application of a NILM system that mapped the power signatures of various electrical devices to ADLs. The advantage of this technique was that the environment in the home was not altered as monitoring occurred through the external power meter box.

Another study by Noury et al. (2011) defined relationships between ADLs and HEAs. The approach mapped power signatures detected on the power line to the usage of HEAs in the home using an annotated training dataset of house power consumption. It then identified the performance of instrumental ADLs from the relationships between ADLs and HEAs.

A similar study by Belley, Gaboury, Bouchard, and Bouzouane (2014) recognised ADLs by measuring the power signatures of HEAs through the external power meter box. The power signatures could characterise the number, types, consumption and the operational states of all HEAs from a household. The study used a similarity measure to classify a new power signature to the detected appliance and associated activity.

Other studies have reported the use of smart water meters for monitoring ADL activities. A study by Srinivasan, Stankovic, and Whitehouse (2011) proposed a disaggregation technique to link water usage to individual fixtures in the home. Another study by Fogarty, Au, and Hudson (2006) attached simple microphones to a home's plumbing system. This solution has several advantages as it requires a limited number of sensors. However, it is not considered appropriate for homes which have plumbing infrastructure that is not easily accessible.

### 1.1.4 Combinations of sensor technology used for monitoring the elderly

One type of sensor may not provide sufficient information about ADLs for all situations (Ranjan & Whitehouse, 2015). For example, PIR sensors cannot supply data associated with ongoing instrumental activities in the kitchen. Monitoring techniques that involve different sensor types may provide a solution to deficiencies which have been shown with individual sensors. Table 1.1 presents examples of research studies that used different combinations of

sensors for monitoring ADLs. All studies have reported an increase in the accuracy of monitoring ADLs. The combination of environmental sensory technologies can require a large number of sensors and can be expensive.

Table 1.1. Examples of research studies that combined sensor technologies.

| **Study** | **Types of sensor used** | | | | | | | | **Monitored ADLs** |
|---|---|---|---|---|---|---|---|---|---|
| | **PIR** | **VC** | **RT** | **BS** | **PM** | **WS** | **POS** | **TS** | |
| Intille et al. (2006) | | * | | * | * | * | * | * | I |
| Helal, Chen, Kim, Bose, and Lee (2012) | | | * | | * | | | | I |
| Prakash, Kemp, and Rogers (2014) | | * | * | | | | | | I |
| Ariani, Redmond, Chang, and Lovell (2012) | * | | | | * | | | | P |
| Alwan et al. (2003) | * | | | * | * | * | | * | I/P |
| Tong, Chen, and Gao (2015) | * | | | * | | | * | * | I |
| Nag and Mukhopadhyay (2014) | * | | | | * | | * | * | I |
| Cook and Holder (2011) | * | | | * | * | | | * | I |
| Bang, Kim, Song, and Park (2008) | * | | | | | * | | | P |
| Biswas et al. (2010) | * | | | | | * | | | P |
| Hein et al. (2010) | * | * | | | | * | * | | I |
| Roy, Bouzouane, Giroux, and Bouchard (2011) | * | * | | | * | * | | | I |
| Lundström, Järpe, and Verikas (2016) | * | | | * | * | | | | I |
| Sim, Phua, Yap, Biswas, and Mokhtari (2011) | | | * | * | * | * | | | I |
| Suryadevara et al. (2012) | | | | * | | * | | | I |
| Debes et al. (2016) | * | | | * | | | * | | I |

PIR= PIR sensor, VC= video camera, RT= RFID tags, BS= Binary switches, PM= pressure mat, WS= wearable sensors, POS= power sensors, TS= temperature sensors, P=physical ADLs, I=instrumental ADLs.

An early study by Intille et al. (2006) investigated a technique for monitoring the elderly within a one-bedroom research environment equipped with numerous environmental sensors (e.g. binary switches and pressure sensors). Another study by Helal et al. (2012) reported using a RFID reader attached to the wall of the entranceway of a house (the Gator Tech Smart House) to identify residents approaching the house using RFID tags attached to their key rings. The systems also used numerous pressure mats that were fitted underneath the floor to localise occupants and to categorise their instrumental ADLs.

Alwan et al. (2003) reported an ADL monitoring system which used PIR sensors and pressure

mats to identify the occupant's locations. The study also used a stove temperature detector, switches on cabinet doors and a multi-function bed sensor capable of detecting the presence of the home occupant along with some other features such as respiration and pulse. The combination of these sensors was able to detect various instrumental ADLs under a sensor fusion paradigm. For example, if a person used the couch in the living room, pressure mats and location sensors could verify this activity.

A recent study by Nag and Mukhopadhyay (2014) used PIR sensors to detect human motion, pressure mats to identify the sitting activity and multiple power sensors to monitor the use of HEAs. While using a network of environmental sensors may help detect a wider range of ADLs, it is considered to be obstructive to the elderly. It is also considered to be costly as it requires installation of many devices during the construction of a house, and maintenance thereafter. Other studies have reported the use of intrusive sensors such as wearable devices, microphones and video cameras (Bang et al., 2008; Biswas et al., 2010; Hein et al., 2010). The major challenges found body-worn sensor technologies are that subjects may feel uncomfortable when wearing the sensors or may forget to wear them. The use of video camera and microphones has been found to provide a large amount of information on activities. These systems have not been popular due to privacy concerns.

Another limitation to the studies outlined in Table 1.1 is that they only combined sensory technologies to monitor either instrumental or physical ADLs. An early study by Celler et al. (1995) proposed that improvements could be made in these approaches by including both types of ADLs to provide a comprehensive monitoring system that could detect emergency situations and symptoms of decline in the functional status of the elderly.

## 1.2 The purpose of the study

This study aims to develop and validate a data-driven monitoring framework which can provide constant monitoring of both physical and instrumental ADLs of elderly people living alone in their homes. The monitoring framework uses a combination of inexpensive and non-intrusive sensors (i.e. Kinect sensors and a single power meter) which can be used in existing homes to monitor ADLs.

Due to the absence of a formal definition and the scarcity of abnormal activities, it is

challenging to map low-level sensory data to high-level abnormal events. It is also difficult to model different aspects of diverse activities that characterise everyday living. This study aims to develop techniques:

- to use multiple sensors (i.e. Kinect sensors and a power meter) to capture and represent the normal behaviours of a home occupant during physical and instrumental ADLs

- to model sensor observations related to normal behaviours

- to detect abnormal behaviour patterns in the occupant's monitored behaviours.

## 1.3 Significance of the research

This research is significant in terms of advancing computer science techniques for monitoring ADLs of elderly people and providing support to this age group through helping them to live independently.

The research proposes novel data-driven techniques and combined them with existing techniques in order to provide an integrated framework for monitoring both physical and instrumental ADLs in the existing homes of the elderly. Existing monitoring techniques are limited in that they use a costly network of environmental sensors, intrusive video cameras or obstructive wearable devices. This research proposes a framework that captures data from a novel combination of Kinect sensors and a power meter. This minimally intrusive combination of sensors is cost effective as it allows retrofitting of sensors to existing homes without the need for expensive renovation. These devices are not obstructive because the power meter is installed in the power panel and only one Kinect sensor needs to be installed in each regular-sized room.

The research improves existing monitoring approaches by presenting a novel unsupervised data-driven fuzzy approach to monitor key aspects of physical ADLs based on unlabelled Kinect depth maps. Current fuzzy techniques that monitor physical ADLs require a pre-determined number of fuzzy sets to be defined over attributes which reduce the scalability and accuracy of those techniques. The proposed fuzzy approach uses a novel unsupervised technique which automatically defines different numbers of fuzzy membership functions that

describe the person's body postures. These functions exclude noise and outliers in the data.

This research is also significant as it introduces a novel unsupervised method to monitor the daily patterns of instrumental ADLs. This approach uses a fuzzy rule set that is learned from an unlabelled training dataset of the home power consumption and the occupant's locations to model the occupant's instrumental ADLs. A novel unsupervised technique within this approach identifies instrumental ADLs based on the occupant's interactions with HEAs. Another novel statistical technique is also proposed to distinguish power signatures that are automatically generated by self-regulated devices (e.g. refrigerators) from the rest of power signatures.

At a community level this research contributes to governments' efforts in helping the growing elderly population live independently in their homes. The system can help caregivers to detect hazardous situations and any variations in the daily activities of elderly people and provide help when necessary. The techniques proposed in this study could also be used for monitoring in other industries such as agriculture or manufacturing.

## 1.4 Research questions

The following major research question has been addressed by the research study:

How can a framework incorporating unlabelled data from inexpensive and non-intrusive sensors (i.e. Kinect sensors and a power meter) be developed for unsupervised monitoring of both physical and instrumental ADLs of elderly people living alone?

To address the main question, the three sub-questions below must be considered:

- **Sub-question 1**: How can data from multiple sensors (i.e. Kinect sensors and a power meter) be used to represent physical and instrumental ADLs of the monitored elderly person?

- **Sub-question 2**: How can techniques be developed that automatically learn from the proposed data representation to generate models of physical and instrumental ADLs?

- **Sub-question 3:** How can techniques be developed that detect unexpected patterns and

abnormal behaviours using the models of physical and instrumental ADLs?

## 1.5 Summary of contributions

The main contributions of this research include:

**Providing a framework to concurrently monitor both physical and instrumental ADLs:** The ADLs of elderly people which need to be monitored include both physical and instrumental ADLs. No well-established framework for concurrently detecting abnormal behaviours during physical and instrumental ADLs has previously been reported. A hybrid framework has been proposed in this thesis in order to achieve this aim. The inputs to this framework are supplied by several Kinect sensors, each covering a functional subarea in the house, and a power sensor installed in the power box of the house. The outputs are alarms generated in emergency situations and reports of the similarity of instrumental ADLs to the learned normal behaviour.

**Proposing an unsupervised data-driven fuzzy approach to model key aspects of physical ADLs and detect abnormal behaviour patterns based on unlabelled Kinect depth maps:** Current techniques to detect abnormal behaviour patterns in physical activities classify sensor data into certain ADLs and determine a threshold for the signatures of each activity by using a labelled training dataset. These approaches are prone to many false classifications due to the wide range of activities and the considerable variability in behavioural patterns. Labelling a large amount of training data also requires considerable labour and time. Several studies have used fuzzy logic to enhance the robustness of monitoring approaches in regards to variations in ADLs (e.g. Brulin et al. (2012) ). The parameters associated with fuzzy rules in these existing fuzzy approaches are defined experimentally, which limits the applicability of those approaches to various domestic settings and individuals.

The fuzzy approach proposed in this thesis monitors the important aspects of ADLs without limiting the number of ADLs or having to determine the exact types of activities undertaken by the elderly. The approach automatically defines several fuzzy sets to replicate the variability of ADLs based on attributes extracted from the body postures of the occupant. This approach learns epochs corresponding to different activities in each

monitored location. It learns normal behavioural patterns based on training data associated with each epoch. This is achieved through identifying frequent co-occurrences among fuzzy attributes through the use of a fuzzy association rule mining algorithm. The occupant's abnormal behaviour is detected in monitoring data through identifying patterns which differ from the occupant's normal behaviours, based on their location, time of occurrence, duration and the occupant's body posture.

**Proposing an unsupervised approach to the automatic generation of fuzzy membership functions:** Existing fuzzy techniques to monitor physical ADLs require a pre-determined number of fuzzy sets to be defined for all attributes. The range of fuzzy sets generated by these techniques does not address the impact of outliers and "noisy" measurements in the data. This thesis proposes an unsupervised approach, called VBMS-RS, to address these issues. VBMS-RS is based on the variable bandwidth mean shift algorithm and robust statistics to automatically generate location-specific fuzzy sets to parameterise the dataset of an attribute. The analysis of the data distribution is unsupervised as the VBMS-RS first determines the number of modes from the probability density function of data and then uses this value as the number of fuzzy sets. The associated parameters of fuzzy sets that represent the dataset are learned automatically and exclude noise and outliers in the data.

**Proposing an unsupervised technique to identify instrumental ADLs from the occupant's interactions with HEAs:** Many studies have proposed the monitoring of instrumental ADLs through load monitoring from a centralised location and the identification of the operational state of HEAs by disaggregating the composite power signal. Most of these techniques need a network of power sensors, a labelled dataset, or prior knowledge about the characteristics of HEAs to identify their usage.

This thesis presents an unsupervised technique that identifies instrumental ADLs from the occupant's interactions with HEAs within the home. This approach employs an association rule-mining algorithm to map the power signatures of HEAs to the occupant's physical locations. Power signatures are obtained using a power meter, installed in the electrical panel of the home. The physical locations of the occupant are measured via non-intrusive Microsoft Kinect sensors. The association rules are used to verify whether a power signature observed on the power line resulted from the occupant interacting with

HEAs. The interaction is then labelled as a specific instrumental ADL using contextual information. A novel technique has also been proposed to distinguish the power signatures of self-regulated HEAs such as a refrigerator from the power signatures of other HEAs.

– **A fuzzy based approach to monitor the daily patterns of instrumental ADLs based on the occupant's interactions with HEAs:** Unlike many existing instrumental ADL monitoring approaches that classify sensor data into a specific set of activities, an unsupervised fuzzy approach is proposed to robustly monitor the daily pattern of instrumental ADLs based on interactions with HEAs. A fuzzy rule set is learned from an unlabelled training dataset to model important features associated with the occupant's interactions with HEAs. This rule set is then used in a fuzzy inference system to robustly monitor the occupant's pattern of using HEAs and to generate daily reports about any deviation from the learned regular pattern.

## 1.6 Thesis organisation

The thesis is organised into eight chapters which are described below:

**Chapter 1** introduces the background of the study as well as description of the sensory technologies which are available to monitor elderly people. It also explores the significance and challenges of this research, followed by sections about the research questions, contributions of the study, and the outline of the thesis.

**Chapter 2** reviews scholarly research related to the study, focussing on the classification and the detection of abnormal behaviour patterns in ADLs followed by. The chapter describes the nomenclature in the ADL monitoring followed by techniques developed for ADL detection and recognition. It also presents an account of techniques devised for abnormality detection in general which is followed by a review of those abnormality detection techniques that have been applied in the area of monitoring ADLs.

**Chapter 3** explains the research methodology adopted followed by an account of the study's phases and associated tasks. It also describes the testbed that was used to collect

experimental data and describes the captured data. The computer science techniques used in this study are detailed followed by a brief description of the platforms used to implement those techniques.

**Chapter 4** introduces an unsupervised approach based on fuzzy logic to monitor the physical ADLs of the elderly using data supplied by Kinect sensors. This chapter introduces the problem of monitoring the physical activities of elderly people followed by a section on the training steps and monitoring phases associated with the approach. This chapter also demonstrates the experimental evaluations for the proposed approach based on the collected dataset. The chapter concludes with a discussion of the results and a summary of the chapter.

**Chapter 5** introduces a method for automatically obtaining robust location-specific fuzzy sets to characterise the normal range of attributes extracted from physical ADLs for each monitored location. It elaborates problems associated with the fuzzy sets used in Chapter 4. The chapter then describes modifications required to the structure of fuzzy rules to incorporate the proposed location-specific fuzzy sets and the procedure for generating location-specific fuzzy sets to represent normal ADLs. This is followed by a section demonstrating experimental results related to the collected dataset. The chapter concludes with a discussion and a summary.

**Chapter 6** introduces an unsupervised technique to identify instrumental ADLs from the interactions of the occupant with HEAs. After an introduction to the problem of estimating instrument ADLs from sensory data, it lists the steps for training the system and subsequently identifying instrumental ADLs in newly acquired data. This is followed by a presentation of the results of training the system, using the collected dataset, and a demonstration of the accuracy of the approach in the classification stage. The chapter concludes with a discussion and a summary.

**Chapter 7** proposes an approach for monitoring instrumental ADLs based on interactions with HEAs. It presents the steps of training the approach and identifying deviations from the normal behaviour in the subsequent monitoring data. The experimental results obtained for testing the approach are described next. The chapter concludes with a discussion and a summary.

**Chapter 8** provides a general discussion and conclusion as to how the research questions have been addressed. It also presents concluding remarks in regard to different proposed techniques in this study. The limitations of the study and further research directions are also explored at the end of this chapter.

## 1.7 Summary

This chapter has provided an introduction to the thesis research. A growing population of elderly people and their willingness to live independently in their homes have been explored. These issues drive the need for systems that can provide lifestyle monitoring and notify caregivers of abnormal behaviour patterns. Different types of sensors available for this purpose were reviewed. The existing monitoring systems that are equipped with different sensor technologies to provide telecare for the elderly people were discussed. It was argued that existing approaches either monitor physical ADLs and detect emergency situations related to them (e.g. falls) or monitor instrumental ADLs. There are several affordable types of sensor used for monitoring ADLs. Video cameras, wearable sensors, and PIRs are usually used to monitor physical ADLs while for monitoring instrumental ADLs, the interactions with objects are identified via numerous sensors attached to them. The importance of improving existing monitoring approaches by incorporating both physical and instrumental ADLs was highlighted.

The purpose of the study was to propose an unsupervised approach that monitors both physical and instrumental ADLs of elderly people via bringing together a combination of non-intrusive and easy-to-deploy sensors. The chapter also outlined the significance of the study and the specific research questions directing it. The next chapter reviews previous studies associated with monitoring the ADLs of the elderly and discusses the problems associated with those approaches, which this study addresses.

# CHAPTER 2:
# LITERATURE REVIEW

This chapter outlines a review of the literature related to the research. The chapter provides an introduction to the nomenclature of ADL monitoring in Section 2.1. It then explores literature on the techniques developed for activity detection and recognition (Section 2.2). The chapter presents an account of techniques devised for abnormality detection in general (Section 2.3) which is followed by a review of the techniques of abnormality detection for both physical and instrumental ADLs (Section 2.3). The chapter concludes with a summary in Section 2.5.

## 2.1 Introduction

Monitoring techniques are necessary for the rising demand for telecare to assist aged people to live independently in their homes. These monitoring techniques facilitate detection of emergency situations and timely response to changes in elderly people's ADLs resulting from a decline in their functional health status. Such timely interventions by caregivers can help prevent potential health crises (and in some cases deaths) and extended hospitalisation of the elderly. These systems have been reported since the mid-1990s.

A study by Celler et al. (1995) presented an early system for continuous monitoring of a home occupant's functional health status based on their interactions with domestic objects and movements within the environment. The study described a technique which monitored the occupant's movement between rooms and activity performance in specific areas of each room via magnetic switches in doors and infrared sensors on the walls. Some activities were identified using sound sensors.

Other researchers have proposed several other monitoring approaches. These studies have also attempted to define different levels of semantics for modelling, recognising and analysing of human behaviour. These studies have used different nomenclature to describe these levels (Cook & Krishnan, 2014). A study by Andr et al. (2012) proposed a model were sensor data were classified into event (e.g. the motion of human body), action, activity, and behaviour based on their time scales (see Figure 2.1). A sensor event was defined at the lowest level as a simple and small part of an action represented by a change in the state of a motion sensor (e.g. the output signal changing from high to low). An individual's actions and interactions with

HEAs in the home (e.g. opening a door and using a kettle) was detected at a higher level. Human activities were defined at the next level as a set of actions executed in a specific order. The ADLs were recognised at this level by classifying the detected sequences of actions in relation to time and location. The highest level of this model included the behaviours and daily routines.

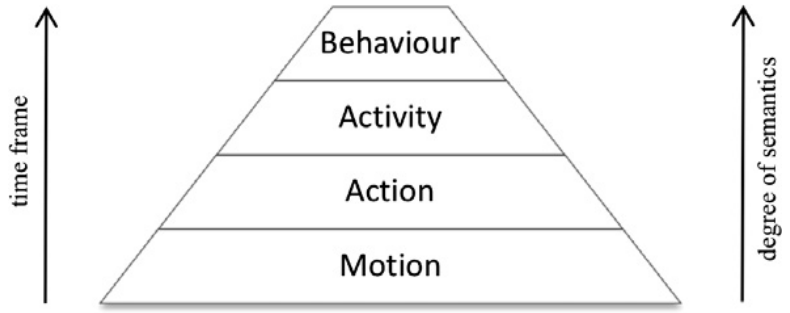


Figure 2.1. Classification of different semantic levels in human behaviour analysis (from Andr et al., 2012)

Performing common types of physical ADLs (e.g. sitting, walking and sleeping) and maintaining the routine for instrumental ADLs (i.e. cooking and grooming) can indicate physical and cognitive abilities of elderly people (C. Franco, Demongeot, Villemazet, & Vuillerme, 2010). This has led to researchers modelling the sensor observations at the activity and behaviour levels. This modelling requires a training dataset of sensory data to be obtained from ADLs inside the home and used to develop a model of activities. The model is then employed for monitoring the occupant to allow for the (1) detecting and classifying ADLs; (2) detecting abnormalities in ADLs such as falls (Peetoom et al., 2015). The following section outlines techniques developed for detecting and classifying ADLs.

## 2.2 Techniques for detecting and classifying ADL

Numerous techniques have been developed for collecting information about activities and using this information for detecting and recognising ADLs. The goal has been to map a set of sensor observations to a corresponding activity, which helps assess the quality of the performed ADLs through measuring their similarity to the normal profile of the monitored person. Activity recognition researchers have used different supervised and unsupervised machine learning techniques in environments ranging from laboratories to real-life settings. While the

experimental environment is typically occupied by one person, some studies have also involved multiple residents.

The following section provides a review of activity classification which has focused on recognising predefined human activities using a supervised machine learning technique. The section is followed by reviewing research on activity pattern discovery which employed unsupervised data mining techniques to detect ADLs as frequent patterns observed in sensor data.

### 2.2.1 Activity classification techniques

One method which has been proposed for activity classification is the use of a supervised machine learning technique to map low-level features from the sensor data to human activities. Accurate activity recognition in real-life settings is challenging because human activities are complex and considerably diverse. A commonly used framework for this task has been described by Duda, Hart, and Stork (2012) and is shown in Figure 2.2. This framework involves collecting a labelled (annotated) training dataset of sensor data for specific activities. Several features are then extracted from the sensor data and machine learning techniques are used to create a model of ADLs. The model is then used by the classification component to label unseen testing data with activities. The following sections provide details of research studies which have used different machine learning techniques.

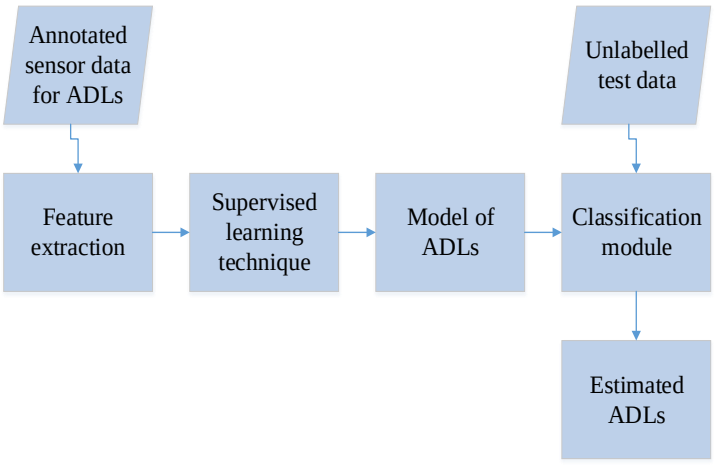


Figure 2.2. General framework for supervised classification of ADLs (Duda et al., 2012).

#### *2.2.1.1 Support Vector Machines (SVMs)*

The use of support vector machines (SVMs) has been explored for classifying ADLs. The algorithm for developing SVMs uses a supervised learning technique to develop decision boundaries that categorise sensor data into different ADLs. Each SVM can separate one class of ADLs from the rest. Given a labelled dataset of ADL features, the learning process of a SVM generates a hyperplane that maximises the separating margin between two classes. Support vectors are training points which are near the margin of this separating hyperplane. If the data distributions of different classes are not linearly separable, the algorithm of SVMs employs kernel functions (e.g. polynomial or Gaussian kernel) to map such input data to a higher dimension. This allows for data of different ADLs to become linearly separable.

A study by Kadouche, Pigot, Abdulrazak, and Giroux (2011) trained SVMs for user classification. The study used data captured from motion, temperature, light, hot water, cold water, and electricity usage sensors to extract ADL patterns. SVMs were then trained based on the ADL patterns of each individual to identify the person when performing activities. This research developed SVMs based on the ADLs of eight individuals. The evaluations showed a high prediction precision of the trained SVMs for identifying individuals via their behavioural patterns. Another similar study by Geng, Chen, Fu, Bao, and Pahlavan (2016) trained SVMs for human motion classification with features obtained from the wearable devices. A limited number of activities including walking, running, lying, crawling were targeted at the experiments and the evaluations of this approach yielded a satisfactory average classification rate of 88.69 percent.

#### *2.2.1.2 Artificial neural network*

The use of artificial neural networks (ANNs) is another machine learning technique explored to model and identify ADLs. Artificial neurons are the fundamental processing elements of an ANN, which are interconnected by weighted links to form layers. An ANN employs a single input and output layers and several hidden layers depending on the complexity of the task. Neurons use an activation function to transform the weighted input into output. The weights are adjusted through a process called learning. Different types of ANNs have been found based on various parameters associated with the architecture of a neural network. A study by Mehr, Polat, and Cetin (2016) investigated the performance of different training algorithms of an ANNs for activity classification. The study used labelled data obtained from state-change

sensors attached to objects in an apartment. The dataset represented 13 different activities. The ANNs achieved 92.81% activity recognition accuracy when trained by the Levenberg Marquardt training algorithm.

A One-Pass Neural Network (OPNN) was developed by H. Li, Zhang, and Duan (2008) to perform activity recognition. The OPNN was available online, which allowed for new sensors to be added to the architecture of the monitoring system and for new activities to be accommodated at any stage. The study used a bedroom equipped with a set of sensors to detect the use of furniture such as chairs, the bed, ceiling light switches, table lamps and bed lamps. The dataset was labelled based on responses from questionnaires completed by occupants, which recorded their activities of using HEAs. An evaluation of the OPNN for an unlabelled dataset of the same activities resulted in 92% accuracy in detecting activities.

Despite these promising results, ANNs have been found to be unable to model temporal dependencies. Research by Rivera-Illingworth, Callaghan, and Hagras (2010) described an improved ANN to learn ADLs based on spatial similarity and temporal patterns in sensor data. The proposed ANN had short memory that could deal with temporal variations in input and output patterns. The researchers proposed adding a memory layer to the network with feedback connections from the hidden layer of neurons back to the same neurons to enable the classifier to discern the temporal order of events. The added layer held a copy of the activations of the hidden neurons from the previous step of the activity. A labelled dataset from distributed sensors was used to classify activities including listening to music, working at a computer and sleeping. The study showed an accuracy which exceeded 90% with the unseen test data (Rivera-Illingworth et al., 2010).

#### *2.2.1.3 Bayes classifiers*

Different types of probabilistic methods have also been applied to develop ADL classification techniques. One common technique has been the use of the naive Bayes classifiers. A naive Bayes classifier relies on Bayes' theorem in order to generate the decision boundary in the space of ADL features assuming all input features to be independent of each other. The classifier is trained based on the probability of the co-occurrence of feature values and the activity labels to map feature values from new data to an activity label. For example, Cook and Schmitter-Edgecombe (2009) implemented a naive Bayes classifier to recognise specific

activities (i.e. hand washing, telephone use, preparing meals) using features including the occupant's location, the usage of the stove and water, and the duration between sensor events. The study calculated the similarity of the learned model to each activity when labelling a sequence of sensor observations with an activity. Specific steps in the activity which the resident skipped or performed incorrectly were also identified. Messing, Pal, and Kautz (2009) also evaluated naive Bayes classifiers on video data and activities such as having snacks, drinking water and using the phone were targeted. The experimental evaluation showed that the classifiers achieved 89% accuracy in a laboratory environment.

Another study by Brdiczka, Reignier, and Crowley (2007) proposed a Bayesian classifier system based on video tracking to segment and track moving occupants in a residence. The position, size and orientation of the detected occupant's silhouette was extracted as input for the frame-wise recognition of basic activities (i.e. walking, sitting, sleeping and interacting with the table). A Bayesian classifier was developed for each activity via an expectation maximisation algorithm based on a labelled training data. A threshold on the probability provided by each classifier was applied to determine whether the ongoing activity in new data was a part of the learned classes.

#### *2.2.1.4 Hidden Markov Models*

A Hidden Markov Models (HMM) is a network of Bayesian classifiers which can model the joint probabilities of sequential data and observations based on the learned connections between unobserved (hidden) states. HMMs are the most widely used modelling techniques applied to activity recognition (Brownsell et al., 2011). Each state in a HMM is characterised by a probability distribution function, modelling the frequency of observations which correspond to that state (see Figure 2.3). The Markov process of HMM assumes that for each given time, the conditional probability distribution of any hidden state depends solely on the value of the observation and the value of a finite number of preceding hidden states. When HMMs are used to model ADL scenarios, the sequence of sensor events (denoted by $Y_1$, …, $Y_T$ in Figure 2.3) forms observations and activities (denoted by $S_1$, …, $S_T$) define hidden states. The HMM models correlations between the observations and their interdependence identified from sensory data. This information is used to classify unseen sensor data into an activity.

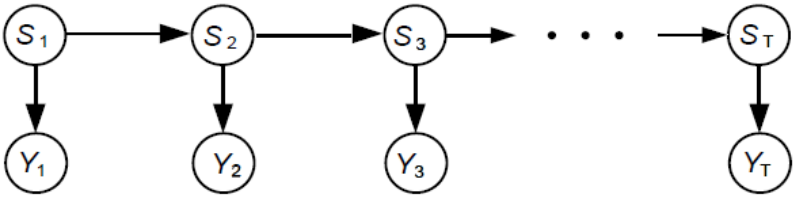


Figure 2.3. An example of conditional relations for a HMM (Charriere et al., 2016).

ADL classification techniques using HMMs assume activities to be sequential. For example, Steinhauer, Chua, Guesgen, and Marsland (2010) trained HMMs for each activity to encode their sequential actions. The HMM with the highest likelihood indicated the type of activity based on observed ADL features. This approach was improved by the study presented by Cook and Holder (2011). The training sequences of sensor events for each target activity were used to model transitions between hidden states based on a Viterbi algorithm. This study also investigated the use of different number of binary sensors to maximize activity recognition accuracy.

Another study by Buettner, Prasad, Philipose, and Wetherall (2009) proposed a more efficient HMM-based activity recognition technique with a precision and recall of approximately 90%. A special type of RFID tag which were equipped with accelerometers was attached to everyday objects in the environment. A labelled training dataset of object-use was collected to train simple HMMs for 14 different ADLs such as making cereal, cleaning windows and taking vitamins. The daily activities from new sensor data were then identified based on the traces of object-use via the trained HMM models.

Despite their popularity, Nguyen et al. (2005) concluded that techniques using HMMs for ADL recognition have several major drawbacks. The study stated that:

- They are incapable of capturing the temporal aspects of activities, meaning that the duration of an ADL is not explicitly modelled;

- Each hidden state can only produce one event, and the model is incapable of detecting changes in the order of events because of its strict independence assumptions for observations;

- Although many of our ADLs can be expressed by a hierarchical structure, HMMs are incapable of representing sub-activities shared among ADLs; and

- Without significant training, an HMM may not recognise different instances of a particular activity.

Several extensions to HMMs have been proposed to address these limitations including hidden semi-Markov models (HSMMs), hierarchical hidden Markov models (HHMMs) and abstract hidden Markov models (Bui, 2002).

A recent study by Clement, Ploennigs, and Kabitzsch (2014) presented an approach based on HSMMs to detect the performance of ADLs from analysing a power meter data. HSMM learned habits of performing specific ADLs based on a labelled dataset of those ADLs. The occupant's currently executed activity was inferred based on the similarity of the sensor data to the learned model of each target activity. A study by van Kasteren et al. (2011) compared the performances of HSMMs and HMMs. The study used magnetic switches to collect data related to activities of two different individuals which involved environmental interactions. The limited set of activities that was targeted included using a dishwasher, having snacks, eating main meals and drinking. The experimental evaluations showed that when the duration of activities was modelled via HSMMs, these models only marginally outperformed HMMs.

HHMMs can model complex activities by splitting them into smaller units (i.e. actions) with a hierarchical structure. These models extend on traditional HMMs to include a hierarchy of hidden states. A study by Karg and Kirsch (2013) presented HHMMs with a shared structure for classifying kitchen activities based on the sequence of visited locations. ADL classification techniques based on HMMs are limited as they are only suitable for applications in which the subject follows specific steps for each daily activity. The training of these models has also been found to be computationally expensive.

#### *2.2.1.5 Conditional random fields*

The everyday activities of a person can be performed in a variety of ways involving a series of different steps. These activities may also be conducted either individually or concurrently. This results in the need for more flexible alternatives to the HMM and its variants. Conditional

random fields (CRF) has been proposed as an alternative approach. CRFs are modelled as undirected graphs which flexibly capture any relationship between a hidden state and an observation variable, hence allowing arbitrary relationships among the observation sequences. Another major advantage of CRFs is that probabilities associated with hidden states take account of future and past observations (Amiribesheli, Benmansour, & Bouchachia, 2015).

CRFs were used in a study by Zhan, Faux, and Ramos (2015) to classify simple and concurrent activities.. The developed model of activities involved two levels; at the lower level the probability of each activity was calculated while the upper level involved a graph representing the correlation between different activities with each edge having a weight. A strong chance that the subject would perform two activities in a concurrent or interleaving manner was indicated by relating those activities by an edge with a high weight. The technique was developed and validated using two datasets of elder routine ADLs and achieved an overall recognition accuracy of 90.04%.

#### *2.2.1.6 Clustering techniques*

Several studies have proposed using clustering techniques to develop ADL classifiers from a training dataset. A study by Hein et al. (2010) manually annotated data from video cameras, in time slices of five seconds, to create a labelled dataset. The motion pattern of the subject in each time slice was extracted and represented by optical flow segments. The k-means clustering algorithm was used to define a codebook of optical flow segments to represent a finite set of ADLs. The extracted motion patterns from a new video stream were assigned to the nearest element of the codebook to recognise the ongoing ADLs. Another study by Belley et al. (2014) also presented a similar technique in which a k-nearest neighbourhood classifier identified the used HEAs based on an annotated dataset of power signatures from HEAs. The ADLs were estimated based on the function and location of these HEAs. Noury et al. (2011) also proposed measuring the power consumption of a house to estimate the time of interactions with specific HEAs. This approach exploited a k-means algorithm to group the time of interactions into epochs of activities. The number of interactions during each epoch was taken into account to monitor the behaviours of an occupant.

#### *2.2.1.7 Fuzzy logic*

Another technique that has been used for ADL recognition is to employ classifiers based on

fuzzy set theory. Such classifiers have been found to be efficient in recognising imprecise sensor values attributed to real world environments and can tolerate slight variations in performed ADLs. For example, a study by Medjahed et al. (2009) used microphones, physiological sensors and infrared detectors to capture data for a fuzzy inference system. The system allowed the user to easily configure the input, output, and inference parameters. The testing of this approach with simulated data provided a classification accuracy of about 97%. The fuzzy inference system in this study used a predefined set of membership functions of inputs and outputs and fuzzy rules. This would result in this approach being unable to cope with noises and uncertain information in sensor readings.

This limitation was addressed in a recent study by Doctor, Iqbal, and Naguib (2014). A fuzzy logic controller, named "Adaptive Online Fizzy Inference System" was developed which was consisted of five steps: capturing behaviours of the elderly person, designing fuzzy membership functions, determining fuzzy rules, designing the agent controller, and life-long learning. The parameters for input/output fuzzy sets were identified using a double-clustering technique. The fuzzy rule set obtained in this study was used to model the patient's habitual behaviours in the environment.

A study by Brulin et al. (2012) presented another fuzzy logic based ADL classification technique based on capturing the posture of elderly people from video data. The silhouette of the person was segmented in the image to extract features such as the subject's position in the room and the aspect ratio of the minimum bounding box. A set of pre-defined fuzzy rules was used to map those features into different body postures including squatting, sitting and lying. Datasets used to evaluate the posture recognition technique involved different training scenarios recorded in a laboratory environment and various testing data acquired from a home environment with perturbations. This system displayed an accuracy ranging from around 65% to 72%.

The approach presented by Brulin et al. (2012) was improved in a recent study by Banerjee et al. (2014) which used Kinect sensors to recognise specific activities of a monitored person (e.g. sitting, standing, and lying on the floor). Once the silhouette was obtained from the Kinect SDK, image moments were extracted and grouped into a pre-defined number of clusters using a fuzzy clustering technique. Cluster centres were then labelled by the user where each label indicated the posture category. The distances between the extracted features and cluster centres

were calculated to classify the new data into activities. The system was tested on datasets from laboratory and real-world settings and showed an average correct classification of nearly 90%.

A recent study by Lundström et al. (2016) has highlighted a number of drawbacks from using supervised recognition. The study concluded that these techniques were inapplicable for real-life settings. Some of the drawbacks noted by the study included:

- These approaches monitor very specific activities but their underlying assumption is that each person performs these activities in a consistent predefined manner, while in reality an individual may perform an activity in different ways. For example, preparing dinner may take different durations, it may start at different times, and the objects with which the subject interacts during the activity may vary each time.

- A consequence of detecting preselected activities is that other activities are ignored while they provide significant information about an elderly person's functional health. Hayes et al. (2007) reported a correlation between variation in the activity level and mild cognitive impairment, which highlights the importance of taking into account all activities regularly performed in a residential environment.

- A significant amount of training data must be labelled and made available to the machine learning algorithm for each individual. The reason is that individuals perform activities differently because of various reasons such as their physical conditions, culture and lifestyle.

### 2.2.2 Activity pattern discovery techniques

Activity pattern discovery techniques provided an advantage over supervised activity classification techniques that require a labelled dataset. These activity classification techniques automatically identify activity patterns in the data prior to those being modelled for recognising ADLs in new sensor data.

Hierarchical activity models could help to identify daily patterns. A supervised classifier detects the lower-level activities, such as eating and sitting, while an unsupervised technique models the combinations of these activities which represent more complex activities. For example, a study by Anderson, Luke, Keller, and Skubic (2008) used a fuzzy logic based

technique to classify body postures into a specific set of states (i.e. upright, on the ground, and in between) from the silhouette of the detected person in video streams. The new activities of the person were recognised from the linguistic summarisations of those states. Some activities that were recognised included walking as having an upright position with a high level of motion and standing as having low motion and being in an upright position. This study employed a predefined set of fuzzy sets and fuzzy rules to classify the occupant's activities from video data. The use of predefined fuzzy sets and fuzzy rules would limit the implementation of such a system in real-life environment.

A popular approach for activity pattern discovery has been to deploy data mining algorithms to discover meaningful and frequent patterns hidden in sensor data. The various data mining approaches used for discovering human activities have mostly investigated the spatial and temporal relations between sensor events. Frequent pattern discovery, better known as frequent itemset mining (Manku, 2016), is a well-known data mining technique for finding items that frequently co-occur. The discovery of ADLs requires the partition of sensor data into time windows which comprise a sequence of events. These events have been used to identify meaningful patterns associated with the occupant's ADLs. For example, the sequence of events over each time window can be put together to form a string. These strings are then treated as individual transactions in the data mining algorithm. The size of window could be strictly temporal or involve a fixed number of events. Various techniques, such as cross-validation (Guesgen & Marsland, 2010), have been proposed to choose a suitable size of window. The challenge involved in monitoring the elderly is identifying patterns of ADLs using these strings.

A number of variations of a frequent itemset mining algorithm have been proposed to discover ADLs from the strings of sensor events. For example, Lühr, West, and Venkatesh (2007) used inter-transaction association rule mining to find significant sensor event associations and their temporal relationships using large amounts of data. The study applied a data mining algorithm to sensor events within a time window to define actions. An associative temporal relationship among actions was used to obtain frequent behaviours regardless of the order of events. The performance of the proposed mining algorithm was evaluated using two datasets of magnet switch sensors in a real-life environment. The window size to define actions and the minimum support of frequent behaviours were determined experimentally.

Another variant of the frequent itemset mining algorithm is the *AprioriAll* (Agrawal & Srikant,

1995) which has been deployed in a group of studies to find frequent itemsets as ADLs. For example, Vrotsou, Ellegard, and Cooper (2007) proposed a technique in which *AprioriAll* generated candidate activity patterns (items) from sensor observations. These unrelated patterns where then filtered by applying constraints on their attributes such as the repetition and duration. This study was improved by Chikhaoui, Wang, and Pigot (2011) which used a network of distributed sensors, such as motion detectors and door switches to recognise ADLs from frequent patterns of sensor events. Each sensor event was associated with a timestamp specifying the time of the event. The *AprioriAll* algorithm was used to discover all episodes that had a particular significance. An episode was defined as a set of sensor events that occurred close to each other in a given order. A hierarchical characterisation of activities was proposed in which complex activities were identified in a bottom-up fashion by first estimating actions via sensor events. A mapping function was then used between the frequent patterns and the activity models to classify new sensor data.

Another study by Hoque and Stankovic (2012) employed *AprioriAll* algorithm to recognise ADLs using data from state-change sensors installed into objects such as a dishwasher and cups cupboard. All sensor events during a room visit were segmented into an occupancy episode that included the room ID, entrance time and a list of objects used. The activities of each room were identified using the *AprioriAll* algorithm via the groups of objects that had been frequently used together. Each of these groups were called frequent itemsets. Once the duration of each frequent itemset was determined as the difference between the start time of the first and the last sensor events, the approach clustered frequent itemsets based on their temporal characteristics. Each obtained cluster represented a particular activity starting at a specific time and lasting for a specific duration. These clusters were then labelled by the user to recognise new occupancy episodes as activities.

Data mining techniques do not consider the temporal order of events in the process of finding association. Some approaches have addressed this limitation by encoding the temporal relation in sensor events. The first step was to determine the start and end times for sensor events which result in the formation of intervals. This is considered to be practical approach as data streams generated by most sensors can be segmented into intervals. For example, in data supplied by sensors installed on home electrical devices, the interval of a related activity can be indicated through the difference between the starting time and the ending time of an appliance usage. Once sensor events are associated with intervals, Allen's temporal logic (see Figure 2.4 for

some examples) has been employed to identify frequent temporal relations between intervals (Amirjavid, Bouzouane, & Bouchard, 2014; Papamatthaiakis, Polyzos, & Xylomenos, 2010).

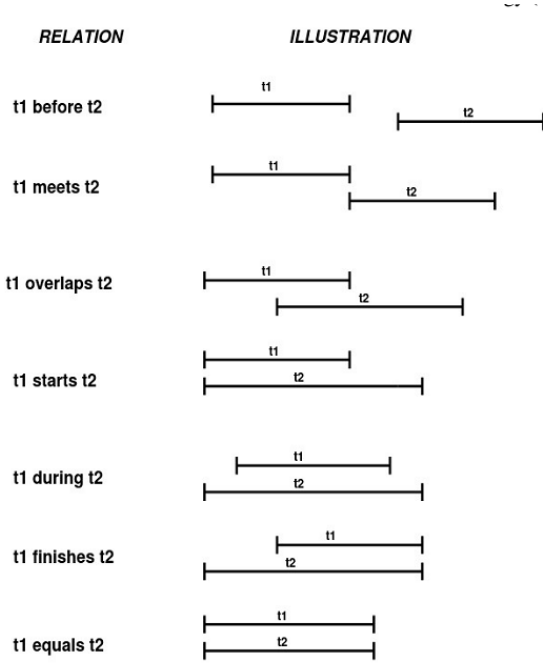


Figure 2.4. Example of Allen's temporal relations (Allen & Ferguson, 1994).

A study by Papamatthaiakis *et al.* (2010) integrated Allen's temporal relations with mining association rules to segment the most important temporal relations in sensor events when characterising activities. The study considered the same temporal relationships in sensor events at the classification stage to calculate the similarity of new data to each candidate activity. The accuracy of this technique was evaluated using two datasets from real-life environments. The results showed that, when compared with a classifier such as decision tree, the data mining technique performed slightly better in recognising ADLs.

Another data mining algorithm for discovering activities from sensor data was described by Gu et al. (2009). The study proposed mining a set of "*Emerging Patterns*" (EPs) from the sequential events obtained from two sources of data captured from wearable motion and RFID sensors. An EP is a feature vector associated with an activity that describes significant concurrent changes between the two sources of data. The study applied sliding time windows to a training dataset to find EPs and used those EPs to classify both simple activities and complex activities that can be performed in interleaving and concurrent manners. The accuracy of the technique was evaluated using multiple datasets and the results indicated that the

technique could recognise sequential activities more effectively than other types of activities.

Another study by Rashidi, Cook, Holder, and Schmitter-Edgecombe (2011) introduced an unsupervised data mining algorithm for identifying frequent and repeatable sequences of sensor events that represent ADLs. The study argued that the proposed data mining technique could detect discontinuous sequences of sensor events that could have varied orders. The detected sequences were clustered into activity definitions using a sequence clustering technique. The cluster centroids represented the activities to be tracked and recognised in the system. A version of HMMs was developed to model and recognise target activities as they occur in the environment. All HMMs were evaluated for each new sequence of sensor events and the one which best supported the sequence of events was chosen as the activity label for the sequence. A testbed environment was used to validate the ability of the technique for discovering frequent activities. An evaluation of the experiment revealed that the clustering technique could find 80% of cluster representatives corresponding to some pre-defined activities and the developed HMM model could recognize 73.8% of target activities.

A study by Gu, Chen, Tao, and Lu (2010) proposed another data mining based approach for automatically discovering and recognising specific activities from interactions with RFID-tagged objects. This approach searched the relevant instructions for each activity on websites to mine a set of objects involved in performing the activity together with the probability of them being used. A fingerprint was then mined for each activity as a set of objects that were used during that activity. Those fingerprints were then deployed to label a new sequence of observations (i.e. object-use) with an activity label. One drawback of this approach was that it required the monitor person to carry the sensor all the time.

The abovementioned ADL recognition techniques have yielded promising results in experimental settings. Kim, Helal, and Cook (2010) proposed that these techniques present a number of challenges when used for monitoring the well-being of elderly people in their homes: These included the following:

- Activities can be performed concurrently or can overlap. An occupant may also stop the current activity (e.g. cooking in the kitchen) for a short time, and start doing another activity such as visiting the toilet. These techniques do not take account of these real-life conditions.

- It is difficult to label sensor data since a number of activities can be performed for different purposes. For instance, entering the kitchen can be for performed for feeding activity or cleaning.

- A home occupant can perform the actions involved in an activity in many ways and yet the activity is performed normally. For instance, interactions with specific objects in the environment for 30 minutes of cooking can occur in many combinations some of which have not been performed before by the person.

Other monitoring approaches have been proposed which may overcome these challenges. These approaches do not aim to recognise the exact type of ADLs, but to find deviations and abnormalities in sensor data collected from the behaviours of an elderly person. The following sections outlines the techniques generally used for abnormality detection and provide a review of those applied in the application of monitoring ADLs.

## 2.3 Techniques for abnormality detection

Abnormality detection can be defined as the task of identifying data samples which differ from other data available in a dataset. According to Hawkins (1980), "*an outlier is an observation that differs so much from other observations as to arouse suspicion that it was generated by a different mechanism*." A further definition by Bamnett and Lewis (1978) is "*an observation (or subset of observations) which appears to be inconsistent with the remainder of that set of data*." These definitions are general which makes each anomaly detection tailored to the specific application domain. An example of two-dimensional data distribution for observations involving three clusters of typical data and three outliers X, Y, and Z is shown in Figure 2.5. The example shows that the three outliers are isolated and inconsistent with the main components of normal data.

Abnormality detection has been considered a crucial task in many research fields as the occurrence of outliers can be associated with significant performance degradation in a system's operation. For example, when monitoring credit card usage, an outlier may specify an unauthorized interaction of a stolen card. Abnormality detection in elderly people's behaviours may also help recognise changes in their normal lifestyle and emergency situations such as faints or falls where caregivers' rapid response is essential.

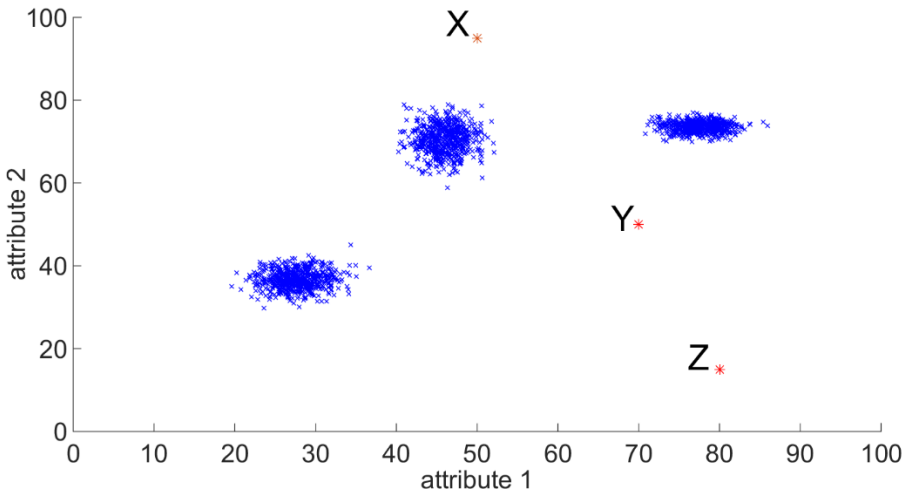


Figure 2.5. Example of data distribution for a two-dimensional dataset of observations including three clusters of normal data and three outliers.

Many studies have explored how different kinds of outliers can be detected from various types of data. The simplest technique has been to apply a user-specified decision threshold on data. Data are labelled to be "abnormal" if the threshold is exceeded. For example, when a fall detection technique monitors the posture of an elderly person, the specific threshold (e.g. 30 degrees) can be set based on the orientation of the body (Pierleoni, Belli, et al., 2015). The drawback of this technique is the difficulty of selecting the appropriate threshold for different environment settings and its inability to address variations in different subjects' behaviours. Abnormality detection techniques address this issue by learning a model of normal (and abnormal) behaviour from a training dataset of the monitored person's ADLs. These approaches have been categorised into two distinct types depending on the machine learning technique used to develop the model and whether the data are labelled and include examples of abnormalities. A summary of abnormality detection techniques is provided in Table 2.1.

Table 2.1. A summary of abnormality detection techniques.

| **Type of Supervision** | **Classifier used** | **Characteristics of the training dataset** |
|---|---|---|
| Type I: supervised | Multi-class | A labelled dataset of normal and abnormal examples |
| Type II: unsupervised | One-class | A labelled/unlabeled dataset of normal examples |

Type I abnormality detection assumes the availability of labelled training instances of both normal and abnormal classes. The Type 1 outlier detection technique is explained in Figure 2.6

(a). Such techniques usually employ supervised classification to develop a model (e.g. a decision boundary) for both normal and abnormal classes based on the dataset. The class for any new data sample is determined by comparing the data against the learned model. The model for normal instances can be further subdivided into sub-classes of normal data depending on the application and requirements of the system. Techniques categorised as Type I have been found to not always be suitable as they are susceptible to over fitting and cannot generalise well to address different variations in both classes of data (Pimentel, Clifton, Clifton, & Tarassenko, 2014). One reason for this has been the scarcity of comprehensively labelled training data that represent every possible normal and abnormal behaviour. Another limitation of these techniques is that they cannot always handle new types of outliers that are not present in the training dataset. For example, many fall detection techniques that develop a classifier using specific types of falls cannot be applied to unseen types of falls which are not learned by the classifier. A further drawback is that labelling a training dataset is usually time-consuming.

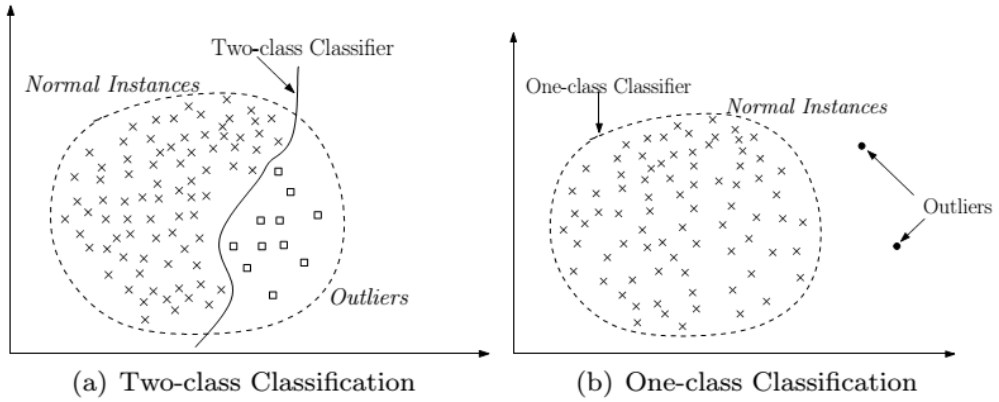


Figure 2.6. Examples of the decision boundary learned by (a) Type I and (b) Type II outlier detection techniques (Chandola, Banerjee, & Kumar, 2009).

In Type II abnormality detection, the assumption is that the normal instances are far more frequent and easy to obtain than outliers. The Type 2 outlier detection technique is explained in Figure 2.6 (b). The advantage of the techniques in this category is that they do not require labeling a training dataset. The one-class classifier learns a boundary around normal instances according to the training data and subsequently uses it to pinpoint potential outliers as data points that would not fit the model (e.g. the remote points separated from the component distributions of normal data). These techniques require that the training dataset be sufficiently comprehensive (i.e. represents various normal behaviours) to permit generalisation. The rest of this section elaborates on techniques in this category.

#### *2.3.1.1 Statistical techniques*

Statistical techniques are considered to be most applicable to single dimensional datasets. Sensor statistics over a period of time are employed to develop a normal behaviour pattern (i.e. a normal range over the universe of discourse of sensor data). If a new data point falls outside the learned normal range, it is categorised as abnormal. The two dominant statistical approaches that have been employed include the mean-variance test (Grubbs, 1969) and box-plot (Laurikkala et al., 2000). In the former, it is assumed that normal data can be modelled via a Gaussian distribution N (μ, $\sigma^2$), where μ and $\sigma^2$ are the mean and the variance of the data. The root of $\sigma^2$ is standard deviation. A new data point is marked as an outlier if it lies two or more standard deviations away from the mean. Outliers therefore fall outside a normal range of $[\mu - A * \sigma, \mu + A * \sigma]$. $'A'$ specifies the confidence interval for labelling a new data point as an outlier. For $A$ =2 and $A$ =3, the confidence values that the new data does not belong to the normal behaviour are almost 95% and 99%, respectively. This technique is data-driven as $\mu$ and $\sigma$ are learned directly from training data. The disadvantage of this technique is that it requires a high number of sample data points so that the determined range statistically represents the normal behaviour of the monitored person (i.e. the sample mean and standard deviation of sample data points represent those of the theoretically infinite population).

An alternative approach is the box plot which is a graphical representation approach for examining an unlabelled dataset of a univariate attribute. For example, box plot was used in a study by B. Das, Chen, Dasgupta, Cook, and Seelye (2010) to distinguish between normal and abnormal activities in an elderly residence. A box plot was used to display a box on the data, extending from the lower quartile (Q1) of the data to their upper quartile (Q3). The location of the median of the data is marked inside the box. A box plot also shows whiskers through lines extending from the box. The ends of the whiskers are called extreme points. Data outside the extreme points are considered as outliers. In Tukey boxplot, the extreme points are located 1.5×IQR times lower than Q1 or 1.5×IQR times higher than Q3 (Rousseeuw & Hubert, 2011). IQR is the inter quartile range, obtained as Q3-Q1. Figure 2.7 shows the respective box plot for the *y* axis of data distributions shown in Figure 2.5. Outlier points X and Y in Figure 2.7 are located outside the whiskers.

A Box plot makes no assumptions about the data distribution model and is optimal when applied to data with a unimodal distribution. Outliers located between the component

distributions of data with separate component distributions cannot detected by using box plot parameters. This technique also requires symmetry data distribution. The extreme points are determined by adding the same amount to Q3 and subtracting from Q1.

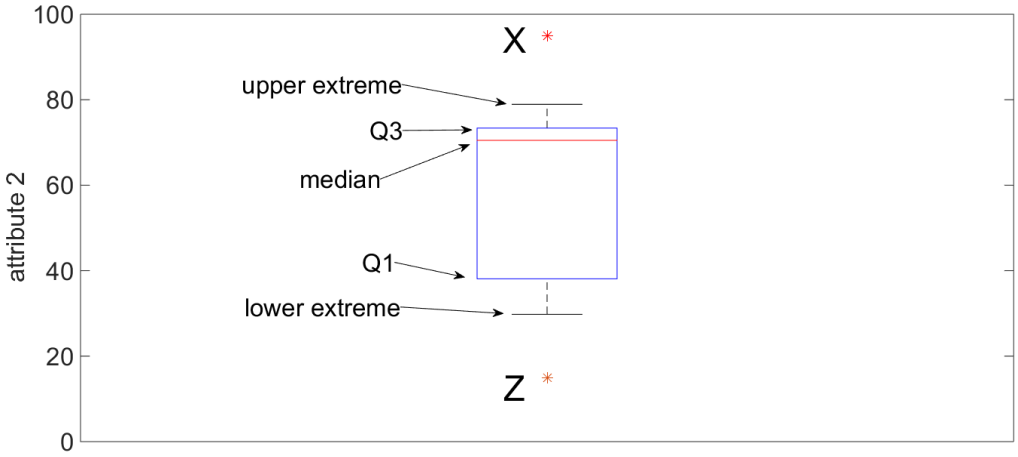


Figure 2.7. The box plot of the *y* axis values of the data points in Figure 2.5 and the two outliers X and Z. The point Y in Figure 2.5 is not an outlier with respect to the *y* axis.

#### *2.3.1.2 Probabilistic techniques*

Probabilistic techniques have also been applied to detect abnormalities in data. Such techniques estimate the probability density function (PDF) of training samples and define a threshold on the resulting PDF to obtain the normal range of data. A new data point is considered an outlier if it does not fall within this normal range. The estimation of the PDF of multivariate training samples is a well-established area of research (Scott, 2015). These techniques to estimate PDF are categorised as either parametric or nonparametric.

Parametric techniques used to estimate PDF assume that training samples are generated from some underlying parametric distribution and those parameters can be estimated if enough samples are available. Fitting a Gaussian distribution to training data has been the most frequently employed form of parametric probabilistic approaches. The training stage typically estimates the mean and variance of the Gaussian distribution based on training samples. More complex forms of data distribution can be modelled using a mixture of Gaussians known as GMMs. A study by Scholz (1985)) estimated parameters of GMMs using optimisation algorithms (e.g. maximum likelihood estimation) which maximise the likelihood of the model given a set of training samples. An incrementally learning technique was used by Fink, Zio, and Weidmann (2015) to learn a model of normal data from a set of sample data. Once a GMM

was estimated from the data, the likelihood of a new data point $x$ to the model $t$ was calculated by Equation 2.1

$$P\left(x\middle|\mu_i, \Sigma_i\right) = \sum_{i=1}^{M} \alpha_i \, g(\mathrm{x}|\mu_i, \Sigma_i) \tag{2.1}$$

where M is the number of component Gaussian distributions, $\alpha_i$ $(i = 1, \ldots, M)$ are the mixture weights, $x$ is the input value and $g(\mathrm{x}|\mu_i, \Sigma_i)$ $(i = 1, \ldots, M)$ are the component Gaussian distributions. Each component distribution is calculated using Equation 2.2.

$$g(\mathrm{x}|\mu_i, \Sigma_i) = \frac{1}{(2\pi)^{\frac{d}{2}} \sigma_i(x)^{\frac{1}{2}}} \exp\left\{\frac{1}{2\Sigma_i} (\mathrm{x} - \mu_i)^{\mathrm{T}} (\mathrm{x} - \mu_i)\right\} \tag{2.2}$$

where $\mu_i$ and $\Sigma_i$ represent the mean and covariance matrix of the training samples. $d$ specifies the dimensionality of the sample data. Given a new data point, a score for being normal can be calculated using Equation 2.1 and once this score is less than a specific threshold, the data point is marked as outlier.

Mixture models may require large numbers of training examples to estimate model parameters. Another drawback reported was that the chosen functional form for the data distribution may not accurately represent the distribution that generated the data (Pimentel et al., 2014).

Non-parametric probabilistic techniques used to estimate PDF typically employ a kernel density estimator. Outliers are identified as those data points that fall in the low density area of the learned density function. A kernel density estimator places a kernel function (e.g. Gaussian) on each training data sample and estimates the local PDF for that location with respect to the kernel bandwidth (the radius of the kernel). This means the local PDF for each data point is calculated by summing the contributions from kernels within a specific proximity of the data point. The data points in dense regions receive a higher value in the PDF and those in the tails of the distributions receive very low values.

A study by Tarassenko, Hann, and Young (2006) proposed a non-parametric approach for detecting abnormalities in physiological information of patients. The study used a non-

parametric probabilistic model of normality which was learned using a training dataset of normal high-risk patients. The model was estimated using a combination of k-means clustering and Gaussian kernels. A number of clusters were identified using k-means and the PDF of the training data was estimated by calculating the local PDF of each cluster centre using Gaussian kernels. The model of normality was employed to detect abnormality in test data acquired from a patient. An alert was generated if a novelty score for test data exceeded a threshold.

#### *2.3.1.3 Techniques based on one-class SVM*

Training a one-class SVM is another unsupervised technique for forming a novelty boundary in the feature space of an unlabelled dataset to separate normal data from outliers (Yu et al., 2013). The location of outlier decision boundary is determined using the support vectors (i.e. those training data that lie closest to the boundary of normal data distribution). The one-class SVM projects the normal data onto a high-dimensional space using a kernel function in an attempt to draw the smallest hyper-sphere that separates normal and abnormal data with a maximum margin. To make the classifier more tolerant to outliers, a parameter needs to be set by the user to allow a proportion of the normal data to fall outside the decision boundary of the "normal" class. The kernel functions range from linear dot product, through polynomial nonlinear, and to a Gaussian function. Labelling new test data typically involves determining whether the test data falls outside the boundary of normal data (i.e. the boundary where the outliers lie). The problem associated with using this approach has been that the performance of the classifier is highly affected by the parameters defined by the user (Pimentel et al., 2014).

A study by Gardner, Krieger, Vachtsevanos, and Litt (2006) described the application of a one-class SVM in detecting seizures in humans. The intracranial electroencephalogram (EEG) time-series was mapped onto its respective sequences of novelty scores through the classification of one-second-window energy-based statistics computed from the signal. The separating hyper plane for the classifier was obtained using training data of normal EEG. Data containing seizure events were detected as those representing significant changes in the feature space. Another study L. A. Clifton, Yin, and Zhang (2006) also proposed an SVM-based abnormality detection technique for monitoring combustor operation. It employed a one-class SVM to predict combustion instability using multivariate combustion data. Wavelet analysis was used first for feature extraction, from which detail coefficients were extracted as two-dimensional features. Novelty scores computed using the one-class SVM classifier were

obtained to detect unstable operation of the combustion machine.

#### *2.3.1.4 Data mining techniques*

Data mining techniques for abnormality detection include clustering techniques (e.g. k-means, Fuzzy C-Means (FCM) and DBSCAN) and rule extraction techniques, such as association rule mining (Agrawal, Imieliński, & Swami, 1993) and frequent episode rule mining (Agrawal & Srikant, 1995).

Clustering techniques characterise boundaries for normality in the data space using a small number of unlabelled normal samples. The training data are grouped into clusters and a representative point for each cluster is obtained (i.e. the cluster centre). A score for abnormality in a test data point is calculated as its minimum distance to the nearest cluster centre. The test instance is labelled as an outlier if it is not close to any of the learned clusters.
Clustering methods use different approaches to identify cluster centres. K-means and FCM are categorised as partitioning clustering algorithms which partition the dataset into a pre-defined number of clusters. The initial partitioning of the dataset iteratively changes in order to optimise an objective function. The k-means algorithm initially chooses *k* random data points as cluster centres. The data points in the dataset are then assigned to clusters based on their distances to the cluster centres. The locations of data points for each cluster are then averaged to update the location of the cluster centre. This process is repeated until a specific criterion is met (e.g. the locations of cluster centres do not change during two consecutive iterations).

The FCM technique clusters data using a similar approach to k-means. Each data point in the dataset is assigned to different clusters to a certain degree. The centre of a cluster is the average of all data points, weighted by their degree of belonging to the cluster. The algorithm starts by choosing specific numbers of data points as cluster centres. Once the degree of membership of all data points in different clusters is calculated, the locations of cluster centres are updated. The algorithm then repeatedly recalculates the membership degrees of data points and updates the location of cluster centres until their locations do not change beyond a specific threshold during two consecutive iterations. This shows that each cluster includes data points that have the maximum degree of membership in that cluster.

A study by D. A. Clifton, Bannister, and Tarassenko (2007) used the k-means clustering

technique to monitor the operation of aerospace gas-turbine engines, where k was determined empirically. Novelty scores were constructed based on the distance of test data from their closest cluster centre. Test data with a novelty score exceeding a threshold were classified "abnormal" with respect to the model. Since each cluster was represented via the location of the cluster centre, this technique is unable to represent clusters with arbitrary shapes. Techniques based on k-means are also sensitive to outliers since they can significantly affect the location of cluster centres.

DBSCAN is a density-based clustering algorithm that finds clusters of an arbitrary shape. It has two application-specific parameters: *MinPnts* which determines the minimum number of data points in each cluster and *Eps* which specifies the radius in which two points in a cluster are reachable. The DBSCAN algorithm selects an arbitrary unprocessed point *p* from the dataset and generates a new cluster with *p* as the core object if *Eps*-neighbourhood of this point contains more than *MinPts* data points. *p* is then labelled as *processed*, and all its neighbours are selected as core objects and go through the same process to grow the cluster. Once this process is completed, a new unprocessed point is selected and this process is repeated until no new cluster can be developed (i.e. there are no new points that can be added to any clusters).

Rule based data mining methods generate rules that represent frequent patterns in a training dataset. The set of these rules represent the regular behaviour of the monitored system (Chandola et al., 2009). Any test sample that does not trigger any rule is considered as an outlier. Various methods have been proposed to generate such rules. Association rule mining techniques extract rules that associate frequent itemsets in their antecedent and consequent. In a given database of transactions with each transaction including a limited list of items, frequent itemsets are those items that co-occur frequently in the database. The assumption of association rule mining techniques is that outliers occur very rarely in the dataset. Valid support and confidence thresholds for the association rules are chosen to prevent outliers being represented by any rule.

A number of association rule mining algorithms have been proposed in research literature. An early study by He, Xu, Huang, and Deng (2004) used association rule mining to detect abnormal network traffic by characterising significant data patterns in a training dataset. Another study by Tajbakhsh, Rahmati, and Mirzaei (2009) described a fuzzy version of this algorithm in order to detect network intrusions. Fuzzy linguistic values were defined over the

domain of network traffic attributes. The data patterns that co-occurred frequently in the training dataset were characterised as fuzzy rules. This fuzzy rule set was then used to detect those abnormal data that had a low compatibility to the rule set.

Techniques for mining frequent episodes extend the association rule mining algorithms since they take into account the order of items in sequential data. Such techniques generate rules from the sequences of sensor events in which each rule represents a frequent sequence of events known as a frequent episode. Outliers are those test sequences that do not match any rule.

A technique for mining frequent episodes was presented by Y. Liu, Zhao, Chen, Pei, and Han (2012) to monitor a person's visited locations inside a home. The approach collected sequences of *n* visited locations (*n* was a user specified parameter) in a training phase and mined frequent episodes to identify frequent trajectories inside the home. A monitoring phase was used to compare the sequences of visited locations with the frequent trajectories in order to detect abnormal behaviours.

#### *2.3.1.5 Fuzzy based techniques*

Deploying inference systems based on fuzzy logic is another technique for abnormality detection. The fuzzy rule base associated with a fuzzy inference system is flexible and incremental as new fuzzy rules can be added and existing rules. Fuzzy rules can be generated from a training dataset of both normal and abnormal samples or only normal samples. Each rule usually characterises a specific behaviour of the system. The output from the fuzzy rule set can be used to detect deviations from the normal behaviour of the system.

A recent study by Chakraborty, Chakraborty, and Mukherjee (2016) reported on the development of a fuzzy inference system to detect Parkinson's disease in the elderly. This study captured a dataset of biomedical measurements of elderly people's voice and employed clustering techniques to extract fuzzy rules from the input and output dataset. The output of fuzzy rule set was a continuous value ranging from 0.1 to 1.5 with values higher than a pre-defined threshold indicated the disease. The result indicated that the detection accuracy of the system was up to 97%.

## 2.4 Abnormality detection in ADLs of the elderly

Abnormality detection has been considered as a challenging task in the realm of monitoring elderly people's ADLs due to the absence of a formal definition and the scarcity of events that indicate such behaviours (Lundström et al., 2016). The first stage in the detection of the abnormal behaviour is to define a sequence of actions as an activity. Activities are then be regarded as abnormal based on different attributes, such as the posture of the person, the order of actions, duration, time, location, and the frequency of the activity. The subject's posture and the time, duration and location associated with an activity are monitored to detect hazardous events such as falls, whereas the other attributes are used for detecting deteriorating health over a longer period. A recent study by Peetoom et al. (2015) on approaches developed to detect abnormality in elderly people's ADLs suggests that these can be categorised as follows:

1. Those that aim to detect short-term abnormal behaviours in physical activities which result in dangerous incidents. This category of abnormal behaviours can usually be identified by monitoring systems over a short period. For example, a fall can be detected within a few seconds of lying on the floor and becoming unconscious can be detected within several minutes.

2. Those that detect deviations from the subject's daily routine in a longer period (e.g. daily and weekly). These deviations are mostly detected by analysing instrumental ADLs and indicate a deteriorating functional ability of elderly people.

This categorisation suggests that most studies are not able to detect both short-term abnormal behaviours during physical activities and long-term deviations from the routine of instrumental ADLs. This is due to the combination of sensors employed by these approaches not providing relevant data for monitoring both physical and instrumental ADLs. Monitoring the former requires identifying the subject's body postures (e.g. sitting, walking, and lying) along with the time and location of the activity. This is achieved mostly by employing video cameras or wearable sensors. Monitoring instrumental ADLs on the other hand involved using environmental sensors to detect interactions with objects and measuring the person's ability to follow a daily routine for important tasks, such as cooking and grooming.

Another important reason is the difference in the intervals at which monitoring approaches

examine behaviours related to physical and instrumental ADLs. The focus in monitoring physical ADLs is typically on the short-term behaviours of the occupant. Once an abnormality (e.g. a sudden fall) is detected, an alarm is raised to notify a caregiver about a potential emergency situation. This is different from monitoring instrumental ADLs where the focus is to examine behaviors over a longer period of time. For example, a set of activity metrics may be calculated for an entire day to detect a noticeable drift from the occupant's normal profile (Noury et al., 2011).

Different types of output also need to be generated for monitoring physical and instrumental ADLs. Monitoring physical ADLs results in generating alarms as it aims at detecting emergency situations that need a rapid response by a caregiver or family member. This is in contrast to monitoring the daily routine for instrumental ADLs in which once a drift is detected across several days, a notice is sent to caregivers to help them identify deteriorating health.
The following subsections will provide a review on research related to abnormality detection in physical and instrumental ADLs.

### 2.4.1 Abnormality detection in physical ADLs

Many elderly people face hazardous events during physical ADLs (such as becoming unconscious or falls) and may sustain an injury or remain on the floor for long durations until someone discovers them. Different factors can cause such abnormal behaviours during physical ADLs including side effects of medications and muscle weakness. Approaches that are proposed for detecting these events mostly target fall incidents using different sensor technologies such as cameras and wearable sensors. The majority of these approaches rely on simple thresholding of the sensor outputs. Other approaches have applied machine learning techniques to distinguish hazardous events from normal ADLs by using a training dataset. The following sections provides a review of literature on approaches used to detect abnormalities in physical ADLs.

#### *2.4.1.1 Thresholding techniques with wearable sensors*

Several studies have applied fixed thresholds on kinematic information obtained from wearable sensors, such as accelerometers and gyroscopes to detect abnormalities in physical ADLs. Research by Jay Chen, Kwong, Chang, Luk, and Bajcsy (2005) proposed an accelerometer-based approach that monitored body-orientation changes. A potential fall would be indicated

if the orientation angle of the body was less than a user-defined threshold. The orientation change was then calculated over one second before and two seconds after the initial impact with the floor by calculating the dot product of the acceleration vectors. Despite many efforts to improve this algorithm, it was not able to distinguish between real-world falls and ADLs. Another similar study by Bourke and Lyons (2008) positioned a gyroscope on the subject's chest and used threshold values for angular velocity, angular acceleration, and the change in the trunk angle to detect falls.

A recent study by Pierleoni, Belli, et al. (2015) proposed another thresholding-based fall detection technique which used information supplied from an accelerometer, a gyroscope and a magnetometer to detect falls. The system raised an alarm if the body orientation was below a pre-determined threshold for a certain amount of time. The proposed algorithm was evaluated with a dataset of simulated falls and normal ADLs and results confirmed the detection accuracy of both types of activity.

A similar approach was proposed by Q. Li et al. (2009) which applied a thresholding technique on data from accelerometers and gyroscopes. The sensor data were first categorised as belonging to static postures (i.e. standing, bending, sitting and lying) or motions between the static postures. Features including angular velocity and linear acceleration were extracted to detect fall incidents as unintended motion transitions before a static lying posture. The study reported that the proposed technique could not accurately differentiate specific activities (e.g. falling into bed and falling against the wall from a seated posture).

#### *2.4.1.2 Machine learning techniques with wearable sensors*

Monitoring approaches which involve wearable sensors have used different types of machine learning techniques such as k-nearest neighbour (k-NN) classifiers and SVMs to distinguish falls based on a training dataset of the elderly person's activities. The wearable sensors are labelled with different activities including falls and then used to train the classifier. These were categorised as Type 1 classifiers as shown in Table 2.1.

A recent study by Yuan, Yu, Dan, Wang, and Liu (2015) attached an accelerometer and a gyroscope to different parts of the monitored subject's body to distinguish between falls and ADLs. A large set of statistical features was extracted from the sensors' outputs and principal

component analysis (PCA) condensed this feature space into fewer dimensions. The performance comparison of six machine learning techniques, for a labelled dataset, showed that the k-NN classifier was the most accurate in detecting falls. A similar result was obtained by Özdemir and Barshan (2014) who attached six sensors to different parts of the subject's body. Once the data from the wrist sensor reached a peak, raw data from other sensors in a 4 second time window around this peak point were processed to extract features.

Another recent study by Lustrek et al. (2015) partnered SVMs with a decision tree classifier to detect falls using location sensors attached to different body parts of the subject. The sensor data were pre-processed and the results were used to classify the subject's posture. The estimated postures were combined with the subject's locations to detect falls. The occurrence of a fall was confirmed as those situations that both classifiers output as a fall. Evaluation results revealed that taking into account the subject's location improved the fall detection accuracy by approximately 30 percent.

Another study by Pierleoni, Pernini, et al. (2015) also employed SVMs to develop a fall detection system using intervals of data supplied by a smart phone. For those intervals featuring a potential fall, features were extracted and fed into SVMs to detect fall events. SVMs were also used by S. H. Liu and Cheng (2012) to detect falls from signals provided by a wrist accelerometer. The study used a time sliding window to extract body orientation angle and the motion of the hand as the input of the SVMs. The SVMs were trained using a labelled dataset of simulated ADLs including falls. Although this approach required a labelled training dataset, the results proved to be more accurate than those of traditional thresholding techniques.

Techniques relying on wearable devices to detect short-term abnormal behaviours have two key limitations (Khan & Hoey, 2016). These techniques have been found to provide a high rate of false alarm in real-life settings. This is because many normal ADLs can cause high acceleration of body parts (e.g. jumping or sitting down suddenly) that can result in sensor measurements being similar to those for real falls. Another drawback has been that some people find wearing a device uncomfortable when sleeping, changing cloths and bathing, hence raising issues about the maintenance of wearable devices.

#### *2.4.1.3 Machine learning techniques with video cameras*

Several researchers have proposed video based monitoring techniques to detect short-term abnormal behaviours. These techniques overcome the limitations found with using wearable sensors. The silhouette of the monitored person is first segmented from video stream and features are then extracted to describe ADLs. These features include the aspect ratio of the minimum bounding box, the ratio of the major axes of the fitted ellipse, and the body orientation. Machine learning techniques are employed to distinguish short-term abnormal behaviours in physical ADLs.

Hsueh, Lin, Chang, Chen, and Lie (2015) proposed a video/audio based approach which used a Bayesian network to detect abnormal behaviours. The trajectories of occupants along with audio features were first extracted from labelled sensor data and then used to build the Bayesian network model. The model was utilised to detect abnormal events in new sensor data. This approach was validated using data collected from a real environment and results showed that this outperforms the Naive Bayesian model.

Another video based approach was reported by Seki (2009) in which an omni-directional vision camera was used to collect data and a fuzzy framework was created for detecting abnormal activities. The approach extracted the subject's body orientation, the location and the time of activities to generate fuzzy rules. The degree of abnormality for each observed pattern of features was determined by calculating its frequency in a training dataset. One limitation to this approach was that each frame was evaluated independently which resulted in ignoring the duration of activity patterns. Another limitation was that the fuzzy sets were defined arbitrarily to obtain fuzzy attributes describing ADLs.

Another approach proposed by Rougier, Meunier, St-Arnaud, and Rousseau (2011) detected falls via thresholding the body orientation and the ratio of the major axes of the fitted ellipse on the subject's silhouette. This approach had some limitations as it was unable to extract features that characterise the 3D posture of the person during falls with the use of a single camera. For example, a fall which happens in the viewing direction of the camera cannot be differentiated from other postures because of the very small differences in the orientation of the subject's body.

This issue was addressed by Zambanini, Machajdik, and Kampel (2010b) where a network of video cameras was employed to detect falls via the silhouettes of the monitored person. The video stream from each camera combined to estimate the 3D posture of the person, termed early fusion. Evaluation results showed that monitoring 3D posture of the occupant would significantly improve the accuracy of fall detection.

Another study by Rougier, Meunier, et al. (2011) improved on this approach by proposing an unsupervised fall detection technique using late fusion of data from multiple cameras. From each camera stream, the subject's silhouette was extracted for each frame and then falls were detected via analysing human shape deformation. The assumption was that during a fall, the subject's posture changes rapidly and this is followed by a lack of significant movement. Several edge points from the silhouette were selected in each frame. The matching distances of those edge points from two consecutive frames were then calculated. The matching distances were classified by a GMM into normal or abnormal. The GMM was trained by an unlabelled dataset of normal activities. The system classified input data as representing a fall incident if GMM labelled data as abnormal and that situation was followed by low movement of the person for a specific period.

Yu et al. (2013) research reported on the use of one-class SVMs to detects falls in video images. After capturing a dataset of an occupant's ADLs for a specific number of days, features including body orientation and skeleton structure were extracted to determine a decision hyperplane for the SVM classifier. The study reduced false alarms by introducing two rules for cases in which an abnormal posture is detected; these would verify whether a large movement in the body posture occurred during the fall and whether the occupant lied on the ground for a certain duration. Evaluations using a dataset of simulated falls showed that the one-class SVMs performed better by nearly 10% compared with the GMMs proposed earlier by Rougier, Meunier, et al. (2011).

Banerjee et al. (2014) concluded that systems using video cameras are limited as they have three key drawbacks: (1) the segmentation of the subject relies on background modelling in the colour image space, which is difficult in real-life conditions due to colour and light variations; (2) operating in low light or no light conditions is only possible if an active source of infrared light is available; and (3) for multi-camera systems, the installation and calibration of the cameras in the same reference frame become a major concern.

#### *2.4.1.4 Thresholding techniques with Kinect sensors*

Researchers have used the recently developed Microsoft Kinect sensors to detect emergency situations such as falls in homes of elderly people. This motion sensing device includes a depth sensor to capture 3D data under any ambient light conditions. The depth information is utilised to estimate a skeletal model of any person in Kinect's field of view along with their segmented silhouette.

A number of recent studies have reported the use of Kinect sensors to detect abnormal activities. A fall detection system was proposed by Planinc and Kampel (2013) which relied on the location of skeleton joints with respect to the ground plane. The occupant's spine was estimated from an analysis of full-body 3D data supplied by a Kinect sensor. The study defined potential fall events as scenarios where the occupant's spine rapidly transformed from a state of vertical to horizontal and did not return to vertical within a specified period. One limitation of this approach was that for real-life environments the tracking of all skeletal joints cannot be carried out in a reliable manner. This is due to the tracked person being occluded by furniture resulting in their skeletal joints not being directly visible from the sensor (Kwolek & Kepski, 2016). This has lead researchers to search for other techniques to characterise the 3D silhouette of the person to detect falls.

A recent study by Yang, Ren, and Zhang (2016) described a Kinect-based fall detection technique in which the silhouette of the moving individual along with the floor plane equation were estimated from depth images. This study analysed the orientation of the human body and the distance between the silhouette's centroid and the floor plane to detect a fall incident. This approach used some pre-defined thresholds which make its application limited across different real-life settings. An evaluation of results in laboratory environments showed that it could detect fall incidents effectively.

#### *2.4.1.5 Machine learning techniques with Kinect sensors*

Some Kinect-based fall detection studies have used machine learning techniques to avoid the drawbacks associated with the simple thresholding of the extracted features. A study by Dubey, Ni, and Moulin (2012) proposed a fall recognition system which combined depth maps with colour information. The subject's motion was characterised via extracting Motion History Images (MHI) from both colour images and depth maps. SVMs then detected a fall through a

set of geometrical moments extracted from each MHI channel. The SVMs were trained using a labelled dataset of 12 activities including falls captured from a laboratory environment. A similar study by C. Zhang, Tian, and Capezuti (2012) trained SVMs to detect fall incidents from deformation of the subject's height and skeleton joint angles. A high fall detection accuracy of 94% was achieved using a testing dataset of specific types of fall (i.e. fall from a chair and fall from standing) captured from a laboratory environment.

A recent study by Stone and Skubic (2015) proposed a two-stage fall detection system from Kinect data. The first stage generated a time series characterising the vertical status of the detected person over time. A sliding widow in the second stage analysed this time series to identify segments in which the subject was lying on the floor. A set of features was extracted to characterise the dynamic of the body motions during potential fall incidents. An ensemble of decision trees was then used to calculate a confidence of fall for each segment. The decision trees were trained using a labelled dataset of fall and non-fall activities. This approach was compared against other fall detection algorithms and was found to achieve better results.

Many Kinect-based fall detection approaches have applied fuzzy rule-based systems in the form of fuzzy If-Then rules. The use of fuzzy sets to parameterise input variables allowed some degree of variation in different samples of ADLs. The simple structure of fuzzy rules is easy to interpret. Kepski et al. (2012) presented a fuzzy rule-based system for fall detection which obtained data from a Kinect and a wearable device. The study extracted the acceleration and speed of the body's motion from wearable sensors and these were combined with the distance of the person's centre of gravity to the floor as measured by a Kinect camera. These features were the inputs to a set of manually defined fuzzy rules which distinguished fall incidents from other activities.

Another recent study by Kwolek and Kepski (2016) proposed a similar fuzzy approach in which data captured by an accelerometer were thresholded to detect potential falls. The processing of Kinect depth maps was initiated each time a potential fall was detected. A set of features including the aspect ratio of the subject's bounding box and the distance of their centroid from the floor was obtained from processing the depth maps. Features from both Kinect camera and accelerometer data were then used by a two-level fuzzy inference engine where, on the first level, two different fuzzy inference systems were used to determine the lying posture and motion transition associated with a fall. The second level of the inference engine

classified the output of the first level into a fall or non-fall activity via the use of a pre-defined set of fuzzy rules. Experiments performed on a dataset of simulated falls showed better performance using this technique compared with using SVMs as the classifier.

Planinc and Kampel (2012) reported a similar fuzzy-based fall detection technique in which the body orientation and the height of the subject's spine were estimated as the inputs of a fuzzy inference system to classify the posture of the body into on the ground, in between and upright states. The confidence values for the subject being in different states were thresholded for fall detection. Although evaluation results showed a fall detection accuracy of 98.6% on 72 testing videos, this method was evaluated using a set of predefined fuzzy rules with a dataset collected from a laboratory environment.

### 2.4.2 Abnormality detection in instrumental ADLs

A number of studies have reported on monitoring instrumental ADLs of elderly people in order to detect long-term deviations from their daily routine. Abnormalities over a long period (e.g. day or week) are infrequent and hard to simulate. Instead of modelling abnormalities, researchers typically modelled normal behaviours using data samples collected from the elderly person's ADLs. Outliers were defined as those behaviours deviating from the developed model. These approaches mostly belong to the category of Type II described in Table 2.1 (Yu et al., 2013). The majority of studies used environmental sensors (e.g. PIR sensors, magnetic switches and RFID tags) to estimate ongoing instrumental activities based on the subject's locations and/or environmental interactions. The following section provides a review of research on some of the commonly used techniques for abnormality detection in instrumental ADLs.

#### *2.4.2.1 Statistical techniques*

Among various techniques described for outlier detection (see Section 2.3), statistical techniques are frequently used for monitoring elderly people's long-term behaviours. Some studies have monitored the mobility of the elderly inside their homes to detect abnormal behaviours. Frequency rank order statistics were used by Shieh, Chuang, Wang, and Kuo (2006) to monitor the mobility changes of the elderly at home using PIR sensors. A day was divided into intervals and the number of sensor triggers during each interval was counted. The numbers associated with eight successive intervals were then mapped into a binary sequence of eight bits to represent a pattern of movement in the house. The average deviation of

frequencies of movement patterns were calculated for a test day to measure the deviation of the subject's behaviour from their normal profile. This technique required a high number of training samples so that the calculated features represent the normal behaviour of the monitored person.

A similar study by Virone et al. (2008) monitored an elderly individual's mobility using PIR sensors installed in every room of a residence. Two metrics were obtained for each hour of the day namely, *occupancy rate* and *activity level*. The former measured the duration for which the occupant visits each room and the latter specified the number of sensor triggers for each room. A normal variation range was defined for each metric using the mean and the standard deviation of the training data. To monitor the occupant's behavioural patterns, the hourly values of the two metrics were computed, and when they were found to be outside the ranges of normal variation, the system generated an alarm. The technique was tested on a dataset from real-life settings and validations showed that monitoring the occupant for each hour of the day could result in a high rate of false alarms.

#### *2.4.2.2 Probabilistic techniques*

A limited number of studies have described the use of probabilistic techniques for detection of abnormal of physical ADLs. Elbert, Storf, Eisenbarth, Ünalan, and Schmitt (2011) combined the statistical technique described previously by Virone et al. (2008) with a probabilistic technique to detect deviations in the long-term behaviours of elderly people. Attributes such as the start time and duration of ADLs were extracted from a labelled dataset of specific activities obtained from PIR sensors. GMMs were trained to characterise the normal variation range of attributes during different activities. The likelihood of new sensor data belonging to each activity was calculated based on the probability of those data being generated by the GMM model of that activity. A final score in a range of zero to one was obtained via averaging the likelihood of GMMs. Values closer to one indicated less deviation from the normal behaviour patterns. Experimental results showed different behaviour patterns on weekends than during weekdays which would require building separate models.

Various approaches have been proposed for modelling the duration of activities using GMMs. A study by Alam, Reaz, and Husain (2011) that explored MIT's PlaceLab and MavHome datasets found that GMMs were efficient for learning regular activity durations and could

highlight deviations. Switching Hidden Semi-Markov Models have also been successfully employed to model durations and to detect outliers (Duong, Bui, Phung, & Venkatesh, 2005). Another study by Shin, Lee, and Park (2011) used a one class SVM to monitor the activity level and mobility of the elderly through motion detectors. Each day was divided into one-hour intervals, and for each interval, a one-class SVM classifier was developed to model a decision boundary for the normal data patterns so as to identify outliers. This boundary was obtained through applying a Gaussian kernel function to the data. Evaluations on a dataset captured from a real-setting environment showed that the classification results of the one class SVM were influenced by the variance parameter of the kernel function. The optimal hypersphere resulted in a correct classification rate of nearly 98%.

A recent study by Tong et al. (2015) developed an approach based on hidden state conditional random field (HCRF) to monitor ADLs via modelling sub-activity relations. A labelled dataset of ADLs captured by environmental sensors was used to train the HCRF model. The likelihoods of the activity in testing data to target ADLs were calculated to detect abnormal activities. The results showed that the HCRF this approach outperforms other approaches that were based on using SVMs.

#### *2.4.2.3 Clustering techniques*

A number of researchers have employed clustering techniques to find abnormalities in the sequence of visited locations. These studies are based on the assumption that different types of ADLs are related to spatial regions in a home. The clustering techniques in these studies determined a boundary of normal behaviour and defined outliers as data points outside the boundary or located far from any cluster.

A study presented by Hsu, Lu, and Takizawa (2010) collected a person's visited locations for a week using active RFID sensors. After a sliding window extracted movement patterns, a fuzzy c-means clustering algorithm was used to identify behavioural models. A new observation distant from all cluster centres was identified as an outlier. Bamis, Lymberopoulos, Teixeira, and Savvides (2008) also modelled the order of visited locations using a k-means clustering algorithm. The study clustered room occupancy durations and the patterns of visiting different rooms via using timestamped data from PIR and door sensors. The distance of the occupancy pattern to the closest cluster centre was calculated for each day as an indication of

deviation from the regular daily routine.

Another study by Lotfi, Langensiepen, Mahmoud, and Akhlaghinia (2012) also employed clustering techniques, including SOM, k-means and FCM, for monitoring the pattern of visited locations in a house. The evaluation results confirmed the effectiveness of modelling the start time and durations of ADLs in finding abnormal behaviours in the elderly homes especially when the occupant was suffering from dementia.

#### *2.4.2.4 Data mining techniques*

Data mining techniques have shown promise for modelling the frequent behaviour patterns of the elderly using unlabelled sensor data. Munstermann et al. (2012) identified such patterns during instrumental ADLs using data from binary sensors attached to different objects. The study identified nine instrumental activities based on the practical knowledge of caregivers and these were modelled via the set of objects used during each activity. When the sensor data were transformed into sequences of activities, a sequential mining algorithm generated a model of frequent transitions between activities along with the probability of each transition. The sensor data for a new day were similarly transformed into activities and the probability of transitions between activities were compared with the learned model to decide whether the behaviour was normal. The evaluation of this technique showed that choosing a certain threshold value would lead to a precision of 96.5%.

Another data mining technique, named sensor activity pattern (SAP), was recently proposed for modelling the spatio-temporal order of visited locations in a home (Suryadevara & Mukhopadhyay, 2015). The frequent patterns of visited locations were identified during several time periods of the day. An unlabelled dataset collected from PIR sensors was used to determine each frequent pattern which could be considered as a particular ADL. To monitor the ongoing ADLs, the likelihood of the patterns of visited locations relative to the learned ADLs was determined.

Data mining techniques have also been used to monitor the order of actions during ADLs such as cooking, grooming, and taking medicine which are complex and contain sequences of actions. Jakkula and Cook (2008) concluded that the order of interactions with objects constituting ADLs is important as it can help indicate abnormality in behaviours. This study

collected an unlabelled dataset of environmental interactions (sensor events) from a network of binary switches attached to objects, with each sensor event tagged with a date and time. Allen's temporal logic was employed via a data-mining algorithm to find frequent temporal relationships between sensor events. A probabilistic approach was then used to determine if a new sequence of sensor events was abnormal based on its similarity to the frequently occurring sequences of sensor events. The evaluation results of this approach based on synthetic data only showed that it is capable of identifying abnormal events based on the temporal information of sensor events.

A recent study by Lundström et al. (2016) proposed using random forests to detect abnormalities in the time and space of ADLs. This approach trained a random forest for each activity to model most meaningful patterns of sensor data related to the activity. These models were used in the monitoring stage to flag temporal and spatial deviations of activities. A limited number of activities were modelled by this approach and validation experiments showed the high effectiveness of this approach in detecting deviating behaviours.

#### *2.4.2.5 Fuzzy logic approaches*

Machine learning techniques have a number of limitations for modelling human behaviours. This is due to their lack of tolerance to the inherent variations in performing ADLs and uncertainty in sensor data. Fuzzy logic has been used extensively in ADL monitoring approaches to address this limitation. For example, Martin, Majeed, Lee, and Clarke (2007) proposed a fuzzy system for monitoring an elderly person's instrumental ADLs. After classifying the sensor events into activities in the training stage, the approach determined the usual time and duration of activities using a fuzzy version of the *AprioriAll* algorithm. It is reported that the use of fuzzy logic has enabled this approach to summarise the monitoring data in a manner understandable to caregivers. The disadvantage of this approach is that it only monitors a limited set of ADLs.

This shortcoming was addressed by the fuzzy system developed by Mahmoud, Lotfi, and Langensiepen (2012) where abnormal days were identified using sequences of the visited locations obtained from PIR sensors. This study extracted two statistical attributes via the use of PCA to characterise the occupancy patterns of rooms during the training period. Several fuzzy rules were manually defined to map the attributes into degrees of abnormality. The

system verified the occurrence of an abnormal situation when both attributes exceeded their normal variation range.

The monitoring of instrumental ADLs and visited locations inside an elderly person's home has been shown to provide useful information about elderly people's functional abilities. The disadvantage of this approach is that the information it provides does not always help to accurately determine the physical wellbeing of the elderly (Suryadevara & Mukhopadhyay, 2015). It was extremely difficult to verify the subject's wellbeing when no appliance was used or the location of the monitored person did not change. A more comprehensive framework is therefore required to monitor both physical and instrumental ADLs.

## 2.5 Summary

The literature review in this chapter showed that although detecting abnormal behaviour in both the physical and instrumental ADLs of elderly people is crucial, there is a lack of research in the area of monitoring both types of activities concurrently. Most techniques adopted for monitoring ADLs were found to be based on simple thresholding or supervised machine learning algorithms. These techniques were shown to have drawbacks with the former not able to be generalised to fit across different environments while the latter requiring the laborious generation of a labelled training dataset of activities. These approaches were limited as they can only monitor a pre-defined list of activities and confine emergency situations to fall incidents by using a pre-assumed model of body motion.

The review of literature has found that most approaches proposed for monitoring physical ADLs have used either intrusive video cameras or asked the subject to wear sensors which might easily be forgotten. The application of Microsoft Kinect depth sensor for monitoring elderly people's activities in a minimally intrusive manner is in its infancy stage. The related studies have been limited to simple thresholding techniques that can only detect falls among a wide range of abnormal behaviours. The review of literature also found that most approaches for monitoring instrumental ADLs involved either using a network of environmental sensors or a power sensor in the electricity box of the house. The use of environmental sensors requires a costly installation of many sensors during the construction of a house while using a power sensor in the electricity box needs a prior knowledge about HEAs in use or a labelled dataset of the home power consumption.

Sensory data captured from real life settings has been found to be noisy and there are inherent variations in ADLs. Monitoring approaches based on fuzzy logic have addressed noisy sensory data and variations in ADLs since they incorporate fuzzy sets to represent ADL attributes. Existing fuzzy monitoring approaches have been found to be limited as they have focused on using a fixed number of pre-defined fuzzy sets over attributes and detecting abnormalities based of pre-defined fuzzy rules. Fuzzy sets in these approaches do not accurately represent activities of the subject and incorporate outliers in sensor data.

The next chapter presents the methodology of this research which aims to address the abovementioned gaps in the current knowledge.

# CHAPTER 3:
# RESEARCH METHODS

This chapter presents the research methods and phases employed to develop a novel hybrid ADL monitoring approach for the elderly living alone. The chapter is divided into a number of sections. Section 3.1 describes the adopted methodology and Section 3.2 provides the research framework to answer the research questions. Section 3.3 provides an account of the phases of the study and the tasks performed in each phase. Section 3.4 explains metrics used to evaluate the effectiveness of the research framework in this study. Section 3.5 describes the testbed used to collect experimental data, the data collection procedure and the characteristics of the adopted sensors. Section 3.6 reviews the computational intelligence techniques employed in this study. This is followed by an account of the platforms used to implement those techniques and a summary of the chapter in sections 3.7 and 3.8, respectively.

## 3.1 Research methodology

A research methodology is a formulation of techniques for addressing a problem, which involves components such as phases, tasks, and tools (Basili, 1993). Establishing a framework to describe the method for any research is considered to be important. The form taken by a research methodology may either be experimental or analytical. As monitoring ADLs of the elderly is a quantitative domain and the study involved the examination of various computer science techniques, a mixed approach within experimental methodology was adopted for the research. This included the combination of engineering and empirical approaches. The engineering approach is one of the standard approaches used in the research related to monitoring ADLs of the elderly. It involves solving a research problem by iteratively improving on a proposed solution until no further improvement is observed (Easterbrook, Singer, Storey, & Damian, 2008). An empirical approach involves using data from case studies to quantitatively evaluating the improvement of the developed solution (Wohlin, Höst, & Henningsson, 2003).

A description of the steps undertaken for the overall research process is shown in Figure 3.1. The present research was initiated with defining the research objectives and performing an exhaustive study of the related literature to identify problems relevant to the research

objectives. The proposition of a solution to those problems was the next step. This was followed by conducting experiments based on a case study, where a dataset was collected from sensors installed in a testbed, to iteratively refine the developed solutions. The final stage was reporting the findings.

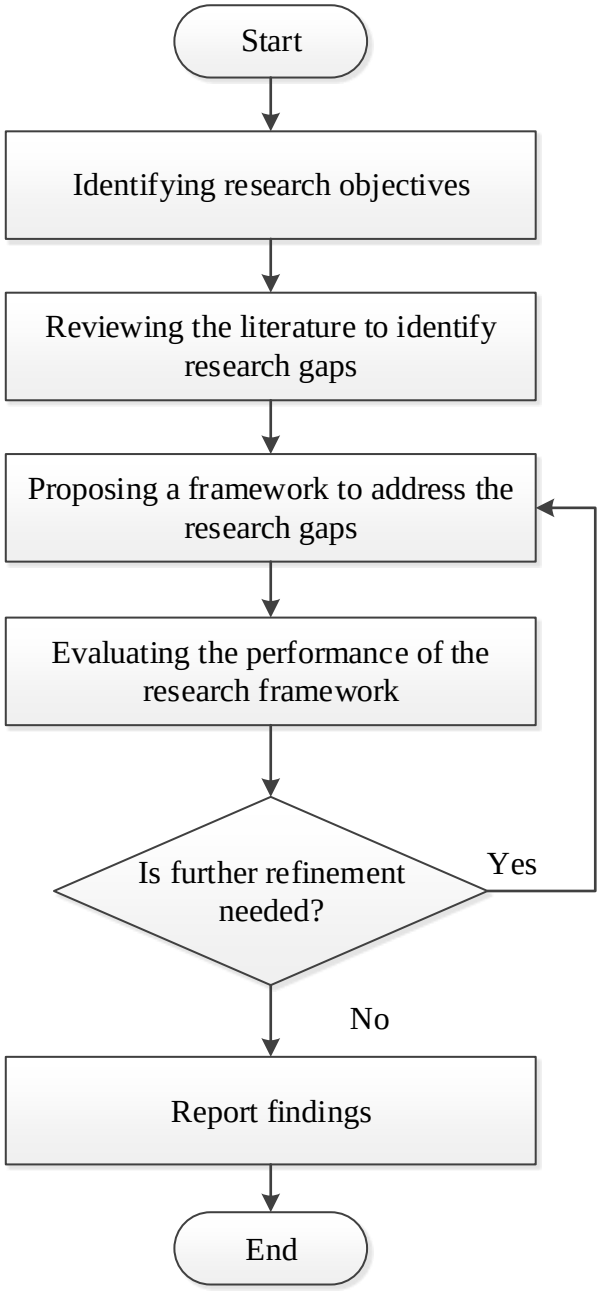


Figure 3.1. The overall research process adopted in this study.

The engineering approach was used in the research process to develop and refine the research solution iteratively until no further improvement on the proposed solution was observed. The empirical approach was used in the research process to evaluate the improvement of the

developed research solution using data from a case study. It was also employed for reporting the significance of the findings.

## 3.2 Research framework

This research has developed a hybrid-monitoring framework to address the research questions and to achieve the overall objectives as outlined in Chapter 1. The framework focused on the use of a combination of Kinect sensors and a single power sensor for the continuous monitoring of an elderly person's physical and instrumental ADLs. Kinect sensors were employed in functional areas of the monitored house to capture the 3D structures of physical activities and the occupant's locations in the room. The power sensor was installed in the power box to measure the power consumption of the house.

The extensive review of the literature in Chapter 2 concluded that monitoring physical and instrumental ADLs requires different aspects of ADLs to be modelled. Differences also occur in the type of output and the time intervals at which the approaches for monitoring physical and instrumental ADLs examine elderly people's behaviour. To address these requirements, the hybrid framework combines two approaches which monitor the occupant's physical and instrumental ADLs based on unlabelled data collected from the sensors. The approach for monitoring physical ADLs is called AMP-ADLs and the approach for monitoring instrumental ADLs is called AMI-ADLs. The AMP-ADLs approach alarms a caregiver through notifying them of abnormal behaviours during physical ADLs while AMI-ADLs generates daily reports showing deviations from the regular routine of instrumental ADLs.

The method adopted to develop each of these monitoring approaches involved three general stages as shown in Figure 3.2. Each stage addressed a sub question of the research and provided the information necessary to undertake the subsequent stage.

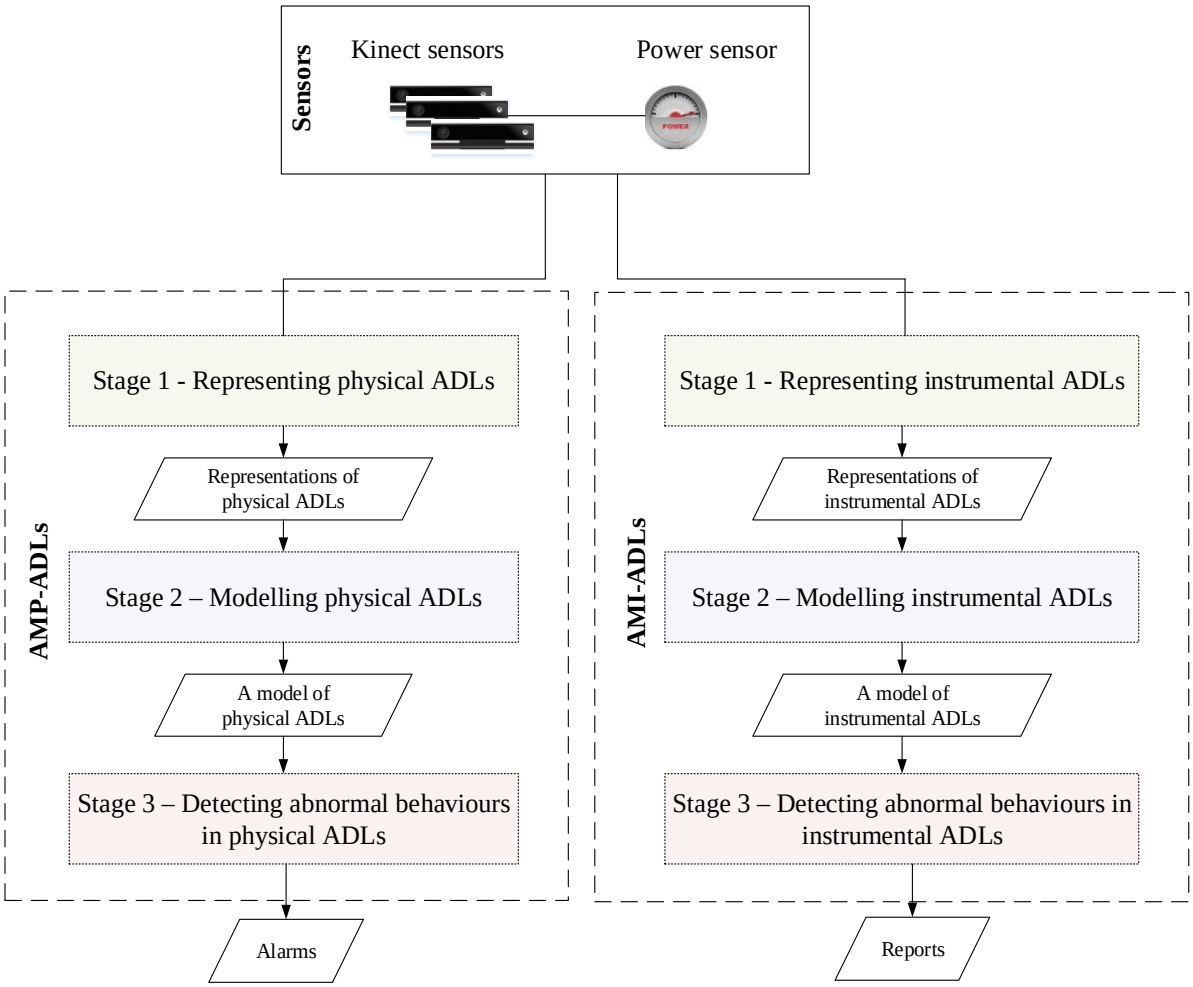


Figure 3.2. The general approach taken for monitoring physical and instrumental ADLs of an elderly person.

The first stage of the two approaches was developed to answer the first research question (i.e. *How can data from multiple sensors (i.e. Kinect sensors and a power meter) be used to represent physical and instrumental ADLs of the monitored elderly person?*). It involved extracting features of the occupant's activities from unlabelled data captured by sensors. Examples of features representing physical ADLs included the occupant's body orientation and their location in the room. Different features were also extracted for monitoring instrumental ADLs. This was achieved by measuring the combination of the composite power consumption of the house and the occupant's locations in order to extract features of regular usage of specific HEAs. The combination of the extracted features in this stage was used to represent the occupant's physical and instrumental ADLs within the house.

The second stage of the monitoring approaches involved developing techniques to model normal behaviour patterns associated with physical and instrumental ADLs. This stage was

developed to attempt to answer the second research question (i.e. *How can techniques be developed that automatically learn from the proposed data representation to generate models of ADLs?*).

The model of physical ADLs included a set of fuzzy rules characterising key attributes of physical ADLs in order to help detect hazardous abnormal events. The model of instrumental ADLs involved a different set of fuzzy rules characterising the regular usage of HEAs. The fuzzy logic was employed to enhance the robustness of the models in regards to capturing fine variations in elderly people's activities (e.g. variations in their posture and the time and duration of activities).

The final stage of the monitoring approaches aimed to answer the third research question; *How can techniques be developed that detect unexpected patterns and abnormal behaviours using the models of ADLs*?

This stage involved development of techniques to analyse and classify new data from ADLs. Unlike many existing approaches, the adopted techniques in this stage did not recognise the exact types of ADLs. This was because ADLs are performed differently in each household due to different room configurations and the occupant's preferences. The similarity of new sensor observations to the developed models of normal behaviour were categorised into abstract labels. The labels associated with monitoring physical ADLs were "normal" and "abnormal" which were obtained based on the similarity of the monitored physical ADLs to their respective model. Abstract labels for monitoring instrumental ADLs included "*low*", "*normal*", "*high*" which were given according to the regularity and frequency of the daily usage of HEAs in comparison with the occupant's normal routine. Deviations from the normal routine inform caregivers of the possibility of a decline in the cognitive ability or general health of the person.

The combination of these three stages was followed to develop the two monitoring approaches in the hybrid framework.

## 3.3 Research Phases

The research was undertaken in five specific phases from data collection to validating the developed techniques. These phases and the relationship between each phase is illustrated in Figure 3.3.

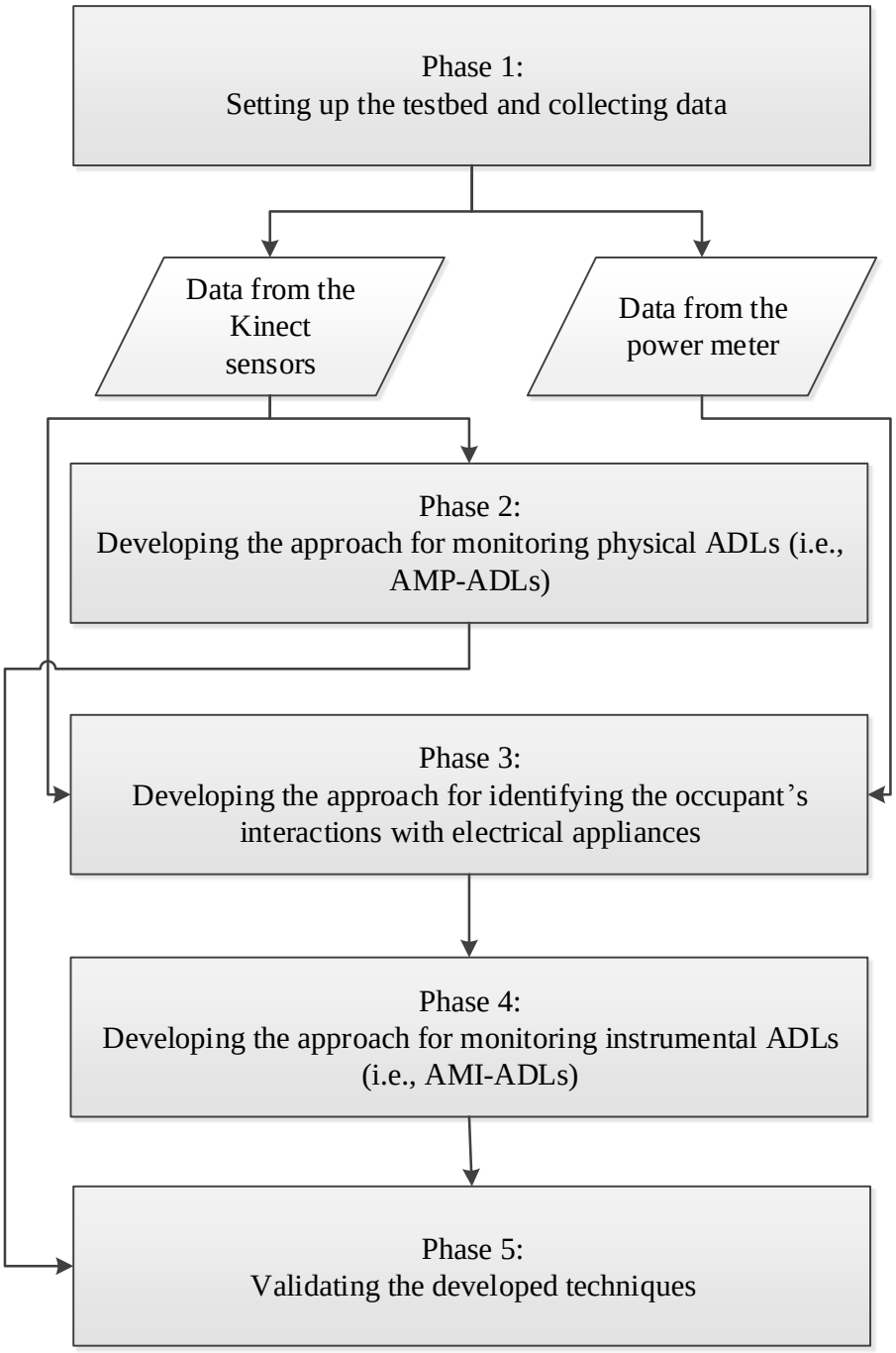


Figure 3.3. Flowchart diagram showing the research phases.

*Phase 1- Setting up a testbed and collecting data:* This phase involved retrofitting sensors in a real-world environment and capturing a dataset. The dataset comprised continuous Kinect observations of the occupant's ADLs and continuous composite power consumption of the house, captured from a power sensor. Section 3.5 provides more details about this phase.

*Phase 2 – Developing an approach for monitoring physical ADLs*. This phase investigated data mining techniques for monitoring different attributes of physical ADLs, including the occupant's posture and the time, duration and location of activities. A prototype unsupervised approach based on fuzzy logic was developed for this monitoring with details presented in Chapter 4. This approach was then improved through a set of modifications as presented in Chapter 5.

*Phase 3 – Developing an approach for identifying the occupant's interactions with HEAs*. This phase investigated a data mining technique which identifies the performance of instrumental ADLs based on the composite power consumption of the house and the occupant's locations. The rationale behind combining these sources of data was to distinguish power signatures on the power line generated as a result of the occupant's interactions from those automatically generated by HEAs (e.g. by self-regulated and thermostatically operating devices including refrigerators or washing machines). It also facilitated the approach to differentiate between the usage of HEAs which have similar power consumption patterns. Details for this approach are presented in Chapter 6.

*Phase 4 – Developing an approach for monitoring instrumental ADLs*. This phase investigated the use of simple features for monitoring key aspects of performing instrumental ADLs from the usage of HEAs. The developed approach generated daily reports showing the elderly person's deviations from their habitual performance of instrumental ADLs. Chapter 7 provides an examination of this approach. An overview of the adopted steps in this monitoring framework is presented in Chapter 8.

*Phase 5 – Validation of the developed techniques*: This phase was used to evaluate the performance of the developed methodology against other alternative techniques using the collected testing dataset of various normal and abnormal behaviour patterns. Each chapter includes a validation of results against other techniques.

## 3.4 Evaluation metrics for the research framework

The problem of monitoring an elderly person's behaviour falls into the category of binary classifications. A binary classification model classifies each recording of the elderly person's behaviours into one of the two classes of normal or abnormal. This gives rise to four possible

classifications for each testing recording, namely true positive (TP, the number of correctly classified recordings of abnormal behaviour), false positive (FP, the number of incorrectly classified recordings of normal behaviour), false negative (FN, the number of incorrectly classified recordings of abnormal behaviour) and true negative (TN, the number of correctly classified recordings of normal behaviour). These categories are shown in Table 3.1.

Table 3.1. Definition of terms used in equations 3.1 and 3.2.

| Abnormal situation / System classification | Occurs | Does not occur |
|---|---|---|
| Abnormal | TP | FP |
| Normal | FN | TN |

The performance of a developed classifier to monitor ADLs of an elderly person was evaluated through calculating its classification accuracy for testing recordings of both normal and abnormal behaviour patterns. These accuracies were defined as below:

$$Accuracy\ for\ normal\ behaviours(\%) = \frac{TP}{TP+FN} \times 100 \qquad (3.1)$$

$$Accuracy\ for\ abnormal\ behaviours(\%) = \frac{TN}{TN + FP} \times 100 \qquad (3.2)$$

## 3.5 The testbed of the study

To the best of the researcher's knowledge, no public dataset exists which supplies a combination of continuous power consumption and Kinect data for ADLs inside a private residence. The research established a testbed to capture such data for developing and validating the approaches presented in this study. The testbed provided a real-life setting for an individual living alone where ADLs of the researcher were captured using sensors set up in a variety of locations. A more detailed description of this testbed is presented below.

### 3.5.1 Specifications of the testbed

The testbed used for capturing the experimental data was a single-bedroom apartment consisting of a living room, a kitchen, a dining room, a bedroom, and a combined toilet and bathroom. The layout of this testbed, the setup of the Kinect sensors, the range of the depth

sensor of each Kinect (i.e. the shaded region in each room), and the location of the important furniture used during ADLs are shown in Figure 3.4.

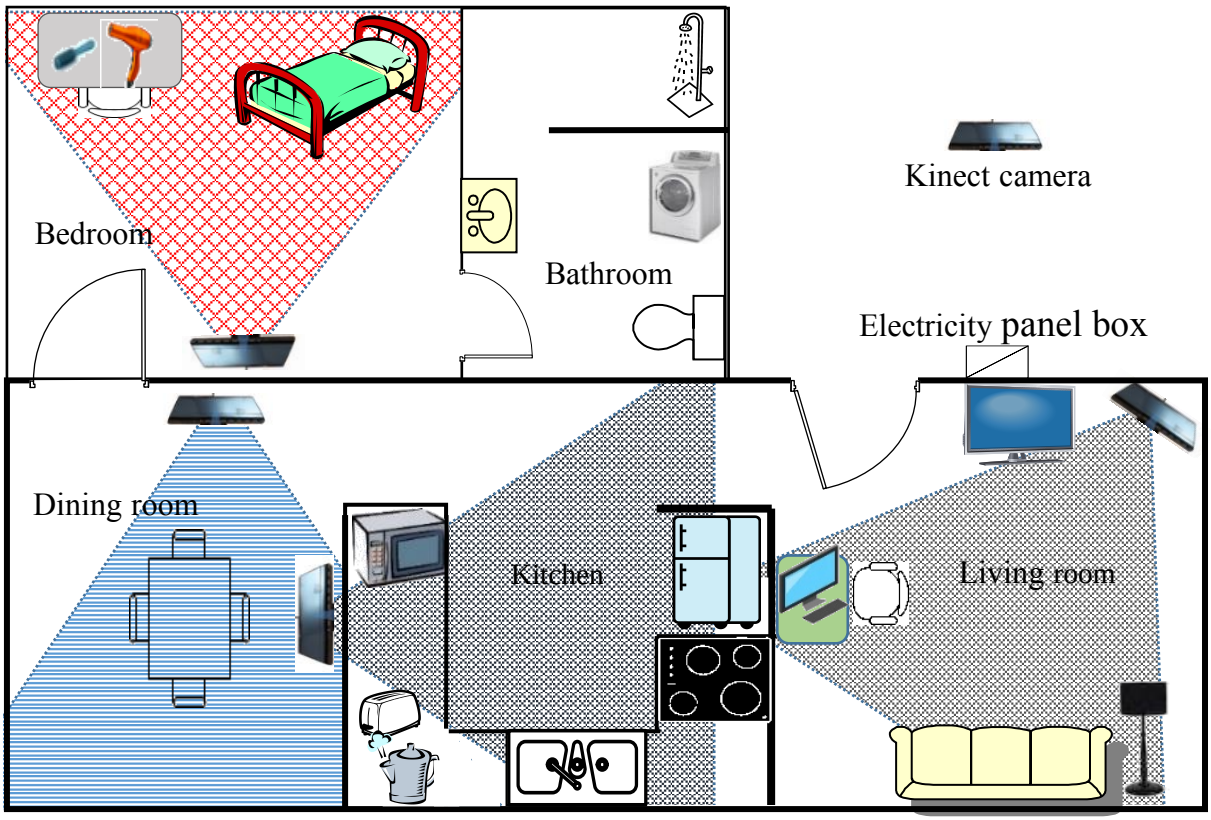


Figure 3.4. Furniture locations and the layout of the testbed.

The Kinect data were captured using four Kinect sensors installed in the kitchen, living room, dining room, and bedroom as shown in Figure 3.4. All sensors were set up to cover the location of furniture used during ADLs except for those in the bathroom. The Kinect sensors were positioned approximately one and half metres from the floor using tripods and had different downward angles to cover as much of the floor plane of the monitored room as possible. The system used for recording these data consisted of four Windows 8.1 notebook computers, with one notebook per Kinect device. Each Kinect was assigned an ID (i.e. the first letter of the corresponding room monitored by the Kinect) to represent the room being monitored by the sensor, as shown in Table 3.2.

Table 3.2. Kinect IDs in the testbed

| ***Location*** | ***Kinect ID*** |
|---|---|
| Living room | L |
| Kitchen | K |
| Dining room | D |
| Bedroom | B |

Figure 3.4 indicates the location of the electricity box external to the home where a power sensor was installed to measure the composite power consumption of the house. Power consumption data were transmitted wirelessly to the notebook computer responsible for recording the living room Kinect data. A list of typical ADL-related HEAs used in the testbed is shown in Table 3.3. This table also shows the location of each appliance. These devices were considered to represent the typical setting of an elderly person's home.

Table 3.3. Monitored HEAs and their locations in the testbed

| ***Appliance*** | ***Location*** | ***Appliance*** | ***Location*** |
|---|---|---|---|
| Washing machine | Bathroom | Computer | Living room |
| Toaster | Kitchen | TV | Living room |
| Refrigerator | Kitchen | Floor lamp | Living room |
| Electric cooktop | Kitchen | Hair dryer | Bedroom |
| Kettle | Kitchen | Microwave | Kitchen |

The furniture in the testbed also included other items frequently used by the occupant during ADLs such as a dining room table, and a living room sofa which was used for taking an afternoon nap, reading, and watching TV.

### 3.5.2 Description of the sensors

The data in this study were captured using a combination of Kinect sensors and a power meter. The following sections describe the technical aspects of each type of sensor.

#### *3.5.2.1 Kinect Sensor*

3D information from the monitored environment was captured by using off-the-shelf and inexpensive Kinect sensors. As mentioned in Chapter 1, Kinect was initially introduced as a motion-sensing device for the Microsoft gaming system Xbox 360 (Kinect, 2013) in order to enable users to interact with the console using their gestures and voice commands. The camera can provide 3D structures of the environment and video images in one instrument.

Microsoft introduced the first generation of Kinect sensors (i.e. Kinect V1) in 2010 (see Figure 3.5). This version emits a specific pattern of infrared light over the camera field of view. The reflection of this pattern is then captured by an infrared sensor and is employed to illustrate the distance between objects in the scene and the sensor via depth maps. Two major problems associated with this technology include interference that can result from using multiple Kinect sensors and the limited field of view of the depth sensor. When the fields of view of two Kinect sensors interfere with each other (i.e. the same area of the room is observed by both depth sensors), the interference of infrared patterns emitted by the two Kinect sensors causes an unreliable estimation of depth by both sensors. Another problem which has been noted is that the field of view is limited to only 58.5 degrees horizontally and 46.6 degrees vertical. This limits the detectable range of a room in which a person can be detected (one to four metres from the sensor).


Figure 3.5. First-generation Kinect sensors.

The Kinect V2 associated with the Xbox One gaming consoles was introduced in 2013 in order to address these limitations (see Figure 3.6). The Kinect V2 hardware contains a 1080p colour camera and a 70-degree horizontal by 60-degree vertical field of view wide-angle depth sensor. The depth sensor comprises an infrared projector and an infrared camera.

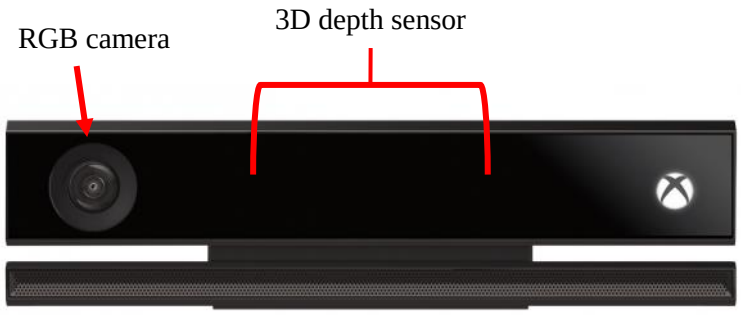


Figure 3.6. Kinect V2 sensor consisting of a depth sensor and a colour camera.

The depth sensor in Kinect V2 is based on Time-Of-Flight technology which emits bursting short infrared lights and captures the reflections of the lights. The delay between the emitted and the received light reflection is calculated to obtain lighting-independent 3D information of the scene (Rob, 2013). The depth maps obtained from Kinect V2 sensors with overlapped fields of view are considered to be reliable (Dal Mutto, Zanuttigh, & Cortelazzo, 2012).

A number of software development tools are available to acquire and process the Kinect sensor data. Kinect for Windows software development kit (SDK) (Kinect for Windows SDK 2.0, 2015) and the OpenNI framework (OpenNI, 2013) are the most popular software tools in this area. Kinect for Windows SDK, which supports many Windows-based programming platforms, involves drivers, tools, APIs, and code samples for developing Kinect-enabled applications. In addition to raw sensor streams, the SDK can provide (Webb & Ashley, 2012):

- 3D coordinates of the detected persons' skeletal joints in a range of [0.5 4.5] metres
- depth map of the scene
- human body segmentation (silhouette) for up to six people
- infrared image of the scene
- colour image of the scene

The skeletal tracking feature of the SDK tracks up to six individuals and provides 3D positions of 25 skeleton joints per tracked person at a frame rate of 30 Hz. The location of each joint in the body along with its ID in the SDK are shown in Figure 3.7. These points form a skeletal representation of the human are provided with an associated state (e.g. tracked, not tracked, or

inferred) indicating the tracking status.

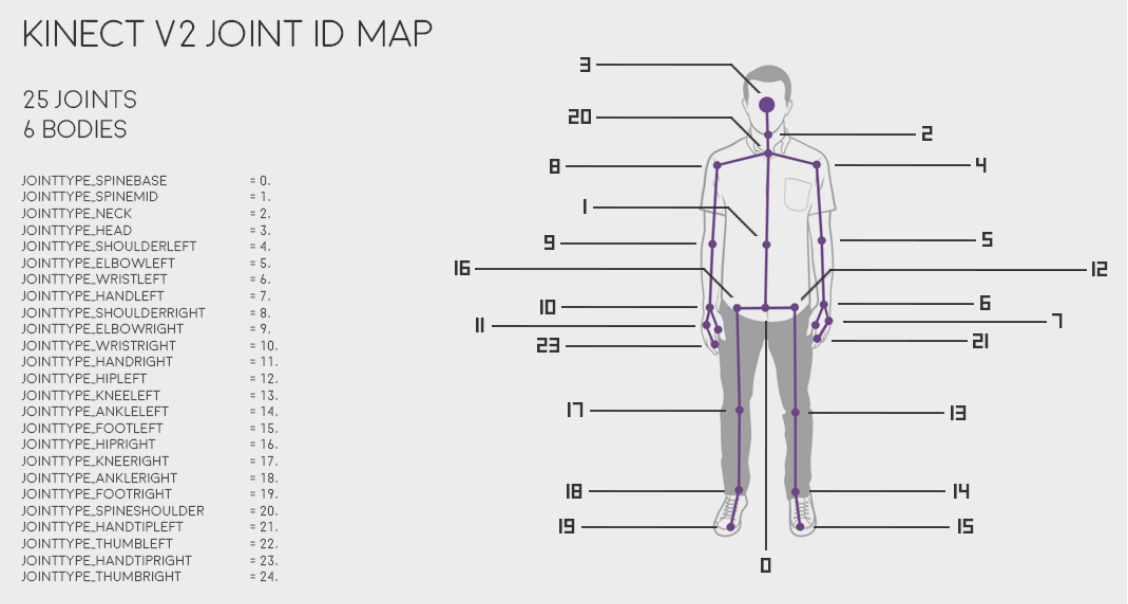


Figure 3.7 Kinect V2 skeletal joint representation (Ashley, 2015).

To represent the 3D coordinates of the skeleton joints, the Kinect sensor uses a Cartesian coordinate system centred at the sensor, as shown in Figure 3.8. The positive *y*-axis extends upward, the positive *z*-axis points along the viewing direction, and the positive *x*-axis extends to the left. The values of joint positions in the x and y axes range from approximately -2.2 to +2.2 and -1.6 to +1.6, respectively. The values of positions in the *z*-axis range from 0.0 to 4.5 indicating the range of tracking in metre. This allows a single Kinect V2 sensor to effectively monitor most of a regular-size room. Person localisation using this type of skeletal tracking method is nonintrusive, in comparison with wearable sensors that the home occupant must remember to put on.

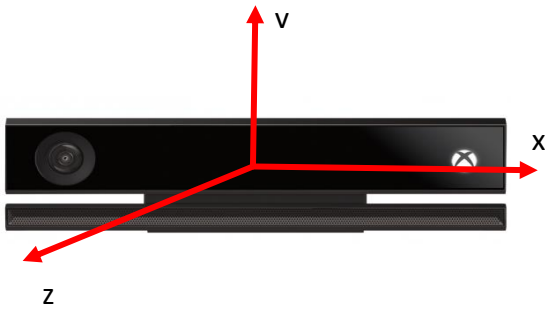


Figure 3.8. *x*, *y*, and *z* coordinates for representing the position of skeleton joints.

The SDK can supply the detected person's silhouette and the depth map of the scene based on the depth maps produced from the sensors data. The Kinect can be used to monitor individuals' ADLs in their home without compromising their privacy as it does not provide a colour image of the scene (Banerjee et al., 2014). The specifications of Kinect V2 are listed in Table 3.4. This version of the Kinect sensor was adopted to capture the 3D structures of activities in the testbed as it was considered to have a number of advantages over Kinect V1.

Table 3.4 Specifications of Kinect V2

| ***Feature*** | ***Specification*** |
|---|---|
| Depth distance | 0.5 - 4.5 metres |
| Depth map | 512 x 424, 30 Hz |
| Colour image | 1920 x 1080, 30 Hz |
| Depth sensor horizontal viewing angle | 70 degrees |
| Depth sensor vertical viewing angle | 60 degrees |
| Minimum latency | 20-60 ms |

#### *3.5.2.2 Power sensors*

Two types of power sensor were used in the testbed. One type was placed in the main electrical panel box to measure the composite power consumption of the house. The other was placed between different HEAs and their respective power outlets to obtain the ground truth of their power consumption. Note that the monitoring approach presented in this study needs the power sensor at the main electricity box to be installed and the second power sensor was deployed for measuring the ground truth and validating results.

**Power sensor installed in the main electrical panel box:** A power sensor called Ranger Power Master 1000 (PM1000F) (Outram Research Ltd., 2014) was installed in the main power box and continuously measured the composite power consumption of the house. The equipment that was included with the sensor was a traditional current clamp (to measure the current signal) and a power plug to measure line to neutral and neutral to earth voltages (see Figure 3.9).

Figure 3.9. The Ranger PM1000F sensor and accessories (Outram Research Ltd., 2014)

The sensor pack includes a software tool which can be installed on a host computer. The software can be used to measure voltage, current and power factor, with a rate of 20 milliseconds to once every 12 hours. The sensor has an associated Bluetooth interface to allow the software to retrieve sensor measurements wirelessly in a range of up to 10 metres from inside the house.

**Power sensor used for individual HEAs:** A Power-Mate 10AHD Serial power sensor (Power-Mate 10AHD Serial, 2016) was selected to measure the consumption characteristics of individual HEAs. It is an easy-to-use device which has a special power plug. The power consumption of a device can be measured by simply unplugging the appliance from the power outlet. The Power-Mate special plug can then be plugged into the outlet and appliance plugged into the rear of the special plug. The Power-Mate 10AHD Serial device is shown in Figure 3.10.


Figure 3.10. Power-Mate 10AHD Serial.

An example of measuring the power consumption of a TV is shown in Figure 3.11. For appliances hardwired to power lines, such as ceiling lights, the rated power consumption obtained from their power consumption label was used.


Figure 3.11. Example of measuring the power consumption of a TV using Power-Mate 10AHD Serial.

The sensor measures specific parameters from the power line and sends information such as voltage, current, and power factor via a built-in serial (RS-232) output to the associated software in a computer. The recording rate in the software can be configured to record at different time intervals from every second to several minutes.

### 3.5.3 The collected dataset

The collected dataset includes a training dataset in which the researcher simulated a daily timeline, including typical activities of an elderly person living alone. The collected dataset also included a number of testing datasets to evaluate the performance of different techniques proposed in this study.

#### *3.5.3.1 The training dataset*

The data in the training dataset were obtained from the combination of power meters (i.e. PM1000F and several Power-Mate 10AHDs) and several Kinect cameras during 30 days. Elderly people living alone tend to have a fixed daily routine of ADLs (Elbert et al., 2011). The researcher simulated a consistent daily routine of ADLs which would help identify subsequent

abnormal behaviours and deviations from the routine. The daily timeline followed to simulate the activities is shown in Table 3.5. The table indicates the location and the HEAs used by the occupant for each activity. The table also shows the type of sensor(s) that could collect data about each activity.

Table 3.5. The timeline followed each day to simulate activities for the training dataset

| ***Time*** | ***Activity*** | ***Location*** | ***Sensors*** | ***Appliances*** |
|---|---|---|---|---|
| 7:00 | Getting up | Bedroom | Kinect | N/A |
| 7:10 | Taking a shower | Bath room | N/A | N/A |
| 7:35 | Grooming | Bedroom | PS - Kinect | H* |
| 7:50 | Preparing breakfast | Kitchen | PS - Kinect | T, K, M, R, E |
| 8:10 | Eating breakfast | Dining room | Kinect | N/A |
| 8:30 | Using the computer | Living room | PS - Kinect | Computer |
| 9:00 | Washing dishes | Kitchen | Kinect | N/A |
| 9:30 | Using a computer | Living room | PS - Kinect | Computer |
| 12:00 | Cooking lunch | Kitchen | PS - Kinect | T, K, M, R, E |
| 12-30 | Eating launch | Dining room | Kinect | N/A |
| 13:00 | Watching TV | Living room | PS - Kinect | TV |
| 14:30 | Taking a nap | Living room or bedroom | Kinect | N/A |
| 15:30 | Making tea | Kitchen | PS - Kinect | K |
| 15:40 | Using the computer | Living room | PS - Kinect | computer, L |
| 18:00 | Cooking dinner | Kitchen | PS - Kinect | T, K, M, R, E |
| 18:40 | Eating dinner | Dining room | Kinect | N/A |
| 19:30 | Watching TV | Living room | PS - Kinect | TV, L |
| 21:30 | Sleeping | Bedroom | Kinect | N/A |

*H= hair dryer, T=toaster, K=kettle, M=microwave, R=refrigerator, E=electric cooktop, L=living room lamp, and PS=power sensor.

The variations in how an individual perform ADLs were simulated during activities shown in Table 3.5. The occupant carried out the activities with variations in their durations, starting

times or actions. The occupant was absent from the home for some periods of time when he left the house for shopping and other activities. The occupant also took afternoon naps in the bedroom or on the sofa in the living room to simulate the real-life variation in the location of ADLs. The occupant varied the activities for different days. For example, on some days the occupant went out in the afternoon while he would usually use the computer at this time of the day. All these variations were represented by the collected training dataset.

Observations were taken from each Kinect, at one-second intervals. Data were collected for each time the occupant was observed. This resulted in more than three million Kinect observations of normal behaviour patterns associated with ADLs. The number of observations captured from each Kinect in the testbed is shown in Table 3.6. It was observed that the occupant spent majority of time in the living room area. Nearly 900,000 observations were captured from kitchen activities while the occupant was preparing a meal or refreshment or cleaning as shown in Table 3.5. Observations taken from the dining room area were in the order of half a million and were mostly related to eating and cleaning activities. Approximately 800,000 observations were collected from the bedroom. This resulted from an average of 7.5 hours sleeping during night, one hour taking occasional afternoon naps, and several minutes on after-shower rituals (e.g. blow-dry).

Table 3.6. Characteristics of Kinect datasets obtained from different monitored locations.

| ***Kinect ID*** | ***Location*** | ***Number of observations*** |
|---|---|---|
| K | Kitchen | 889,445 |
| L | Living room | 1,023,542 |
| D | Dining room | 421,036 |
| B | Bedroom | 785,236 |

The Kinect SDK (Kinect for Windows SDK 2.0, 2015) was deployed to capture data from Kinect sensors. Each stored Kinect observation included a depth map, 3D positions of the occupant's skeleton joints, a binary silhouette mask of the occupant, a timestamp, and a Kinect ID. Some examples of the collected observations are shown in Figure 3.12.

Kinect ID: D, Frame: 2096, Date: 2015-04-21, Time: 16-13-53

(a) (b) (c)

Kinect ID: K, Frame: 45, Date: 2015-04-20, Time: 09-55-46

(d) (e) (f)

Kinect ID: L, Frame: 11012, Date: 2015-04-22, Time:18-33-17

(g) (h) (i)

Kinect ID: B, Frame: 45368, Date: 2015-03-09, Time: 13-18-33

(j) (k) (l)

Figure 3.12 (a) Example of Kinect observations. (a), (d), (g) and (j) show activities of having dinner in the dining room, making breakfast in the kitchen, sitting at a computer desk in the living room, and blow-dry in the bedroom, respectively. (b), (e), (h), and (k) show the respective depth map of the scene and (c), (f), (i), and (l) illustrate the occupant's silhouettes detected by Kinect SDK.

A timestamp consisting of a frame number, date and time of the day was also recorded for each

Kinect observation. The frame number indicates how many other observations have already been captured by the respective Kinect during that day. For example, Kinect ID 'D' and frame number 2096 was taken from the dining room as shown in Figure 3.12 (a). Timestamps were used for synchronising the different sources of data in the dataset.

It should be noted that all attributes associated with the subject's body shape were obtained from depth maps (e.g. part (b) in Figure 3.12) and the respective binary masks of the subject (e.g. part (c) in Figure 3.12). Figure 3.12 provides the colour images to illustrate the scene. Each Kinect observation was associated with a skeleton frame of the occupant. All skeleton frames from a particular Kinect for each day were saved in a separate text file. Each frame included the 3D positions of 25 skeletal joints, in the form of *x*, *y* and *z* coordinates. An example of these coordinates for a skeleton frame in the dataset is shown in Figure 3.13. The name of each joint ID can be found in Figure 3.13. Each skeleton frame had an associated timestamp so it could be synchronised with other types of data (i.e. depth maps, the occupant's silhouettes and power consumption) stored in the dataset. For example, a timestamp might be "12 2015-04-03 10-06-33" which indicates the frame number (12), date (2015-04-03) and time of the observation (10-06-33).

The power consumption of the house was measured at one-second intervals, using PM1000F power meter. This frequency can be achieved by the use of inexpensive power sensors (Marchiori, Hakkarinen, Han, & Earle, 2011) and is adopted based on the assumption that only one appliance is switched on/off between the measurements. The measurements of the power consumption recorded for the dataset are shown in Table 3.7. Active and reactive powers (Arrillaga, Watson, & Chen, 2000) were supplied directly by the power sensor. The sensor uses Equation 3.3 to measure the active power.

$$P = I \times V \times \cos(\Theta) \tag{3.3}$$

$\Theta$ in Equation 3.3 is the angle between voltage ($V$) and current ($I$). Reactive power was calculated through Equation 3.4.

$$Q = I \times V \times \sin(\Theta) \tag{3.4}$$

| Joint ID | *x* | *y* | *z* |
|---|---|---|---|
| 1: | 0.1658834 | 0.042834 | 2.104234 |
| 2: | 0.1309665 | 0.3645723 | 2.041522 |
| 3: | 0.09624073 | 0.6733708 | 1.966303 |
| 4: | 0.0786925 | 0.7788246 | 1.992168 |
| 5: | -0.02559494 | 0.4727924 | 1.914269 |
| 6: | -0.08591931 | 0.2625551 | 2.007757 |
| 7: | -0.1473993 | 0.1488807 | 2.145067 |
| 8: | -0.16559 | 0.08463367 | 2.222207 |
| 9: | 0.2456914 | 0.51015 | 1.894187 |
| 10: | 0.3685612 | 0.313965 | 1.955285 |
| 11: | 0.4142971 | 0.1020837 | 2.049423 |
| 12: | 0.4108421 | 0.03667326 | 2.076071 |
| 13: | 0.1106208 | 0.03405551 | 2.070805 |
| 14: | 0.07956149 | -0.1973553 | 2.155784 |
| 15: | 0.009970853 | -0.2117011 | 2.224953 |
| 16: | 0.07654364 | -0.2475743 | 2.127875 |
| 17: | 0.2152837 | 0.05009888 | 2.063318 |
| 18: | 0.2958736 | 0.1782732 | 2.155258 |
| 19: | 0.3322443 | -0.2530912 | 2.223233 |
| 20: | 0.2867146 | -0.320666 | 2.173521 |
| 21: | 0.1049214 | 0.598042 | 1.987249 |
| 22: | -0.1711686 | 0.03021169 | 2.251483 |
| 23: | -0.158307 | 0.06588595 | 2.189 |
| 24: | 0.4075494 | -0.02902544 | 2.071115 |
| 25: | 0.4354644 | 0.00133979 | 2.039818 |

Figure 3.13. Example of 3D positions of joints composing the skeleton frame.

The combination of date and time was recorded as a timestamp helping to synchronise power consumption measurements with Kinect data.

Table 3.7. Power measurements in the dataset.

| ***Description*** | ***Unit/Format*** |
|---|---|
| Active Power | Watt |
| Reactive Power | var |
| Date | dd/mm/yyyy |
| Time | hh-mm-ss |

The continuous power measurements of each day was stored in a separate text file. An example of measurements obtained on 3/11/2015 is shown in Table 3.8. During the first seven measurements, the consumption of the house was around 100 Watts and 1 var and then it raised

suddenly to around 130 Watts and 1 var at the eighth measurement. Some text files had data missing for different timestamps, resulting in the missing of 1,054 measurements. No two or more consecutive measurements were missed. For each missing measurement, the values of the active and reactive power consumption during the preceding and following measurements were averaged and added to the dataset.

Table 3.8. Example of measurements obtained from the PM1000F power meter.

| ***Active Power*** | ***Reactive Power*** | ***Date*** | ***Time*** |
|---|---|---|---|
| 100.72 | 0.902 | 3/11/2015 | 10-44-34 |
| 100.73 | 0.902 | 3/11/2015 | 10-44-35 |
| 100.73 | 0.902 | 3/11/2015 | 10-44-36 |
| 100.7 | 0.902 | 3/11/2015 | 10-44-37 |
| 100.64 | 0.901 | 3/11/2015 | 10-44-38 |
| 100.79 | 0.901 | 3/11/2015 | 10-44-39 |
| 100.68 | 0.902 | 3/11/2015 | 10-44-40 |
| 127.2 | 0.927 | 3/11/2015 | 10-44-41 |
| 132.3 | 0.939 | 3/11/2015 | 10-44-42 |
| 132.45 | 0.938 | 3/11/2015 | 10-44-43 |

Example diagrams for the aggregated active power signal (cut at 500 Watts) and the reactive power for the operation of HEAs, including a refrigerator, captured during a 24-hour period is displayed in Figure 3.14.

Information about the names of HEAs, the rooms where they were located, and their power consumption ranges was collected in order to capture the ground truth about the power consumption of the house. In order to measure the power consumption range of each individual appliance, the Power-Mate 10AHD Serial was placed between the appliance and its respective power outlet and the appliance was then turned on and off 10 times. The ranges of active and reactive power consumption of the HEAs in the testbed is displayed in Table 3.9.

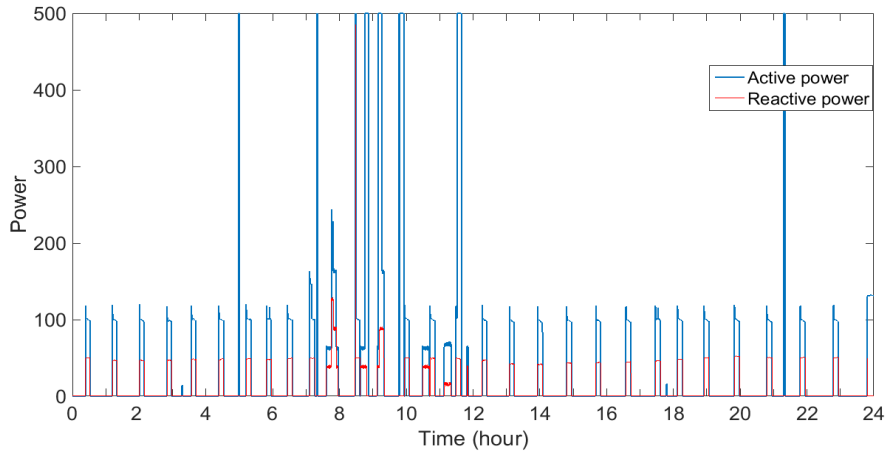


Figure 3.14. An example of active and reactive power signals (cut at 500 Watts) captured during the operation of HEAs including a refrigerator.

Table 3.9. The power consumption of each individual appliance in the testbed.

| ***Appliance*** | ***Active power (Watts)*** | ***Reactive power (var)*** |
|---|---|---|
| TV | 60 ± 5 | 100 ± 8 |
| Computer | 85 ± 7.2 | 60 ±4 |
| Microwave | 1700 ± 64 | 500 ±12 |
| Toaster | 900 ± 40 | 0 |
| Kettle | 1900 ± 62 | 0 |
| Refrigerator compressor | 110 ± 8 | 60 ± 5.5 |
| Refrigerator light | 45 | 0 |
| Living room light | 40 | 0 |
| Electric cooktop | 850 ± 83, 1900 ± 64 | 0 |
| Mobile charger | 9± .5 | 15 ± 1 |
| Washing machine (1) | 15 ± 1.3 | 10 ± 3.9 |
| Washing machine (2) | 250 ± 14 | 220 ± 12 |
| Washing machine (3) | 250 ± 12 | 450 ± 19 |
| Washing machine (4) | 500 ± 39 | 750 ± 15 |
| LED Lights (kitchen, dining room, bathroom, bedroom) | 10 – 15 | 0 |

The researcher logged the time and names of the HEAs interacted with to capture the ground truth of activities. An example of this is provided below:

"The computer 10:12:30 AM, 2015-04-22".

#### *3.5.3.2 The testing datasets*

The performance of the developed approaches for monitoring physical and instrumental ADLs was assessed based on two testing datasets captured from the testbed. *Testing_Data 1* consisted of Kinect recordings representing scenarios of normal and abnormal behaviour patterns during physical activities. For each of the four monitored locations in the testbed, 30 recordings were captured for normal behaviour patterns and 30 for abnormal behaviour patterns (240 in total). Each recording involved one or a combination of the ADLs performed by the occupant in their routine and for normal durations in their respective locations. For example, activities including: sitting behind the computer desk, watching TV and taking a nap on the sofa were performed in the living room. A testing recording for the living room could involve one or a combination of these activities.

Although the same ADL might be carried out multiple times across different test recordings, each instance the ADL was performed with perturbations (including starting time, duration, and the posture of the occupant) in order to simulate real-life variations in ADLs. Other variations in ADLs were also recorded in which the location of the furniture used during ADLs (e.g. dining table, sofa, and computer desk) was slightly modified.

Recordings of abnormal behaviour patterns were captured according to use-cases to test the output of the monitoring system (Guesgen & Marsland, 2010). Software engineers define use-cases as a collection of possible scenarios used to study the behaviour of a system under different inputs and configurations (Wang, Pastore, Goknil, Briand, & Iqbal, 2015). The use-cases were developed to describe scenarios that may happen to the elderly and indicated the expected output of the monitoring system (e.g. raising an alarm). The use-cases for each monitored location described an initial normal behaviour followed by an abnormal behaviour pattern and the expected output of the system. A use-case defined in this study is shown in Figure 3.15 as an example.

**A use-case for the living room**

**Goal**: To detect unusual durations of ADLs

**Initial state**: The occupant is in the living room sitting on the sofa.

**Description**: It is 2 PM and the occupant is watching TV. Then he turns off the TV and lies down on the sofa to take a nap. However, his nap takes 2 hours longer than usual.

**Normal behaviour**: The occupant occasionally has a 1-2-hour nap on the sofa in the afternoon.

**Expected output**: The occupant has a sleeping posture lasting significantly longer than usual duration. This could be because of his deteriorating health. An alarm should be raised to notify a caregiver.

Figure 3.15. An example of the use-cases defined to evaluate the performance of the developed approaches in detecting ADLs that have a considerably long duration.

The *Testing_Data 2* was developed to evaluate the effectiveness of the proposed approach for identifying instrumental ADLs from the usage of HEAs (see Chapter 6); and the proposed approach to detect drifts from habitual performance of instrumental ADLs (see Chapter 7). The dataset included two recordings of continuous data from the combination of power meters (i.e. PM1000F and several Power-Mate 10AHDs) and Kinect cameras. Each recording was made for a duration of nine days (18 days in total) and represented three-day periods of normal routine of instrumental ADLs, slight drifts from this routine and major drifts from it (see Table 3.5). The drifts away from the normal routine were upward (the person performed more instrumental ADLs) in one recording and downward (the person performed less instrumental ADLs) in the other. The ground truth of instrumental ADLs was determined from the recording of the time and name of the HEAs used by the occupant.

## 3.6 Computational intelligence techniques

This section provides a description of the computational techniques and concepts used in the research. The section first describes the fuzzy set theory and fuzzy logic techniques. This is followed by explaining the Plug-in rule and the skewness adjusted boxplot techniques. The section concludes with details on the data mining techniques employed in the research

### 3.6.1 Fuzzy sets

Fuzzy set theory was proposed by Zadeh (1965) and has been utilized to solve many problems including clinical diagnosis (H. Pazhoumand-Dar & Yaghobi, 2010; Sarabadani Tafreshi,

Klamroth-Marganska, Nussbaumer, & Riener, 2015), driving safety monitoring (Wu, Chen, Yeh, & Li, 2013), and data classification (Moeinzadeh, Nasersharif, Rezaee, & Pazhoumand-dar, 2009; Hossein Pazhoumand-dar & Yaghoobi, 2013). The technique allows for computing with words and using linguistic quantifiers such as '*low*' or '*high*'. The degrees of membership of elements in a fuzzy set are allowed to vary in a range of [0 1]. If *U* is the universe of discourse of a variable, then the degree of membership in a fuzzy set *A* defined over *U* is denoted by

$$\forall x \in U, \mu_A(x) \in [0\ 1]$$

where *x* is an element in *U* and $\mu_A(x)$ is the degree of membership of each *x* in *A*. This is different from the classical theory in which the membership of elements is restricted to two values, i.e. $\mu_A(x)$= 1 if $x \in A$ or $\mu_A(x)$=0 if $x \notin A$. Element *x* can belong to more than one fuzzy set in different degrees. The degree of membership to a fuzzy set is typically defined using a membership function (MF); it defines how each point in the universe of discourse of input is mapped to a degree of membership in range of [0 1]. Support of a MF is the part of *U* that is characterized by non-zero degree of membership (Zadeh, 1978). Different types of MFs can be associated with a fuzzy set; the most common types include triangular, trapezoidal, z-shaped and Gaussian, as shown in Figure 3.16 (a), (b), (c), and (d), respectively.

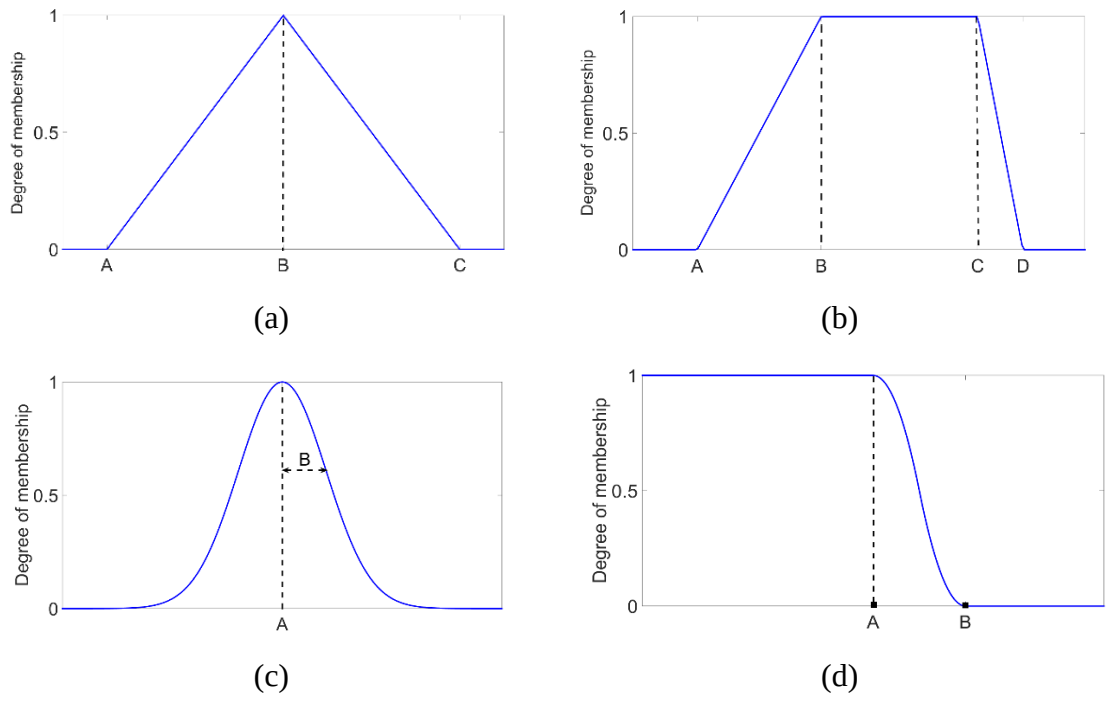


Figure 3.16. Different types of membership functions used in fuzzy set theory; (a) Triangular, (b) trapezoidal, (c) Gaussian, and (d) z-shaped.

As shown in Figure 3.16 (a), the parameters of triangular MFs are defined by a triad $(A, B, C)$, with point *A* representing the left foot of triangular MF, *B* is the location of the center, and *C* is the location of the right foot. A triangular MF is defined using Equation 3.5.

$$\mu_A(x) = \begin{cases} 0 & if\ x \leq A \\ \dfrac{x - A}{\mathrm{B} - \mathrm{C}} & if\ \mathrm{A} < x \leq B \\ \dfrac{\mathrm{C} - x}{\mathrm{C} - \mathrm{B}} & if\ \mathrm{B} < x \leq \mathrm{C} \\ 0 & if\ \mathrm{C} \leq x \end{cases} \tag{3.5}$$

A trapezoidal MF is characterized by four parameters *A, B, C, D* (with $A < B \leq C < D$) as shown in Figure 3.16 (b). These determine the *x* coordinates of the four corners of the underlying trapezoidal defined over the attribute space. Specifically, points *A* and *D* specify the left and right feet. Parameters *B* and *C* specify the shoulders for the trapezoidal. A trapezoidal MF is define using Equation 3.6.

$$\mu_A(x) = \begin{cases} 0 & if\ x \leq \mathrm{A} \\ \dfrac{x - \mathrm{A}}{\mathrm{B} - C} & if\ A < x < \mathrm{B} \\ 1 & if\ B \leq \mathrm{x} \leq \mathrm{C} \\ \dfrac{\mathrm{C} - x}{\mathrm{C} - \mathrm{B}} & if\ \mathrm{C} < x \leq \mathrm{D} \\ 0 & if\ \mathrm{C} \leq x \end{cases} \tag{3.6}$$

A Gaussian MF or a bell-shaped MF is specified according to two parameters A and B, as indicated by Equation 3.7.

$$\mu_A(x) = e^{\frac{-(x-A)^2}{2B^2}} \tag{3.7}$$

In Equation 3.7, parameter *A* represents the mean and parameter *B* is the standard deviation of the Gaussian function - *B* controls the width of the bell.

A z-shaped MF is defined by two parameters *A* and *B*, as shown in Figure 3.16 (d). Equation 3.8 shows how z-shaped MF is defined using these two parameters.

$$\mu_A(x) = \begin{cases} 1, & x \leq A \\ 1 - 2\left(\frac{x-A}{B-\mathrm{A}}\right)^2, & u < x \leq \frac{\mathrm{A+B}}{2} \\ 2\left(\frac{x-\mathrm{B}}{\mathrm{B-A}}\right)^2, & \frac{\mathrm{A}+v}{2} < x \leq \mathrm{B} \\ 0, & \mathrm{B} \leq x \end{cases} \tag{3.8}$$

### 3.6.2 Fuzzy logic

One popular concept associated with fuzzy set theory is fuzzy logic, introduced by Zadeh (1973). A fuzzy inference system (FIS) seeks to map numerical input values onto fuzzy sets and use fuzzy rules to generate numerical outputs; this way a FIS allows flexibility for making decisions under conditions of uncertainty in the data. The most popular fuzzy inference systems are: (1) Sugeno type and (2) Mamdani type. The main difference between these two lies in the way the numerical output is generated.

A Sugeno FIS has no output fuzzy set and it uses a weighted average of rule outputs to compute the crisp output of the system. As there is no intuitive method for determining the numerical output of fuzzy rules, this type of FIS is particularly popular to be used for dynamic non-linear control systems. Fuzzy rules in Mamdani type FIS use linguistic terms in their output to qualitatively describe the system behaviour. As those linguistic terms in rule outputs are associated with MFs, the evaluation of fuzzy rules results in obtaining a combined MF. Defuzzification of this MF is performed to calculate the final crisp output. This intuitive nature of the fuzzy rules makes a Mamdani type FIS interpretable and suitable in particular for decision support applications such as monitoring ADLs.

The research described in this thesis uses Mamdani type FIS and will be referred to it as FIS. The process of a FIS is shown in Figure 3.17. The process involves four main blocks, namely the fuzzifier, the fuzzy rule set, the inference engine, and the defuzzifier. Each of these components are described in detail below.

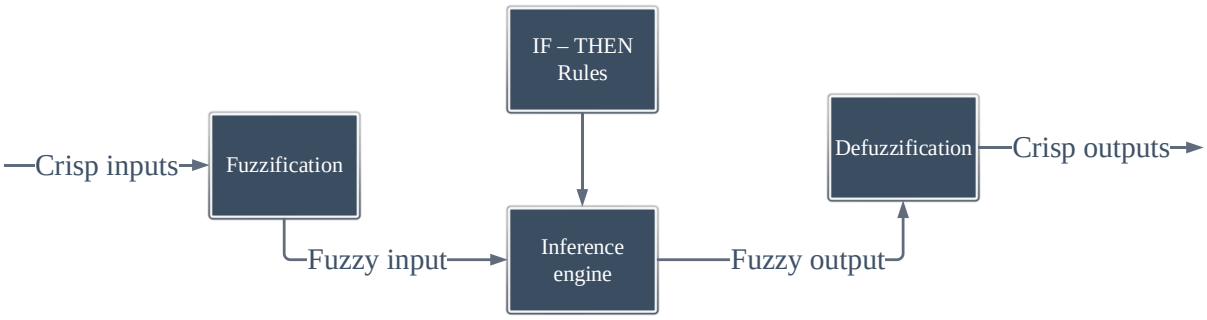


Figure 3.17. The process of fuzzy logic inference (L. Li, Song, & Ou, 2011)

***Fuzzifier***: It constitutes the first step of a FIS process. The role of this block is to map the crisp input data into degrees of membership functions of fuzzy sets defined over the input variables.

***Fuzzy rules***: The rule base structured in a set of fuzzy IF–THEN propositions in the form of 'IF a set of conditions is true, THEN a set of consequences can be true". The IF part and the THEN part of a rule are referred to as the antecedent and the consequent of the rule, respectively. Fuzzy rules can be obtained by using the knowledge of experts or extracted directly from numerical data. A set of IF–THEN rules is consistent if it does not contain contradictory rules.

The antecedent and consequence of rules are comprised of linguistic variables. These variables are described by fuzzy terms. Such rules are in the following form:

$$IF\ x_1\ is\ A_1\ AND\ x_2\ is\ A_2\ \dots\ AND\ x_n\ is\ A_n\ THEN\ y_1\ is\ B_1\ AND\ y_2\ is\ B_2\ \dots\ AND\ y_n\ is\ B_n$$

where $x_1$, …, $x_n$ are the input variables and $A_1$,…, $A_n$ are the fuzzy sets associated with the input variables. $y_1$, …, $y_n$ are the output variables and $B_1$,…, $B_n$ are the fuzzy sets associated with those variables. As observed in the example of fuzzy rule above, statements in both antecedent and consequent of the rules may involve fuzzy logical connectives (e.g. *AND* and *OR*). The conjunction (fuzzy *AND*) and disjunction (fuzzy *OR*) in the antecedent of rules are referred to as T-norm and S-norm, respectively, which aggregates membership functions in the input variable. Assume fuzzy rules have two input variables, $x_1$ and $x_2$, and one output variable $y_1$. Let two fuzzy sets $A_1$ and $A_2$ to be associated with the two input variables in a fuzzy rule. The fuzzy "AND" and "OR" are written as:

$$\mu_{A_1\ AND\ A_2} = T(\mu_{A_1}, \mu_{A_2})$$

$$\mu_{A_1\ OR\ A_2} = S(\mu_{A_1}, \mu_{A_2})$$

where $\mu_{A_1}$ and $\mu_{A_2}$ are MFs associated with $A_1$ and $A_2$, respectively. $T(.,.)$ and $S(.,.)$ are T-norm and S-norm operators, respectively. There are different types of T-norm and S-norm operators. For example, Zadeh's T-norm and S-norm are shown in Equations 3.9, and 3.10. respectively.

$$T(\mu_{A_1}, \mu_{A_2}) = min[\mu_{A_1}, \mu_{A_2}] \tag{3.9}$$

$$S(\mu_{A_1}, \mu_{A_2}) = max[\mu_{A_1}, \mu_{A_2}] \tag{3.10}$$

***Inference engine***: The inference engine operates on fuzzy rules to generate a fuzzy output based on crisp input values. Fuzzifier determines the degrees of membership of numerical inputs in the fuzzy sets associated with input variables. Fuzzy operators (AND and OR) are then used to evaluate the antecedent of all rules. Those rules whose antecedent has a degree of membership with respect to the input are triggered. The next step is rule implication which involves obtaining the membership degree of the fuzzy set in the consequence of the triggered rules with respect to the truth degree specified by their antecedent. There can be defined plenty of implication functions. The most common way is to truncate the MFs in the consequent using the *min* function (known as Mamdani implication). Back to the example of fuzzy rules defined above, the *min* implication function for each rule is calculated as Equation 3.11.

$$\mu_{B_1'(y)} = \min\left(\min\left(\mu_{A_1}(x_1), \mu_{A_2}(x_2)\right), \mu_{B_1}(y_1)\right) \tag{3.11}$$

In Equation 3.11, $\mu_{B_1'(y)}$ is the membership function associated with the rule output, which is derived from truncating $\mu_{B_1}(y)$ with the degree of truth of the antecedent of the triggered rules. Fuzzy outputs of the triggered rules are combined into a single fuzzy set in a process called aggregation. An S-norm operator is typically used to combine these fuzzy outputs. For example, in Mamdani FIS, the fuzzy output of the system is obtained using Equation 3.12.

$$\mu_{out}(y) = \max_{n=1,\ldots,N} \left( \mu_{B_1'}^{n}(y) \right) \tag{3.12}$$

where $\mu_{B_1'}^{n}(y)$ is the membership function associated with the output of *n*-th fuzzy rule and *N* is the total number of fuzzy rules. Upon obtaining $\mu_{out(y)}$, the next step is to use a defuzzifier to convert the fuzzy output of the system into a numerical value.

***Defuzzifier***: There are several defuzzification methods to generate a crisp value from the fuzzy output of a FIS. These include centroid of area, mean of maximum, smallest of maximum and largest of maximum.

The centroid of area defuzzifier calculated the crisp output of the system as the centre of mass in the fuzzy output (see Equation 3.13).

$$\mathrm{y}^{*} = \frac{\iint_{-\infty}^{\infty} \mathrm{y}\, \mu_{\mathrm{out}}(\mathrm{y})\, \mathrm{d_y}}{\iint_{-\infty}^{\infty} \mu_{\mathrm{out}}(\mathrm{y})\, \mathrm{d_y}} \tag{3.13}$$

Intuitively, this defuzzifier finds the point where a vertical line would slice the aggregate output fuzzy set into two equal masses. The mean of maximum defuzzifier is obtained using Equation 3.14

$$\mathrm{y}^{*} = \frac{\sum_{\mathrm{n=1}}^{\mathrm{N}} \mathrm{x_n^{*}}}{\mathrm{N}} \tag{3.14}$$

where $x_n^{*}$ $(i = 1, \ldots, N)$ indicates the maximal values of $\mu_{B_1'}^{n}(y)$ obtained from Equation 3.11. Smallest of maximum and largest of maximum defuzzifier are calculated using Equations 3.15 and 3.16, respectively.

$$\mathrm{y}^{*} = \min_{\mathrm{n=1,\ldots,N}} \mathrm{x_n^{*}} \tag{3.15}$$

$$\mathrm{y}^{*} = \max_{\mathrm{n=1,\ldots,N}} \mathrm{x_n^{*}} \tag{3.16}$$

### 3.6.3 Plug-in rule

The Plug-in rule technique (Sheather & Jones, 1991) provides a data-driven procedure for selecting the bandwidth of kernel function (the degree of smoothing applied to the data) for nonparametric kernel density estimation of data.

Plug-in rule performs the estimation of the PDF of data per different values for the bandwidth of the kernel function and the bandwidth that minimises an error function is selected. The procedure of selecting the bandwidth is as follows.

1. Compute $IQR = Q_3 - Q_1$, where $Q_1$ and $Q_3$ are the first and the third quartiles of the data.
2. Compute $a = 0.92 \times IQR \times n^{-1/7}$ and $b = 0.912 \times IQR \times n^{-1/9}$.
3. Calculate $\hat{T}_D(b) = \frac{1}{-\{n(n-1)\} \times b^7} \sum_{i=1}^{n} \sum_{j=1}^{n} \emptyset^{vi} [\frac{1}{b(x_i - x_j)}]$ where $\emptyset^{vi}$ is the sixth derivative of the normal kernel (Wand & Jones, 1994, p. 177).
4. Calculate $\hat{S}_D(a) = \frac{1}{\{n(n-1)\} \times a^5} \sum_{i=1}^{n} \sum_{j=1}^{n} \emptyset^{iv} [\frac{1}{a(x_i - x_j)}]$ where $\emptyset^{iv}$ is the fourth derivative of the normal kernel.
5. Calculate $\hat{\alpha}_2(h) = 1.357 \times (\frac{\hat{S}_D(a)}{\hat{T}_D(b)})^{1/7} h^{5/7}$.
6. Obtain *h* by solving the following equation:

$$\left[\frac{R(K)}{\{m_2^2(K)\hat{S}_D(\hat{\alpha}_2(h))\}}\right]^{\frac{1}{5}} n^{-\frac{1}{5}} - h = 0$$

where $m_2(K) = \int z_1^2 K(z) dz$ and $R(K) = \int K(z) dz$. For more information, including the technique used to solve the above equation, the reader is referred to Sheather and Jones (1991).

Note that the histograms provided in this thesis were obtained using the plug-in rule technique with the bin size of each histogram equal to the bandwidth calculated from applying the plug-in rule to the respective data.

### 3.6.4 The skewness adjusted boxplot technique

The skewness adjusted boxplot (SAB) technique is a graphical tool (with a robust measure of

skewness) used in robust statistics (RS) for the purpose of outlier detection (Rousseeuw & Hubert, 2011). Given a continuous unimodal data, SAB first calculates a robust measure of skewness of the underlying data distribution called medcouple (MC). It then outputs a normal range for the data, which excludes possible outliers in the data.

If $x_n$ $(n = 1, \dots, N)$ is a univariate data, the MC of the data is calculated as below (Brys, Hubert, & Struyf, 2004):

$$MC = \underset{x_i \le m_n \le x_j}{\text{med}} k(x_i, x_j) \tag{3.17}$$

where for all $x_i \neq x_j$ the kernel function $k$ is given by:

$$k(x_i, x_j) = \frac{(x_j - m_n) - (m_n - x_i)}{x_j - x_i} \tag{3.18}$$

In Equation 3.18, $m_n$ is the median of data points. If $x_i = x_j = m_n$, let $m_1 < \dots < m_s$ be the indices of the data points which are associated with the median $m_n$. The kernel $k$ is then defined as Equation 3.19.

$$k\left(x_{m_i}, x_{m_j}\right) = \begin{cases} +1, & if\ i + j - 1 < s \\ 0, & if\ i + j - 1 = s \\ -1, & if\ i + j - 1 > s \end{cases} \tag{3.19}$$

In case the distribution is skewed to the right, MC gets a positive value up to +1. MC becomes negative (up to -1) in a left-skewed distribution. A symmetric distribution has a zero MC. Once the value of MC is obtained for the data, SAB calculates the normal range (NR) for the data as

$$\text{NR} = \begin{cases} [Q_1 - 1.5\, e^{(-4MC)}\ IQR\ ; Q_3 + 1.5\, e^{(3MC)} IQR] & \text{if } MC \le 0 \\ [Q_1 - 1.5\, e^{(-3MC)}\ IQR\ ; Q_3 + 1.5\, e^{(4MC)} IQR] & \textit{otherwise} \end{cases} \tag{3.20}$$

where $Q_1$ and $Q_3$ are the first and the third quartiles of the data and $IQR = Q_3 - Q_1$. For a left-skewed distribution (with a MC <0), the cut-off interval of the distribution will be the upper range shown in Equation 3.20. The lower range in Equation 3.20 is for right-skewed

distributions having a positive MC. All data points outside the NR range of a distribution are marked as potential outlier.

### 3.6.5 Data mining techniques

Data mining techniques analyse data for discovering useful patterns hidden in large quantities of data (Berry & Linoff, 1997). Various data mining techniques were used in this study for monitoring ADLs of elderly people including mean shift and variable bandwidth mean shift clustering techniques, association rule mining and fuzzy association rule mining. These techniques are discussed in more detail in the following sections.

#### *3.6.5.1 Mean shift clustering*

Mean shift is a general non-parametric clustering procedure which does not rely on the number of clusters having known beforehand (Comaniciu & Meer, 2002). A non-zero radially symmetric kernel is used in this algorithm to estimate the local density of data-points with respect to a specific bandwidth as the radius of the kernel. The location of the kernel centre shifts iteratively to find the local maxima or modes of the underlying data distribution. The output of the algorithm is the location of modes in the data distribution and the cluster of data associated with each mode. Given a univariate dataset of *N* data points $x_i$ $(i = 1, \dots, N)$, a kernel function *K*, and the bandwidth parameter *h*, kernel density estimator for the dataset is obtained using Equation 3.21.

$$\bar{f}(x) = \frac{1}{\mathrm{Nh}} \sum_{\mathrm{i}=1}^{\mathrm{N}} \mathrm{K}\left(\frac{\mathrm{x} - \mathrm{x_i}}{\mathrm{h}}\right) \tag{3.21}$$

where the kernel function is defined as Equation 3.22.

$$K(x) = c_k k(x) \tag{3.22}$$

$c_k$ in Equation 3.22 is a normalization constant to assures $K(x)$ integrates to 1. The gradient of the density estimator $\bar{f}(x)$ is calculated using Equation 3.23.

$$\nabla \hat{f}(x) = \frac{2\, c_k}{Nh^2}\left[\sum_{i=1}^{N} g\left(\frac{x - x_i}{h}\right)^2\right]\left[\frac{\sum_{i=1}^{N} x_i g\left(\frac{x - x_i}{h}\right)^2}{\sum_{i=1}^{N} g\left(\frac{x - x_i}{h}\right)^2} - x\right]$$

(3.23)

$g(x) = -k'(x)$ is the derivative of the kernel profile in Equation 3.23. The second term in Equation 3.23 is called the mean shift vector denoted as $m(x)$.

The mean shift clustering algorithm can be summarised as follow (Comaniciu & Meer, 2002):

1. Choose the location of an unprocessed data as the initial location of the kernel and move mean shift vector represented iteratively till convergence (i.e. $\nabla \hat{f}(x) = 0$).
2. Record the location of kernel at convergence as the location of a mode of density function, and group all data points covered by the kernel, during its successive locations, as the cluster associated with the mode.
3. Repeat step 1 to 2 until no unprocessed data is left.

#### *3.6.5.2 Variable Bandwidth Mean shift clustering*

Variable bandwidth mean shift clustering (VBMS) is a nonparametric clustering technique which does not require the number of clusters to be defined (Comaniciu, Ramesh, and Meer (2001). It estimates the density function of data by taking the average of locally scaled densities that are obtained by applying kernels centred at each of the data points. The output of this technique is location of modes in the data distribution and the cluster of data associated with each mode. Usually the kernel *K* is taken to be a radially symmetric, nonnegative function centred at zero such that $K(x) = k(\|x^2\|)$. Given data points $x_i$ $(i = 1, \ldots, N)$ as input, steps of the VBMS algorithm are as follows:

1. Use the plug-in rule to find an initial bandwidth $h_0$ for the kernel $K(x)$ and estimate the PDF of data using Equation 3.24.

$$\bar{f}(x) = \frac{1}{nh_0}\sum_{i=1}^{N}\left(\frac{x - x_i}{h_0}\right)$$

(3.24)

2. Obtain $\lambda = e^{\frac{1}{N}\sum_{i=1}^{N} \log\ (\bar{f}(x_i)}$

3. Compute the adaptive bandwidth $h(x_i)$ for each data point $x_i$ using Equation 3.25.

$$h(x_i) = h_0[\frac{\lambda}{\bar{f}(x_i)}]^{1/2} \tag{3.25}$$

$h_0$ in Equation 3.25 is a fixed kernel bandwidth obtained from the plug-in rule (in step 1) and λ is a proportionality constant parameter, which divides the range of density values into low and high densities. When the local density for a given data point $x_i$ is low (i.e. $\bar{f}(x_i) < \lambda$), $h(x_i)$ increases relative to $h_0$, implying more smoothing in the estimated density for the point $x_i$. The bandwidth becomes narrower for data points where their estimated density $\bar{f}(x_i)$ is greater than λ.

$$m(x) = \left[\frac{\sum_{i=1}^{N} x_i g\left(\frac{x - x_i}{h}\right)^2}{\sum_{i=1}^{N} g\left(\frac{x - x_i}{h}\right)^2} - x\right] \tag{3.26}$$

where d is the dimension of the data and $g(x) = -k'(x)$

4. Choose the location of an unprocessed data as the initial location of kernel and compute mean shift vector represented in Equation 3.26 iteratively until convergence.
5. Record the location of the kernel at convergence as the location of a mode in the PDF of data and group all data points covered by the kernel, during its successive locations, as the cluster associated with the mode.
6. Repeat step 4 to 5 until no unprocessed data is left.

#### *3.6.5.3 Association rule mining*

Research by Agrawal et al. (1993) presented the problem of mining association rules with the motivation coming from improving sales strategies via analysis of 'market-basket' data. An example of such an association rule may be that 70% of people who purchase item *X* will also purchase product *Y* with some degree of confidence. A formal statement of the problem introduced by Agrawal et al. (1993) is as follows:

Let the set of all binary items to be denoted by $I = \{i_1, \cdots, i_m\}$ and *D* be a transaction database where each transaction *T* is a binary vector containing a set of items such that

$$T(k) = \begin{cases} 1, if\ T\ has\ the\ item\ i_k \\ 0, \qquad\qquad otherwise \end{cases}$$

*X* is satisfied by a transaction *T* if for all items $i_k$ in *X*, $T(k) = 1$. An association rule is an implication of the form $X \rightarrow Y$ where $X \subseteq I$, $Y \subseteq I$ and items in $Y$ are not present in *X*. The rule $X \rightarrow Y$ has a support of *sup* percent, if the fraction of transactions in *D* that contains $X \cup Y$ is at least *sup*. The rule $X \rightarrow Y$ is satisfied in the transaction set *D* with confidence $0 \leq conf \leq 1$ if *conf* percentage of transactions in *D* that contain *X* also contain *Y*. The confidence of a rule $X \rightarrow Y$ can be determined by computing:

$$conf(x \rightarrow y) = \frac{\sup(x \cup y)}{\sup(x)}.$$

The support of a rule specifies the percentage of transactions in *D* that contain both the consequent and antecedent of the rule. The confidence of a rule is the ratio of transactions that contain both the consequent and antecedent of the rule to the total number of transactions that contain only the antecedent of the rule.

The aim of mining association rules is to generate all rules that satisfy user specified thresholds of minimum support and minimum confidence. The following two steps are performed in order to achieve this aim:

Step 1. *Generate all frequent itemsets*: The algorithm generates all combinations of items that have support above a certain threshold *minsupport*.

*Step 2. Generate association rules:* For a given frequent itemset $FI = i_1, \cdots, i_k$ $(k \geq 2)$, the algorithm generates all rules $X \rightarrow Y$ that $X \cup Y = FI$ and the rule confidence is greater than a threshold *minconf*. The antecedent of each of these rules would be a subset $X \subseteq FI$ such that *X* has k-1 items, and the consequent would be items in $FI - X$.

#### *3.6.5.4 Fuzzy association rule mining*

The study by Agrawal et al. (1993) introduced an association rule-mining algorithm for the problem of mining transactional databases that have attributes capable of taking one of a limited and fixed number of items (e.g. the name of a product in a supermarket). This algorithm has some limitations when applied to the problem of monitoring ADLs. ADL monitoring results in datasets that contain numerical attributes obtained from sensors data. The original association rule-mining algorithm proposed by Agrawal et al. (1993) cannot directly be used for datasets of numerical attributes as transformation of the numerical attributes into binary attributes is required.

A study by Kuok, Fu, and Wong (1998) introduced the fuzzy association rule-mining algorithm as one solution to this problem. It integrated fuzzy logic into association rule-mining algorithm where each rule is in the form 'IF *X* is *A* THEN *Y* is *B*'. *X* and *Y* are attributes from the database and *A* and *B* are fuzzy terms characterising *X* and *Y*, respectively. For each transaction database *D* with transactions $T = \{t_1, \cdots, t_M\}$ and a set of numerical attributes $I = \{a_1, \cdots, a_K\}$ assume the value of attribute $a_k$ $(1 \leq k \leq K)$ can be retrieved from the *m*-th transaction using $t_m[a_k]$. Let each attribute $a_k$ to be associated with a set of fuzzy sets $F_{a_k} = \{f_{a_k}^1, \dots, f_{a_k}^J\}$. Each fuzzy set $f_{a_k}^j$ in $F_{a_k}$ represents the *j*-th fuzzy set in $F_{a_k}$ and has an associated linguistic term as well as a membership function $\mu_{f_{a_k}^j}(x)$ such that $\mu_{f_{a_k}^j}(x) : dom(a_k) \rightarrow [0, 1]$. This allows the rules to be mined in the form of:

$$IF\ X\ is\ A\ THEN\ Y\ is\ B$$

where $X = \{x_1, \cdots, x_p\}$ and $Y = \{y_1, \cdots, y_p\}$ are a subset of *A* and $X \cap Y = \emptyset$. $A = \{f_{x_1}, \dots, f_{x_p}\}$ and $B = \{f_{y_1}, \dots, f_{y_p}\}$ are fuzzy sets defined over *X* and *Y*, respectively. Each fuzzy association rule is interpreted as when "*X* is *A*" is satisfied, it can be inferred that "*Y* is *B*" is also satisfied. Kuok et al. (1998) states that the word satisfied here means "*there are sufficient amount of records which contribute their votes to the attribute fuzzy set pairs and the sum of these votes is greater than a user specified threshold*". (Kuok et al., 1998, p. 3).

The support of each rule is a value in range of [0 1]. It is calculated by summing all votes of transactions with respect to the itemset described in the rule which is calculated using Equation

3.27.

$$Supp(X, A) = \frac{\sum_{t_i \in T} \prod_{x_j \in X} \left\{ \alpha_{a_j} t_i [x_j] \right\}}{total(T)} \tag{3.27}$$

In the above equation

$$\alpha_{a_j} t_i [x_j] = \begin{cases} \mu_{f_{x_j \epsilon A}(t_i[x_j]), if\ \mu_{f_{x_j}} \geq \omega} \\ 0, \qquad otherwise \end{cases}.$$

The confidence of a rule is the ratio of transactions that support both the consequent and antecedent of the rule, divided by the total number of transactions that contain only the antecedent of the rule. It is calculated using Equation 3.28

$$\mathrm{Supp}(\langle X, A \rangle, \langle Y, B \rangle) = \frac{\sum_{t_i \in T} \prod_{z_j \in Z} \{ \alpha_{c_k} t_i [z_k] \}}{\sum_{t_i \in T} \prod_{x_j \in X} \{ \alpha_{a_j} t_i [x_j]}$$

(3.28)

where $Z = X \cup Y$, $C = A \cup B$, and $\alpha_{a_j} t_i [x_j]$ is obtained from the following equation.

$$\alpha_{c_k} t_i [z_k] = \begin{cases} \mu_{f_{c_k \epsilon C}(t_i[z_k]), if\ \mu_{f_{c_k}} \geq \omega} \\ 0, \qquad otherwise \end{cases}$$

The same two steps described at the end of Section 3.6.5.3 is followed to generate fuzzy association rules.

## 3.7 Platform

All programming codes developed for the collection of research data were undertaken using C# and the Microsoft .Net framework. Development. Analysis and validation of the techniques were carried out using MATLAB™. The MATLAB (MATrix LABoratory) software is a computing platform that is very flexible and adaptable for visualisation of data via 2D and 3D surface plots, histograms, etc. This platform offers a range of products for implementation of algorithms as it endowed with rich functions for matrix and data manipulation. The integrated fuzzy logic toolbox in MATLAB provides various functions for designing and analysing of systems based on fuzzy logic. This toolbox allows the user to implement rules and specify

parameters associated with a fuzzy inference system to interactively view and analyse the behaviour of the developed system using a graphic user interface.

## 3.8 Summary

This chapter described the research methods used in the research study. Section 3.1 described the research methodology. This was followed by Sections 3.2 which outlined the steps for the research are activity representation, behaviour modelling, and abnormality detection using fuzzy rule based systems. The five phases defined to develop the monitoring framework to answer the research questions were explained in Section 3.3. Section 3.4 discussed the metrics used to evaluate the effectiveness of the developed approaches. Descriptions of the experimental place, deployed sensors, and the collected datasets were also explained in Section 3.5.

Various data mining techniques, such as mean shift, VBMS, association rule mining, and fuzzy association rule mining, were discussed in Section 3.6. This was concluded with a description of the platform used and a summary of the chapter. The next chapter presents an approach for monitoring physical ADLs of an elderly person living alone.

# CHAPTER 4:
# MONITORING PHYSICAL ADLS USING KINECT DEPTH MAPS

This chapter presents an approach, called AMP-ADLs, for monitoring physical ADLs of an elderly person living alone. Stages of this approach are undertaken to answer the research questions regarding monitoring of physical ADLs. The chapter first introduces the problem of monitoring physical ADLs of the elderly through sensor data and briefly reviews limitations of existing approaches (Section 4.1). This is followed by describing the stages of the AMP-ADLs approach in Section 4.2. The experimental results related to the collected dataset are explained in Section 4.3. A discussion of these results followed by a summary of the findings of the chapter are provided in Section 4.4 and Section 4.5, respectively.

## 4.1 Introduction

The aim of many telecare environments is to deploy automatic sensor-based techniques that can monitor the physical wellbeing of their elderly occupants and detect abnormal behaviour patterns and hazardous situations. Abnormality detection in this type of context is particularly challenging as sensor data represent only normal behaviour patterns. It is also challenging as the modelling of multiple types of abnormal situations can be difficult. Monitoring techniques usually involve two phases. The first phase is a training stage in which they model important aspects of normal behaviour patterns that are indicative of the occupant's wellbeing. The second phase is a monitoring stage where the developed model is used to distinguish any abnormalities which do not match the normal profile of the occupant.

Several supervised techniques that can monitor the performance of a limited set of ADLs (e.g. walking and sleeping) have been reported over the last few decades. Training these techniques typically depends on a labelled dataset which can be difficult to acquire. Numerous studies have proposed unsupervised approaches for monitoring physical ADLs in which metrics relevant to assessment of elderly people's wellbeing are automatically monitored based on sensor data (Zerrouki, Harrou, Sun, & Houacine, 2016). Physical independence, mobility, and time orientation are prominent metrics that have been used in these studies. Physical independence can be associated with performing ADLs in a normal duration. Mobility indicates the ability to move in the environment and visit different locations during the day (Fillenbaum,

1984). Time orientation involves functions that show awareness of time and location (i.e. performing ADLs at the right time and location).

Attributes related to ADLs have been extracted from sensor data to measure metrics described above. The choice of attributes depends on the type of sensors used. Attributes describing the occupant's body posture and motion during ADLs have been extracted when the visual data or depth maps of the scene were available. Such attributes help to monitor physical independence and mobility of the person.

The time of ADLs in visual data have also been monitored for an indication of time orientation and independence of the person. For example, the behaviour patterns of walking around at midnight and sleeping for an extended duration in the late morning are considered as abnormal because they suggest deterioration of the elderly person's perception of time and illness (G. C. Franco, Gallay, Berenguer, Mourrain, & Couturier, 2008). Monitoring the duration of behaviour patterns can also help in many situations to judge whether a specific behaviour pattern is abnormal. A normal behaviour of sitting on the kitchen floor for a few seconds for cleaning purposes can be distinguished from a similar activity which lasts for two hours. The longer activity in this example can be associated with undesirable incidents such as fainting.

To model attributes related to ADLs, different techniques such thresholding and statistical measures have been adopted (Noury et al., 2011; Virone, Noury, & Demongeot, 2002). Most of these techniques are unable to accommodate fine variations in real-life ADLs and generate so many false alarms in real-life settings. Several studies have incorporated fuzzy logic into their techniques to achieve this robustness. The parameters associated with fuzzy sets in existing fuzzy approaches are defined experimentally, limiting the applicability of those approaches to various domestic settings and individuals.

This chapter describes an unsupervised and data-driven approach (i.e. AMP-ADLs) based on fuzzy logic to monitor physical ADLs of the elderly using depth maps supplied by Kinect sensors. AMP-ADLs extends upon existing fuzzy based monitoring approaches in the following respects:

- Presenting a data-driven technique to identify epochs of activities for each monitored location. Usually ADLs are associated with locations inside the home and hence each

room is occupied during specific hours of the day. For each monitored location, the day is divided into a number of activity epochs, the duration of which learned from the data. This is in contrast to existing approaches where the day is divided into a number of fixed periods (Martin, Majeed, Lee, & Clarke, 2006; Seki, 2009) and the occupant's ADLs are modelled during each period.

- Presenting a technique to automatically learn the duration of frequent activities from Kinect depth maps. The duration of frequent ADLs carried out in each location usually depends on the nature of the activity. For example, while the activity of watching TV may take one or more hours, making tea is shorter. A technique is presented in this approach to work out the duration of frequent ADLs performed in each monitored location.
- Using a data-driven technique to tune the parameters of membership functions defined over ADL attributes extracted from Kinect depth maps. This is in contrast to existing approach where a set of pre-defined membership functions are assumed for ADL attributes.

## 4.2 The proposed approach

The AMP-ADLs approach in this chapter is comprised of three stages: *representing physical ADLs*, *modelling physical ADLs* and *detecting abnormal behaviours*. The layout of this approach is displayed in Figure 4.1.

The first stage is to represent physical ADLs. It comprises a number of steps. The first step is to collect an unlabelled training dataset of Kinect observations from the occupant's physical ADLs. A set of attributes of the occupant's ADLs is then extracted from Kinect depth maps. Membership functions are defined for each depth map attribute to determine the membership of the attribute values to the linguistically labelled fuzzy sets. Each combination of fuzzy labels for depth map attributes represents a specific body posture of the occupant observed at a specific location. The last step in this stage is *defining fuzzy sets for epochs of activities* for each monitored location, corresponding to usual times where the occupant is active in the location (Section 4.2.1.3). The output of this stage is the fuzzy representations of the occupant's physical ADLs. These representations are in the form of combinations of fuzzy labels for depth map attributes and the time of activities.

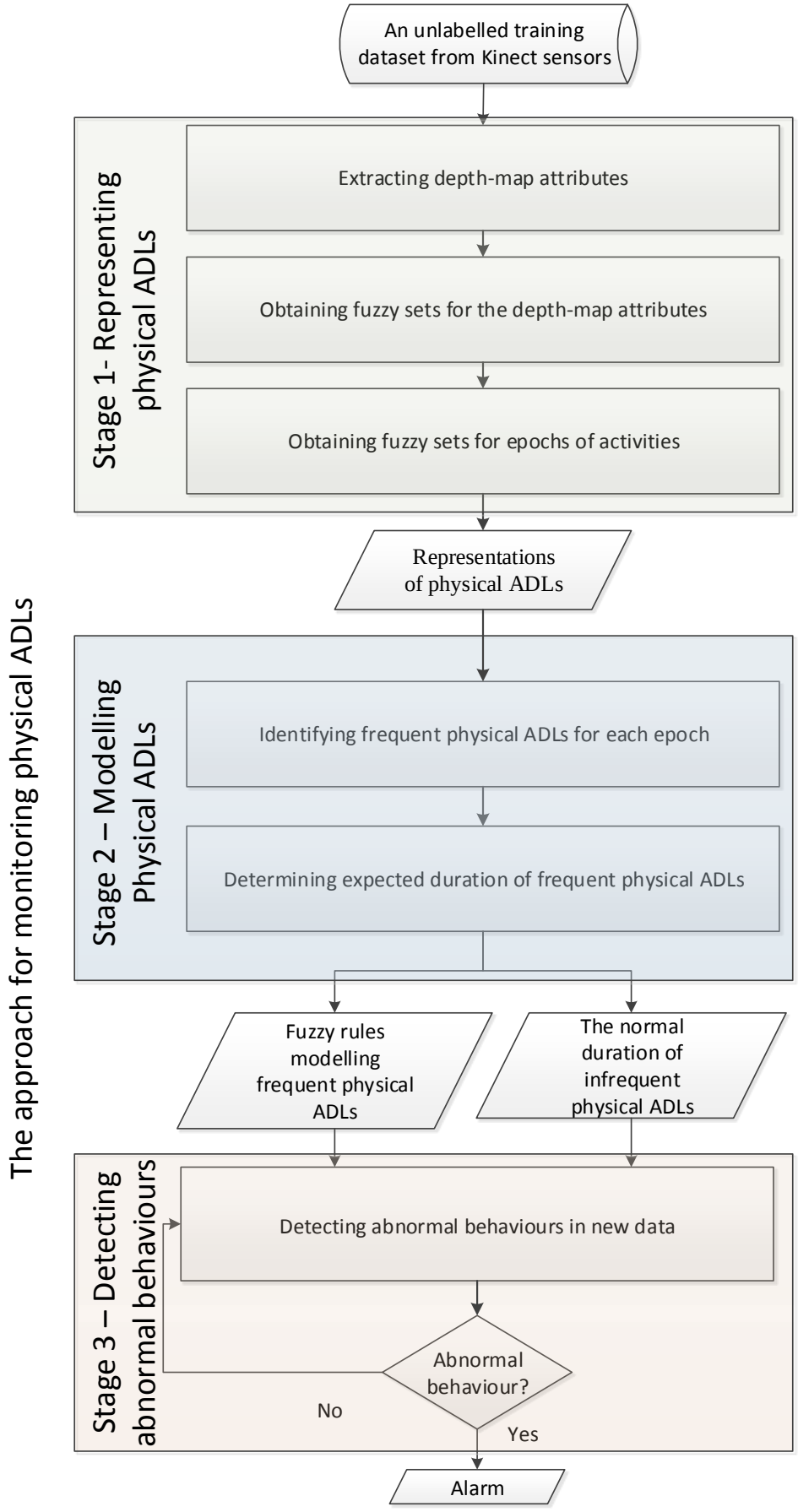


Figure 4.1. An overview of AMP-ADLs.

An example of a physical activity representation is

{*body_orientation* = '*high'*, *body_aspect_ratio*='*high'*, *body_location_x_axis*= '*medium*', *body_location_y_axis*= *medium*, *Time*= '*epoch 2*'}

where *body_orientation, body_aspect_ratio, body_location_x_axis* are depth map attributes and *Time* specifies the time of the activity. '*high'*, '*medium*', and '*epoch 2*' are fuzzy labels.

The second stage of AMP-ADLs automatically generates a model of physical ADLs. It first applies a fuzzy association rule-mining algorithm on the representations of physical ADLs to identify frequent physical ADLs for each epoch. This stage then determines the expected duration of frequent physical ADLs within each epoch. The output of this stage for each monitored location is the duration of infrequent physical ADLs and a set of fuzzy rules that models frequent physical ADLs.

The last stage of AMP-ADLs is to detect unexpected patterns and abnormal behaviours using the model of physical ADLs. It uses the fuzzy rules and information on the normal duration of infrequent ADLs in order to detect abnormal behaviours. The three stages of AMP-ADLs are described in detail in section 4.2.1 to 4.2.3.

### 4.2.1 Stage 1 – Representing physical ADLs

This stage addresses the first research sub-question in monitoring physical ADLs. It takes an unlabelled training dataset of Kinect depth maps to generate fuzzy representations of the occupant's physical ADLs. The training dataset is called $D_{training}$ and includes observations of normal behaviours during physical ADLs from all Kinect sensors in the house. $D_{training}$ is composed of several datasets $d_r$ $(r = 1, \cdots, R)$ each captured by a Kinect sensor. $R$ indicates the number of monitored locations (i.e. the number of Kinect sensors).

This stage involves three steps. The first step extracts a set of attributes from the depth maps in $D_{training}$ (Section 4.2.1.1). The second step defines fuzzy membership functions for each depth map attribute in order to convert the attribute values into fuzzy labels (details in Section 4.2.1.2). Each combination of fuzzy labels for depth map attributes represents a specific body posture of the occupant observed at a specific location. For each monitored location, the last

step determines fuzzy sets characterising epochs of activities (Section 4.2.1.3). These steps are explained below.

#### *4.2.1.1 Extracting depth map attributes*

A large set of attributes has been adopted to describe body postures for the purpose of classification and monitoring physical ADLs. Some of these attributes are intera-frame, describing the posture of the person at each individual frame, while the others are inter-frame. Inter-frame attributes characterise the change of body postures during consecutive frames.

A feature selection procedure was performed to evaluate the effectiveness of different subsets of attributes in characterising physical ADLs. A labelled dataset of Kinect depth maps was collected during an experiment in which various ADLs were performed in the living room area of the testbed and a Kinect sensor captured the activities. Different possible combinations of attributes were then extracted from the Kinect data and an activity classification score was calculated for each combination. The best score was obtained for the subset of $\{AR, \theta, C_X, Cy\}$ with a classification error rate of 6.25%. *AR* is the aspect ratio of the 3D bounding box for the detected person. $\theta$ is the orientation of the body, and $C_x$ and $C_y$ denote the horizontal and vertical coordinates of the silhouette's centre of gravity, respectively. This set of attributes is referred to as the depth map attributes in the remainder of this thesis.

Robust enough to minor variations of postures, the combination of *AR* and $\theta$ can describe the global shape of the subject's body during ADLs while $C_x$ and $C_y$ specify the location of ADLs. Figure 4.2 (a) shows an individual in the living room area of the testbed and Figure 4.2 (b) depicts the bounding box of the person's silhouette (the red rectangle) with the location of the silhouette's centre of gravity shown via the red dot in the bounding box. Details on the calculation of different attributes and the procedure of the performed feature selection are provided in Appendix A. Note that the colour images of the testbed are displayed only to provide a visualisation of the scene and all attributes were obtained from Kinect depth maps.

(a)

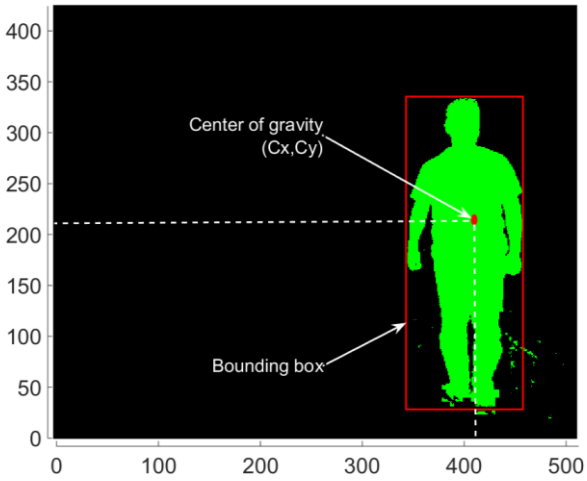


(b)

Figure 4.2. (a) Colour image for a Kinect observation in the living room area of the testbed (b) the bounding box and centre of gravity calculated for the detected person in the scene.

The map attributes $\{AR, \theta, C_x, C_y\}$ denoted as $\{a_k\}$ $(k = 1, \dots, 4)$ are extracted from each Kinect observation in $D_{training}$. This results in obtaining a feature vector in the form of $\{a_1, a_2, a_3, a_4, r, time\_stamp\}$ for each Kinect observation. $r$ indicates the ID of the Kinect sensor that has captured the observation and $time\_stamp$ denotes the time of observation in the form of hh:mm:ss. The example of eight consecutive Kinect observations (the depth map of the scene and the corresponding binary mask of the subject) taken from the kitchen area of the testbed is shown in Figure 4.3. The corresponding feature vectors for these observations are shown in Table 4.1. In this table, $r$ is 2 to indicate that the Kinect sensor in the kitchen has captured the observations.

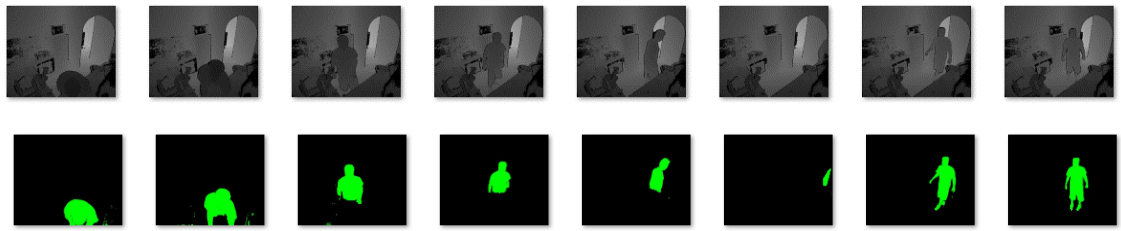

(a) (b) (c) (d) (e) (f) (g) (h)

Figure 4.3 (a) – (h) Example of observations taken by the kitchen Kinect sensor. For each observation, the depth map of the scene and the corresponding binary mask of the subject are shown.

Table 4.1. The depth map attributes extracted from the Kinect observations shown in Figure 4.3.

| ***Observation*** | ***AR*** | ***θ*** | ***Cx*** | ***Cy*** | ***r*** | ***Time_stamp*** |
|---|---|---|---|---|---|---|
| a | 0.7530 | 18.74 | 315.45 | 368.25 | 2 | '10-18-23' |
| b | 0.7530 | 18.50 | 315.27 | 368.07 | 2 | '10-18-24' |
| c | 0.7439 | 18.30 | 314.54 | 367.59 | 2 | '10-18-25' |
| d | 1.1161 | 54.43 | 304.83 | 335.92 | 2 | '10-18-26' |
| e | 1.488 | 78.22 | 249.63 | 238.87 | 2 | '10-18-27' |
| f | 1.4112 | 72.87 | 283.50 | 210.44 | 2 | '10-18-28' |
| g | 1.6530 | 69.58 | 362.93 | 192.80 | 2 | '10-18-29" |
| h | 2.2432 | 70.77 | 484.38 | 203.40 | 2 | '10-18-30' |

#### *4.2.1.2 Obtaining fuzzy sets for the depth map attributes*

The role of this step is to convert the crisp values of the depth map attributes into fuzzy linguistic labels. For example, the value of $\theta$ might be converted into the fuzzy label *'low'* when the occupant lies on the floor. As the range of each depth map attribute varies, the mapping of values to fuzzy labels needs to be determined for each attribute separately.

Let $dom(a_k) = [l_{a_k}, h_{a_k}]$ denote the domain of a depth map attribute $a_k$ across all observations in $D_{training}$. $l_{a_k}$ and $h_{a_k}$ in $dom(a_k)$ are the minimum and maximum values of $a_k$, respectively. A fixed number ($J$) of fuzzy sets are defined over the domain of $a_k$. The set of these fuzzy sets is represented by $F_{a_k} = \{f_{a_k}^1, \ldots, f_{a_k}^J\}$. Each fuzzy set $f_{a_k}^j$ in $F_{a_k}$ represents the $j$-th fuzzy set in $F_{a_k}$ and has an associated linguistic fuzzy label as well as a membership function $\mu_{f_{a_k}^j}(x)$ such that $\mu_{f_{a_k}^j}(x) : dom(a_k) \rightarrow [0, 1]$.

A set of fuzzy labels is associated with the obtained fuzzy sets for each choice of *J*. Different sets of fuzzy labels for *J*=3, 5 and 7 are shown in Table 4.2. For example, when *J*=5, and thus five fuzzy sets are defined over each depth map attribute, the fuzzy labels associated with these fuzzy sets are *Low*, *LowerMedium*, *Medium*, *UpperMedium*, and *High*.

Table 4.2. Fuzzy labels associated with different numbers of fuzzy sets defined for the depth map attributes.

| ***J*** | **Set of linguistic terms** |
|---|---|
| 3 | *{low, medium, high}* |
| 5 | *{Low, LowerMedium, Medium, UpperMedium, High}* |
| 7 | *{very low, Low, LowerMedium, Medium, UpperMedium, High, very high}* |

Triangular MFs are used to represent these fuzzy sets. This is because triangular MFs can be easily calculated and also they show good performance when no information about the distribution of attribute values is available (Pedrycz, 1994). The three parameters that define a triangular MF are learned from the training dataset of each attribute. This involves using the FCM clustering technique to group all values of attribute $a_k$ into *J* clusters. The boundaries of each cluster and the location of the cluster centre are used to determine the cluster membership function parameters.

Let the upper and lower bounds of cluster $j$ $(1 \leq j \leq J)$ that contains data points $C_j = \{p_1, \dots, p_n\}$ to be defined by $u_{C_j} = Max(C_j)$ and $l_{C_j} = Min(C_j)$, respectively. The cluster centre is denoted by $c_{C_j}$. Equation 4.1 is used to define the MF associated with fuzzy set $f_{a_k}^j$.

$$\mu_{f_{a_k}^j}(x) = \begin{cases} 0 & if\ x \leq l_{C_j} \\ \frac{x - l_{C_j}}{c_{C_j} - l_{C_j}} & if\ l_{C_j} < x \leq c_{C_j} \\ \frac{u_{C_j} - x}{u_{C_j} - c_{C_j}} & if\ c_{C_j} < x \leq u_{C_j} \\ 0 & if\ \mathrm{x} < u_{C_j} \end{cases} \tag{4.1}$$

An example of the distribution of $\theta$ for 30 days of observations across four locations in the

testbed is shown in Figure 4.4 (a). The results of determining clustering-based MFs for this attribute ($J$=5) are shown in Figure 4.4 (b).

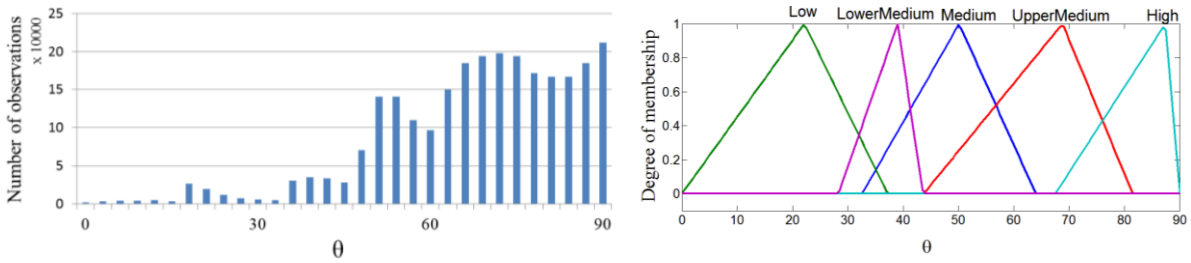


(a) (b)

Figure 4.4. Learning the parameters of triangular MFs; (a) the histogram of $\theta$ for 30 days of Kinect observations and (b) the results of determining five triangular MFs.

The MFs associated with the obtained fuzzy sets are used to convert each attribute's crisp values into their respective fuzzy labels. Table 4.3 shows the results of this conversion for the observations shown in Table 4.1. Note that in this example $J$=5.

Table 4.3. Fuzzy labels of depth map attributes' values shown in Table 4.1.

| ***Observation*** | ***AR*** | ***θ*** | ***Cx*** | ***Cy*** | ***r*** | ***Time_stamp*** |
|---|---|---|---|---|---|---|
| a | *Low* | *Low* | *Medium* | *VeryHigh* | 2 | '10-18-23' |
| b | *Low* | *Low* | *Medium* | *VeryHigh* | 2 | '10-18-24' |
| c | *Low* | *Low* | *Medium* | *VeryHigh* | 2 | '10-18-25' |
| d | *Medium* | *Medium* | *Medium* | *High* | 2 | '10-18-26' |
| e | *Medium* | *High* | *Low* | *Medium* | 2 | '10-18-27' |
| f | *Medium* | *High* | *Low* | *Medium* | 2 | '10-18-28' |
| g | *High* | *High* | *High* | *Low* | 2 | '10-18-29'' |
| h | *High* | *High* | *VeryHigh* | *Medium* | 2 | '10-18-30' |

#### *4.2.1.3 Obtaining fuzzy sets for epochs of activities*

The human behaviour pattern is observed to vary in a cyclical manner over a period of 24 hours, which has been referred to as circadian rhythmic variability (CAV) (Shin et al., 2011). This step performs the following three operations to convert the time of Kinect observations into fuzzy labels according to the occupant's CAV:

1. Identifying epochs of activities performed in each location
2. Defining fuzzy sets for each location to represent the identified epochs
3. Converting the time of training observations into their respective fuzzy labels.

The timestamps of training Kinect observations captured from each location is used to perform the first operation. The behaviour patterns that occur at similar times are grouped using a clustering technique. The result for each monitored location is a set of epochs during which each group of activity is expected to occur. For example, the behaviour patterns during morning, afternoon, evening or night are grouped into different epochs of activities.

The amount of activity for a set of observations from a particular Kinect sensor, $d_r$, and within a particular time period is obtained by counting the number of observations recorded in that period. The time of observations is converted from their original format in the dataset (i.e. hh:mm:ss) to numbers ranging from zero to 24. The minutes in the timestamp of observations are divided by 60, resulting in a decimal number. This is then added to the hour part of the timestamp. For example, 22:45:22 is converted into 22+(45/60) = 22.75. The result of this conversion for location $r$ is a series of crisp values $t_r$ $(0 \leq t \leq 24)$ representing the time of ADLs. The set of these data points constitutes an unknown probability density function $f_r$.

An example of this density function for a living room through the histogram of the data points is shown in Figure 4.5. The number of observations for each bin is determined for 30-minute intervals. As this series is built over a number of days, peaks typically correspond to distinct recurrent activities at a particular time such as watching the nightly news. Each peak in the density function of time of activities can be linked to major epochs in the CAV of the occupant. Since there are variations in the time of activities, each peak is usually associated with a component distribution.

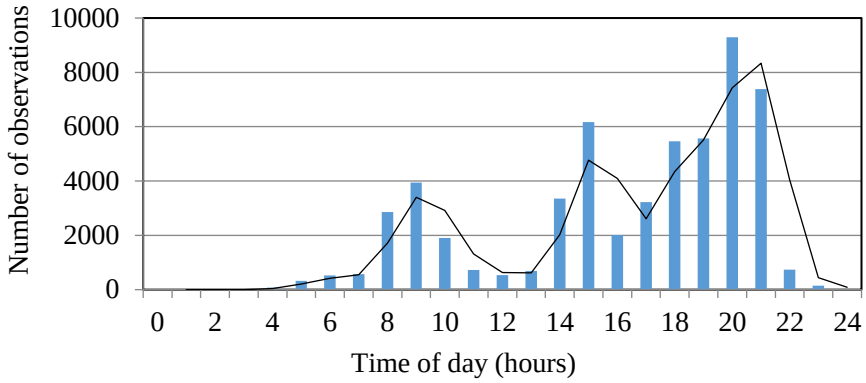


Figure 4.5. An example of hourly count of observations for a living room area during 30 days.

The mean shift clustering algorithm (see Section 3.6.5.1) is used to find modes (local maxima) of $f_r$ representing the epochs of activities. This algorithm provides the locations of modes and the cluster of data associated with each mode. For example, the locations of modes in the data distribution shown in Figure 4.5 are provided to be 9, 15 and 20.

Choice of bandwidth parameter *h* in the mean shift algorithm is considered critical (Comaniciu & Meer, 2002). A large *h* might result in incorrect clustering and merging distinct clusters. A very small *h*, on the opposite, might result in a large number of clusters. In the implementation of the mean shift algorithm *h* is determined using the plug-in rule (see Section 3.6.3).

The location of modes and the cluster of data associated with each mode for a monitored location are used to represent epochs of activities through fuzzy sets. Each detected mode is represented by a fuzzy set and the variation in the cluster of data associated with the mode determines the width of the fuzzy set.

Several studies suggest that the duration of ADLs follows a Gaussian distribution (Rashidi & Cook, 2010; Tang, Yoshihara, Takeda, Botzheim, & Kubota, 2015). This hypothesis is validated by Alam et al. (2011). Each detected mode *i* for a monitored location *r* is therefore modelled by a fuzzy set with a Gaussian MF denoted as $epoch_r^i$. Let $mod_r^i$ and $\sigma_r^i$ be the location of a detected mode and the standard deviation of data points associated with that mode, respectively. The MF to represent $epoch_r^i$ is defined as Equation 4.2.

$$\mu_{epoch_r^i}(x) = e^{\frac{-(x-mod_r^i)^2}{2(\sigma_r^i)^2}} \tag{4.2}$$

Figure 4.6 shows the induced fuzzy sets associated with the epochs of activity shown in Figure 4.5. This figure displays that the CAV of the occupant has three epochs of major activities in the living room. It also shows that the occupant performed more ADLs in this location after 01:00 PM since two different epochs were estimated after this time.

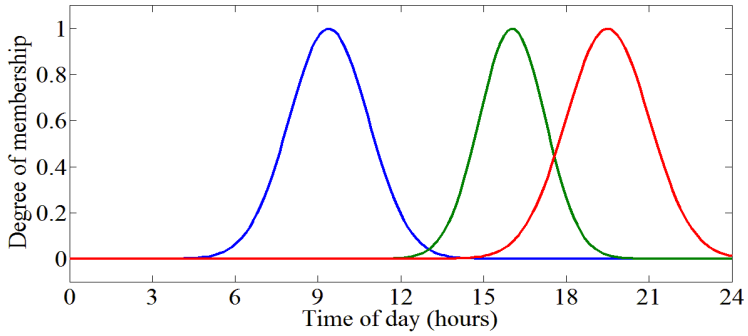


Figure 4.6 An example of Gaussian membership functions for the time of observations in a living room area.

The procedure for determining activity epochs is repeated for each monitored location and a different number of fuzzy sets are obtained for each location, corresponding to the ADLs and their duration in that location.

For each location, the time of observations in the training dataset is then converted into the label of fuzzy set with the highest membership value. For example, the time of observations shown in Table 4.1 is converted into fuzzy labels shown in Table 4.3. Note that it is assumed all these observations belong to the first detected epoch for the kitchen ($r = 2$) and thus, the times of observations were represented by $epoch_2^1$.

The index of location, the combinations of fuzzy labels for the depth map attributes along with the time of activities constitutes representations of the occupant's physical ADLs in the house.

Table 4.4. Replacement of time of fuzzified observations in Table 4.3 with their fuzzy sets.

| *Observation* | *AR* | *θ* | *Cx* | *Cy* | *r* | *Time_stamp* |
|---|---|---|---|---|---|---|
| a | *Low* | *Low* | *Medium* | *VeryHigh* | 2 | $epoch_2^1$ |
| b | *Low* | *Low* | *Medium* | *VeryHigh* | 2 | $epoch_2^1$ |
| c | *Low* | *Low* | *Medium* | *VeryHigh* | 2 | $epoch_2^1$ |
| d | *Medium* | *Medium* | *Medium* | *High* | 2 | $epoch_2^1$ |
| e | *Medium* | *High* | *Low* | *Medium* | 2 | $epoch_2^1$ |
| f | *Medium* | *High* | *Low* | *Medium* | 2 | $epoch_2^1$ |
| g | *High* | *High* | *High* | *Low* | 2 | $epoch_2^1$ |
| h | *High* | *High* | *VeryHigh* | *Medium* | 2 | $epoch_2^1$ |

### 4.2.2 Stage 2 – Modelling physical ADLs

This stage addresses the second research sub-question in monitoring physical ADLs. It uses the fuzzy representations of activities from the previous stage to generate a model of physical ADLs for each location.

The process of this stage first identifies the set of frequent and infrequent physical ADLs in each monitored location and then works out the expected duration of ADLs in each set. A set of fuzzy rules is then generated for each location to model the frequent ADLs. The fuzzy representation of each frequent ADL constitutes the antecedent of the respective fuzzy rule and the expected normal duration of that ADL is characterised as the consequent of the rule.

#### *4.2.2.1 Identifying frequent physical ADLs in each location*

The depth map attributes in Kinect observations belonging to each epoch $epoch_r^i$ associated with location *r* are examined at this step to determine a set of frequent behaviour patterns during physical ADLs. This is carried out using the fuzzy association rule-mining algorithm described in Section 3.6.5. This algorithm examines the co-occurrence of fuzzy labels for the depth map attributes and provides association rules that have levels of support. The combination of fuzzy attributes in each association rule represents a behaviour pattern during physical ADLs. The level of support of each behaviour pattern indicates the proportion of observations in $epoch_r^i$ corresponding to that behaviour pattern.

A threshold value *MinSupp* is adopted to prune the set of generated association rules according

to their levels of support. Each behaviour pattern in the result is considered as a frequent behaviour pattern, indicated as $b_q^{epoch_r^i}$. $q$ indicates the index of frequent behaviour pattern obtained for $epoch_r^i$. These are used to generate a list of frequent behaviour patterns ($FP_{epoch_r^i}$) of the occupant during epoch $epoch_r^i$ associated with location *r*. For example,

$$b_1^{epoch_2^1}: \{AR = 'Low', \theta = 'Low', Cx = 'Medium', Cy = 'VeryHigh'\}$$

and

$$b_2^{epoch_2^1}: \{AR = 'Medium', \theta = 'High', Cx = 'Low', Cy = 'Medium'\}$$

can be respectively the two frequent behaviour patterns of standing in front of the counter and standing in front of the sink in the kitchen (*r*=2) in the first epoch of activity (i.e. $epoch_{d_2}^1$). If only these two frequent behaviours are found for $epoch_2^1$, $FP_{epoch_2^1}$ = { $b_1^{epoch_2^1}$, $b_2^{epoch_2^1}$}. The Kinect observations from each epoch $epoch_r^i$ are then divided into two datasets:

1- $D_{frequent\ behaviours}^{epoch_r^i}$, containing Kinect observations from epoch $epoch_r^i$ that have a combination of attributes corresponding to a frequent behaviour pattern in $FP_{epoch_r^i}$. In the example provided above, $D_{frequent\ behaviours}^{epoch_2^1}$ is composed of observations a, b, c, e, f, and g (see Table 4.4).

2- $D_{infrequent\ behaviours}^{epoch_r^i}$, containing the rest of the observations in $epoch_r^i$. In the example above, $D_{infrequent\ behaviours}^{epoch_2^1}$ is composed of observations d and h (see Table 4.4) as the behaviour patterns in those observations are not correspond to any frequent behaviour pattern in $FP_{epoch_2^1}$.

Note that the body posture and location of individuals are stationary during most ADLs. For example, people usually maintain their location and general posture when sitting on the sofa for watching TV and sleeping in the bed. The observations for those stationary postures therefore comprise the majority of the training dataset and are very likely to be included in $D_{frequent\ behaviours}$.

Behaviour patterns that a monitored occupant performs for only a few times during collecting the training dataset usually share a little portion of the training dataset and they compose $D_{infrequent\ behaviours}$. For example, assume that the occupant usually sits on a sofa in a living room area. During the collection of the training dataset occupant may have also sat on the floor for a few occasions. Observations for sitting on the floor would be classified as infrequent behaviour and compose $D_{infrequent\ behaviours}$. Some other behaviour patterns that were short might be also included in $D_{infrequent\ behaviours}$. For example, assume that the occupant spends most of their time sitting on a sofa in the living room area and spends few seconds each time for walking around in this area. Observations for walking around in the living room would be classified as infrequent behaviour.

These datasets are used in the next step to determine the expected durations of both behaviour classes (i.e. frequent and infrequent ADLs). The system uses the results to monitor the duration of frequent behaviour patterns (e.g. sleeping in bed). This also allows the occupant to repeat the same infrequent behaviour patterns (e.g. sitting on the floor in the living room area) for a similar duration without the system raising alarms.

#### *4.2.2.2 Determining expected duration of physical ADLs*

Fuzzy sets are defined in this step to model the expected duration of frequent behaviours associated with an epoch of activity. Fuzzy rules are then generated based on the results to model frequent physical ADLs of the occupant. The duration of infrequent physical ADLs in each monitored location is also identified.

From Stage 1 epochs of activities are determined for each monitored location. Assume that $FP_{epoch_r^i}$ holds frequent behaviour patterns associated with $epoch_r^i$. The following two steps are performed to model the expected duration of frequent behaviours associated with this epoch.

1. Sequences of consecutive observations that correspond to each frequent behaviour pattern $b_q^{epoch_r^i}$ in $FP_{epoch_r^i}$ are found in $D_{frequent\ behaviours}^{epoch_r^i}$. This is done by sorting observations in $D_{frequent\ behaviours}^{epoch_r^i}$ according to their original timestamp and then putting all consecutive observations which have the same fuzzy attributes as $b_q^{epoch_r^i}$

into a sequence $Seq_q^{epoch_r^i}$. Each frequent behaviour pattern $b_q^{epoch_r^i}$ in $FP_{epoch_r^i}$ would be related to a set of sequences shown as

$$Behaviour_q^{epoch_r^i} = \left\{\text{Seq}(1)_q^{epoch_r^i}, \ldots, \text{Seq(y)}_q^{epoch_r^i}\right\}.$$

2. The mean and standard deviation of durations of sequences in $Behaviour_q^{epoch_r^i}$ are calculated as $m_q^{epoch_r^i}$ and $\sigma_q^{epoch_r^i}$, respectively. Using these two values the fuzzy set $Duration_q^{epoch_r^i}$ is defined over the time domain to model the duration of behaviour pattern $b_q^{epoch_r^i}$. A z-shaped membership function (Berkan & Trubatch, 1997) is associated with this fuzzy set with two parameters $u = (m_q^{epoch_r^i})$ and $v = (m_q^{epoch_r^i} + 3\sigma_q^{epoch_r^i})$ to characterise its break points (see Equation 4.3).

$$\mu_{Duration_q^{epoch_r^i}}(x) = \begin{cases} 1, & x \leq u \\ 1 - 2\left(\frac{x-u}{v-u}\right)^2, & u < x \leq \frac{u+v}{2} \\ 2\left(\frac{x-v}{v-u}\right)^2, & \frac{u+v}{2} < x \leq v \\ 0, & v \leq x \end{cases} \tag{4.3}$$

An example of a z-shaped MF with $u = 800$ and $v$=2450 is shown in Figure 4.7. The output of the function is 1 for durations less than $u$. For those longer than $u$ the function slopes down to its extreme point (i.e. 2450) where its output becomes zero. This means that the MF does not support a behaviour pattern that lasts longer than 2450 seconds.

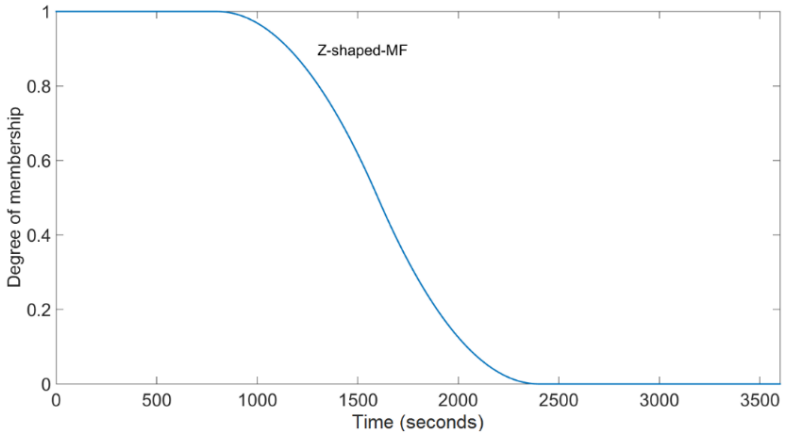


Figure 4.7. An example of a z-shaped MF with u = 800 and v=2450.

The above two steps are repeated to obtain fuzzy sets that model the duration of all frequent behaviour patterns during physical ADLs. A fuzzy rule base is then generated to model the frequent behaviour patterns. Each rule describes a frequent behaviour pattern in its antecedent and has the duration of that behaviour pattern in its consequent. Table 4.5 shows an example where each fuzzy rule is in the form of:

"IF *Location* is $r$ AND *Time* is $epoch_r^i$ AND $AR$ is $A_1$ AND $\theta$ is $A_2$ AND $Cx$ is $A_3$ AND $Cy$ is $A_4$ THEN *Duration* is $Duration_q^{epoch_r^i}$"

Here $A_1$, $A_2$, $A_3$, and $A_4$ are fuzzy sets of the depth map attributes defining a frequent behaviour pattern. $Duration_q^{epoch_r^i}$ is the fuzzy set describing the expected duration of the behaviour pattern. $r$ is the ID of a particular Kinect camera and $epoch_r^i$ is the fuzzy set for the $i$-th epoch of activities for location $r$. The rule base in Table 4.5 can be segmented based on the number of monitored locations and the number of detected epochs of activities for each location. Assume that there are four monitored locations with each location having three epochs of activities and for each epoch five frequent behaviour patterns are detected. The number of fuzzy rules in this case is:

*Number of fuzzy rules= locations × number of epochs × number of frequent behaviours=60.*

Table 4.5. An example of fuzzy rule set obtained from the training phase.

| | | | ***Antecedent*** | | | | ***Consequent*** |
|---|---|---|---|---|---|---|---|
| ***Index*** | ***r*** | ***Time*** | ***AR*** | ***θ*** | ***Cx*** | ***Cy*** | ***Duration*** |
| $rule_1$ | 1 | $T_{d_1}^1$ | *medium* | *high* | *low* | *low* | $Duration_2^{epoch_{d_1}^1}$ |
| $rule_2$ | 1 | $T_{d_1}^2$ | *high* | *high* | *medium* | *high* | $Duration_1^{epoch_{d_1}^2}$ |
| $rule_3$ | 2 | $T_{d_2}^1$ | *high* | *high* | *medium* | *high* | $Duration_1^{epoch_{d_2}^1}$ |
| $rule_4$ | 3 | $T_{d_3}^1$ | *medium* | *medium* | *high* | *medium* | $Duration_2^{epoch_{d_3}^1}$ |
| ⋮ | ⋮ | ⋮ | ⋮ | ⋮ | ⋮ | ⋮ | ⋮ |

This step also determines the maximum duration of infrequent behaviours in each monitored location. This duration for a monitored location $r$ is called $EA_r$ and is estimated based on

processing all $D_{infrequent\ behaviours}$ obtained for that location. Sequences of consecutive observations in $D_{infrequent\ behaviours}$ associated with all epochs of activities are obtained and three standard deviations of their lengths is regarded as the value of $EA_r$. For example, assume that there are only three sequences of infrequent behaviours identified for a kitchen area ($r$=2) and the durations of these sequences are 240, 100, and 50 seconds. $EA_2$ in this case would be 294 seconds.

### 4.2.3 Stage 3 – Detecting abnormal behaviours

This stage is devised to address the third research sub-question in monitoring physical ADLs. An algorithm is developed to detect abnormal behaviours in physical ADLs based on the set of fuzzy rules and the duration of infrequent ADLs that are obtained for each monitored location.

This algorithm calculates the depth map attributes from the occupant's activity in each new Kinect observation. The activity is represented by the ID of the Kinect sensor and the combination of fuzzy labels representing the time of activity and the depth map attributes. If this combination corresponds to a frequent activity represented by the antecedent of a fuzzy rule associated with the same Kinect ID, the duration of the activity during consecutive observations is calculated and evaluated against the consequent of that fuzzy rule. An alarm is raised when the duration of the activity no longer matches to the consequent part of the rule.

If no fuzzy rule can be matched to the activity in the observation, the system monitors the duration of the activity for a specific amount of time before raising an alarm. During that time if the occupant performs a frequent activity, the system starts monitoring the new frequent activity. This avoids generating false alarms for occasional abnormal postures lasting for few seconds (such as bending to fasten the shoe ties).

Steps of this algorithm are shown in Figure 4.8. *NormalDuration* is to indicate the duration of a currently ongoing frequent behaviour pattern. *AbnormalDuration* holds the duration of an ongoing behaviour which is not in the list of frequent behaviours (i.e. it is either an infrequent or an abnormal behaviour).

**The Algorithm for Monitoring Physical ADLs Based on Kinect Depth Maps**
**Input:** fuzzy rules and $EA_r$ for all locations ($r = 1, \dots, R$)
**Output:** an alarm to notify a caregiver

---

1. $NormalDuration = 0$;
2. $AbnormalDuration = 0$;
3. $CurrentBehaviour = 0$;
4. while (True)
5. | if (new observation)
6. | | obtain $O_m$
7. | | compute *QueryBehaviour* using Equation 4.5
8. | | if ($QueryBehaviour$)
9. | | | $AbnormalDuration = 0$
10. | | | if ($CurrentBehaviour == QueryBehaviour$)
11. | | | | $NormalDuration\ ++$;
12. | | | | if $\mu_{Duration_q^{epoch_r^i}}(NormalDuration) == 0$
13. | | | | | trigger Alarm
14. | | | | end if
15. | | | else
16. | | | | $CurrentBehaviour = QueryBehaviour$;
17. | | | | $NormalDuration = 1$;
18. | | | end if
19. | | else
20. | | | $AbnormalDuration++$;
21. | | | $NormalDuration = 0$;
22. | | | if AbnormalDuration $> EA_r$
23. | | | | trigger Alarm
24. | | | end if
25. | | end if
26. | end if
27. end while

Figure 4.8. The algorithm for monitoring physical ADLs in the monitoring phase.

Line 6 extracts attributes from a query Kinect observation. These attributes are shown as $O_m = \{o_m^1, o_m^2, o_m^3, o_m^4, o_m^5, o_m^6\}$. $o_m^1$ is the ID of the Kinect sensor and $o_m^2$ is the time of observation. Components $o_m^3, o_m^4, o_m^5$, and, $o_m^6$ are the values of *AR*, $\theta$, $C_x$ and $C_y$, respectively. Line 7 evaluates $O_m$ against the fuzzy rule set to see whether the occupant's activity in the query Kinect observation corresponds to a frequent activity. This is done using a fuzzy concept called firing strength (Kukolj, 2002). The firing strength of a rule is the degree of satisfaction of the antecedent of the rule by the elements of $O_m$. Let $V = \{v_1, v_2, v_3, v_4, v_5, v_6\}$ be the set of variables in the antecedent of rule $rule_p$ and $A = \{f_1, f_2, f_3, f_4, f_5, f_6\}$ be the fuzzy sets associated with those variables. Also let $\{\mu_{f_1}, \mu_{f_2}, \mu_{f_3}, \mu_{f_4}, \mu_{f_5}, \mu_{f_6}\}$ be the set of membership

functions of A such that $\mu_{f_w}$ $(w = 1, \cdots, 6)$ represents the membership function of $f_w$. The following formula is used to calculate the firing strength of $rule_p$ with respect to $O_m$.

$$f_{<O_m, rule_p>} = \prod_{w=1}^{6} \mu_{f_w}(o_m^w) \tag{4.4}$$

where $\prod$ is the standard fuzzy intersection operator defined as

$$\prod(\mu_{f_1}, \cdots, \mu_{f_n}) = \min\{\mu_{f_1}, \cdots, \mu_{f_n}\}.$$

The best match to $O_m$ is given by the rule with the maximum firing strength (see Equation 4.5). The index of that rule is recorded in $Query\_behaviour$ to indicate which frequent behaviour pattern is observed in the query Kinect observation.

$$QueryBehaviour = \arg\max_{1 \le p \le P} f_{<O_m, rule_p>} \tag{4.5}$$

Line 8 in Figure 4.8 checks if $QueryBehaviour$ is not zero. This implies that the query Kinect observation has matched a frequent behaviour pattern and thereby $QueryBehaviour$ is holding the index of the respective rule. If $QueryBehaviour$ is not zero, Line 10 checked whether the behaviour of $Query\_behaviour$ has also been observed in the previous observation. If yes, the duration of the ongoing identical (matched) behaviour, defined as $NormalDuration,$ is incremented and evaluated against the consequent of the fuzzy rule indexed as $QueryBehaviour$ $(i.e., rule_{QueryBehaviour})$.

Equation 4.3 models the duration of a behaviour up to three standard deviations from the mean value of the duration of its training samples. When *NormalDuration* is no longer satisfying the consequent of $rule_{QueryBehaviour}$, the approach is at the 99% confidence interval that the duration of the ongoing behaviour no longer belongs to the behaviour modelled by the rule. An alarm is raised in this case (Line 13). If $QueryBehaviour$ has a new value corresponding to a frequent behaviour pattern, this new value is assigned to *CurrentBehaviour* (Line 16) and *NormalDuration* is then re-initialised to 1 (Line 17). The algorithm in this case starts monitoring the duration of the new behaviour pattern.

If $O_m$ cannot be matched to any rules in the fuzzy rule set, it means that the observed behaviour pattern of the occupant either corresponds to one of the infrequent behaviours or belongs to an abnormal situation (e.g. falling on the floor). If this condition persists during consequent observations, the system keeps incrementing $AbnormalDuration$ while monitoring the scene. An alarm is raised when this variable reaches $EA_r$(line 23).

The Kinect SDK estimates the number of individuals detected in the room. This feature is used to stop monitoring when more than one person is in the room. This indicates that observations during occasions that other people were present in the room are not classified.

## 4.3 Experimental results

No public dataset was known to be available to provide continuous Kinect data for ADLs inside a residential home. The collected dataset from the testbed was used to test the effectiveness of the AMP-ADLs approach. It included a training dataset of continuous Kinect observations for the activities carried out over 30 days to simulate ADLs of an elderly occupant living alone. It also had a testing dataset. This dataset, which is called *Testing_Data 1*, involved several recordings of scenarios for normal and abnormal behaviours.

The results of applying the techniques associated with stages 1 and 2 on the training dataset are presented through Section 4.3.1 to Section 4.3.4. These sections also demonstrate the impact of the number of fuzzy sets defined over the depth map attributes on the characteristics of fuzzy rules and values of $EA_r$. Section 4.3.5 describes the results of evaluating the performance of the monitoring approach based on Testing*_Data 1*.

### 4.3.1 Results of extracting fuzzy depth map attributes

The MFs generated for the depth map attributes with $J$=3 are shown in Figure 4.9. The fuzzy labels of the three MFs for each attribute were named as '*low', 'medium'*, and *'high'*. The MFs generated for the depth map attributes with $J$=5 are shown in Figure 4.10. The fuzzy labels of the five MFs for each attribute were '*veryLow', 'low', 'medium', 'high'*, and *'veryHigh'*. The MFs generated for the depth map attributes with $J$=7 is shown in Figure 4.11. The fuzzy labels of the seven MFs for each attribute were '*veryLow', 'low', 'lowerMedium', 'medium', 'higherMedium', 'high'*, and *'veryHigh'*.

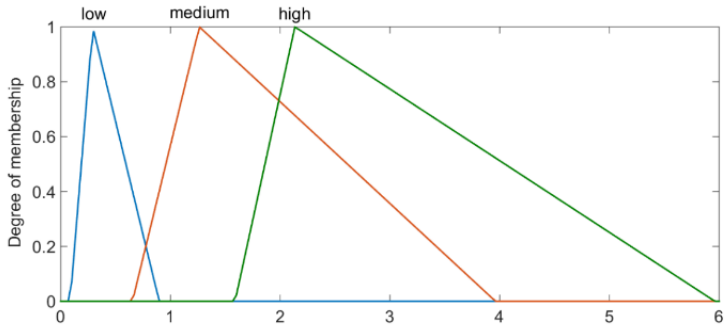


(a)

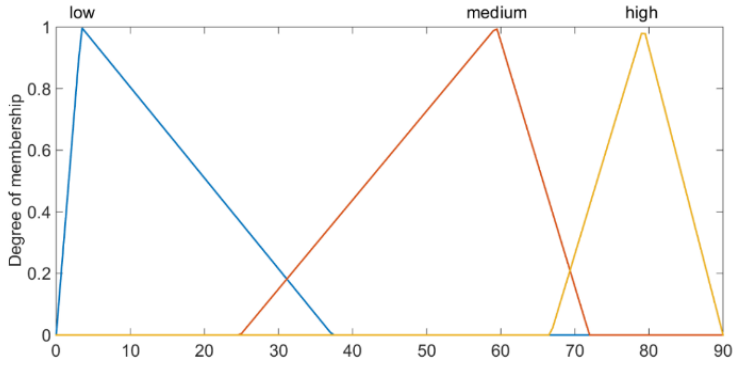


(b)

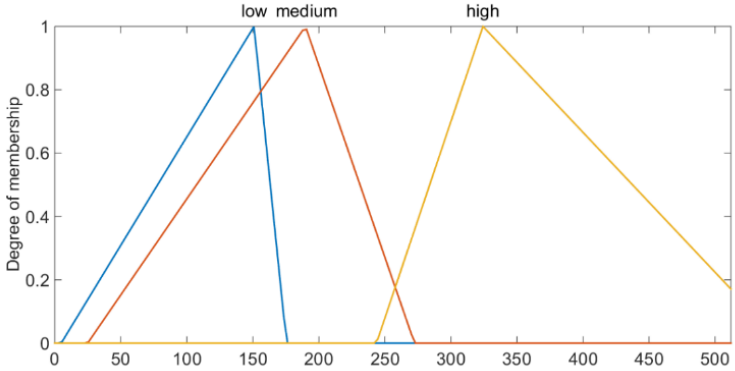


(c)

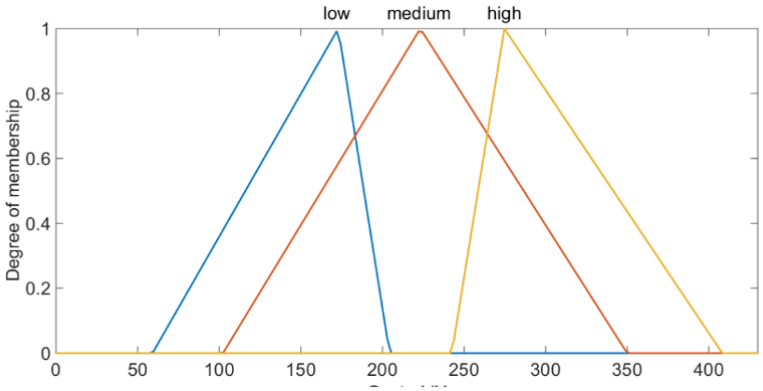


(d)

Figure 4.9. MFs generated for (a) *AR*, (b) $\theta$, (c) *Cx*, and (d) *Cy* via using the FCM algorithm with *J*=3.

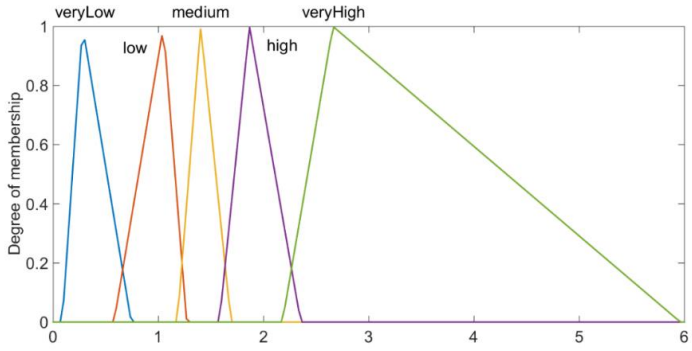


(a)

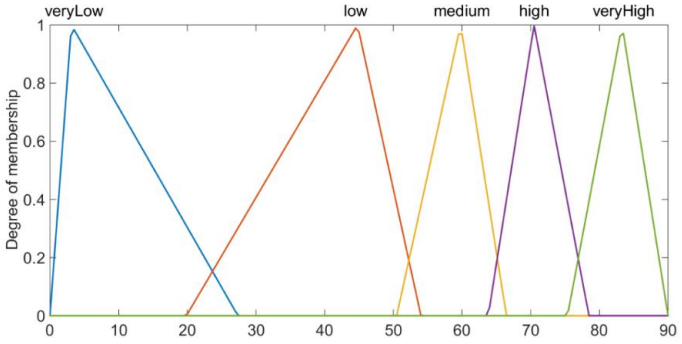


(b)

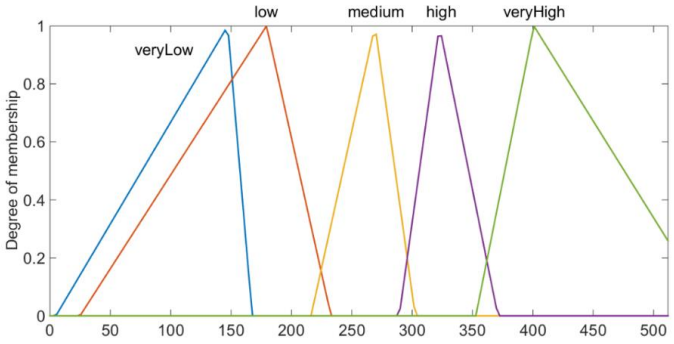


(c)

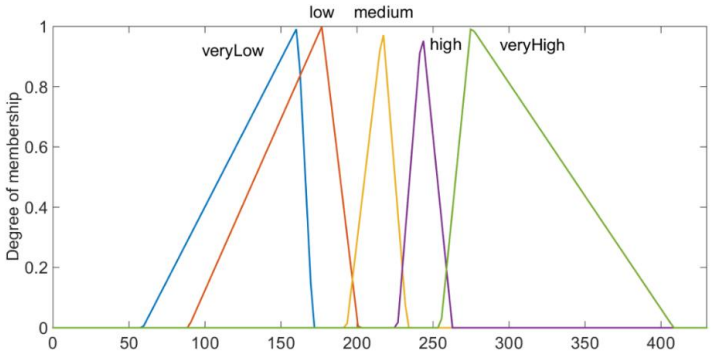


(d)

Figure 4.10. MFs generated for (a) *AR*, (b) $\theta$, (c) *Cx*, and (d) *Cy* via using the FCM algorithm with *J*=5.

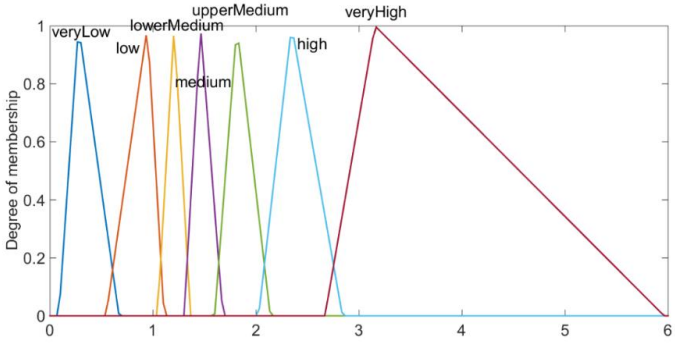


(a)

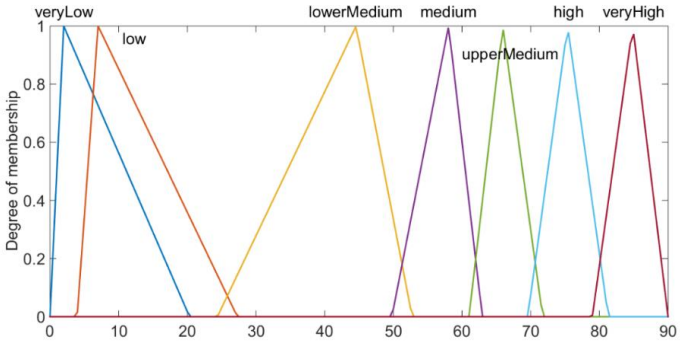


(b)

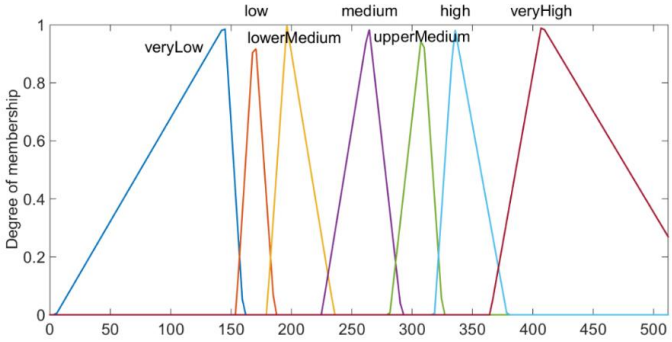


(c)

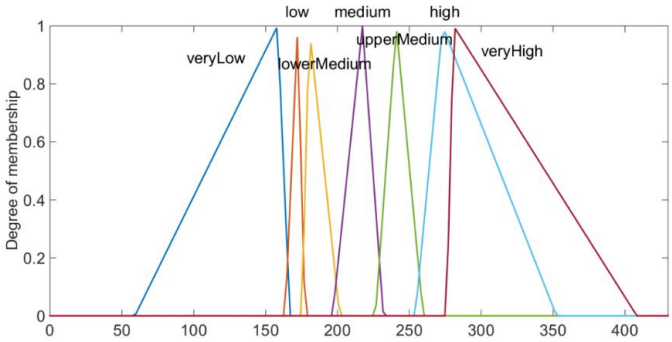


(d)

Figure 4.11. MFs generated for the depth map attributes with *J*=7; MFs for each attribute were given linguistic terms, namely *veryLow*, *low*, *lowerMedium*, *medium*, *upperMedium*, *high*, and *veryHigh*.

It can be inferred that increasing *J* correlates with support area of the generated MFs being smaller. This indicates that slight variations in the occupant's postures during physical ADLs could easily change the pattern of fuzzy labels obtained for the depth map attributes. It is then very likely that when *J* is set to a high value (e.g. 7) multiple fuzzy rules would be generated to model the same ADL. This is because each time the person slightly changes their posture during an ADL, a new combination of fuzzy attributes would be obtained. These combinations would cause fuzzy rules to be generated if they are frequent enough.

### 4.3.2 Results of identifying epochs of activities

The results of identifying epochs of activities are presented in this section. The accuracy of the proposed technique for identifying epochs of activities was estimated through comparing its results with the ground truth for epochs of activities. The ground truth for epochs of activities was obtained based on the daily schedule followed by the researcher to simulate activities (shown in Table 3.5). The histogram for the time of activities for different locations with the ground truth of epochs represented as different colour rectangles is shown in Figure 4.12 (a)-(d). The vertical axis represents the number of observations. Five peaks were detected in the histogram for the kitchen (Figure 4.12 (a)) which corresponded to the five major activities carried out in this area during the collection of the dataset (i.e. preparing the breakfast, cleaning, preparing the lunch, making a refreshment, and preparing dinner). Variations in the starting time of these activities during the data collection period resulted in the formation of component distributions in the data. The combination of these component distributions resulted in a mixture of distributions on the histogram. Each component distribution in this mixture represents an epoch of activity. For example, the typical time for preparing lunch was 12:00 PM (see Table 3.4) and ranged from 10:30 AM to 13:00 PM. Lunch and dinner times had higher peaks than breakfast. This figure also shows less presence of the occupant in the kitchen immediately after lunch. This suggests the occupant spending time elsewhere, such as the dining room or living room.

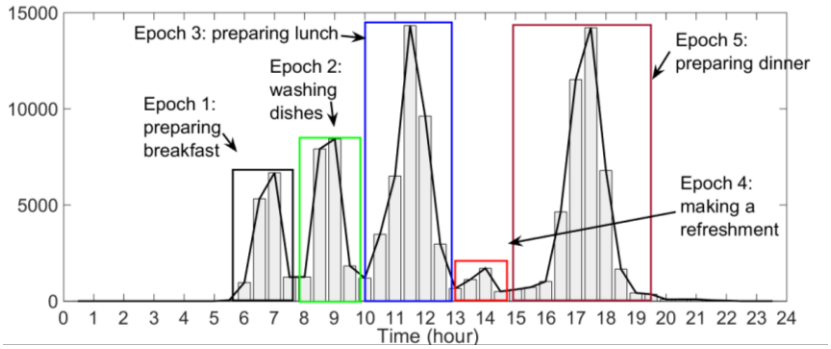


(a)

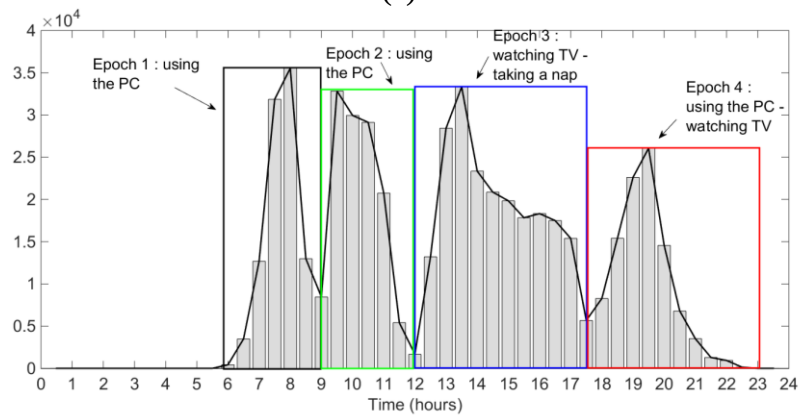


(b)

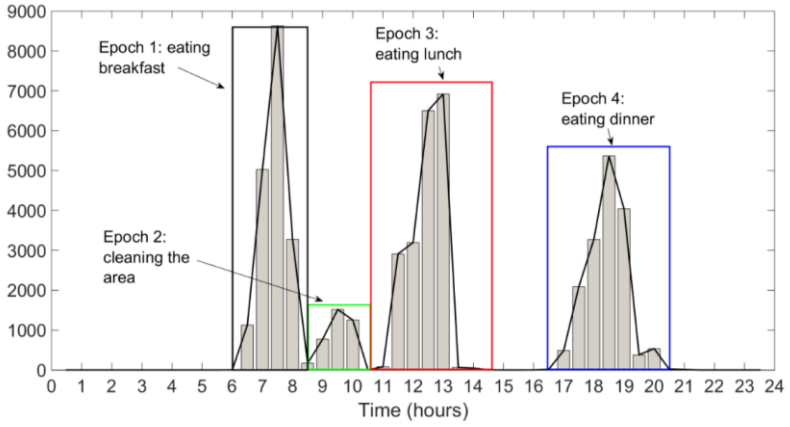


(c)

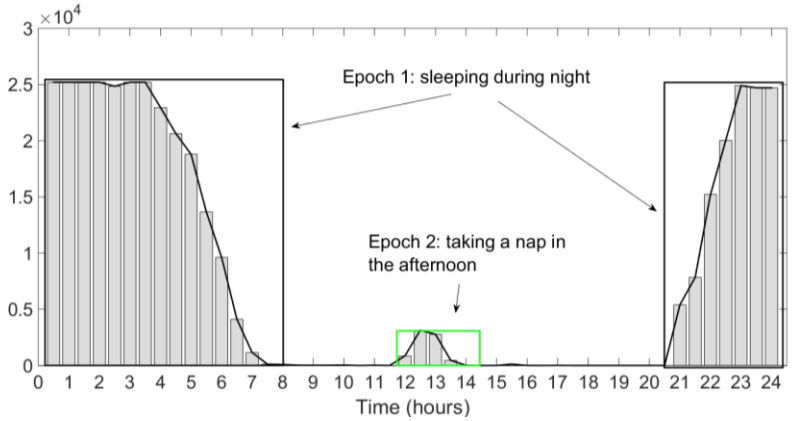


(d)

Figure 4.12. The histogram for the time of observations from the (a) kitchen, (b) living room, (c) dining room, and (d) bedroom datasets with epochs of activities segmented from the ground truth.

The ground truth for the living room is shown in Figure 4.12 (b). By taking Figure 4.12 (a) into consideration, it is evident that the living room was usually occupied after breakfast, washing dishes in the kitchen and lunch. The living room was also occupied between 18:00 and 22:00 for watching TV or using the computer. The ground truth for epochs of the bedroom is shown in Figure 4.12 (d). This figure displays two separate segments labelled as Epoch 1 (black rectangles) which represents sleeping in the bed. The duration of activities for this epoch was calculated by taking into account the total duration of continuous observations for the two segments. When the occupant went to bed at 22:00 PM and slept until 06:00 AM the following morning, the duration of this activity for the right-hand side segment (i.e. 2 hours) was added to that of the observations for the left-hand side segment (i.e. 6 hours).

MFs were generated based on the proposed technique in Section 4.2.1.3 to model epochs of activities for each location. The different parts in Figure 4.13 display the obtained MFs for different locations in the testbed. The estimated epochs were found to accurately represent those obtained from the ground truth. This is due to the use of mean shift clustering algorithm which grouped all observations belonging to the same component distribution as belonging to the same cluster. For example, the living room area was occupied during specific periods in a daily routine to perform specific ADLs. Performing each activity in this area caused a component distribution in the time of activities. This resulted in the mean shift algorithm correctly identifying the epochs for these activities. Most of epochs for the living room, kitchen, and dining room were associated with overlapping MFs as shown in Figure 4.13. The extent of overlapping determines the amount of variation the system allows in the occurrence time of activities at the monitoring stage from the occurrence time in their training samples.

Existing ADL monitoring systems have employed different clustering algorithms for estimating epochs of activities. Those alternatives were also implemented and the accuracy of the proposed technique was compared against them. Details for this comparison are presented in Appendix B.

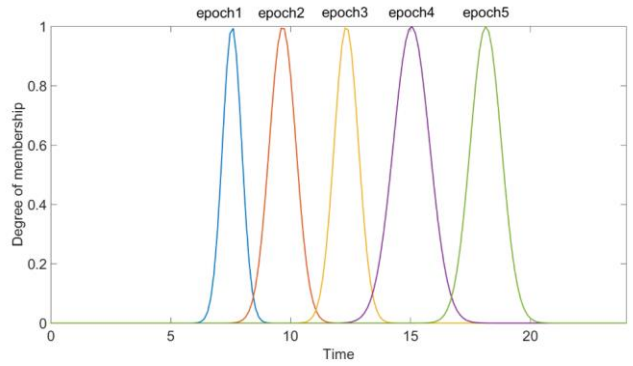


(a)

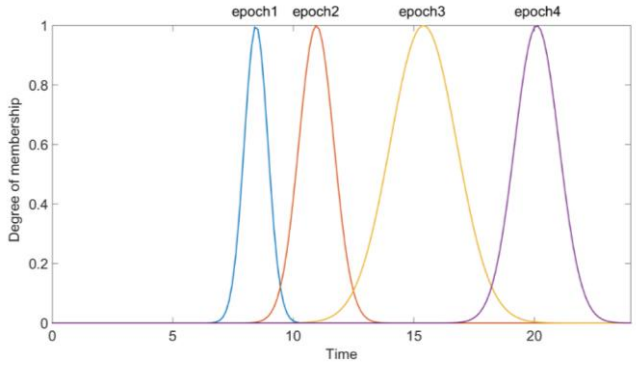


(b)

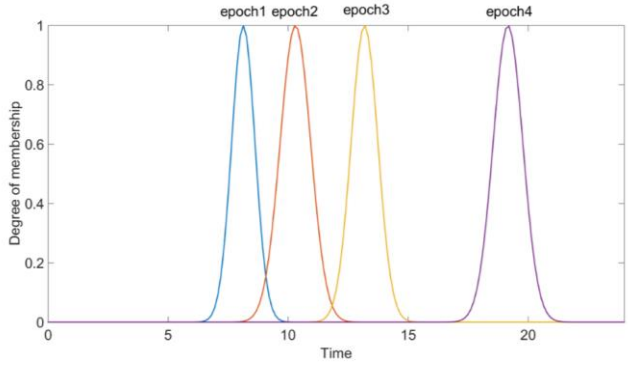


(c)

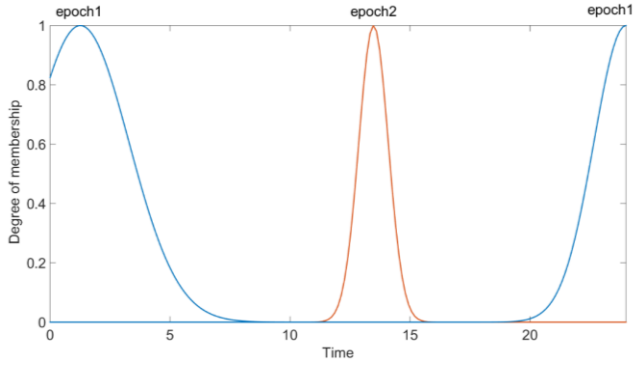


(d)

Figure 4.13. MFs generated to model epochs of activities in different locations of the testbed: (a) the kitchen, (b) living room, (c) dining room, and (d) bedroom.

### 4.3.3 Results of identifying frequent behaviour patterns

This section presents the results of determining frequent behaviour patterns for each epoch of activity for different configurations of *J*.

The plots of support level versus the number of behaviour patterns from processing different activity epochs for different locations with *J*=3 is shown in Figure 4.14. Examination of these plots showed that they all have similar characteristics, in that once the support level reduces to less than 2%, it flattens out and approaches zero. This indicates that the association rules with less than 2% support represented very small proportion of the occupant's behaviours, hence representing infrequent behaviours. *MinSupp* was set such that rules with at least 2% support were picked as to represent frequent behaviours. Reducing *MinSupp* to a smaller value such as 1% increased the number of fuzzy rules for different values of *J*. Subsequent analysis of the classification results associated with using either of the values of *MinSupp* (1% or 2%) showed no significant difference between the two.

The numbers of frequent behaviour patterns in the kitchen dataset during epochs 1 to 5 were estimated to be 11, 14, 8, 10, and 8 (51 in total) as shown in Figure 4.14 (a). In the case of the dining room, however, these numbers for the four detected epochs were smaller, resulting in a sharper fall in the diagrams in Figure 4.14 (b). This may be due to the occupant usually visiting the dining room to have a meal during most of those epochs. The performed activities were therefore limited to sitting behind the dining table and eating food. Epoch 2 for the dining room was associated with a higher number of frequent behaviours because cleaning up the room was carried out in this epoch.

The detected epochs 1-4 for the living room had 7, 7, 10 and 8 (32 in total) frequent behaviour patterns respectively with greater than 2% support (see Figure 4.14 (b)). Epochs 1 and 2 had the same number of frequent behaviour patterns since the activities carried out during these two were almost the same (sitting behind the computer).

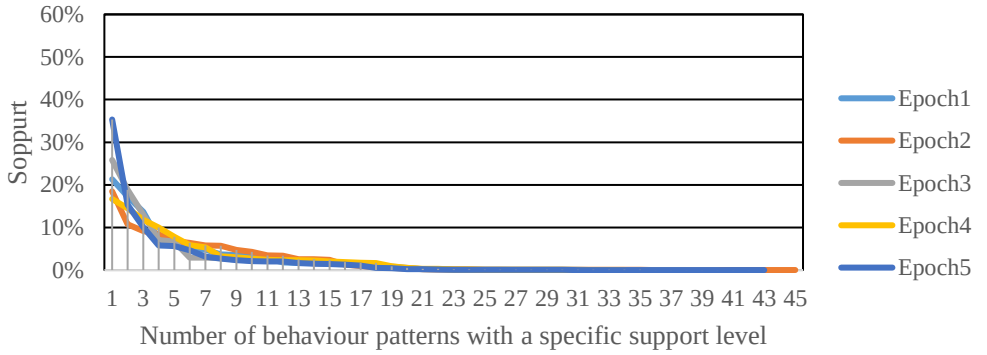


(a)

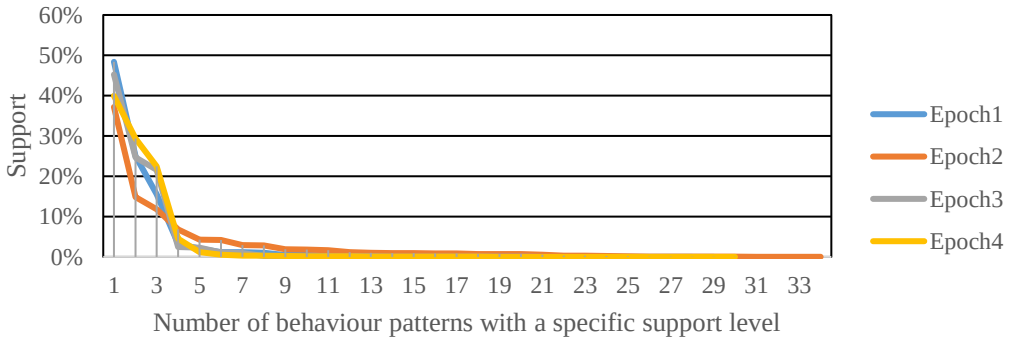


(b)

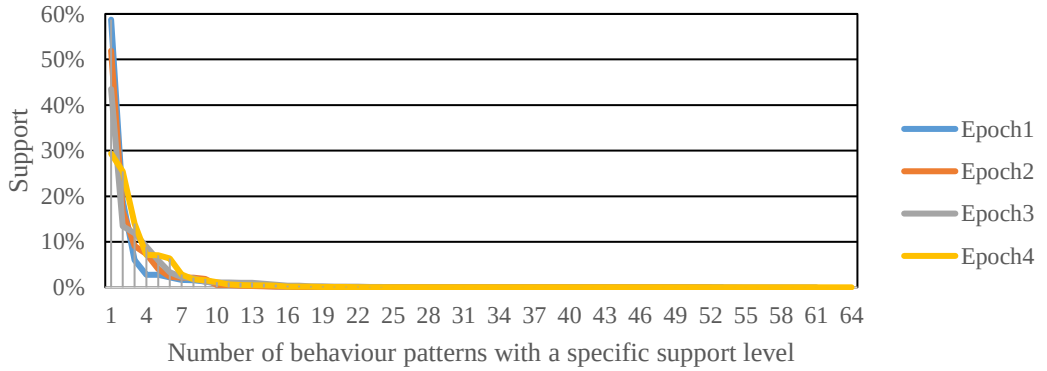


(c)

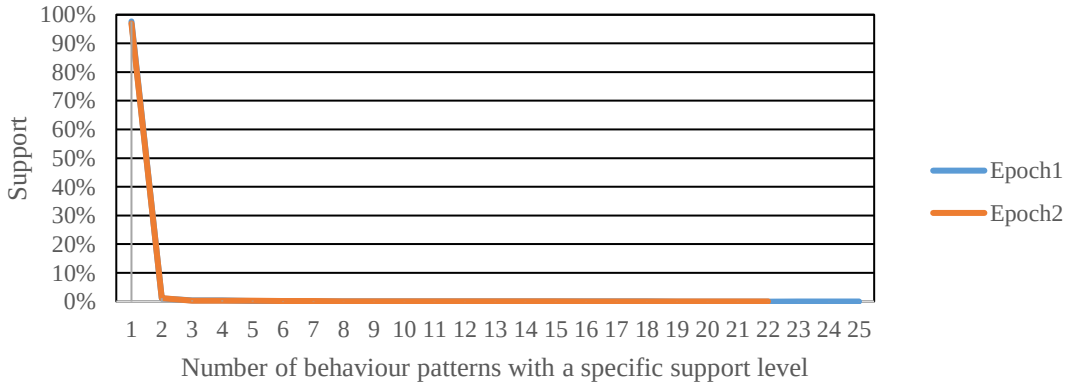


(d)

Figure 4.14. The number of behaviour patterns with a specific level of support obtained for epochs associated with J=3 in the dataset: (a) kitchen, (b) dining room, (c) living room, and (d) bedroom.

The numbers of frequent behaviours for both detected epochs in the bedroom were one, as shown in Figure 4.14 (d). Each epoch belonged to the same activity of sleeping in bed. The support of this activity in each epoch was more than 95%. Although during these two epochs other activities such as blow-drying (by standing by the mirror) and walking around in the room were performed, the ratio of observations of sleeping in bed to those of the other activities was very high. For example, the ratio of observations associated with blow-drying performed in Epoch 1 to all other observations for that epoch was less than 1% (less than *minsupp*).

In another experiment, *J* was set to higher values (i.e. 5 and 7) and plots of the support level versus the number of behaviour patterns were examined. The parameter *minsupp* for these configurations was also set to 2% because the support level flattened out once it reduced to less than 2%.

Figure 4.15 shows these plots when *J*=7. A comparison of the results in Figure 4.14 and Figure 4.15 shows that increasing the value of *J* elevated the number of frequent behaviours for each epoch. This is because the supports of fuzzy sets were smaller when the number of fuzzy sets for the depth map attributes increased. Therefore, the occupant's ADLs were represented through a higher number of combinations of fuzzy attributes.

The total number of rules obtained for different values of *J* to represent frequent behaviour patterns in each monitored location is summarised in Table 4.6.

Table 4.6. The number of fuzzy rules obtained from the output the proposed MF generation techniques for different monitored locations.

| | ***Number of rules*** | | | | |
|---|---|---|---|---|---|
| | ***Kitchen*** | ***Living room*** | ***Dining room*** | ***Bedroom*** | ***overall*** |
| *J* = 3 | 51 | 32 | 19 | 2 | 104 |
| *J* = 5 | 58 | 37 | 24 | 2 | 121 |
| *J* = 7 | 61 | 43 | 28 | 2 | 134 |

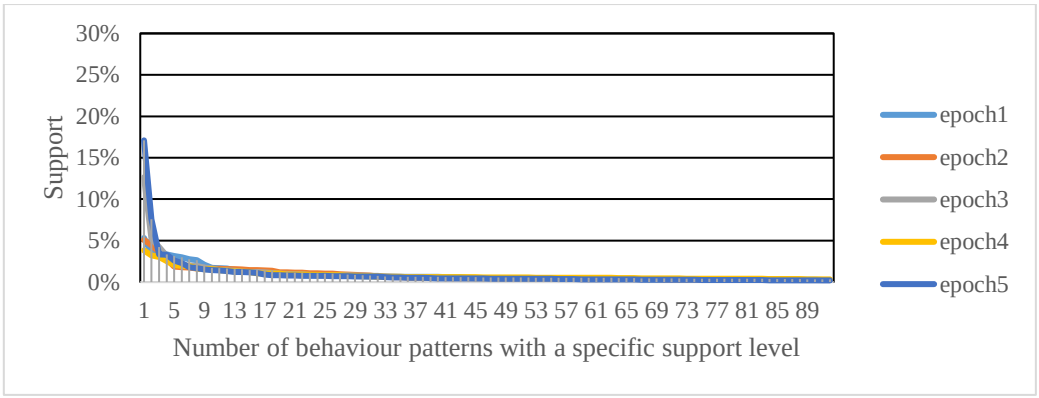


(a)

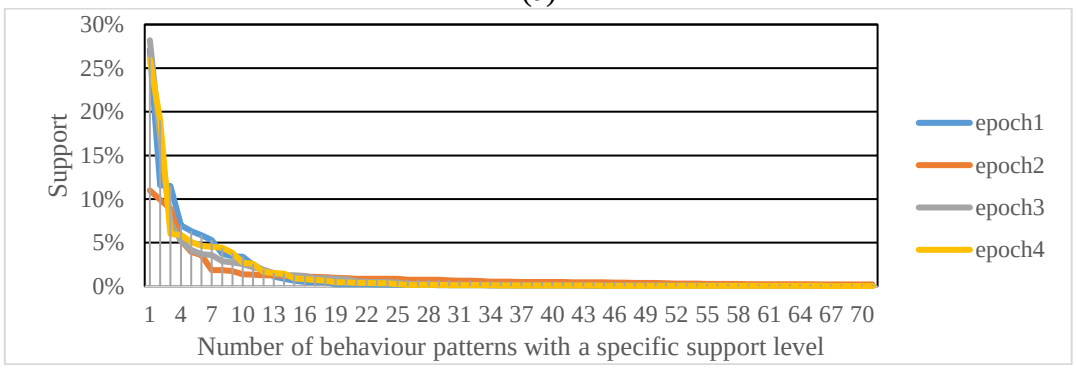


(b)

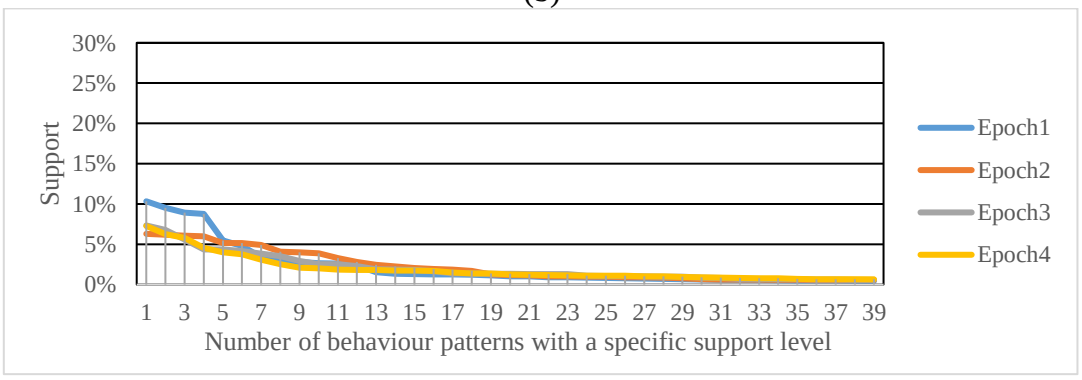


(c)

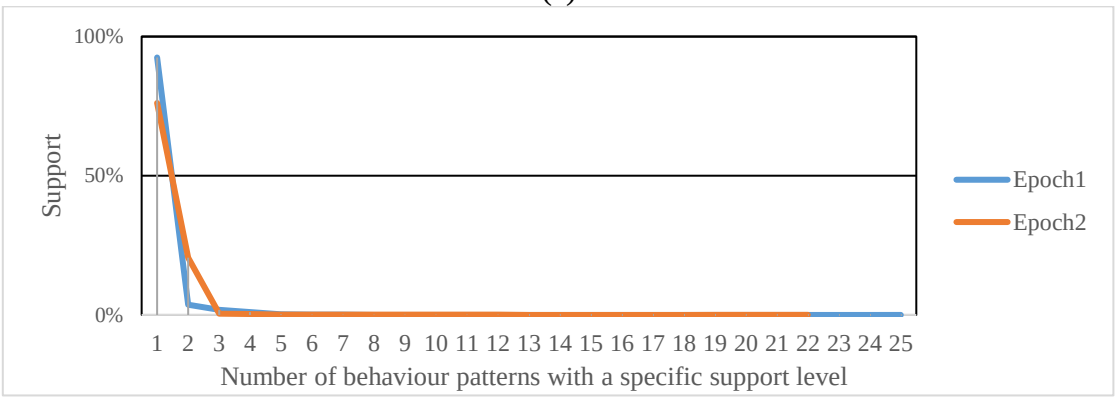


(d)

Figure 4.15. The number of frequent behaviour patterns with a specific level of support obtained for epochs associated with J=7 in the dataset: (a) kitchen, (b) dining room, (c) living room, and (d) bedroom.

### 4.3.4 Results of modelling the duration of behaviour patterns

The results of modelling the duration of frequent behaviours using different values of *J* are presented in this section. The z-shaped MFs representing the duration of the frequent behaviour of sleeping in bed for epochs 1 and 2 with *J*=3 is shown in Figure 4.16. The MF for Epoch 1 represents a duration of approximately nine hours and the MF for Epoch 2 displays a duration of approximately three hours. This is because Epoch 1 is for the activity of sleeping at night which usually took six to eight hours and Epoch 2 is for the activity of occasionally taking a one- or two-hour nap in the afternoon. There were instances in the training dataset where the sleeping activity took more than the usual duration. These instances increased the standard deviation of durations of this activity.

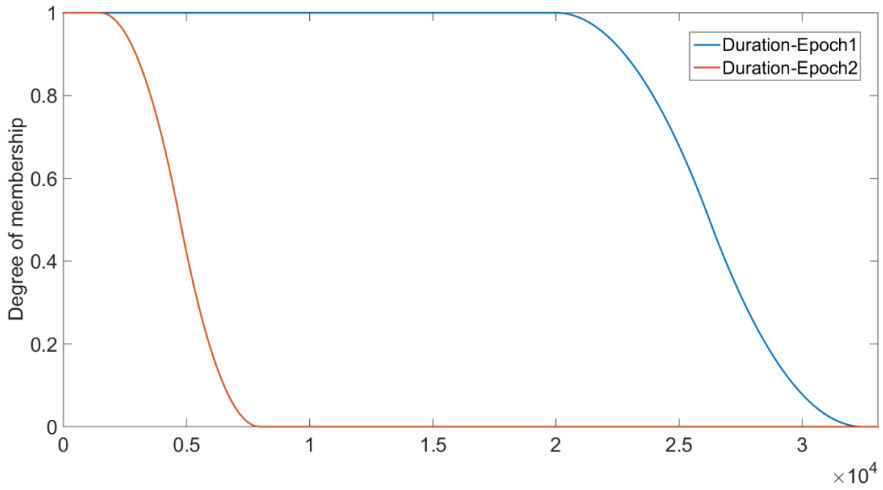


Figure 4.16. The duration of two frequent behaviours obtained from the bedroom dataset with *J*=3. The horizontal axes represent time in seconds.

The MFs generated to represent the duration of frequent behaviour patterns for the kitchen using different values of *J* are shown in Figure 4.17. Increasing *J* generally decreased the estimated duration of behaviour patterns. Increasing *J* also increased the sensitivity of the fuzzy attributes. By setting *J* to a high value, variations in people's body postures and the slight changes in the attribute values during activities resulted in formation of various representations of frequent behaviour patterns.

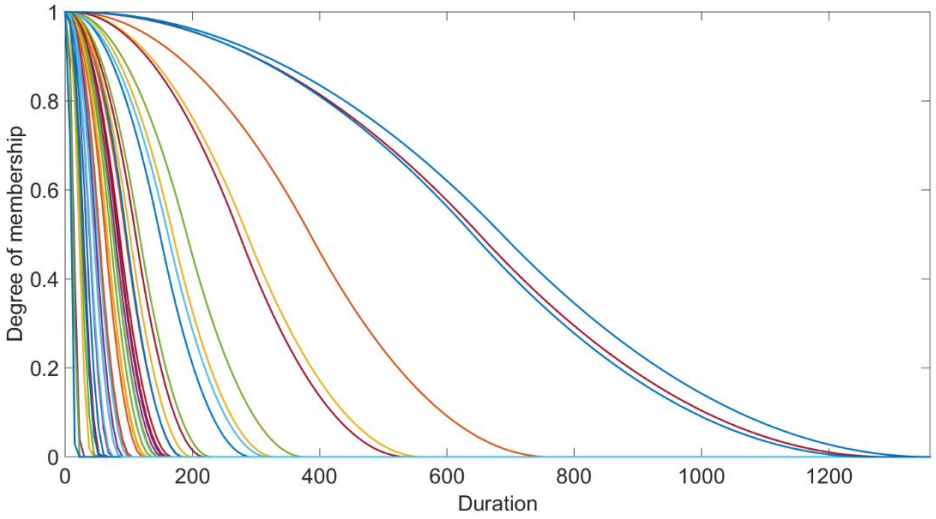


(a)

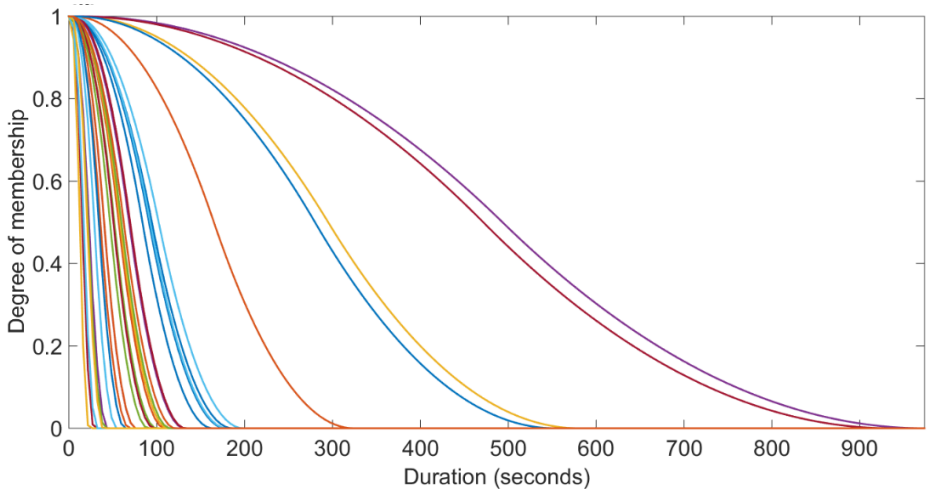


(b)

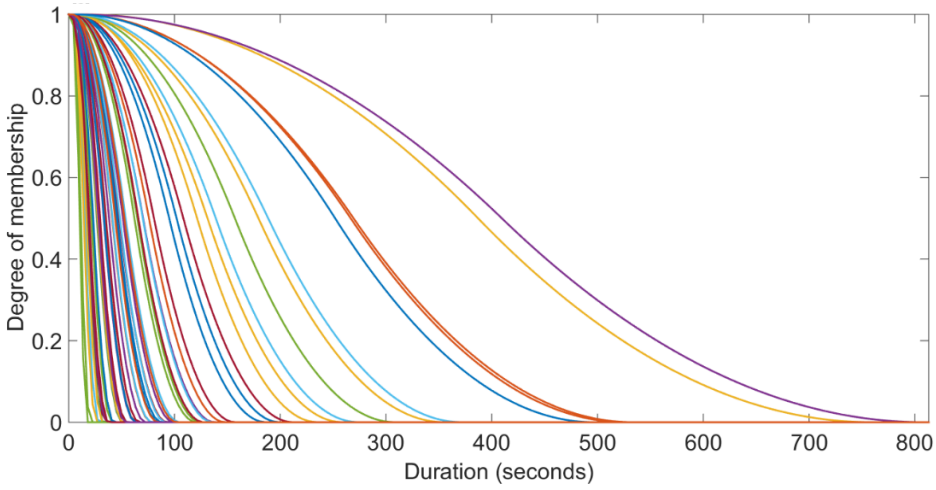


(c)

Figure 4.17. MFs generated to represent the duration of frequent behaviour patterns for the kitchen dataset, using (a) $J$=3, (b) $J$=5, and (c) $J$=7.

Examples of Kinect observations belonging to the longest activities in the kitchen identified for $J$=7 is visualised in Figure 4.18; for each example, the colour image and its corresponding binary mask of the subject is displayed. It was observed that the longest identified activity was standing by the kitchen countertop (preparing a meal) followed by two different behaviour patterns for the same activity of standing by the cooktop. The combinations of fuzzy attributes for these two behaviour patterns were

$$\{AR=\text{'high'}, \theta=\text{'high'}, Cx=\text{'lowerMedium'}, Cy=\text{'upperMedium'}\}$$

and

$$\{AR=\text{'high'}, \theta=\text{'veryHigh'}, Cx=\text{'lowerMedium'}, Cy=\text{'upperMedium'}\}.$$

These combinations only differ in their fuzzy label for $\theta$. This variation was due to the occupant's different body postures during the activity.

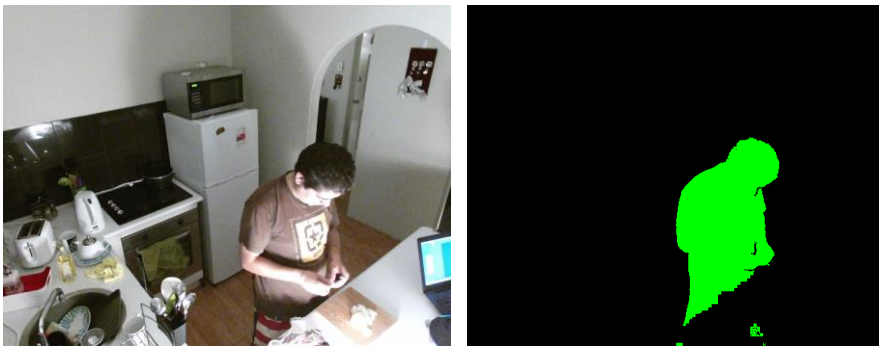

(a)

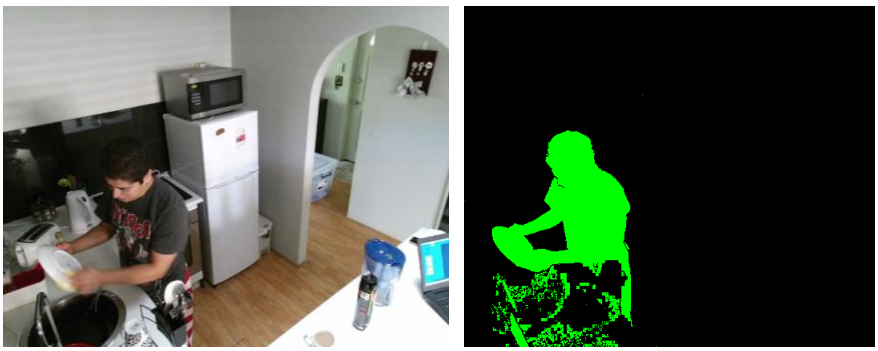

(d)

Figure 4.18. Examples of observations belonging to longest identified frequent behaviour patterns obtained from the kitchen with $J$=7.

The duration of the frequent behaviour patterns obtained for other values of $J$ (i.e. 3 and 5) was examined. It was confirmed that for other values of $J$, the longest durations still were for those

activities in the same order. The duration detected for these activities increased as the value of *J* decreased. This was due to the wider support of MFs obtained when *J* increased.

Different values of *J* were used to obtain $EA_{\mathrm{r}}$ for the monitored locations. Table 4.7 shows the results for these configurations. Increasing *J* had a positive impact on $EA_{\mathrm{r}}$ obtained for most locations in Table 4.7. For a low value of *J* (e.g. *J*=3), the support of the respective MFs for the attributes widens. Slight variations of the occupant's posture during most ADLs did not result in changes in the combinations of fuzzy labels. This resulted in more observations associated with frequent behaviours, hence a shorter $EA_r$ for most monitored locations.

Table 4.7. Values of $EA_r$ obtained for different configurations of *J*. The figures represent time in seconds.

| ***Number of MFs*** | ***Living room (r=1)*** | ***Kitchen (r=2)*** | ***Dining room (r=3)*** | ***Bedroom (r=4)*** |
|---|---|---|---|---|
| *J*=3 | 725 | 256 | 212 | 640 |
| *J*=5 | 861 | 281 | 315 | 680 |
| *J*=7 | 905 | 478 | 400 | 682 |

### 4.3.5 Results of monitoring the test dataset of normal and abnormal activities

The *Testing_Data* 1 (see Section 3.5.3) was used to evaluate the accuracy of the AMP-ADLs approach. It consisted of 60 recordings for each of the monitored locations. Half of these recordings were associated with scenarios of different normal behaviour patterns and the other half of the recordings were associated with different abnormal situations. Each of these recordings was tested using different configurations of *J*.

The performance of AMP-ADLs was evaluated by calculating its classification accuracy for testing recordings of both normal and abnormal behaviour patterns. These accuracies were calculated using Equation 3.1 and 3.2 (see section 3.4). The performance of AMP-ADLs with different configurations of *J* is summarized in Table 4.8. The highest average accuracy in classifying abnormal behaviour patterns was estimated to be 75.8% when *J*=7. The highest average performance in terms of classifying normal behaviour patterns was calculated to be 74.2% when *J*=3. This showed that the ability of AMP-ADLs to detect an abnormal behaviour improves when *J* increases while lower values of *J* resulted in more accuracy in classification of normal behaviours. This was because lower values of *J* resulted in fuzzy sets with wider MFs. Greater variation in normal behaviours were tolerated in the test recordings when such

fuzzy sets were used. The ability of the system to identify drifting attribute values as abnormal behaviour reduced as a result of this. The highest average correct classification rate (i.e. 72.1%) for both normal and abnormal behaviour patterns was obtained when *J=3* (see Table 4.8).

The results obtained for several testing scenarios of normal behaviour patterns using different values of *J* are presented in the next section. It is followed by another section elaborating the results of classifying different abnormal behaviours for each configuration of *J*.

Table 4.8. Performance of the AMP-ADLs approach in classifying recordings of normal and abnormal behaviour patterns using different values of *J*.

| ***Number of MFs*** | ***Accuracy for normal behaviours*** | ***Accuracy for abnormal behaviours*** | ***Overall accuracy*** |
|---|---|---|---|
| *J*=3 | 74.2% | 70.0% | 72.1% |
| *J*=5 | 67.5% | 71.7% | 69.6% |
| *J*=7 | 61.8% | 75.8% | 68.3% |

#### *4.3.5.1 Scenarios of normal behaviour patterns*

An examination of scenarios for different normal behaviour patterns was carried out for each of the monitored locations. 30 Kinect recordings were captured for these scenarios, examples of which are described in the following. The results obtained using the rule sets associated with different values of *J* are illustrated for each example.

***Sitting on the living room sofa in the evening****:* An example of a test scenario including one ADL for the living room was for watching TV in the evening. A colour image and its corresponding binary mask of the occupant is shown in Figure 4.19. The occupant sat on the sofa in the living room for 30 minutes in the evening while watching TV resulting in the recording to be consisted of nearly 18000 Kinect observations. The posture of the occupant had slight variations during the recording.

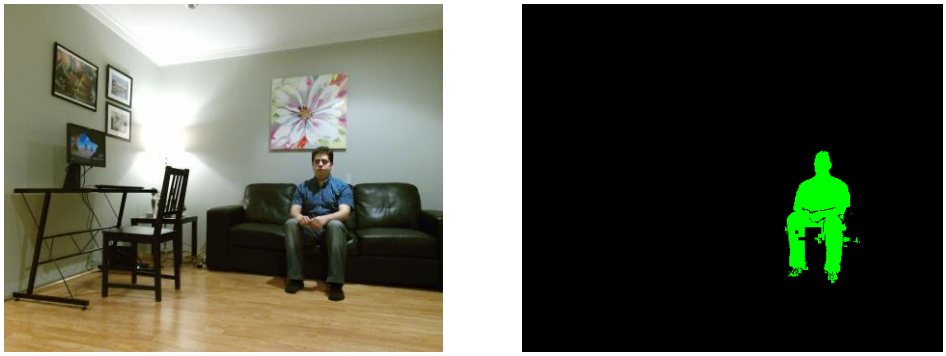

(a) (b)

Figure 4.19. An example of observations for sitting on the sofa in the living room in the evening. (a) The colour image and (b) the corresponding binary mask of the occupant obtained from the Kinect SDK.

The physical ADL in this recording was a part of the occupant's frequent behaviour patterns in the evening. Some fuzzy rules in the rule set associated with each configuration of $J$ represented this behaviour. The triggered rule number in the rule set for different configurations of $J$ during the first 400 observations of this recording is shown in Figure 4.20. Note that rules have been given arbitrary numbers in the respective rule set for each value of $J$. For example, rule number 10 in the rule set for $J=3$ did not necessarily represent the same activity as rule number 10 in the rule set for $J=5$.

For $J$=3 the behaviour pattern {$AR=medium$, $\theta=high$, $Cx=high$, $Cy=low$, $time=Epoch3$} was obtained from the Kinect observations in this recording. This behaviour pattern was present in the antecedent of rule number 21 in the rule set obtained when $J$=3. The blue line in Figure 4.20 indicates that monitoring this recording triggered this rule to fire, which resulted in this recording being considered as normal.

The red line in Figure 4.20 indicates that the attribute values for most Kinect observations in this recording triggered rule number 32 in the respective rule set for $J$=5. However, the combination of fuzzy attributes obtained for some Kinect observations did not match with the antecedent of any rule in the rule set. This was due to slight variations in the segmented posture of the occupant during the ADL. Those Kinect observations were categorised as belonging to infrequent behaviours and the duration of the infrequent behaviour was monitored. The duration for each instance of infrequent behaviour was reset to zero each time rule number 32 fired again during the sequence. The recording was labelled as normal because there was no instance of the duration of the infrequent behaviour exceeding the corresponding $EA_r$.

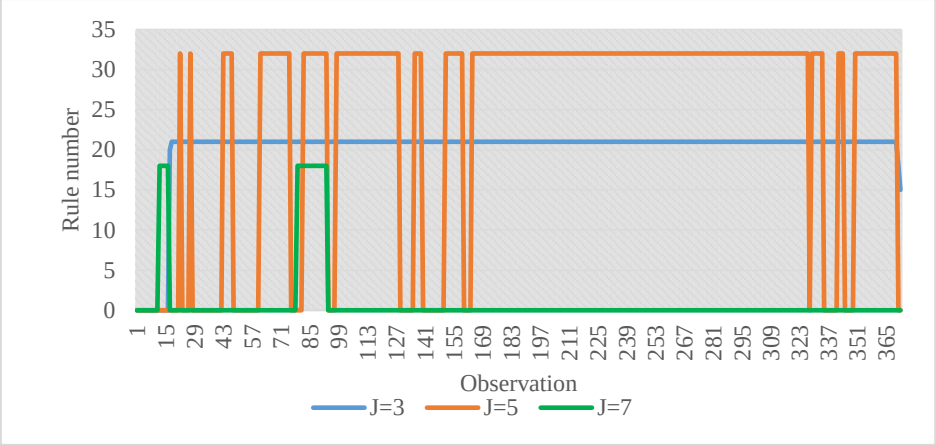


Figure 4.20. Testing a recording of sitting on the sofa in the living room in the evening. The index of the triggered rule in the respective rule set (for different values of *J*) for each observation.

It was observed that degrees of match between rules associated with $J$=5 and the observations in this recording was lower compared to those for $J$=3. The reason was that the supports of MFs becomes narrower when $J$=5. The rules in the corresponding rule set was then more specific and it was less likely that the attribute crisp values for a Kinect observation resulted in a high membership degree in the antecedent part of the triggered rule.

The green line in Figure 4.20 showed that only few observations caused a rule to fire when $J$=7. The system classified all the Kinect observations as showing infrequent behaviour after frame number 100. This was because a slight change in the posture of the occupant caused a new combination of the fuzzy attributes not to be supported by any rule in the respective rule set. The duration of consecutive observations labelled as infrequent behaviour lasted for more than the respective $EA_r$ and resulted in the recording to be labelled as abnormal by this configuration.

***Washing dishes in the kitchen in the morning*:** This scenario was an example of a test recording which included the daily activity of washing dishes in the kitchen in the morning. This activity was performed slightly differently from what was undertaken in the training samples. The occupant intentionally stood in a slightly different location in front of the sink after frame number 96. An example of a colour image along with the occupant's binary mask is shown in Figure 4.21. The occupant's hands usually moved while interacting with objects during this activity. This caused variations in the depth map attributes, mostly in $C_x$ and $AR$.

The results of monitoring observations in this recording are shown in Figure 4.22. It displays the number assigned to the triggered rule in the respective rule set for each value of *J*. All Kinect observations in this recording were related to the same activity.

It was expected that the same rule would be triggered for these Kinect observations. However, the blue line in Figure 4.22 shows that monitoring observations in the recording triggered several rules when *J*=3 (mostly rules 14 and 19). This was because for these observations $C_x$ varied in a range of 240 – 290. Values in the first half of this range had a higher degree of membership in '*medium*' while the other half belongs to '*high*' (see Figure 4.9 (c)). The same situation applied to values of *AR* during the Kinect observations as they varied between 0.75 and 1.3. Different combinations of fuzzy attributes were therefore obtained during monitoring this sequence. These different combinations triggered different rules in the rule set. The occupant changed his location in front of the sink after frame number 96. This change did not change the combination of fuzzy attributes due to the wide support of MFs associated with *J*=3.

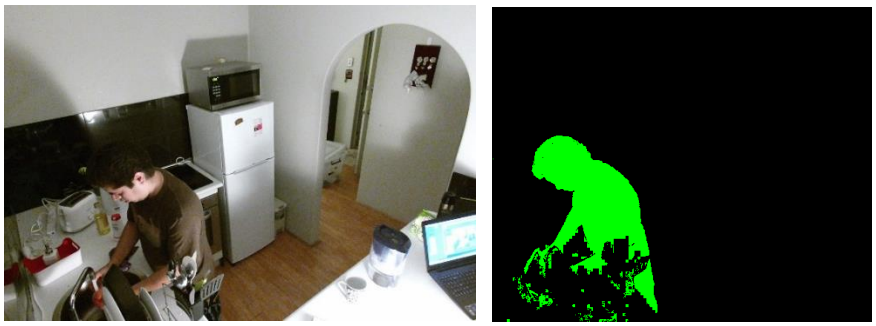

(a) (b)

Figure 4.21. An example of observations related to washing dishes in the kitchen. (a) The colour image and (b) the corresponding binary mask of the occupant obtained from the Kinect SDK.

The red line in Figure 4.22 indicates that fewer observations were supported by rules in the rule set obtained when *J*=5. The combination of fuzzy attributes changed after frame 96 and since no rule was triggered for the new combination, those observations were labelled as belonging to infrequent behaviours. The system continued to monitor the activity to record whether it lasted longer duration than the respective $EA_r$ before raising an alarm. The recording was labelled as abnormal because the next 400 observations did not trigger any rule.

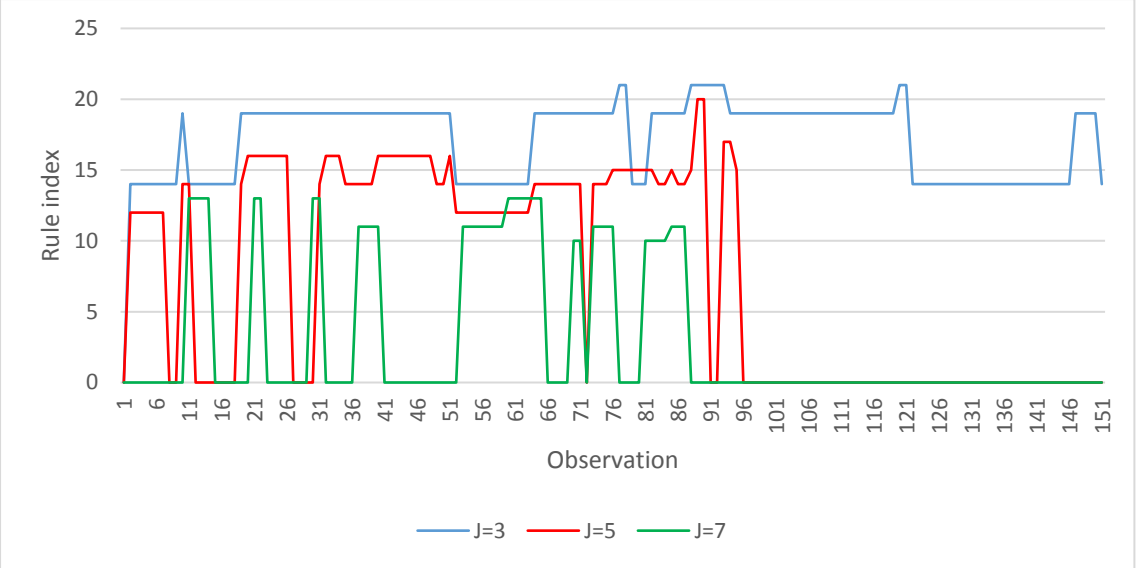


Figure 4.22. Testing a recording of washing dishes based on rule sets associated with different values for *J*. The diagrams show the numbers assigned to the corresponding triggered rules in the rule set (for each value of *J*).

The green line in Figure 4.22 shows that when *J*=7 most observations were categorised as showing infrequent behaviours. This was because slightly different attribute values extracted from this activity resulted in an infrequent combination of fuzzy attribute. Monitoring this recording caused the system to raise an alarm since at the end of monitoring periods no rule supported the slightly different behaviour of the occupant after frame 96.

***Multiple activities of sitting on the sofa and then sitting behind the computer desk in the evening:*** Another example of a testing recording for normal behaviour patterns in the living room included a 35-minute recording for a combination of living room activities the occupant performed in the evening. The occupant's binary masks for the first 21 observations with the index for each observation is shown in Figure 4.23 (a). This figure illustrates that the recording starts with the occupant walking towards the sofa and sitting there for a few seconds (Kinect observations 4 to 14). He then changed his activity and sat behind the computer desk which lasted for the rest of the recording. An example of colour images for observations 11 and 21 is shown in Figure 4.23 (b) and (c), respectively.

The output of the AMP-ADLs approach for the first 21 observations of this recording is shown in Figure 4.24. The diagrams this figure indicates the triggered rule from the rule set associated with different values of *J*.

No rule set supported the observations for the activity of walking towards the sofa or towards the computer desk as shown in Figure 4.24. The monitoring systems associated with the different values of *J* classified those observations as showing infrequent behaviours. The reason was that the ratio of observations in the training data for walking around in the living room to those of more frequent activities (e.g. sitting on the sofa and sitting behind the computer desk) was less than 1%. All observations belonging to walking were thus included in $D_{infrequent\ behaviours}$.

The blue line in Figure 4.24 indicates that at the beginning of sitting on the sofa both observations 4 and 6 resulted in the same combination of fuzzy attributes (i.e. {*AR=medium, θ=high, Cx=high, Cy=low, time=Epoch3*}). This resulted in rule number 21 to be triggered for those observations. The subject's posture changed slightly once he started to write notes while sitting on the sofa as his head was down. This slight change in values associated with *AR* caused the combination of fuzzy attributes to change to {*AR=low, θ=high, Cx=high, Cy=low, time=Epoch3*}. Rule 18 corresponding to the new combination of fuzzy attributes was thus fired for observations 8 to 14. Note that this rule was developed in the training phase since the behaviour of writing notes while sitting on the sofa was observed frequently during the training period.

The posture of the occupant for sitting behind the computer desk slightly changed during observations associated with this activity. Although the same rule was expected to fire for all those observations, different rules in the rule set were triggered because of slightly different postures.

The red line in Figure 4.24 illustrates that the AMP-ADLs approach with *J*=5 recognised fewer observations associated with sitting on the sofa as showing frequent behaviours. The occupant's activity in those observations triggered several rules in the system with almost 50% similarity to the behaviour patterns in the training dataset.

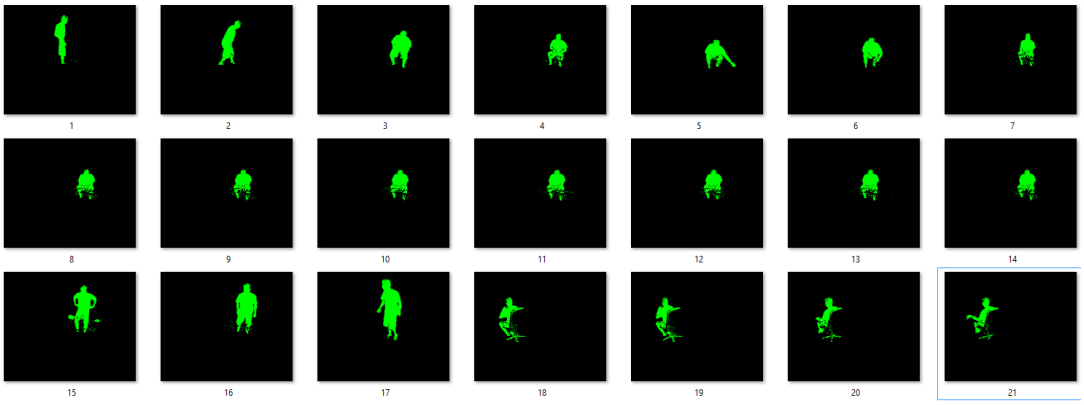

(a)

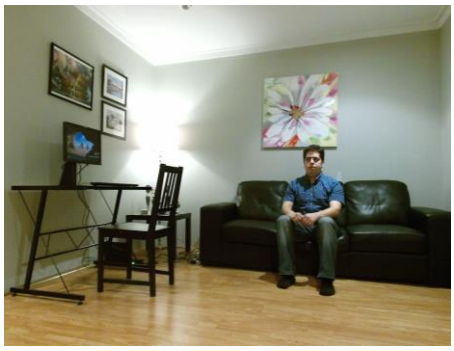

(b)

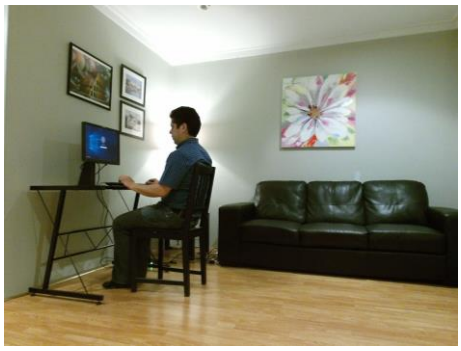

(c)

Figure 4.23. (a) Binary images of the occupant during the first 21 frames of a test recording involving multiple ADLs; walking in the room, sitting on the sofa and then sitting behind the computer desk. (b) A sample colour image for the activity of sitting on the sofa, and (c) an example of a colour image for sitting behind the computer desk.

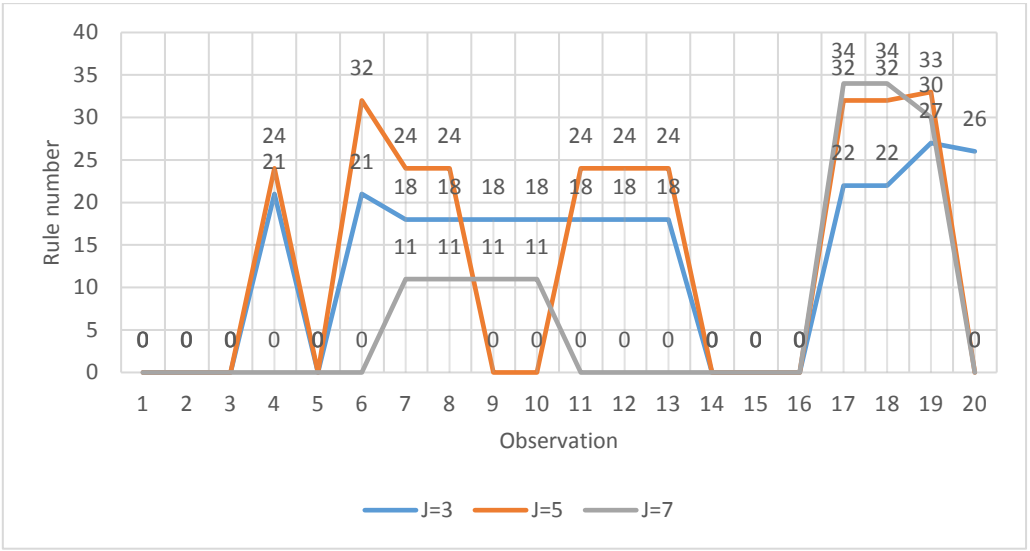


Figure 4.24. Testing a recording of multiple ADLs with the rule set based on different values of *J*. The number assigned to the corresponding triggered rule in the rule set (for each value of *J*) is shown for each observation.

Increasing *J* to a value of 7 caused the system to categorise almost half of the observations as representing infrequent behaviours (see the green line in Figure 4.24). For narrower fuzzy sets associated with *J*=7, it was less likely that the value of the attributes during this test sequence fall within the boundaries of the learned fuzzy sets for sitting behind the computer desk.

***A new activity in the kitchen for eight minutes in the morning*.** The occupant carried out a new normal activity in this scenario which was cleaning inside the refrigerator for several minutes. An example colour image is shown in Figure 4.25. This activity was not present in the original training dataset. The posture was significantly different from the other refrigerator-related postures in the training dataset. The combination of fuzzy attributes associated with this new behaviour pattern was therefore not within the bounds associated with the set of learned frequent behaviours for any value of *J*. This resulted in no rule for any configuration of *J* to be triggered during the process of monitoring this recording. The monitoring approach eventually triggered an alarm when the elapsed duration of this new activity exceeded $EA_r$. This scenario is an example where using a more comprehensive training dataset consisting of typical ADLs with more variability would enable the proposed approach to learn a more representative rule base for characterising the behaviour of the occupant.

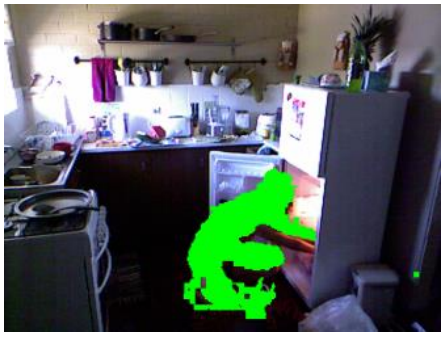

Figure 4.25. A colour image taken from a test sequence of a new behaviour of crouching down on the kitchen floor while cleaning inside the fridge.

#### *4.3.5.2 Scenarios of abnormal behaviour patterns*

*Testing_Data 1* was comprised of 30 use-cases for each monitored location (see Section 3.5.3). These were used to evaluate the accuracy of the developed system in detecting various abnormal behaviours. The use-cases for each monitored location were categorised into three

groups with 10 use-cases associated with each group. Each group tested the ability of the system to detect abnormality in a key aspect of ADLs. These groups were:

(1) *The occupant's postures*: This category defined situations where the body posture observed at a specific location is abnormal. Such abnormality can occur because of a hazardous incident like a fall or a decline in the physical independence of the person (Gokalp & Clarke, 2013). Examples of use-cases in this group were lying on the floor in the dining room and sitting at unusual locations, such as the kitchen floor.

(2) *Time of ADLs*: The behaviour time is very important for the elderly people's behaviour analysis as it is related to individuals' time orientation. Abnormalities in the time of activities can be regarded as an indicator of cognitive impairments (Xavier, Sigulem, & Ramos, 2010). For example, walking around at midnight may indicate insomnia or other diseases. Use-cases in this category demonstrated scenarios where the occupant performs normal activities in abnormal times of the day.

(3) *Duration*: This category defined scenarios where the occupant performs one or a combination of ADLs for a longer duration than normal. It was defined to evaluate the ability of the system to detect extended activities which could indicate an emergency incident such as a fall. For example, a sitting posture can be an abnormal behaviour if it lasts for too long in the case of a faint or a heart attack. A longer duration in performing activities can also indicate a decline in mobility and general wellbeing of the elderly (Cardinaux, Brownsell, Hawley, & Bradley, 2008; Gokalp & Clarke, 2013).

Examples of different categories of use-cases for abnormal behaviour patterns are described below. The results obtained from the rule sets associated with different values of $J$ are illustrated for each scenario.

***Lying on the floor in the kitchen for a duration of 20 minutes.*** This scenario is an example of the first category of use-cases defined for testing the ability of the system to detect abnormality in the occupant's posture during ADLs (i.e. an unusual posture of lying on the kitchen floor). The use-case defined for this scenario is shown in Figure 4.26. The situation described in this use-case may occur if an elderly person shows some dizziness as a symptom of a health issue or a sudden fall.

**Use-case #1 defined for the kitchen:**

**Goal**: To test the ability of the system to detect an abnormal posture of the occupant in the kitchen

**Initial state**: The occupant is washing dishes in the kitchen.

**Description**: It is 9:30 AM when the occupant usually washes dishes from the day before in the kitchen. He suddenly feels faint and lightheaded and lies on the kitchen floor. This situation persists as he continues to lie on the floor for the next 20 minutes.

**Normal behaviour**: The occupant normally does not lie on the floor in the kitchen.

**Expected outcome**: The Kinect observations represent an abnormal behaviour in the kitchen. The system should continue to monitor if this situation persists for a specific duration and then raise an alarm to notify a caregiver.

Figure 4.26. The description of a use-case defined for the abnormal behaviour pattern of lying on the kitchen floor for a duration of 20 minutes.

An example colour image for this recording along with its detected binary mask of the occupant is shown in Figure 4.27. It shows that the occupant's body was within the field of view of the kitchen Kinect sensor.

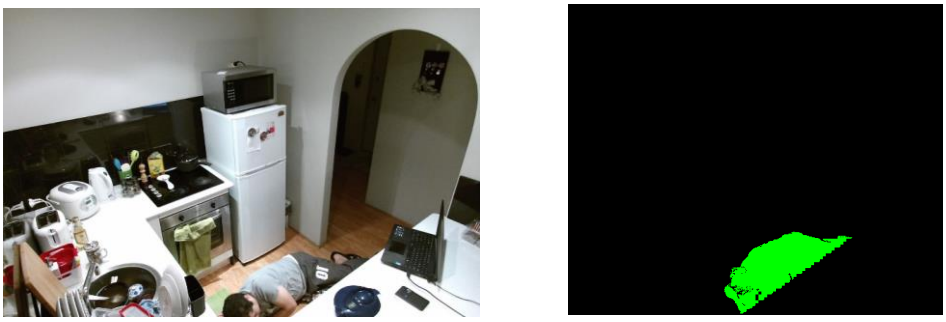

(a) (b)

Figure 4.27. An image from the abnormal behaviour of lying on the kitchen floor. (a) The colour image and (b) the corresponding binary mask of the occupant.

The combination of attributes obtained from the Kinect observations associated with this recording did not trigger any rules in the set of the learned frequent behaviours for any configuration of $J$. The system associated with each value of $J$ considered this behaviour as belonging to the set of infrequent behaviours and the associated duration for this recording was monitored. The AMP-ADLs approach raised an alarm after the elapsed duration of this behaviour exceeded the learned value of $EA_r$ for the kitchen.

***Lying on the floor in the immediate vicinity of the kitchen (partially occluded) for a duration of 20 minutes.*** This scenario was another example of the first category of use-cases where the occupant finishes an activity in the kitchen and then falls over on the floor on his way to the dining room (see Figure 4.28).

An example colour image and the respective binary mask of the occupant for this use-case are displayed in Figure 4.29. The body of the occupant is partially occluded, as only part of the occupant's body is evident to the kitchen Kinect sensor.

The first 19 Kinect observations in this recording involved the activity of standing by the electrical cooktop in the kitchen (the initial state of the use-case). The rest of the observations are related to the abnormal behaviour of lying on the floor. Figure 4.30 shows the output of different configurations of $J$ for this test recording. This figure indicates that all configurations of $J$ resulted in the observations of standing by the electrical cooktop to be classified as belonging to a frequent behaviour pattern. The diagrams for $J$=7 and $J$=5 in Figure 4.30 indicate that none of the observations associated with lying on the floor caused rules to fire, which resulted in an alarm to be raised eventually by those configurations.

**Use-case #2 defined for the kitchen:**

**Goal**: To test the ability of the system to detect an abnormal posture of the occupant where it is partially occluded.

**Initial state**: The occupant is standing by the electric cooktop in the kitchen.

**Description**: It is 6:00 PM which is the time when the occupant usually cooks dinner and goes to the dining room to eat. While walking, he suddenly overbalances and falls on the floor right outside the kitchen. This situation can happen to elderly people as they may lose balance.

**Normal behaviour**: The occupant normally does not lie at the mentioned location.

**Expected outcome**: The posture of the occupant indicates an abnormal situation of lying on the floor outside the kitchen. The system should monitor if it persists for specific duration and then raise an alarm to notify a caregiver.

Figure 4.28. A use-case defined for abnormal behaviour pattern of lying on the floor outside the kitchen for a duration of 20 minutes.

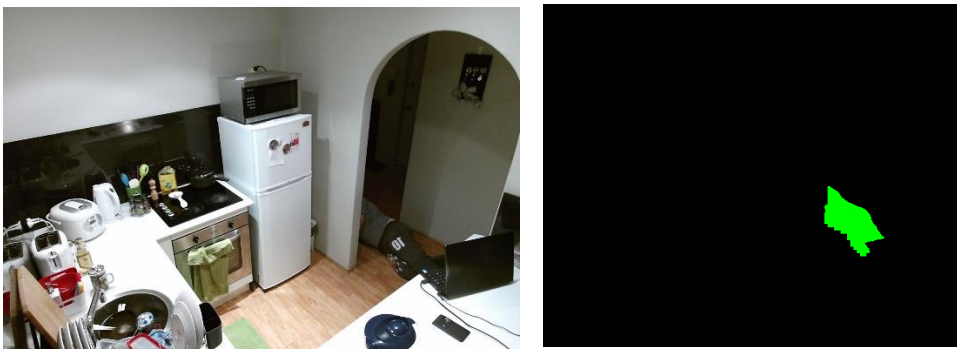

(a) (b)

Figure 4.29. An observation of the abnormal behaviour of lying on the floor outside the kitchen. (a) The colour image and (b) the corresponding binary mask of the occupant.

This recording was classified as normal when the rule set from the configuration of $J$=3 was employed. The combination of fuzzy attributes for lying on the floor was present in the antecedent of a fuzzy rule in this rule set which caused the recording to be classified as representing a normal behaviour. This fuzzy rule (rule number 30) was developed during the training phase to represent the frequent behaviour of standing by the counter in the kitchen. The supports of the MFs in this rule were wide enough to encompass attribute values for the occluded posture of lying on the floor in this recording. This resulted in the triggering of this rule (rule number 30) during monitoring the lying posture.

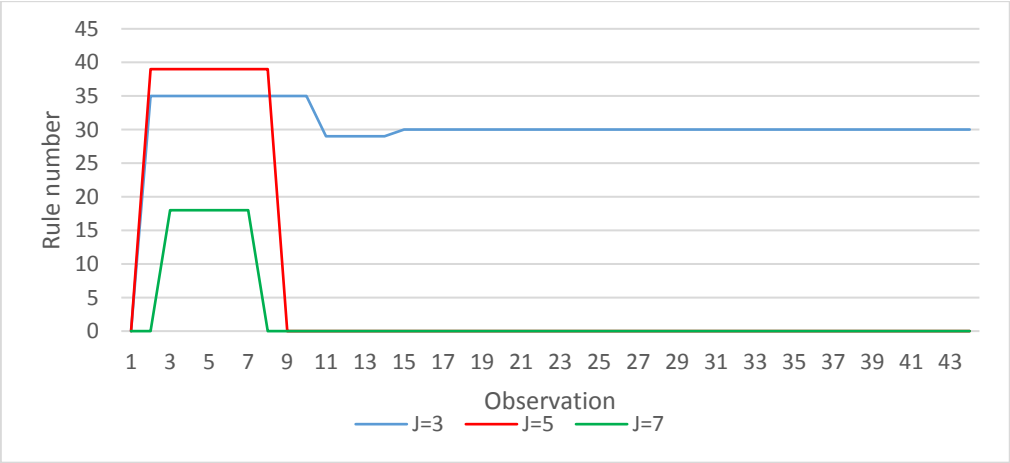


Figure 4.30. Using rule sets associated with different values of $J$ to monitor a test recording of falling on the floor outside the kitchen area. The diagrams show the index of the triggered rule for each observation.

***Sitting on the floor at an unusual location in the living room:*** This scenario is another example of situations representing abnormality in the occupant's posture during monitoring ADLs. The use-case defined for this scenario is shown in Figure 4.31.

**Use-case #3 defined for the living room:**

**Goal**: To test the ability of the system to detect an abnormal posture of the occupant during ADLs.

**Initial state**: The occupant is walking in the living room.

**Description**: It is 09:30 AM when the occupant usually goes to the kitchen to wash the dishes. Because of his deteriorating health he cannot walk and decides to sit on the floor next to the computer desk. He cannot change his posture as his problem persists and eventually faints.

**Normal behaviour**: The occupant normally does not sit on the floor at the specified spot.

**Expected outcome**: As the posture of the occupant indicates an abnormal situation, the system should raise an alarm to notify a caregiver.

Figure 4.31. A use-case defined to represent the abnormal behaviour pattern of sitting at an unusual place on the living room floor.

An example colour image and its binary silhouette of the occupant for this recording is shown in Figure 4.32. The indexes of the triggered rules in the rule set for different values of $J$ are shown Figure 4.33. This figure shows that when $J$=3, rule number 22 (i.e. one of the rules associated with the activity of sitting behind the computer desk) was triggered. This was because the depth map attributes during this abnormal behaviour were represented by a combination of fuzzy sets which also represented the normal behaviour of sitting behined the computer desk. For example, the values of $Cx$ during this behaviour were mostly around pixel location 66 (see Figure 4.32) which fall within the boundary of "*low"* in Figure 4.9 (c). This fuzzy set also represented values of $Cx$ for the behaviour of sitting behind the computer desk. This behaviour pattern was therefore misclassified as being normal and no alarm was raised by the system. By increasing $J$, this value of $Cx$ fell within the domain of a different fuzzy set, making this abnormal behaviour distinguishable from sitting behind the computer desk. For other values of $J$ therefore this recording was correctly classified since no rule was triggered during monitoring the observations.


Figure 4.32. An example colour image of recordings for an abnormal activity of sitting at an unusual location on the floor with value of *Cx* shown in the image.

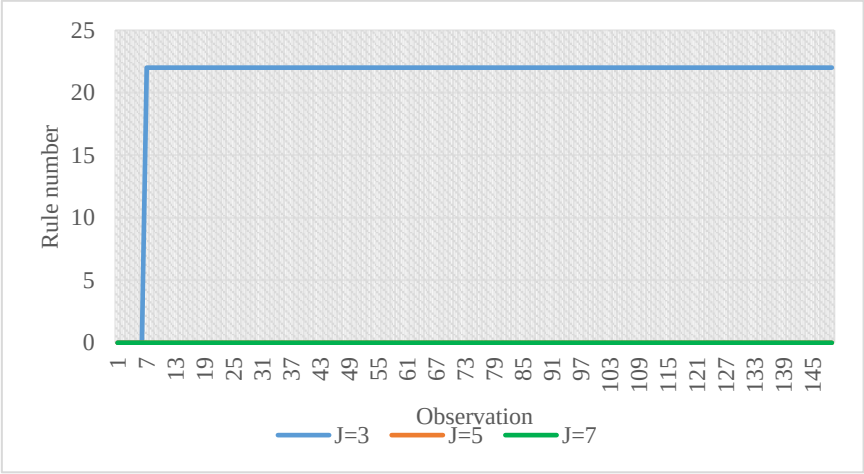


Figure 4.33. Using rule sets associated with different values of *J* to monitor a test recording of sitting on the floor at an unusual location in the living room. The diagrams show the index of the corresponding triggered rule for each observation.

***Performing a normal activity at an abnormal time of the day***. This testing scenario was associated with the second category of use-cases. It depicts an abnormal situation in which the occupant is sitting for 30 minutes on the sofa in the living room at 1 AM in the morning. The use-case associated with this scenario is shown in Figure 4.34.

The behaviour in this sequence was classified correctly by all the configurations of *J* as being abnormal. This is because no epoch of activity was learned for 1 AM in the living room (see Figure 4.13). Although the combination of depth map attributes corresponded to a frequent learned behaviour pattern of sitting on the sofa, no rule from the learned rule set (associated to any configuration of *J*) fired. The behaviour in this sequence fell into the set of infrequent behaviours and the system continued to monitor its duration. Once the elapsed duration for this behaviour was detected to be more than the respective $EA_r$, the system raised an alarm.

**Use-case #4 defined for the living room:**

**Goal**: To test the ability of the system in detecting a normal ADL carried out at an abnormal time of the day.

**Initial state**: The occupant is in the bedroom at 10:30 PM and goes to bed.

**Description**: It is 01:00 AM, and the occupant cannot sleep. He goes to the living room and sits on the sofa.

**Normal behaviour**: The occupant normally does not carry out any ADLs late at night in the living room.

**Expected outcome**: As the time of the activity does not fit the normal profile of the occupant, the system should raise an alarm to notify a caregiver about a possible problem in the normal daily routine of the occupant.

Figure 4.34. A use-case defined for the abnormal behaviour pattern of performing an ADL in an unusual time of the day.

***Sleeping on the sofa for an unusual duration in the afternoon.*** This was an example of test scenarios defined for the third category of use-cases evaluating the ability of the system to detect unusual duration of ADLs. The use-case associated with this scenario is shown in Figure 4.35.

**Use-case #5 defined for the living room**

**Goal**: To detect ADLs with unusual durations.

**Initial state**: The occupant is in the living room.

**Description**: It is 2 PM and the occupant is watching TV while sitting on the sofa. Then he turns off the TV and lies down on the sofa to take a nap. However, because of his deteriorated health, his nap takes 2 hours more than usual.

**Normal behaviour**: The occupant occasionally has a 1-2-hour nap on the sofa in the afternoon.

**Expected outcome**: As the posture of the occupant indicates a sleeping activity and has lasted considerably longer than usual duration, an alarm should be raised to notify a caregiver.

Figure 4.35. A use-case defined for abnormal behaviour pattern of sleeping on the sofa in the living room for a long duration.

An example colour image along with the occupant's binary mask from this recording is shown in Figure 4.36. The monitoring systems developed for different configurations of *J* could not

classify this recording correctly. In the training dataset, different sleeping positions of the occupant during sleeping on the sofa were learned through different combinations of fuzzy attributes. As a result, multiple rules were developed to represent those slightly different postures for this activity. Since the occupant changed his sleeping position a few times in the test recording, different fuzzy rules were triggered. The monitored duration for the behaviour of sleeping on the sofa reinitialised to one each time a new rule fired and the system kept monitoring the duration of the new matched behaviour pattern. The transitions between rules happened for multiple times by the end of the recording causing the monitored duration of this extended sleeping behaviour not exceeding $EA_r$ for the living room.

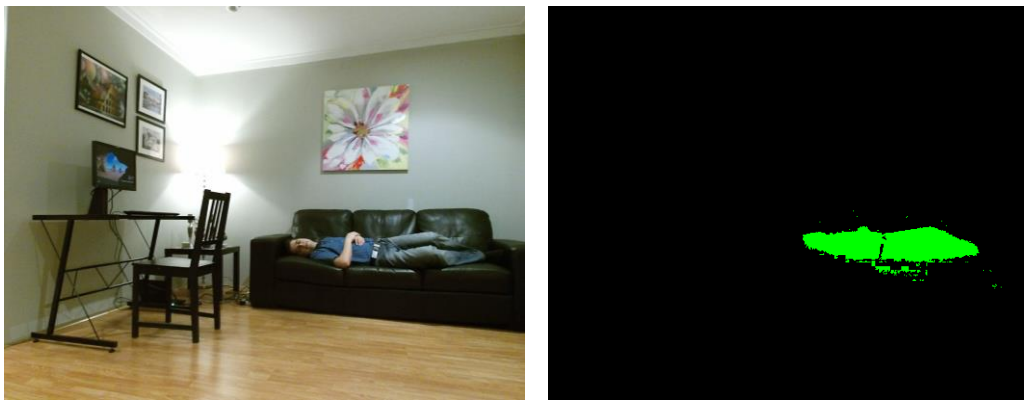

(a) (b)

Figure 4.36. (a) A colour image from in the recording of sleeping on the sofa in the living room and (b) the binary mask of the person.

## 4.4 Discussion

A technique based on the FCM clustering algorithm was employed in this chapter to define a specific number (i.e. *J*) of fuzzy sets over each depth map attribute based on the combined dataset of all monitored locations. The performance of the AMP-ADLs approach with different values of *J* was evaluated and the best overall performance was obtained when *J*=3 as it could correctly classify a greater number testing scenarios of normal and abnormal behaviours. The findings from this chapter revealed that the proposed method for generating fuzzy sets for the depth map attributes had three key drawbacks:

(1) ***A fuzzy rule does not necessarily represent variation of attributes during an activity***. Variations in frequent activities in a particular room typically cause the depth map attributes of that location to have a number of component distributions each associated

with a mode in the distribution. For each dataset of the attributes collected from a particular room, each combination of component distributions represents a frequent activity in that room. Various distributions of the attributes were captured from different rooms. This was the result of different ADLs being recorded for a particular room. For example, the attribute $Cx$ associated with the living room dataset had two modes associated with two separate component distributions (see Figure 4.37). The reason was that the living room was occupied mainly for sitting at a computer desk (the left distribution) and using the sofa for watching TV (the distribution to the right). Values of $Cx$ were therefore concentrated around two separate regions in the attribute space. The values of $Cx$ from the kitchen dataset were concentrated around three locations (see Figure 4.39) as the occupant spent most of his time in the kitchen in front of the sink, the electric cooktop, and the countertop.

The mixture distribution of attributes from the combined dataset of different locations did not have the same component distributions compared to when an individual location was considered. When the datasets from all locations were combined, component distributions of particular activities could joint together to result in a wider component distribution. A component distribution for an activity could also split and become a part of two or more other major component distributions in the combined dataset. This is illustrated in Figure 4.40 where the mixture distribution of $Cx$ obtained by combining datasets from all monitored rooms did not represent the frequent activities mentioned for the living room and kitchen.

The technique presented in this chapter generated a fixed number of MFs for each depth map attribute based on the combined dataset of all rooms. The resulting MFs for each attribute did not necessarily represent the component distributions (frequent activities) associated with the dataset of each location. For example, the left side of the distribution to the left in Figure 4.37 is represented via the fuzzy set '*low'* in Figure 4.9 (c) whereas the values on the right side (more than 165) in that data distribution have a higher degree of membership in the fuzzy set '*medium'*.

Slight variations in attribute training values during activities such as "*sitting behind the computer desk"* may result in various combinations of fuzzy sets and hence the creation of multiple rules for slightly different physical ADLs. This affects the performance of the system

in the monitoring phase. For example, some combinations of fuzzy sets for a normal activity might not be frequent enough to form a fuzzy rule and the system become unable to label those combinations as normal behaviour.

As the MFs generated by the technique in this chapter did not accurately represent ADLs, slight variations in the attribute values could easily change the triggered rule and cause the system to reinitialise the duration of the current behaviour to one. This makes the system unable to monitor the duration of those activities accurately. One example of this situation was described for monitoring the activity described in use-case #5 in the previous section.

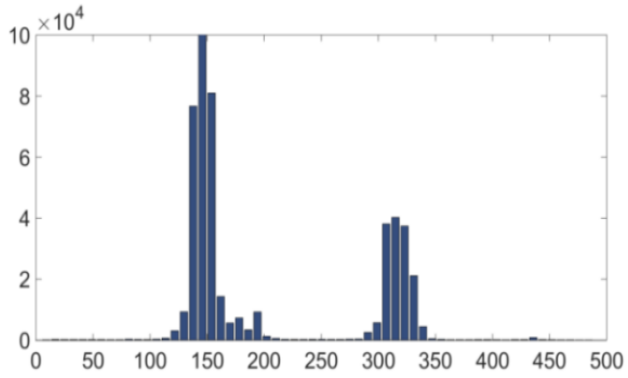


Figure 4.37. The bimodal distribution of $Cx$ associated with the living room dataset.

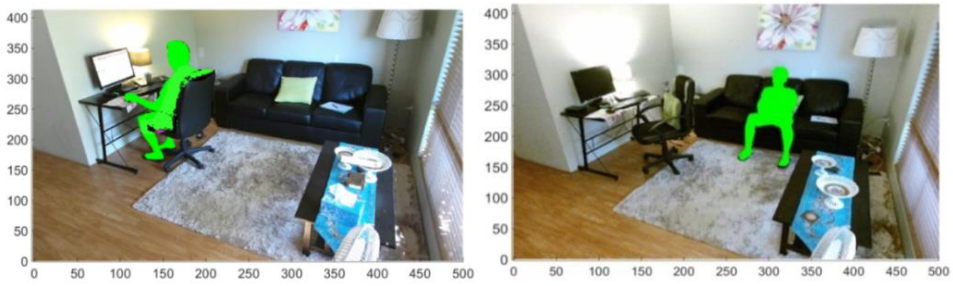


(a) (b)

Figure 4.38. (a) Sitting at a computer desk, and (b) watching TV while sitting on a sofa in the living room. The body of the occupant is masked by its binary silhouette obtained from the Kinect SDK and the numbers in the vertical and horizontal axes indicate pixel location.

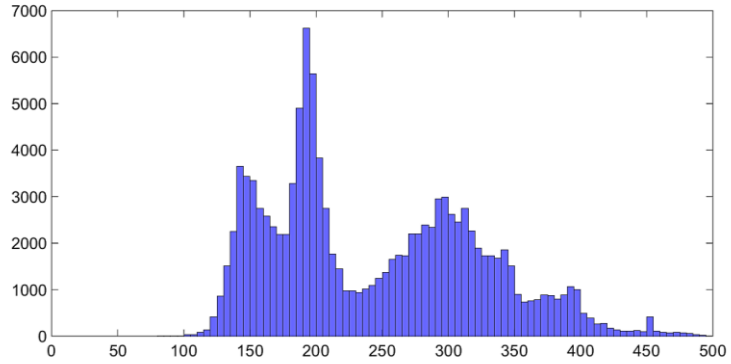


Figure 4.39. The mixture distribution of $Cx$ associated with the kitchen dataset.

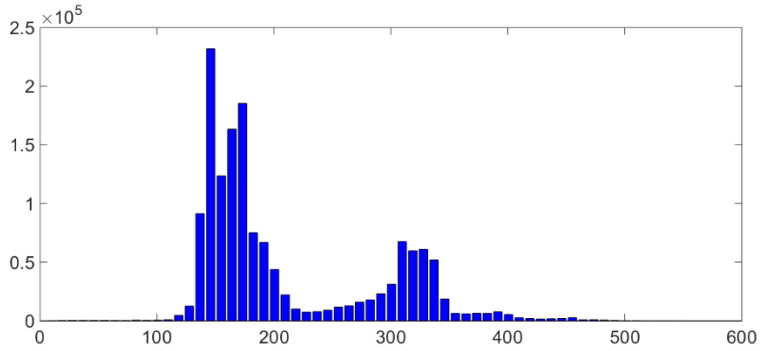


Figure 4.40. The mixture distribution of $Cx$ associated with all monitored areas.

(2) ***The need to define the number of MFs.*** The technique for parameterising the depth map attributes requires the number of MFs to be stipulated by the user. The system can tolerate more variations in normal behaviour patterns when this number is set to a low value but this results in a decline in the ability to detect abnormal situations. Increasing this number on the other hand results in an increase in the accuracy of classifying more abnormal behaviours. This parameter has a high impact on the performance of the monitoring approach and there is a need for a data-driven technique which could calculate this parameter according to the data distribution of attributes.

(3) ***Outliers and noisy measurements in data are incorporated in generating MFs.*** Outliers mostly result from errors in the Kinect human detection algorithm or very rare activities performed by the subject during the training phase. An example of a noisy measurement where the refrigerator door has been included in the binary silhouette of the occupant is shown in Figure 4.41. This caused *AR* to have an unusual value during the training phase.

Figure 4.41. An example of noisy Kinect observation in the training dataset.

Such outliers and noisy measurements are included in the range of generated MFs because the technique adopted in this chapter did not provide a mechanism to filter these from the main data distributions. During monitoring of some abnormal situations it was observed that outliers in the attributes could still trigger a fuzzy rule representing a regular behaviour pattern. This resulted in the system being unable to raise an alarm for those situations. One example of this was observed when applying the AMP-ADLs approach with $J$=3 to monitor the behaviour described in use-case #3 in the previous section.

## 4.5 Summary

This chapter presented an unsupervised fuzzy-logic-based approach for monitoring physical activities tailored to behaviours of each elderly individual using observations obtained from Kinect sensors. An unlabelled training dataset of normal behaviour patterns was collected to model specific dimensions of activities relevant to the wellbeing of the elderly (i.e. the body posture, location, time, and duration of ADLs). This was achieved by extracting a number of depth map attributes that described the occupant's location and posture and representing them via a specific number of fuzzy sets, the parameters of which were learned from the training data. The approach learned epochs of activities in each monitored location and then generated rules modelling frequent behaviour patterns associated with each epoch using a fuzzy association rule-mining algorithm. Unusual behaviours were detected in subsequent data by looking for patterns which differed from the learned normal behaviours.

Evaluation of the approach using testing sequences of various normal and abnormal behaviours showed the impact of the number of fuzzy sets generated for the depth map attributes on the

ability of the system to pick up various abnormal events and correctly classify normal behaviours. It was observed that while this number should be provided empirically, it has a major impact on the sensitivity and specificity of the approach. The evaluations also highlighted the need to elicit location-specific MFs for the depth map attributes to better tolerate slight attribute variations during activities and to address the outliers in the dataset.

The next chapter presents a robust MF generating technique which can automatically determine location-specific MFs for the depth map attributes. This technique is an improvement on the one presented in this chapter in terms of determining the number and parameters of MFs from the dataset of a depth map attribute while excluding outliers in data. It effectively addresses problems mentioned with regard to the proposed MF generating technique in this chapter.

# CHAPTER 5:
# AUTOMATIC GENERATION OF LOCATION-SPECIFIC MEMBERSHIP FUNCTIONS FOR THE DEPTH MAP ATTRIBUTES

Findings from Chapter 4 highlighted the need to elicit location-specific MFs for the depth map attributes in order to better tolerate slight attribute variations during physical activities. That chapter also proposed the need to address the outliers when defining MFs for a dataset. This chapter presents a robust MF generation technique which automatically determines location-specific MFs for those attributes. This technique replaces the one introduced in Section 4.2.1.2 as a part of the AMP-ADLs approach.

The chapter first provides a review of the limitations of the MF generating technique used in Chapter 4 to define MFs over the depth map attributes. This is followed by an explanation of how location-specific MFs for the depth map attributes can be used in fuzzy rules of AMP-ADLs to improve the monitoring of the occupant's physical ADLs (Section 5.2). It then presents the stages of the new MF generation technique to generate different forms of robust location-specific MFs in Section 5.3. The experimental results of evaluation of this technique are presented in Section 5.4 followed by a discussion and summary in Section 5.5 and 5.6 respectively.

## 5.1 Introduction

The AMP-ADLs approach for monitoring a home occupant's physical activities was presented in Chapter 4. The FCM clustering algorithm was employed in that approach to define a fixed number of fuzzy sets for each depth map attribute. For each attribute, these fuzzy sets were obtained based on processing the combined training dataset of all monitored locations. Evaluations revealed that this technique has a number of drawbacks including the inability of the generated fuzzy rules to tolerate variation of the attributes during some frequent activities and to address the impact of outliers and noisy measurements in data. It was also noted that variable number of MFs could better represent different physical ADLs carried out in different rooms. For example, two MFs could better represent the mixture distribution of attribute $Cx$ in the living room dataset (see Figure 4.37) while three MFs could better represent the mixture distribution of $Cx$ for the kitchen dataset (see Figure 4.39). When each MF covers a particular component in the mixture distribution of an attribute from a monitored location, variations

during ADLs in that location can be better tolerated by the fuzzy attributes.

This chapter presents a novel unsupervised technique (i.e. VBMS-RS) to generate location-specific MFs over depth map attributes. The rationale for developing this technique is to improve the accuracy of the AMP-ADLs approach. VBMS-RS is used in this approach instead of the FCM algorithm (presented in Section 4.2.1.2) in order to generate different number of MFs over a depth map attribute for each location. VBMS-RS is based on VBMS and RS.

The dataset of an attribute captured from each monitored location is processed separately in order to identify component distributions that represent frequent ADLs associated with that location. The analysis of the data distribution for each dataset is unsupervised as VBMS-RS first determines the number of modes in the PDF of data and then uses this value as the number of MFs. The associated parameters of MFs to represent the dataset are learned automatically from the data distribution and the generated MFs exclude noise and outliers in the data. The next section explains how location-specific MFs for the depth map attributes are used in fuzzy rules of the AMP-ADLs approach.

## 5.2 Applying location-specific MFs in the fuzzy rules of AMP-ADLs

The representation of fuzzy rules in AMP-ADLs is modified so that the fuzzy rules employ location-specific MFs to characterise the depth map attributes. From the previous chapter it is observed that the AMP-ADLs approach involves three stages. Fuzzy sets are defined for the depth map attributes in the second step of Stage 1. VBMS-RS is used in that step to generate location-specific fuzzy sets over the depth map attributes. Variable number of fuzzy sets are obtained for a depth map attribute to model ADLs associated with different locations. This results in the generation of a different fuzzy set for each monitored location to be tailored to frequent ADLs performed in that location. Location-specific fuzzy sets are therefore used in the antecedent of fuzzy rules obtained from Stage 2 of AMP-ADLs.

Let $d_r(a_k)$ be the training dataset of attribute $a_k$ $(k = 1, \cdots, 4)$ captured from location *r (r=1, …, R)*. Also let $l_{a_k}$ and $h_{a_k}$ denote the minimum and maximum values of $a_k$ across observations associated with all training datasets of $a_k$. Different number of fuzzy sets are defined over the domain of $a_k$ for different monitored locations. Assume that $F_{a_{k,\mathrm{r}}} = \{f_{a_{k,\mathrm{r}}}^1, \ldots, f_{a_{k,\mathrm{r}}}^{J_{k,\mathrm{r}}}\}$ is the set

of fuzzy sets obtained for attribute $a_k$ for location *r*. Each fuzzy set $f^{j}_{a_{k,\mathrm{r}}}$ in $F_{a_{k,\mathrm{r}}}$ represents the *j*-th fuzzy set in $F_{a_{k,\mathrm{r}}}$ and has an associated linguistic term as well as a membership function $\mu_{f^{j}_{a_{k,\mathrm{r}}}}(x)$ such that

$$\mu_{f^{j}_{a_{k,\mathrm{r}}}}(x) : [\, l_{a_k}, h_{a_k}\,] \rightarrow [0\,, 1].$$

These location-specific fuzzy sets replace the fuzzy sets introduced in Section 4.2.1.2 for characterising the depth map attributes. The fuzzy rules obtained from Stage 2 of AMP-ADLs can then be divided into *R* subsections with each having different fuzzy sets in their antecedents to characterise the depth map attributes. An example of such fuzzy rules is shown in Table 5.1. *k* is equal to 1 in the case of *AR*. Table 5.1 shows that this attribute has three fuzzy sets $f^{1}_{a_{1,1}}, f^{2}_{a_{1,1}}$, and $f^{3}_{a_{1,1}}$ for location *r=1*, and two fuzzy sets, denoted as $f^{1}_{a_{1,2}}$ and $f^{2}_{a_{1,2}}$, for location *r=2*.

Table 5.1 An example of a fuzzy rule set with location-specific MFs.

| | | | | ***Antecedent*** | | | | ***Consequent*** |
|---|---|---|---|---|---|---|---|---|
| | ***Index*** | ***r*** | ***Time*** | ***AR*** | ***O*** | $C_x$ | $C_y$ | ***Duration*** |
| r=1 | $\mathrm{rule}_1$ | 1 | $\mathrm{T}^{1}_{\mathrm{d}_1}$ | $f^{1}_{a_{1,1}}$ | $f^{3}_{a_{2,1}}$ | $f^{1}_{a_{3,1}}$ | $f^{2}_{a_{4,1}}$ | $Duration_1^{e^{1}_{d_1}}$ |
| | $\mathrm{rule}_2$ | 1 | $\mathrm{T}^{2}_{\mathrm{d}_1}$ | $f^{3}_{a_{1,1}}$ | $f^{2}_{a_{2,1}}$ | $f^{1}_{a_{3,1}}$ | $f^{2}_{a_{4,1}}$ | $Duration_1^{e^{2}_{d_1}}$ |
| | $\mathrm{rule}_3$ | 1 | $\mathrm{T}^{2}_{\mathrm{d}_1}$ | $f^{2}_{a_{1,1}}$ | $f^{1}_{a_{2,1}}$ | $f^{2}_{a_{3,1}}$ | $f^{2}_{a_{4,1}}$ | $Duration_2^{e^{2}_{d_1}}$ |
| r=2 | $\mathrm{rule}_4$ | 2 | $\mathrm{T}^{1}_{\mathrm{d}_2}$ | $f^{2}_{a_{1,2}}$ | $f^{1}_{a_{2,2}}$ | $f^{1}_{a_{3,2}}$ | $f^{1}_{a_{4,2}}$ | $Duration_1^{\mathrm{e}^{1}_{\mathrm{d}_2}}$ |
| | $\mathrm{rule}_5$ | 2 | $\mathrm{T}^{1}_{\mathrm{d}_3}$ | $f^{1}_{a_{1,2}}$ | $f^{1}_{a_{2,2}}$ | $f^{1}_{a_{3,2}}$ | $f^{1}_{a_{4,2}}$ | $Duration_2^{\mathrm{e}^{1}_{\mathrm{d}_3}}$ |
| | ⋮ | ⋮ | ⋮ | ⋮ | ⋮ | ⋮ | ⋮ | ⋮ |
| r=R | $\mathrm{rule}_{n-1}$ | R | $\mathrm{T}^{1}_{\mathrm{d}_2}$ | $f^{2}_{a_{1,R}}$ | $f^{1}_{a_{2,R}}$ | $f^{2}_{a_{3,R}}$ | $f^{1}_{a_{4,R}}$ | $Duration_1^{\mathrm{e}^{1}_{\mathrm{d}_2}}$ |
| | $\mathrm{rule}_n$ | R | $\mathrm{T}^{1}_{\mathrm{d}_3}$ | $f^{1}_{a_{1,R}}$ | $f^{2}_{a_{2,R}}$ | $f^{3}_{a_{3,R}}$ | $f^{1}_{a_{4,R}}$ | $Duration_2^{\mathrm{e}^{1}_{\mathrm{d}_3}}$ |

The notation of each fuzzy rule *i* when using location-specific fuzzy sets changes to the following:

*IF Location is r AND Time is* $epoch_r^i$ *AND AR is* $A_r^1$ *AND* $\theta$ *is* $A_r^2$ *AND Cx is* $A_r^3$ *AND Cy is* $A_r^4$ *THEN Duration is* $Duration_q^{epoch_r^i}$.

Here $A_r^1$, $A_r^2$, $A_r^3$, and $A_r^4$ are fuzzy sets of the depth map attributes associated with location *r*, the combination of which defines a frequent behaviour pattern in that location.

The next section describes how VBMS-RS automatically generates robust location-specific MFs for the depth maps attributes. MFs generated by this technique are robust with respect to noisy and outlier sensor data as they only cover main components in the distribution of data.

## 5.3 The procedure of VBMS-RS

The procedure undertaken for VBMS-RS is described in this section. The input to VBMS-RS is a training dataset of a depth map attribute, captured by a Kinect sensor from a monitored location, and the output is a number of MFs, defined automatically to characterise the attribute's values. Let the attribute in the given dataset take a series of crisp numerical values $x_n$ $(n = 1, \dots, N)$ and assume that these data points belong to an unknown data distribution. The two-step procedure of VBMS-RS to generate MFs over the attribute is as below:

Step 1. Use VBMS to locate modes (local maxima) in the distribution of the attribute and to cluster data points associated with each mode. VBMS is a nonparametric clustering technique which does not require the number of clusters to be defined. It takes data with an unknown density function and estimates the density of data by taking the average of locally-scaled kernels centred at each of the data points. Each data point is mapped into its corresponding mode to constitute clusters of data. The procedure of VBMS is described in Section 3.6.5.2

Step 2. Use the SAB technique to obtain the normal range of data points for each cluster (where there are no outliers) and accordingly define a MF to represent the cluster.

The output of Step 1 is: 1) the location of modes in the attribute distribution and 2) the cluster of data points associated with each mode. Each data cluster represents a component distribution in the attribute mixture of distributions. When an attribute has a multimodal distribution, the width of the component distribution associated with each mode might be different. Using a

kernel function with one fixed global bandwidth is not considered to be optimal for estimating the location of modes in such distribution and a choice of local bandwidth for each data point can lead to better results (Comaniciu et al., 2001). This is mainly because the density estimator can be adapted to the density of each target data point and can take a larger bandwidth where data points are sparse (Brockmann, Gasser, & Herrmann, 1993). VBMS determines a local bandwidth for the kernel function applied on each data point in a way that kernels corresponding to points in tails of the data distributions receive a wider bandwidth than kernels applied on the data points lying in the large density region of distributions. As a result, the estimated density function for tails of the distributions is further smoothed.

MFs are defined in Step 2 to represent data clusters obtained from Step 1. The number of MFs is equal to the number of modes detected in the attribute data distribution. For each data cluster obtained from Step 1, the location of the cluster centre and its normal range are used to determine the parameters of the respective MF. The SAB technique is employed to determine the normal range of a data cluster.

The SAB technique is a graphical tool (with a robust measure of skewness) used in RS for the purpose of outlier detection. Given data points with a continuous unimodal distribution, SAB first calculates a robust measure of the skewness of the underlying data distribution. It then outputs a normal range for the data points which excludes possible outliers from the regular data. Details associated with this technique can be found in Section 3.6.4.

VBMS-RS can be employed to determine the parameters associated with different forms of MFs to characterise the depth map attributes. The following sections demonstrate how Step 2 of this technique determines the parameters of two different types of MF, namely the triangular and trapezoidal MFs. These two types of MFs are selected because of their simplicity of calculation and ability to represent skewed distributions.

### 5.3.1 Generating triangular membership functions

The parameters of a triangular MF are defined by a triad (A, B, C) with A, B, and C respectively representing the location of the left foot, the centre, and the right foot (see Section 3.6.1). The mode and the normal range of a detected data cluster are used in Step 2 of VBMS-RS to define a triangular MF. This is illustrated through an example in Figure 5.1. Figure 5.1 (a) shows the

histogram associated with an identified cluster from Step 1. A PDF is estimated through normalising this histogram by scaling its maximum height to one. The respective triangular MF obtained from Step 2 to represent the cluster is shown in Figure 5.1 (b).

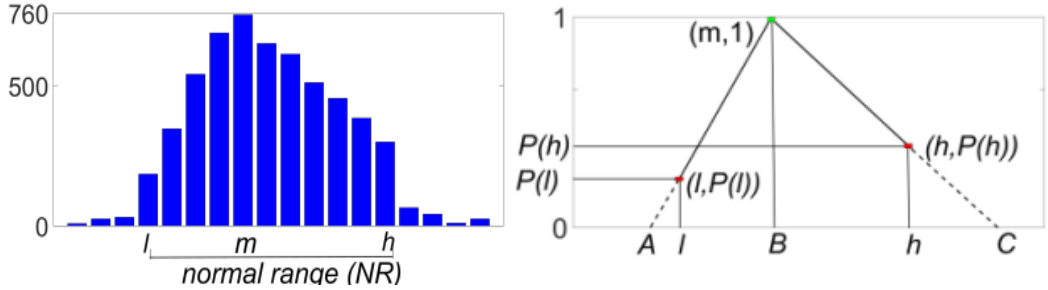


(a) (b)

Figure 5.1. (a) An example of a histogram of a data cluster obtained from Step 1. The vertical axis shows the number of data points in each bin. (b) The triangular MF defined to represent the cluster.

$m$ in Figure 5.1 (a) denotes the location of the mode in the data cluster and $[l, h]$ represents the normal range of the cluster. The following operations are performed in Step 2 of VBMS-RS to define the triangular MF shown in Figure 5.1 (b).

1. Calculate the probability density of the lowest value ($l$) and the highest value ($h$), denoted by $P(l)$ and $P(h)$, respectively (see Figure 5.1 (b)).
2. Extrapolate *A* from the two points ($m$, 1) and ($l$, $P(l)$).
3. Extrapolate *C* from the two points ($h$, $P(h)$) and ($m$, 1).
4. Set *B* as *m* and define the triangular MF using Equation 5.1.

$$\mu^i(x) = \begin{cases} 0 & if\ x \leq \mathrm{A} \\ \dfrac{x - \mathrm{A}}{\mathrm{B} - C_i} & if\ A < x \leq \mathrm{B} \\ \dfrac{\mathrm{C} - x}{\mathrm{C} - \mathrm{B}} & if\ \mathrm{B} < x \leq \mathrm{C} \\ 0 & if\ \mathrm{C} \leq x \end{cases} \tag{5.1}$$

Note that the location of mode has the highest probability in the PDF of a cluster. This location

is adopted as $B$ (the centre of the respective triangular MF) to represent the full membership of the mode in the cluster. In the extrapolating calculations performed in operations 2 and 3, point ($m$, 1) represents the coordinates of the mode in the PDF.

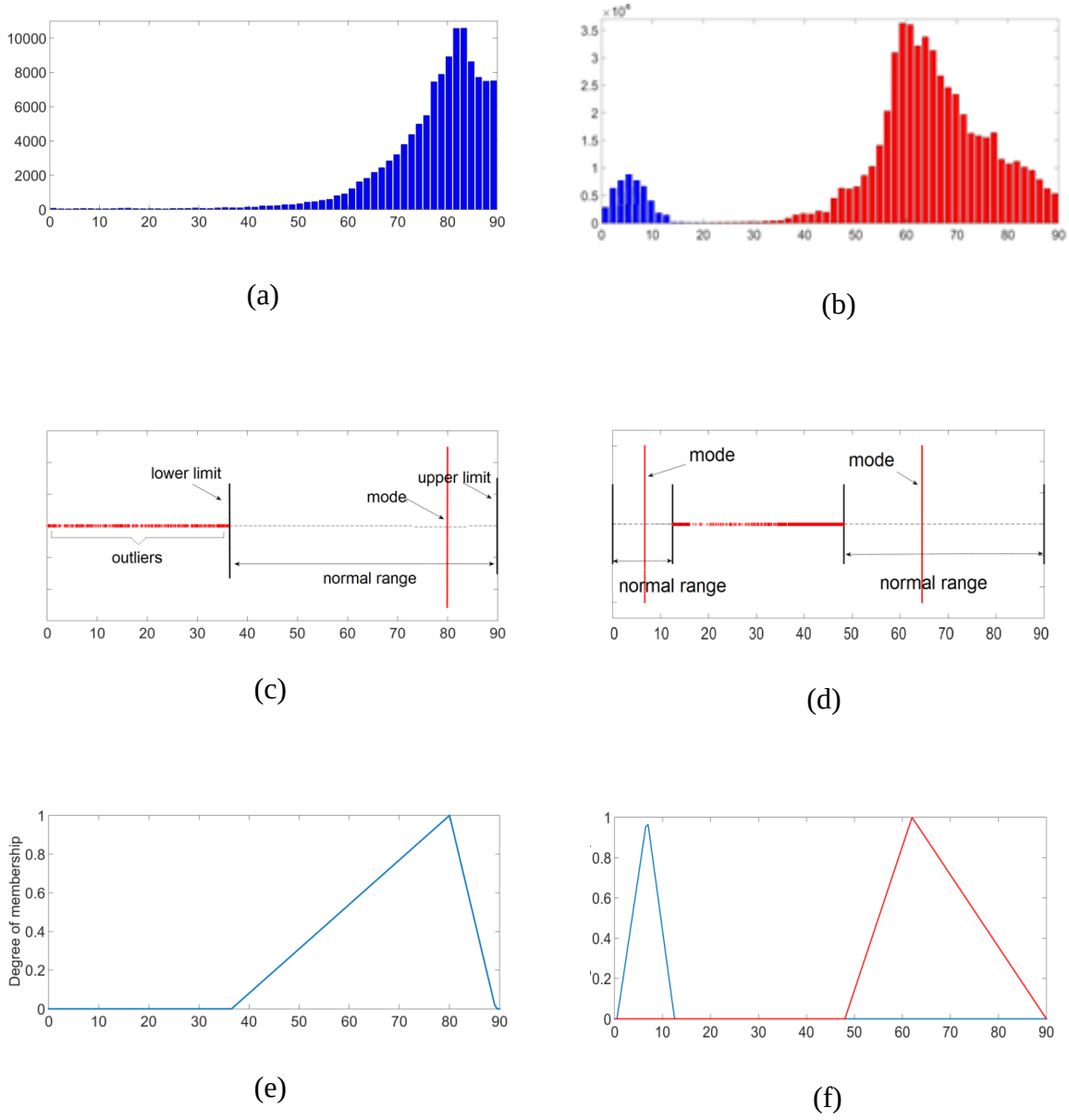


Figure 5.2 (a) and (b) are examples of attributes with a unimodal and bimodal distributions, respectively. (c) and (d) show the normal range and the location of the mode detected for these distributions, respectively. (e) and (f) display the obtained triangular MFs.

Examples of histograms for attributes with unimodal and bimodal distributions are shown in Figure 5.2 (a) and (b), respectively. Each component distribution associated with a detected mode is shown with a different colour. VBMS associated all the data points with the only mode detected in the PDF of the unimodal distribution in Figure 5.2 (a). VBMS has detected two

separate distributions as shown in blue and red colours for the bimodal distributions in Figure 5.2 (b). The normal range and the location of the mode detected for each of the component distributions in Figure 5.2 (a) and (b) are shown in Figure 5.2 (c) and (d), respectively.

The detected normal range of each distribution is shown by the two vertical black lines in Figure 5.2 (c) and (d). The range between these two lines forms the normal range of the cluster. Figure 5.2 (c) shows the distance between the lower limit and the mode of the distribution is larger than that between the mode and the upper limit, hence the skewness of the underlying distribution. The data points shown as red dots outside of the detected normal ranges in Figure 5.2 (c) and (d) are marked as outliers in VBMS-RS and are eliminated. The triangular MFs representing the component distributions in Figure 5.2 (a) and (b) are shown in Figure 5.2 (e) and (f), respectively.

### 5.3.2 Generating trapezoidal membership functions

The trapezoidal MF is defined by four parameters *A*, *B*, *C*, *D* (with $A < B \leq C < D$) in Section 3.6.1. In Step 2 of VBMS-RS these parameters are determined through obtaining the normal range and the first and third quartiles of the data cluster. Figure 5.3 (a) shows the histogram for an example data cluster obtained from Step 1. *Q1* and *Q3* in this example denote the location of the first and third quartiles, respectively. The normal range of the cluster is shown as $[l, h]$. The following operations are performed in Step 2 of VBMS-RS to define the trapezoidal MF shown in Figure 5.3 (b).

1. Calculate the probability density of the lowest value ($l$) and the highest value ($h$) of the cluster, denoted by $P(l)$ and $P(h)$, respectively (see Figure 5.3 (b)).
2. Extrapolate *A* from the two points ($Q1$, 1) and ($l$, $P(l)$).
3. Set *B* and *C* as the locations of *Q1* and *Q3*, respectively.
4. Extrapolate *D* from the two points ($h$, $P(h)$) and ($Q3$, 1).
5. Define the trapezoidal MF using Equation (5.2).

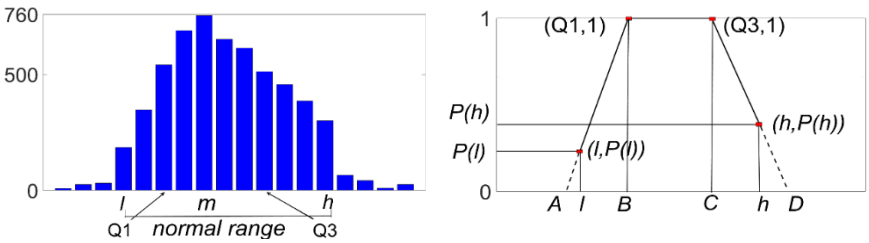


(a) (b)

Figure 5.3. (a) An example of a histogram of a data cluster obtained from Step 1. The vertical axis shows the number of data points in each bin. (b) The corresponding trapezoidal MF defined for the cluster.

$$\mu^i(x) = \begin{cases} 0 & if\ x \leq A \\ \frac{x-A}{B-C} & if\ A<x<B \\ 1 & if\ B \leq x \leq C \\ \frac{C-x}{C-B} & if\ C<x \leq D \\ 0 & if\ C \leq x \end{cases}$$

(5.2)

Data between *Q1* and *Q3* are assigned full membership as they represent the middle 50% of cluster values. Points ($Q1$, 1) and ($Q3$, 1) represent the coordinates of the shoulders in the extrapolation performed in operations 2 and 4.

### 5.3.3 Impact of the shape of a cluster on the support of its MF

The supports of the generated triangular MFs can be greater than those of the trapezoidal MFs. This is dependent on the shape of the data cluster. Figure 5.4 (a) shows an example data distribution with different colours indicating the range of clusters identified from Step 1 of VBMS-RS. The characteristics of the triangular and trapezoidal MFs generated for the cluster shown in red is presented in Figure 5.4 (b). The tail ends of this cluster have been truncated as the cluster is located in the middle of the data distribution. When the extrapolations are performed to obtain parameters of the triangular and trapezoidal MFs, it is evident that the support of the triangular MF is greater than that of the trapezoidal MF. This means that generated triangular MFs generally can tolerate more perturbation of normal data without labelling them as abnormal.

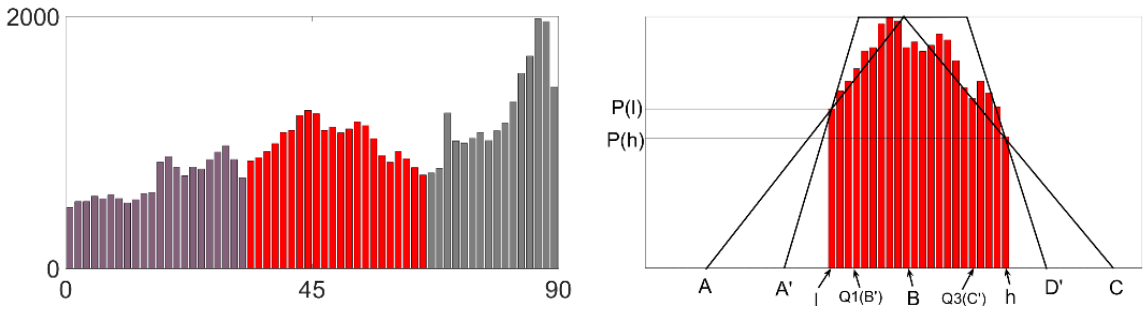


(a) (b)

Figure 5.4**.** (a) An example data distribution - different colours indicate the range of clusters obtained in Step 1. (b) The characteristics of the triangular and trapezoidal MFs generated for the cluster shown in red.

## 5.4 Experimental results

The captured dataset from the testbed (Section 3.5.3) was used to evaluate the performance of VBMS-RS. The evaluation consisted of three stages. In the first stage, the performance of VBMS-RS in parameterising the depth map attributes was compared with other MFs generation techniques. In the second stage, the impact of employing VBMS-RS in the AMP-ADLs approach was evaluated. The performance of the fuzzy rule set obtained based on VBMS-RS was compared with that of the rule sets obtained based on using other MFs generation techniques. Both triangular and trapezoidal MFs were generated in these two stages in order to evaluate the impact of the shape of MFs on the performance of AMP-ADLs. In the last stage, the performance of monitoring physical ADLs using VBMS-RS was compared against other state-of-the-art unsupervised fuzzy monitoring approaches.

### 5.4.1 Comparison of techniques for parameterizing the attributes

The training dataset of each attribute captured from different locations were found to have different data distributions. These datasets were used to compare the parameterisation results between VBMS–RS and other techniques. These techniques involved:

1. Using mean shift (MS) instead of VBMS in Step 1 of the proposed approach followed by the procedure of robust statistics in Step 2. This technique is denoted as MS–RS.

2. Using the FCM clustering algorithm to generate a fixed number of membership functions without the use of robust statistics. This was the same technique used in Chapter 4 to generate MFs over depth map attributes (see Section 4.2.1.2). In the

experiments in this chapter, however, this technique processed the dataset of each location separately and generated location-specific MFs. The number of clusters to be created for a dataset of an attribute associated with a location was set according to the number of modes in the data distribution.

The rest of this section describes the results of comparisons conducted based on the clusters and MFs produced by each of the techniques.

***Attribute with separate component distributions***

An example of an attribute with separate component distributions was $Cx$ captured from the living room area. The data distribution of this dataset is shown via the histograms on the left-hand side of Figure 5.5 (i.e. (a), (d), and (g)). Figure 5.6 (a) illustrates the results of using VBMS–RS for parameterising this dataset. Each component distribution that has been associated with a detected mode is shown with a different colour.

VBMS–RS could correctly divide this attribute into two main component distributions. The component distribution to the right in Figure 5.5 (a) is in the shape of reverse-J (skewed to the left). The corresponding triangular and trapezoidal MFs defined by VBMS–RS represented only the range of the normal data points associated with this component distribution (see Figure 5.5 (b) and (c)). Note that since the normal ranges obtained for both clusters in Figure 5.5 (a) are small, the shoulders of the trapezoidal MFs in Figure 5.5 (c) are small. Therefore, both the trapezoidal and triangular MFs have similar shapes and cover nearly the same area in the attribute space.

VBMS was replaced with MS in Step 1 of the proposed MF generation technique and the experiment was repeated. Results demonstrated that both methods work equally well where the component distributions in the attribute space are separated. MS–RS requires an empirical input (i.e. the bandwidth parameter) whereas the initial bandwidth for VBMS-RS is automatically derived from the data (see Section 3.6.5.2).

In the comparison of VBMS-RS with the FCM technique, the number of membership functions was empirically set to 2 (as this was obvious from a visual examination of the data). This technique correctly identified the two component distributions in the attribute space as demonstrated in Figure 5.5 (g). The triangular and trapezoidal MFs in Figure 5.5 (h) and (i)

were generated, respectively to represent the two detected component distributions. Since this technique does not use robust statistics, the resulting parameterisation of the attribute was not the same as that of VBMS-RS. The MFs generated by this technique had a wider support and thus represented a wider area outside the normal range of the two component distributions. This resulted in the MFs generated by this technique to encompass many rare observations (outliers) around the main component distributions. For example, the triangular MFs generated by FCM gave membership degrees 0.17 and 0.83 to the outlier point $Cx$ =400. This was in contrast to the triangular MFs generated by VBMS-RS which gave zero membership to this outlier point.

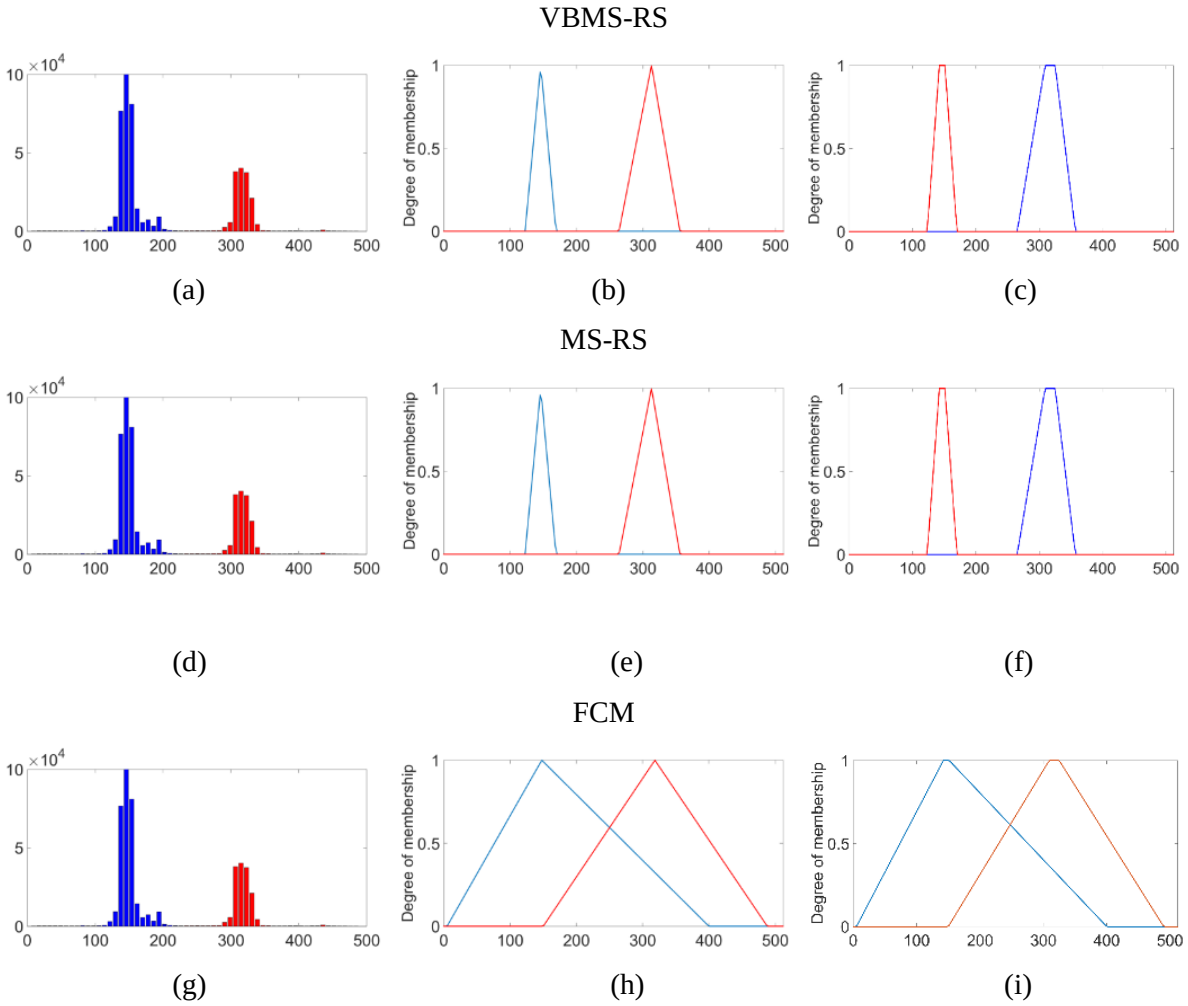


Figure 5.5. Results for different techniques of parameterising an attribute which has two separate component distributions. The different colours in each of (a), (d), and (g) show the ranges of clusters obtained from different techniques. (b), (e), and (h) show the respective triangular MFs, resulted from the output of the 3MF generation techniques. (c), (f) and (i) show the trapezoidal MFs resulted from the output of the 3 techniques.

***Attribute with a unimodal distribution***

One example of attributes which possessed a unimodal skewed distribution was *AR* from the dining room. The data distribution of this dataset is illustrated in images on the left-hand side of Figure 5.6 (i.e. (a), (d), and (g)). The data distribution shown in those images illustrates the skewed distribution of *AR*. Different colours in each of the images indicate the distributions related to the clusters that have been identified using different Mf generation techniques. The triangular MFs generated using the three techniques are illustrated in Figure 5.6 (b), (e), and (h). The results of using the three techniques for generating trapezoidal MFs are provided in Figure 5.6 (c), (f), and (i).

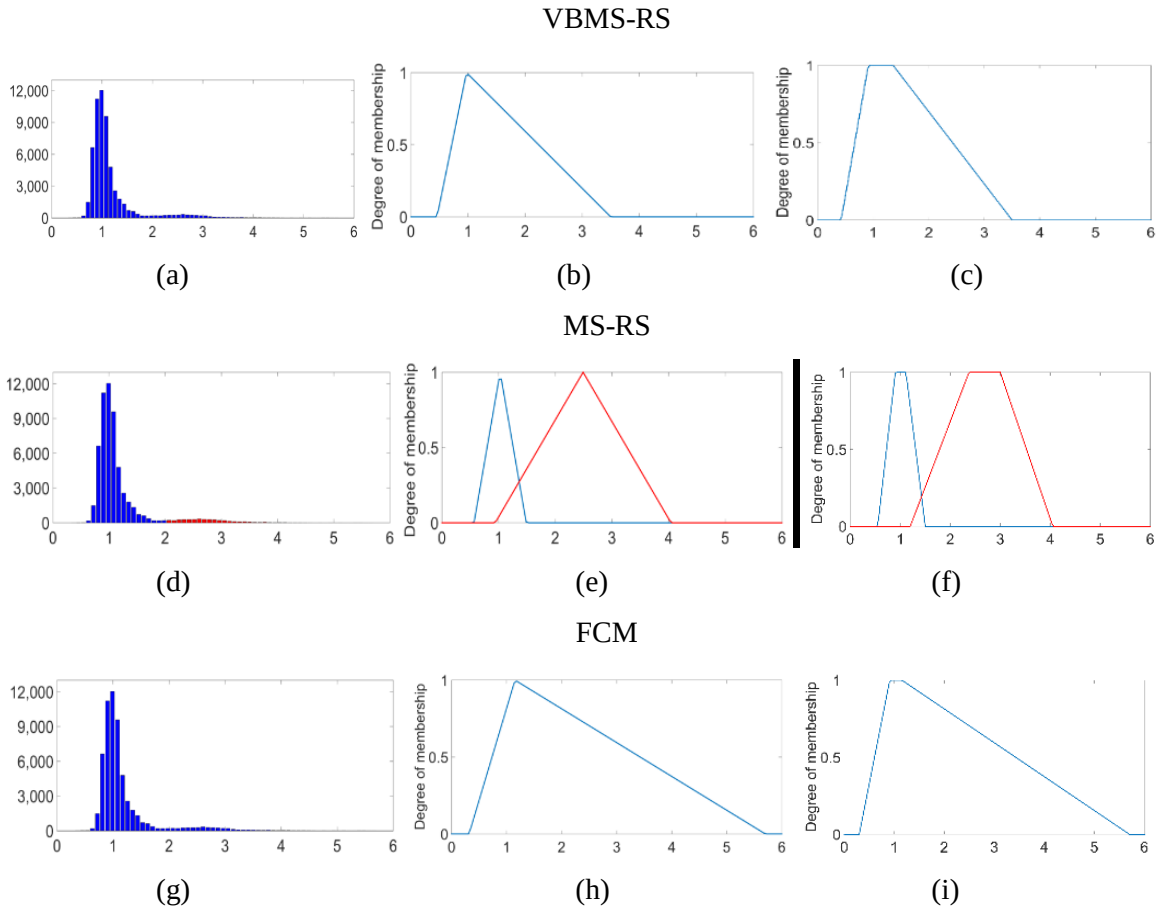


Figure 5.6. Using different techniques for parameterising distribution of *AR* attribute for the dining room dataset. (a), (d), and (g) show the range of clusters obtained using the 3 different techniques. (b), (e), and (h) show the respective triangular MFs resulting from the output of the 3 techniques. (c), (f) and (i) show the corresponding trapezoidal MFs resulting from the output of the 3 techniques.

VBMS-RS correctly associated all data points with the only mode in the distribution (see Figure 5.6 (a)). This was in contrast to the results of using MS-RS (Figure 5.6 (d)) as it broke the distribution into two clusters. This difference was because in VBMS data points that

correspond to the tails of the underlying density received a broader neighbourhood and a smaller importance. This resulted in these points being included in the main component distributions and the tails of the underlying density not being divided into smaller pieces. This is unlike MS as it assigned a fixed global bandwidth to all data points and assigned them the same importance when estimating the PDF of data.

The input value for the number of clusters in FCM was set to 1 because the distribution was unimodal. Figure 5.6 (g) shows that although this technique grouped all data points in the distribution into the stipulated one cluster, the supports of the generated MFs in Figure 5.6 (h) and (i) were much broader than the MFs generated by VBMS-RS. This can lead to non-specific responses for classification of the attribute values (i.e. every point is considered to be in the fuzzy set).

The MFs generated by FCM represented many rare observations (outliers) located between *AR*=4 and *AR*=6. The rules generated based on such MFs could not correctly classify a new abnormal observation within that range. This was in contrast to the results of VBMS-RS as both the triangular and trapezoidal MFs generated by this technique did not represent any data point for outside the normal range [0.5, 3.5]. VBMS-RS yielded better classification results for normal points and handled outlier observations more accurately.

***Attribute with a multimodal distribution***

An example of an attribute with a multimodal distribution was $C_x$ from the kitchen dataset. Examining the Kinect observations for this dataset showed three distinct places for $C_x$ where the occupant performed most of the activities in the kitchen. The PDF of this attribute had three modes, each associated with a component distribution in the attribute mixture distribution. The three components overlap.

The results of parameterising this attribute using the different MF generation techniques are shown in Figure 5.7. Input value for the number of clusters to be created by FCM was set to 3. Results indicated that unlike other techniques, VBMS-RS correctly partitioned the feature space into the right number of MFs, according to the components in the mixture distribution. The results for VBMS-RS and MS-RS differ because VBMS assigned a narrower neighbourhood to the data points lying in large density regions. This example shows that VBMS could identify mixed component distributions more accurately than MS when the

attribute has a mixture of multiple distributions. This finding is consistent with other findings by Comaniciu et al. (2001).

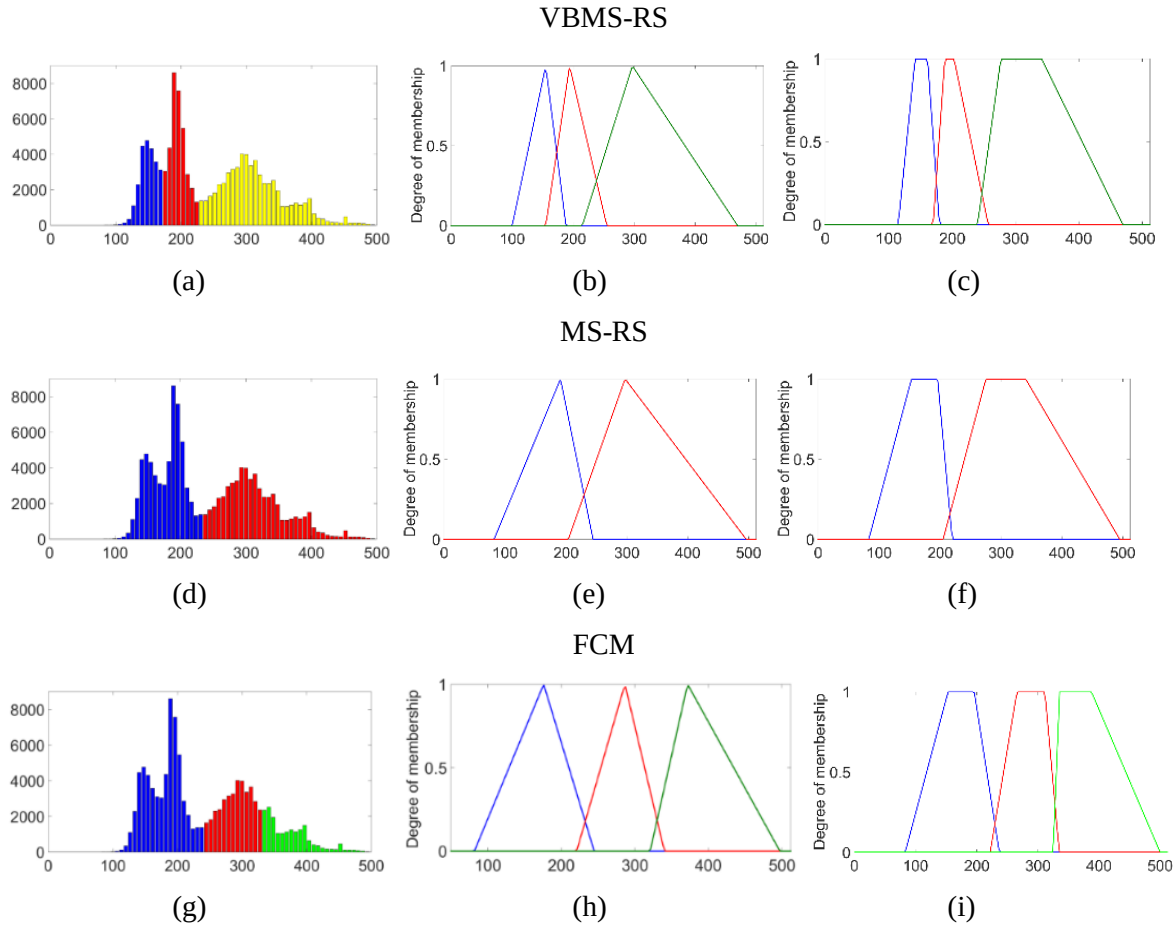


Figure 5.7. Using different techniques for parameterising distribution of *AR* from the dining room dataset. (a), (d), and (g) show the range of clusters obtained using the 3 MF generation techniques. (b), (e), and (h) show the respective triangular MFs resulting from the output of the 3 techniques. (c), (f) and (i) show the corresponding trapezoidal MFs resulting from the output of the 3 techniques.

The ranges of the triangular MFs generated by the three techniques were generally greater than that of the ranges of the trapezoidal MFs (see Figure 5.7). For example, the wider data distribution associated with the right-hand-side cluster (ranging from pixel location 220 to 500) in Figure 5.7 (a) and (d) caused the respective trapezoidal MFs in Figure 5.7 (c) and (f) to have a relatively wider shoulder. This in turn resulted in those MFs receiving steeper descending foots upon performing the extrapolation in Step 2 of VBMS-RS. These MFs also covered less area when compared to their respective triangular MFs in Figure 5.7 (b) and (e). The wider support of triangular MFs allowed more variations of normal data for each cluster which means they could tolerate more variation in physical ADLs without labelling them as abnormal.

The FCM technique partitioned the attribute space by three MFs as shown in Figure 5.7 (g).

Parameters of these MFs were different to those of the results from VBMS-RS. The reason was that this technique aimed to minimise the distance of data points from their respective cluster centres. The locations of the cluster centres identified by FCM did not always correspond to the modes in the distribution of data. As a result of this, the same MF represented both component distributions that have modes on pixel locations 150 and 200 (see Figure 5.7 (h) and (i)).

### 5.4.2 The performance of AMP-ADLs based on using different MF generation techniques

The characteristics of MFs generated by a particular technique have a direct impact on the performance of the corresponding fuzzy rule set for classification purposes. A better technique to estimate the component distributions of an attribute can generate more representative MFs and provide a higher classification accuracy of the corresponding rule set. This section provides the findings from comparing the classification performance of fuzzy rule sets obtained from employing the output of three possible MF generation techniques including VBMS-RS. As the training dataset of Kinect observations involved data from four Kinect sensors and the dataset from each Kinect was associated with four depth map attributes with different numbers of modes in their PDFs, the number of clusters for FCM was empirically set to a specific number (i.e. 3) to suit all situations.

The total number of rules obtained from the output of each MF generation technique is shown in Table 5.2. VBMS-RS resulted in the least number of rules. It was observed that by using this technique slight variations during most physical ADLs were represented by the same combination of fuzzy attributes. This was due to the MFs generated by this technique accurately representing component distributions in the space of attributes which in turn resulted in one fuzzy rule to be generated for modelling each physical ADL. For example, two fuzzy rules were generated to represent the frequent activities of sitting behind the computer desk and sitting on the sofa for each of the four activity epochs in the living room. This caused eight rules to be generated for the living room rule set. In addition to these eight rules, another rule was generated to model the activity of sleeping on the sofa in the afternoon epoch. The set of these nine rules represented the nine physical ADLs frequently carried out by the occupant during the collection of the training dataset (see Table 3.4).

Using the output of other MF generation techniques (e.g. FCM and MS-RS) resulted in a higher number of rules to be generated as indicated in Table 5.2. This was due to the MFs obtained from the output of those techniques not necessarily representing component distributions in the dataset of attributes. This was also due to the slightly different values of attributes during an ADL being represented by different fuzzy sets. This resulted in different fuzzy rules to be generated for modelling slightly different versions of the same activity and a resultant higher number of rules.

The numbers of rules obtained when different techniques generated trapezoidal MFs were slightly higher than the numbers of rules when those techniques generated triangular MFs, as shown in Table 5.2. In most cases, the generated trapezoidal MFs had narrower support than their respective triangular ones. More combinations of fuzzy attributes were then required to represent variations of the attributes during activities. Since the triangular and trapezoidal MFs generated by VBMS-RS represented component distributions well, variations in attributes during activities have been modelled by very similar numbers of rules.

The *Testing_Data 1* used in this study had 60 recordings of different scenarios for normal and abnormal behaviours for each location, with 30 recordings for each category of normal and abnormal behaviours. These were used to evaluate the classification accuracy of the fuzzy rule set obtained using the output of different MF generation techniques. The classification accuracy of using different types of MFs was also evaluated. The results of these evaluations are shown in Table 5.3. The accuracy of the monitoring approach was 86.3% when MS-RS generated triangular MFs in the fuzzy rules. This was largely due to MS-RS not identifying overlapping component distributions of attributes. In some occasions one MF was generated to represent two overlapping component distributions in an attribute, which caused multiple physical ADLs to be represented by one fuzzy rule. For example, values of *AR* for crouching on the kitchen floor (to pick up an object) and bending down (to manipulate objects inside the kitchen cabinet) were grouped into the same cluster although each belonged to different component distributions in the attribute space. The corresponding fuzzy rule was not able to label a recording for spending a long time sitting on the kitchen floor as abnormal behaviour.

Using MS-RS to obtain trapezoidal MFs resulted in a slightly lower classification accuracy than the case of triangular MFs. The supports of the trapezoidal MFs were narrower in comparison with those of their respective triangular MFs and thus slightly different normal

behaviour of the occupant in more number of recordings was misclassified as abnormal.

The classification that resulted from using FCM to generate triangular MFs produced an average accuracy of 80.1%. This was because the rule set obtained based on this technique misclassified normal behaviour patterns that were slightly different from their corresponding training samples. The reason was that FCM divided the component distributions of many attributes into pieces. When most of training values for a given activity belonged to a particular part of the component distribution and the values for test sequences fell into another part, the corresponding fuzzy rule could not fire, hence less accuracy of the classifier. The MFs generated by this technique also represented many outliers in the attributes which resulted in some test recordings that represented an abnormal behaviour to be misclassified as normal. Using FCM to generate trapezoidal MFs produced a less average accuracy of 77.2%.

Table 5.2. The number of fuzzy rules obtained from the output of different MF generation techniques for different monitored locations.

| ***Technique*** | ***Type of MF*** | ***Kitchen*** | ***Living room*** | ***Dining room*** | ***Bedroom*** | ***Overall*** |
|---|---|---|---|---|---|---|
| FCM | Triangular | 30 | 28 | 22 | 2 | 82 |
| | Trapezoidal | 33 | 29 | 23 | 2 | 87 |
| MS-RS | Triangular | 24 | 12 | 9 | 2 | 47 |
| | Trapezoidal | 26 | 13 | 11 | 2 | 52 |
| VBMS-RS | Triangular | 15 | 9 | 6 | 2 | 32 |
| | Trapezoidal | 16 | 9 | 6 | 2 | 33 |

Note that in the experiments in this chapter, FCM processed the dataset of each location separately to generate location-specific MFs. This was different from the MF generation technique presented in Chapter 4 in which FCM processed the combined dataset of all locations for an attribute to generate MFs. The resulting fuzzy rules which used location-specific MFs showed a higher classification performance than those generated in Chapter 4 (see Table 4.8 for comparison). This confirms the hypothesis that location-specific MFs can be used to better represent physical ADLs performed in each location of a house.

The classification accuracy of the fuzzy rules obtained by applying VBMS without RS was also evaluated and the results are shown in Table 5.3. Using VBMS to generate triangular MFs resulted in many test recordings for abnormal behaviour to be label as normal. Since RS was

not employed in generating MFs, the range of the triangular MFs was wider than the range of their respective component distributions and thus they included many outlier values. Although values of attributes in those test recordings for abnormal behaviour were well outside of the normal range of component distributions they caused fuzzy rules for normal behaviours to fire and resulted in those recordings being labelled normal. The generated trapezoidal MFs covered less area (fewer outliers) in the space of each attribute and caused slightly fewer test sequences for abnormal behaviour to be labelled as normal.

The rule set obtained from the triangular MFs generated by VBMS-RS could classify most test sequences correctly with an accuracy of 92.9% (see Table 5.3). Combining VBMS and RS caused most of the triangular MFs to represent only the normal range of the component distributions in the attributes. While the outlier observations for abnormal behaviours were classified correctly, the attribute values during most recordings of normal behaviour were represented correctly by the generated MFs. These recordings of normal behaviour triggered a rule corresponding to a normal behaviour. The misclassified recordings for normal behaviour were those representing new behaviour patterns of the occupant. One example was cleaning inside the refrigerator for eight minutes in the morning, a behaviour which was not present in the training data. The approach could classify such observations correctly by introducing a more comprehensive training dataset consisting of typical ADLs with more variability.

Table 5.3. The classification accuracy of different fuzzy rule sets obtained from the output of different MF generation techniques.

| ***Method*** | ***Type of MF*** | ***Accuracy for normal behaviours*** | ***Accuracy for abnormal behaviours*** | ***Overall accuracy*** |
|---|---|---|---|---|
| FCM (3 clusters) | Triangular | 81.7% | 78.4% | 80.1% |
| | Trapezoidal | 78.0% | 76.3% | 77.2% |
| MS-RS | Trapezoidal | 87.5% | 85.0% | 86.3% |
| | Triangular | 89.0% | 83.7% | 86.4% |
| VBMS | Trapezoidal | 95.0% | 84.2% | 89.6% |
| | Triangular | 95.8% | 83.3% | 89.6% |
| VBMS-RS | Trapezoidal | 93.3% | 89.1% | 91.2% |
| | Triangular | 95.0% | 90.8% | 92.9% |

### 5.4.3 Comparison with other monitoring approaches

The performance of the AMP-ADLs approach was compared with other unsupervised monitoring approaches. These approaches were the two fuzzy monitoring systems presented by Seki (2009) and Brulin et al. (2012). The validation datasets in these studies were collected using 2D cameras in laboratory environments. As these datasets were not publicly available, the dataset collected from the testbed was used for evaluating the performance of all approaches. The fuzzy rule set in the proposed approach was generated by using VBMS-RS and triangular MFs. The results of evaluations are shown in Table 5.4 where the proposed approach is denoted as "AMP-ADLs with triangular MFs".

The approach described by Seki (2009) used omni-directional cameras to extract attributes from the binary mask of a detected person in order to monitor their physical ADLs. The attributes included the area of the silhouette, the orientation of the body, and the coordinates of the silhouette's center of gravity. The crisp attribute values in a training dataset were converted into their fuzzy equivalents. The day was then divided into three-hour overlapping epochs and fuzzy rules were constructed for each epoch to model the frequency of fuzzy attributes (i.e. behaviour patterns). Unusual behaviour patterns were then identified for each epoch as those combinations of fuzzy attributes with low probability of occurrence.

Table 5.4. The performance of different approaches for monitoring physical ADLs in the collected dataset.

| ***Approach*** | ***Accuracy for Normal behaviours*** | ***Accuracy for Abnormal behaviours*** | ***Overall accuracy*** |
|---|---|---|---|
| The approach in Seki (2009) | 74.2% | 67.5% | 70.8% |
| The approach in Brulin et al. (2012) | 73.3% | 70.0% | 71.7% |
| AMP-ADLs with triangular MFs | 95.0% | 90.8% | 92.9% |

The abovementioned attributes were extracted from the binary mask of the occupant in Kinect training observations. Following the technique employed by Seki (2009), six fuzzy sets with evenly distributed triangular MFs were defined over each attribute. The attributes' crisp values were then converted into fuzzy labels. The frequency of observing different behaviour patterns was calculated for each epoch and abnormal behaviours were defined as those patterns with

very small probability of occurrence. The generated fuzzy rules were then used to classify test recordings for different scenarios of normal and abnormal behaviours.

This approach accurately classified 74.2% of the test recording for normal behaviours as shown in Table 5.4. Unlike AMP-ADLs, this approach used a set of pre-defined MFs to convert attributes values into fuzzy labels. These MFs divided the space of each attribute equally into fuzzy intervals, resulting in some activities to be modelled by multiple rules. When attributes in a test recording were slightly different from their training samples, a different combination of fuzzy attributes was resulted and thus the respective fuzzy rule in the rule set could not represent the activity in the recording. The behaviour in such test recordings was therefore labelled as belonging to the abnormal category.

The Seki (2009) approach differed from the AMP-ADLs approach as it did not take into account the duration of infrequent activities and misclassified test recordings of normal behaviour which included an infrequent activity performed for a short period (e.g. bending down in the dining room to pick up an object). The probability of occurrence of the infrequent activity fell below the threshold and caused this approach to raise an alarm.

The approach of Seki (2009) was found to correctly classify 67.5% of test recordings representing abnormal behaviours. It misclassified all sequences of normal activity performed with an abnormal duration. The reason was that, unlike AMP-ADLs, this approach did not monitor the duration of activities and all observations in test recordings of extended activities received a high probability of occurrence.

The fuzzy-logic-based monitoring approach proposed by Brulin et al. (2012) categorised the binary mask of the monitored person in camera images into a set of specific postures. Four image attributes were extracted from each binary mask, namely the aspect ratio of the person's bounding box, the person's centre of gravity in *x* and *y* axis, and the ratio of distance between the centre of gravity pixel location and the bottom of the bounding box to the height of the bounding box. A set of pre-defined fuzzy sets was used to convert the attributes values into fuzzy labels. A set of pre-defined fuzzy rules then categorised the fuzzy labels for each observation into postures of '*lying*', '*sitting*', '*squatting*', and '*standing*'. The fuzzy rules identified emergency situations, such as falls, based on the duration of the person's posture, time of the day and the location of activities.

The same attributes described by Brulin et al. (2012) were calculated from the binary mask of the occupant in Kinect training datasets. The set of fuzzy rules were then used to classify the combination of the duration, time, and location of the person in a test recording into normal and abnormal. As suggested by Brulin et al. (2012), for each combination of postures and locations a fixed maximum duration was considered normal.

This approach could correctly classify 73.3% of the test recordings of normal behaviours, as shown in Table 5.4. Many of the misclassifications occurred due to partial occlusions of the occupant's body in the testbed. The fuzzy rules in Brulin et al. (2012) were defined based on the assumption that the entire human body is visible to the camera. The occupant was partially occluded by the furniture (e.g. the dining table) in some test recordings and thus his postures during those recordings were estimated incorrectly. The system raised an alarm in each instance that the incorrectly estimated posture lasted for more that its threshold.

The Brulin et al. (2012) approach could correctly classify 70% of the recordings for abnormal behaviours, as shown in Table 5.4. Unlike AMP-ADLs, the parameters of the MFs defined over the attributes were set manually rather than based on the data distribution of attributes. The posture of the occupant in some recordings of abnormal behaviours was estimated incorrectly and resulted in the approach misclassifying those recordings. The approach in Brulin et al. (2012) was also limited as it did not model the physical location of ADLs in each room. The abnormal behaviours of lying on the floor in the living room and in the bedroom were confused respectively with the normal behaviours of sleeping on the sofa and sleeping in the bed.

## 5.5 Discussion

The training dataset in this study aimed at simulating a set of typical activities usually performed in the residence of an elderly person living alone. Taking cooking in the kitchen as an example, it involved visiting specific physical locations in the residence on a daily basis with similar durations and starting times for an elderly person. To accurately monitor the duration and the time of ADLs, the combination of fuzzy attributes to represent behaviour patterns should be robust against fine variations in performing ADLs. Using VBMS-RS with triangular MFs resulted in the lowest number of rules, as shown in Table 5.2. Investigating

those rules revealed that different instances of the same ADLs were represented by only one rule. This indicated that variations within individual instances of the same ADL were represented by the same combination of fuzzy attributes, and confirmed the robustness of the generated MFs with regards to those variations.

The results in Section 5.4.1 showed that VBMS-RS generated MFs according to the number of modes of an attribute and robustly excluding outliers. When the attribute values during an abnormal activity fell outside their normal range, no rule represents those values and the activity was considered to be infrequent. The system then raised and alarm once the ongoing duration of the activity elapses the respective $EA_r$. It was observed that the MFs generated by other techniques to parameterise an attribute supported a wider range outside the boundary of component distributions. This results in observations for abnormal situations to receive a positive membership degree from those MFs and the observations to be classified as normal. If fields of view of multiple Kinect sensors in the same room interfere, each Kinect can add its own fuzzy rules to the final rule set. Some rules in this case might model the same activity carried out in the overlapping field of view.

## 5.6 Summary

This chapter examined the use of VBMS-RS as an unsupervised MF generation technique for robustly parameterising the depth map attributes associated with monitoring the behavioural patterns of an elderly person living alone. The technique incorporated variable bandwidth mean shift and robust statistics for automatically generating MFs based on the data distribution of attributes to represent frequent activities. Comparisons were carried out between the results of the proposed technique and other MF generation techniques using trapezoidal the triangular MFs. Results in Section 5.4 demonstrated that, in terms of partitioning an attribute, the MFs generated by VBMS-RS were better at separating the component distributions. This led to more representative MFs and a higher classification accuracy of the corresponding fuzzy rule set. The classifiers constructed using VBMS-RS had a better performance in comparison with the three other techniques in terms of the number of fuzzy rules and classification accuracy. The classifier with triangular MFs generated by VBMS-RS outperformed classifiers that used other approaches for parameterisation of attributes including the one presented in Chapter 4.

A comparison was also made between the performance of other unsupervised physical activity

monitoring approaches (Table 5.2) and the one proposed in this study. The results of this comparison indicated that the AMP-ADLs approach significantly outperforms the existing approaches. The next chapter presents an unsupervised technique to identify instrumental ADLs from the occupant's interactions with HEAs.

# CHAPTER 6: IDENTIFYING INSTRUMENTAL ADLS BASED ON COMBINING KINECT DEPTH MAPS WITH POWER CONSUMPTION OF HEAS

This chapter presents an approach to identify the performance of instrumental ADLs (AIPIA) based on associating the occupant's physical locations with the power consumption of HEAs. The output of the AIPIA is a daily list of identified instrumental ADLs along with their time. AIPIA is a part of the approach for monitoring instrumental ADLs presented in the next chapter. The approach for monitoring instrumental ADLs uses AIPIA to monitor a daily index of instrumental ADLs for the monitored elderly person.

The chapter first introduces the problem of identifying the performance of instrumental ADLs from sensor data and provides a review of the limitations of existing approaches (Section 6.1). It then presents the stages of AIPIA in Section 6.2. This is followed by the experimental results of validating this approach in Section 6.3 where the results of training AIPIA using the collected dataset and assessment of its accuracy are provided. Section 6.4 presents a discussion of the results followed by a summary of this chapter in Section 6.5.

## 6.1 Introduction

Many researchers have developed remote home occupant monitoring approaches which have used a training sensor dataset to model instrumental ADLs (Clement, Ploennigs, & Kabitzsch, 2012; Shin et al., 2011). The developed models have been used for recognition and monitoring of activities to measure elderly people' ability to live independently and to detect their cognitive decline at an early stage.

Several instrumental ADLs such as grooming and cooking can be identified from the occupant's interactions with objects. Studies have embedded binary sensors into objects inside their monitored environments to identify interactions with objects. Implementing the approach proposed by most of these studies poses various limitations including equipping the house with many sensors during its construction and the need for the occupant to wear sensors in some cases (Peetoom et al., 2015).

Reviewing ADL monitoring sensor technologies in Chapter 1 revealed that power consumption

meters have been employed in ADL classification techniques in order to none-intrusively monitor the status of HEAs via their power signatures and consumption patterns (Gaddam, Mukhopadhyay, & Sen Gupta, 2011; Noury et al., 2011). The existing approaches that use a single power meter to identify ADLs require an initialization phase where the number, types, consumption and the operational states of all HEAs from a household have to be stipulated (Aritoni & Negru, 2011). Another challenge of existing approaches is distinguishing power signatures automatically generated by HEAs from those resulted from the occupant's ADLs. Power signatures generated by HEAs are not always the result of ADLs performed by the occupant as some HEAs automatically change their operational state. As a result identifying ADLs via only monitoring power signatures is not always accurate (Ghassemian, Auckburaully, Pretorius, & Jai-Persad, 2011). For example, a refrigerator turns its cooling system on and off multiple times throughout a day to keep its temperature within a specific range. Using a single power sensor also makes it very challenging to differentiate the usage of HEAs that possess similar power consumption patterns. Such HEAs may be used at different locations in the home for different ADLs. For example, the power consumption of a kettle and an iron can be very similar as both use a heating element but are employed for different ADLs;

Combining the occupant's locations with power consumption data can help identifying ADLs which involve different HEAs with similar power consumption patterns. As the majority of instrumental ADLs are performed at specific physical locations in the room, combining the occupant's physical locations inside a room with power consumption of HEAs can help with identifying ADLs which involve different HEAs with similar power consumption patterns. The occupant's physical locations can be estimated from Kinect's depth maps and when combined with power signatures, the usage of HEAs with similar power signatures inside the same room can be differentiated. By combining these sources of data, the power signature of self-regulating HEAs can also be distinguished from those resulting from the occupant's interactions with HEAs.

This chapter presents an unsupervised approach called AIPIA to identify instrumental ADLs based on data fusion between the Kinect depth maps and power consumption of HEAs. An association rule-mining algorithm was employed in AIPIA to map power signatures generated by HEAs to physical locations of the occupant obtained from the depth maps. Power signatures were obtained using a power meter installed in the main electricity panel of the house. Given the location of the occupant, association rules were used to verify whether a power signature

observed on the power line resulted from the occupant interacting with HEAs. The interaction was labelled as a specific instrumental ADL using contextual information. This chapter also introduces a statistical test to identify power signatures automatically generated by self-regulated HEAs.

## 6.2 The AIPIA approach

The AIPIA approach comprises of 2 stages including training and classification stages (
Figure 6.1). The training stage uses a training dataset from Kinect sensors and a power meter as input to automatically establish mappings between relevant power signatures of HEAs and the occupant's physical locations in the house. The output of this stage is used in the classification stage to identify the occupant's interactions with HEAs and label these as different instrumental ADLs. The classification stage provides a timestamped list of identified instrumental ADLs which is used to monitor the wellbeing of the occupant. The following sections provide further details of these stages.

### 6.2.1 Training stage

The training stage is initiated by the collection of an unlabelled training dataset of the home composite power consumption and the occupant's locations as shown in
Figure 6.1. Features are extracted from each source of data after pre-processing operations. These features are separately grouped into clusters and the cluster labels are used to find a set of association rules which specify frequently co-occurring power signatures and the occupant's physical locations.

The outputs of this stage are the boundaries of the detected clusters and the learned association rule set; these are used during the classification stage to identify interactions with HEAs and label them with instrumental ADLs.


Figure 6.1. An overview of the AIPIA approach.

#### *6.2.1.1 Data acquisition and pre-processing*

The aim of this step is to capture a training dataset of the overall power consumption and Kinect depth maps via a combination of a single power meter and a number of Kinect sensors each covering a different functional subarea in the house. Pre-processing operations were then applied to the data captured from each type of sensor.

*Power consumption data*: a single power sensor is installed in the main electricity panel of the

house to capture raw power consumption data at one sample per second intervals. In contrast to conventional intrusive load monitoring techniques that require putting sensors on each appliance, this configuration is achievable using low cost and off-the-shelf power meters and no access to individual HEAs is necessary for installing sensors.

Characteristics of HEAs in-operation are calculated in a two-dimensional space consisting of active power *(P)* and reactive power *(Q)*. Active power is expressed in Watts and is taken into account because any HEA consumes some active power. Reactive power is calculated as some devices use similar amounts of active power. Reactive power is associated with capacitive and inductive elements of a device and is expressed in volt-ampere reactive (*var*).

A noise removal operation is applied on the power consumption data to remove short impulses generated when a device is turned on or off due to a switching transient current. A median smoothing filter is adopted for this aim which replaces the value of each power measurement with the median of its neighbouring values located within a window size $T_m$. The duration of each instance of this type of noise at residential sites has been found to be usually less than a second (Hughes, Chan, & Koval, 1993). A spike may not co-occur with one measurement as it may occur at the end of one measurement and the beginning of the next one, affecting two consecutive measurements in power signal. $T_m$ is chosen to be five seconds as it should be more than twice as long as the longest spike in the data (Chandra, Moore, & Mitra, 1998).

An example of an active power signal over a period of time associated with turn-on and turn-off events of HEAs is shown in Figure 6.2 (a). As the refrigerator is switched on, a spike in the active power signal is noted at the third second. This is followed by the operation of a microwave and a toaster. An example of applying a median filter with $T_m = 5$ seconds on the same power signal is shown in Figure 6.2 (b). This figure shows that the filter removed the effect of the spike noise while preserving step-like changes associated with the events of HEAs being turn-on and turn-off.

*Kinect depth maps*: The environment is divided into several functional subareas and a Kinect sensor is installed in each subarea to capture depth maps of the occupant's ADLs. The only requirement for positioning Kinect sensors is to monitor as many functional areas of the home as possible, including locations where the occupant interacts with important HEAs. The Kinect

software includes a tracking functionality that uses the captured depth map of the scene to provide the 3D spatial locations of a detected person in the environment. It outputs 3D positions of 25 skeletal joints for each detected person (see Figure 6.3) at a frame rate of 30 Hz. Localisation using this type of skeletal tracking method is nonintrusive unlike wearable sensors that the home occupant must remember to put on.

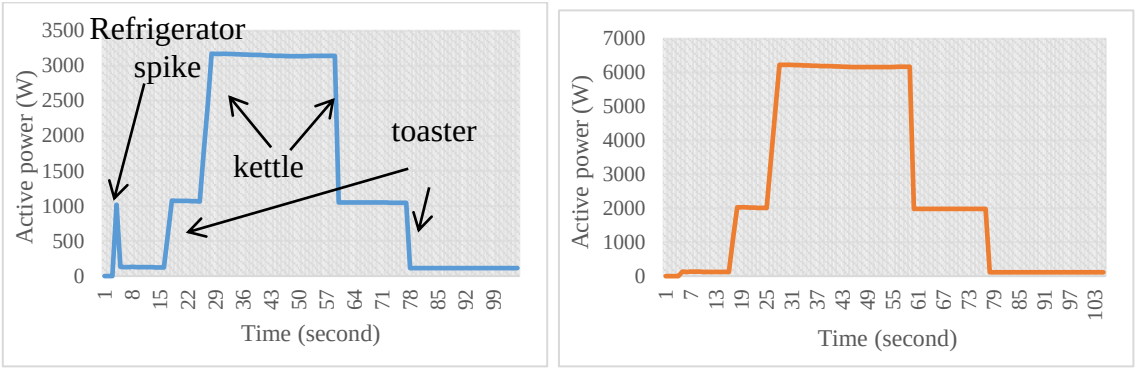


(a) (b)

Figure 6.2. (a) An example of the effect of a spike on the active power signal caused by operation of a refrigerator. (b) Plot after application of a 5-second median filter.

Each Kinect sensor is given a unique ID to represent the room being monitored by the sensor. Observations from each Kinect sensor are taken, and those in which a person is detected are stored. Each stored observation includes 3D positions of 25 skeletal joints for the tracked occupant, a timestamp, and the respective Kinect ID.

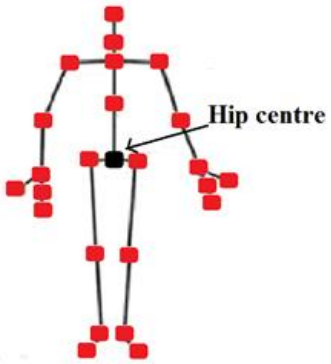


Figure 6.3. The Kinect skeletal joint representation and the location of the hip centre.

Two steps of pre-processing operations are applied to the raw 3D positions of skeletal joints acquired from each Kinect sensor in the monitored environment. The first step stores the 3D

positions of the occupant's hip centre joint (see Figure 6.3) in the form of $x, y,$ and $z$ and discards the information of other joints.

The sequence of raw joint positions is found to contain high frequency jitters and temporary spikes. The second step of pre-processing removes the noise in the obtained positions of the centre of the hip joint using a variant of the Holt Double Exponential Smoothing method (Kalekar, 2004). This method provides smoothing with less latency than in other signal smoothing techniques. The red line in Figure 6.4 shows an example of the occupant's hip joint positions in the *x*-axis and the blue line shows their smoothed values. This figure shows that significant jitters are eliminated - especially those occurred after Frame 130 in the original signal.

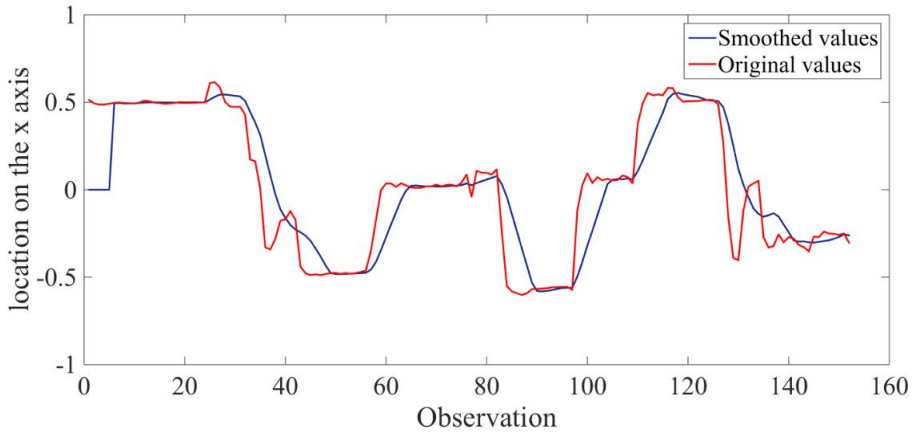


Figure 6.4. An example of the original signal of the occupant's hip joint in *x*-axis along with its smoothed values.

### *6.2.1.2 Extracting features*

This step involves two operations; the *extraction of power signatures* and the *extraction of the occupant's physical location*. The first operation takes the pre-processed composite power signals and extracts power signatures associated with the operation of specific HEAs. The second operation extracts physical locations of the occupant in the monitored home.

*Extracting power signatures:* Every turn-on and turn-off event of an HEA changes the overall power consumed in the home and manifests itself as a positive and negative step change in the composite power signal (see Figure 6.2). Only turn-on events are detected in AIPIA in order to estimate appliance usage in the home. The reason is that many HEAs such as microwaves and toasters are switched on manually, resulting in a positive step-like change in the overall active

power consumption. Many devices however may end their operation automatically after a specific amount of time and a *turn-off* event may not result from an interaction of a person with an HEA.

Since turn-on events of pure resistive loads produce no variation on the reactive power signal, only the active power signal is processed to detect positive step-changes. A positive step-change (i.e. an HEA turn-on event) is detected where the deference in two consecutive active power values exceeds a threshold α. A simple differentiating method is applied on the active power signal to detect turn-on events of HEAs. Each power measurement $P(t)$ with its previous measurement $P(t-1)$ is compared and if the magnitude of difference, i.e. $d_P(t)$, is more than α, the differences in both active $d_P(t)$ and reactive $d_Q(t)$ power signals along with their timestamp (i.e. *t*) are obtained as power signatures and are stored in a list named *power_signatures*. Note that $d_Q(t)$ is the difference between $Q(t)$ and $Q(t-1)$. An example of seven records in *power_signatures* is shown in Table 6.1.

Table 6.1. An example of records in *power_signatures*.

| $d_P$ | $d_Q$ | *Timestamp* |
|---|---|---|
| 45 | 0 | 10-Oct-15, 09:15:04 |
| 1700 | 0 | 10-Oct-15, 11:35:47 |
| 115 | 44 | 10-Oct-15, 12:25:14 |
| 1752 | 651 | 10-Oct-15, 18:42:43 |
| 915 | 0 | 10-Oct-15, 21:11:18 |
| 453 | 0 | 11-Oct-15, 09:23:09 |
| 42 | 0 | 11-Oct-15, 11:40:34 |

The value of α depends on the accuracy of the power measuring sensor and noise on the power line. Its value should be larger than random fluctuations in the power signal so as to avoid detecting those fluctuations as power signatures.

*Extracting the occupant's physical locations*: The 3D positions of the occupant's hip centre joint from all frames acquired in one second are averaged along each of the axes to obtain the 3D location of the occupant at one-second intervals. The calculated 3D locations are then mapped onto the 2D plane of the room using coordinates corresponding to the *x*- and *z*-axes. The resulting 2D locations of the occupant in the scene along with their timestamps and Kinect

IDs are stored in a list named *visited_locations*. The Kinect IDs are used in the subsequent steps to identify the room in which an activity is performed. An example of *visited_locations* consisting of seven records is shown in Table 6.2. Note that the timestamp of some records can be matched to those in Table 6.1.

Table 6.2. Example of *visited_locations* consisting of seven records.

| **Kinect ID** | **The *x*-axis** | **The *z*-axis** | ***Timestamp*** |
|---|---|---|---|
| K | 0.4973 | 2.4705 | 10-Oct-15, 08:47:04 |
| K | -0.4760 | 1.9812 | 10-Oct-15, 11:35:47 |
| K | -0.5653 | 1.9355 | 10-Oct-15, 15:25:11 |
| L | -0.4829 | 2.0520 | 10-Oct-15, 18:42:43 |
| L | 0.4480 | 2.3061 | 10-Oct-15, 21:11:18 |
| B | 0.3475 | 2.2758 | 11-Oct-15, 09:23:09 |
| K | 0.1322 | 2.4330 | 11-Oct-15, 11:40:34 |

#### *6.2.1.3 Grouping power signatures and post processing*

A clustering technique is employed in this step to group power signatures resulting from the same mode of operation of a device. Post-processing operations are then carried out to remove power signatures automatically generated by HEAs.

*Grouping power signatures*: The power signatures of an HEA may have variations in the *P*-*Q* space due to the noise on the power line and errors in sensor measurements. A novel data-driven algorithm is presented to group similar power signatures as belonging to the same device in a particular mode of operation. The steps of this algorithm is shown in Figure 6.5. The input is *power_signatures* obtained from the last step. The algorithm outputs a cluster ID for each power signature in the list.

Each power signature corresponds to a point in $P - Q$ space with two neighbourhood distances, called respectively *A_P_Eps* and *R_P_Eps*, as specific percentages of its active and reactive powers. The algorithm involves repeating certain operations until all power signatures are processed (i.e. labelled with a cluster ID). An arbitrary unprocessed power signature *p* is selected at the beginning of each iteration and all neighbours with respect to *A_P_Eps* and *R_P_Eps* from *p* are then retrieved using function *N(p)* (line 5 of Figure 6.5). The list of neighbours is recorded in *neighbour_p.*

The active and reactive power consumption of different devices can vary in residential enviornments up to 20% (Pihala, 1998). A value of 10% of a point's active and reactive power values is conservatively used in order to calculate *A_P_Eps* and *R_P_Eps* (line 4 of Figure 6.5). Using this technique, larger power signatures are resulted in a wider distance for their neighbours.

The number of neighbours around *p* is compared with *MinPnts* to determine whether *p* belongs to a noisy measurement (line 6 of Figure 6.5). *MinPnts* in this algorithm determines the minimum number of data points constituting a cluster. If *MinPnts* is set to a value of one, then each cluster should contain at least two data points. *MinPnts* therefore is set to this value to filter out unusual power signatures in the P – Q space that result from infrequent situations in which more than one turn-on event occur simultaneously. If there are enough neighbours *(*more than one*)* around *p*, the algorithm assigns a cluster ID to *p*, or alternatively it set the cluster ID of *p* as *noise*.

If *p* has enough neighbours, all neighbours are assigned with the cluster ID of *p* and are marked as processed in a for-loop (lines 10:19). For each of the neighbours, function *N(p)* is used to find their unprocessed neighbours in order to add them to *neighbour_p*. In line 22, *p* is marked as processed and the operations are repeated for another unprocessed point. This is repeated until all data points are marked as processed.

An example of power signatures for an operation mode of a device, including one measurement *q* and one noisy measurement *r* is shown in Figure 6.6. Both indices are shown with red dots. The neighbourhood distances for *q* and *r* are shown with a red-dotted boundary around them. Since *q* has enough neighbours within its neighbourhood distances, it is identified as a cluster member and is tagged using the same cluster ID as its neighbours. *r* has no neighbour within its neighbourhood distances and hence is labelled as *noise*.

***The Algorithm for grouping power signatures***

***Input:*** *a dataset of active and reactive power signatures*

***Output:*** *cluster ID for each data point in the dataset*

```
1  ClId=1
2  Do
3      select an unprocessed data point p from the dataset
4      compute A_P_Eps and R_P_Eps values for p
5      determine neighbour_p =N (p) as neighbours of p
6      if (|neighbour_p| < MinPnts) then
7          set the cluster_ID of p as noise
8      else
9          set cluster_ID of p as ClId
10         for every point in neighbour_p
11             set its cluster_ID as ClId
12             mark it as processed
13             for every point in its neighborhood
14                 if it is unprocessed
15                     add it to neighbour_p
16                 end if
17                 set its cluster_ID as ClId
18             end for
19         end for
20         ClId= ClId+1
21     end if
22     mark p as processed
23 Until all the data points are processed
```

Figure 6.5. The proposed clustering algorithm for grouping power signatures.

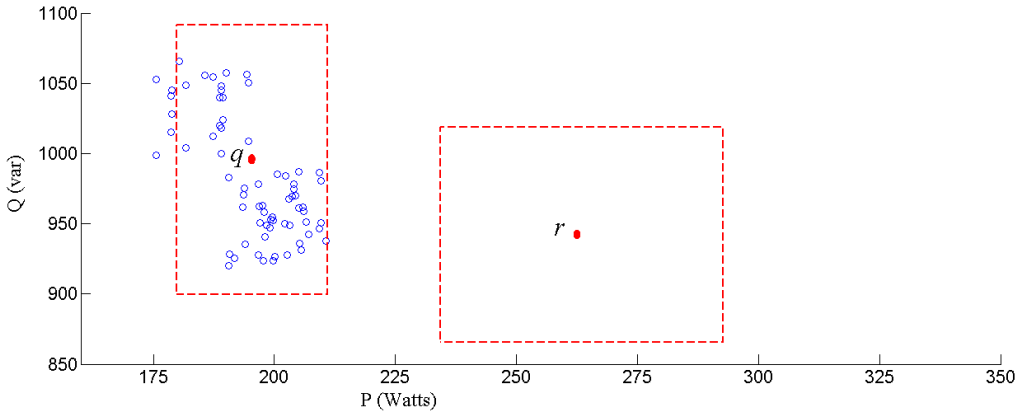


Figure 6.6. Examples of an outlier r and a cluster member q. The searching neighbourhoods of each point are defined as 10% of the point's active and reactive powers to account for variation in power signatures produced by HEAs.

The cluster label of each power signature is added to the power signature's entry in *power_signatures.* Post processing are then applied on *power_signatures* to remove power signatures which are not resulted from the occupant's interactions.

*Post processing of power signatures*: Three stages of post-processing are applied on the processed *power*_signatures.

Stage 1: The first stage is *removal of outliers* which involved removal of data points tagged by the algorithm as *noise*.

Stage 2: The second stage is *Removal of data points of self-regulated HEAs.* It uses the chi-square statistic for goodness of fit (Cochran, 1952) to identify cluster labels generated through the operation of self-regulated HEAs and removes their respective data points from *power_signatures.* An example of the active power signal belonging to the operation of some HEAs, including a refrigerator, is presented in Figure 6.7. The operation cycles of the refrigerator caused several power consumption events of around 100 Watts to be regularly scattered through time.

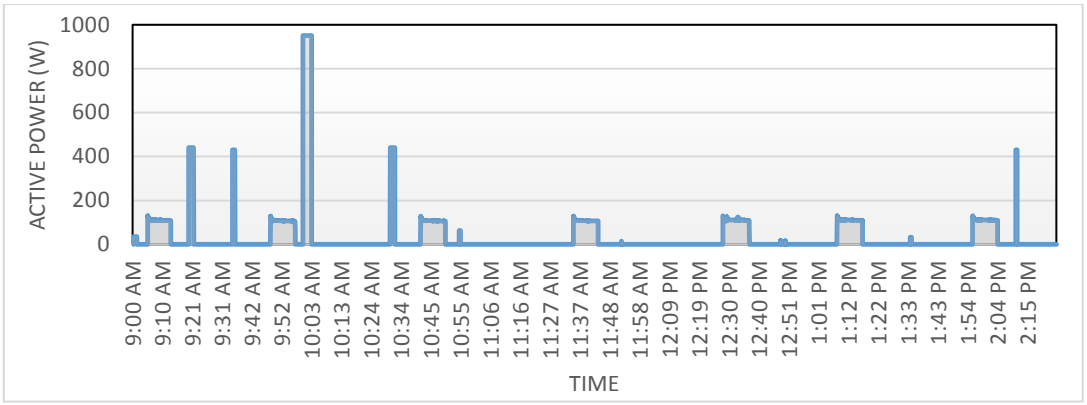


Figure 6.7. An example of an active power signal captured during operation of HEAs including a refrigerator.

The example shown in Figure 6.7 illustrates that turn-on events of self-regulated HEAs tend to spread over a 24-hour cycle and thus the PDF of their time of occurrence follows a relatively uniform distribution. The time of occurrence of turn-on events associated with other devices that operate upon the occupant's interactions follows a non-uniform PDF. This may be because turn-on events of those devices have been found to be heavily concentrated around times when the occupant is active in the home (Hart, 1992).

Chi-square statistic test is employed to categorise each cluster of power signatures into two categories. The first category is *interaction-generated* which corresponds to HEAs that operate upon the occupant's interactions and the second category is *self-regulated* which corresponds to self-regulated HEAs in the home. The Chi-square statistic test categorises each cluster of power signatures using the following steps:

Step 1. Estimating $G(h)$ as the PDF of the time of occurrence of the cluster members (with $h$ indicting the hour of the day). This PDF is obtained by calculating the normalised hourly number of the cluster members. A uniform distribution function $F(h)$ is also estimated based on the assumption that the power signatures in the cluster are generated by a self-regulated HEA. $F(h)$ for the power signatures of the cluster is obtained by averaging their daily number of occurrences during the training period. The result is applied to every $h$ in $F(h)$. The test statistic is then formulated for binary hypothesis testing:

$$H_0: G(h) = F(h)$$

$$H_1: G(h) \neq F(h)$$

(6.1)

If the estimated PDF of a cluster follows an almost uniform distribution across a day, $H_0$ is true and the cluster belongs to the *self-regulated* category. Otherwise if $H_1$ is true, the cluster is categorised as *interaction-generated*.

Step 2. Comparing $G(h)$ with $F(h)$ through calculating the value of $X^2$ statistic test using Equation 6.2.

$$X^2 = \sum_{h=1}^{24} \frac{(G(h) - F(h))^2}{F(h)}$$

(6.2)

Step 3. Classifying the cluster label into one of the two categories. This classification is based on whether the calculated value of $X^2$ is greater than the critical value $\chi^2_{CV}$ which depends on the degree of freedom and a significance level. The number of variables for this case is 24 (the number of hours in a day) and thus the degree of freedom become 23. A number of experiments were carried out using publicly available datasets of power measurements of residential houses (Makonin, Popowich, Bartram, Gill, & Bajić, 2013; Reinhardt et al., 2012) to experimentally determine the significance level. This parameter is accordingly set to 0.05%. The corresponding critical value of $\chi^2_{CV}$ for this classification is thus equals to 35.172 (Lancaster & Seneta, 2005).

All cluster labels are categorised into either of *interaction-generated* and *self-regulated* categories. The boundaries of clusters in each category are determined as the range between the smallest and largest members of the cluster in *P* and *Q* spaces. A list consisting of cluster labels, their category, and their power range in in *P* and *Q* spaces is then developed as *power_cluster_info.* An example of this list is shown in Table 6.3; the group of power signatures labelled as P01 belongs to the *self-regulated* category whereas P02, P03, and P04 belong to the *interaction-generated* category.

Table 6.3. An example of *power_cluster_info* containing boundaries for each cluster of power signatures along with their category type. In this example, P02, P03, and P04 are generated by the power signatures of a refrigerator (light), an electric cooktop, and a microwave, respectively, whereas P01 created by the operation of a refrigerator (cooling).

| ***Cluster label*** | ***Range*** | | ***Category*** |
|---|---|---|---|
| | ***P*** | ***Q*** | |
| P01 | [85 - 121] | [55 – 70] | self-regulated |
| P02 | [31 - 45] | 0 | Interaction- generated |
| P03 | [980 - 1210] | 0 | Interaction-generated |
| P04 | [1380 - 1650] | [340 - 551] | Interaction- generated |
| ⋮ | ⋮ | ⋮ | ⋮ |

The category of each cluster label in *power_cluster_info* is used to remove data points in *power_signatures* that belong to the *self-regulated* category.

Stage 3: Other data points in *power_signatures* generated automatically by thermostatically controlled HEAs (e.g. electric cooktops and coffee makers) may also occur. Once the occupant switched on those HEAs, they repeatedly generate their power signatures during their operation to maintain the temperature. The category of those power signatures in *power_cluster_info* tends to be *interaction-generated* as those HEAs are typically used by the occupant during specific times of the day and thus their PDF throughout the day is different from a uniform distribution. Such automatically generated data points are removed by merging the power signatures of the same cluster with close times of occurrence as one event. The cluster label and timestamp of each data point *p* in *power_signatures* are taken into consideration and that data point is kept if no other data point with the same cluster label has occurred within $w_k$ seconds before *p*.

An example of pulses of power of three HEAs groups of power signatures labelled as P01, P02, and P03 is shown in Figure 6.8. Note that only P02 is thermostatically controlled HEA which produces short-duration pulses of power. The figure shows the active power consumption. Each pulse of power is labelled with a letter. Figure 6.9 (a) demonstrates the timestamp and pulse label for each instance of the power signatures of P01, P02, and P03 shown in Figure 6.8. Figure 6.9 (b) shows that when $w_k = 180$ seconds, this operation merges points within a time window $w_k$ from the point of initialisation and records only the initial timestamp. For example, the two entries associated with P01 in the list of Figure 6.9 (a) are recorded as is (pulses *a* and

*j* in Figure 6.8). This indicates that no merging is performed because the starting times of the first pulse (labelled as *a)* and the second invocation (labelled as *j*) are separated with a long duration. With regard to P02, only entries corresponding to pulses *b* and *g* are kept, while the remaining entries are removed from the list. This is because the length of time between the occurrence of pulses *b* and *g* and the last invocation is more than 180 seconds (in the case of *g*, it is 374 seconds) whereas for *c, d, e, h,* and *i*, the duration between their occurrence and the last invocation is less than 180 seconds.

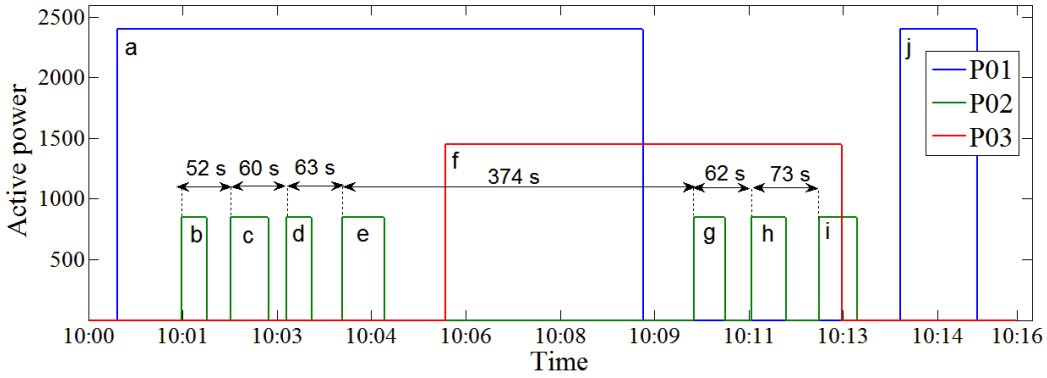


Figure 6.8. Example of power consumption pulses of the three HEAs whose groups of power signatures are labelled as P01, P02, and P03. Only P02 belongs to a thermostatically controlled HEA.

| ***Timestamp*** | ***Cluster ID*** | ***Pulse in Figure*** 6.8 |
|---|---|---|
| 10-Oct-15, 10:00:30 | P01 | a |
| 10-Oct-15, 10:01:38 | P02 | b |
| 10-Oct-15, 10:02:30 | P02 | c |
| 10-Oct-15, 10:03:29 | P02 | d |
| 10-Oct-15, 10:04:28 | P02 | e |
| 10-Oct-15, 10:06:18 | P03 | f |
| 10-Oct-15, 10:10:41 | P02 | g |
| 10-Oct-15, 10:11:42 | P02 | h |
| 10-Oct-15, 10:12:54 | P02 | i |
| 10-Oct-15, 10:14:20 | P01 | j |

(a)

→

| ***Timestamp*** | ***Cluster ID*** | ***Pulse in Figure*** 6.8 |
|---|---|---|
| 10-Oct-15, 10:00:30 | P01 | a |
| 10-Oct-15, 10:00:38 | P02 | b |
| 10-Oct-15, 10:06:18 | P03 | f |
| 10-Oct-15, 10:10:41 | P02 | g |
| 10-Oct-15, 10:14:20 | P01 | j |

(b)

Figure 6.9. Merging of identical symbols in *power_signatures* to remove the effect of short-duration pulses of power of thermostatically controlled HEAs. (a) An example list of data points in *power_signatures*. (b) Merging data resulting from short pulses of power of thermostatically controlled HEAs.

#### *6.2.1.4 Grouping visited locations*

An occupant usually visits specific physical locations in order to interact with HEAs in an indoor environment. The visited physical locations for interacting with a specific HEA are also usually close to each other. This step of the AIPIA includes two operations; to group the occupant's physical locations when interacting with HEAs, and to processes *power_signatures* so each data point in that list includes the respective occupant's location.

The input to the first operation is data points in *visited_locations* the timestamps of which correspond to those of data points in the processed *power_signatures*. A technique similar to the algorithm described in Figure 6.5 is used to assigned cluster IDs to the groups of these locations using their Euclidean distance.

Instead of the two distances (*A_P_Eps* and *R_P_Eps)* in line 3 of the algorithm, a searching distance for the neighbours of a physical location is defined which is denoted as $min_r$. This distance is a context-specific parameter measured directly from the monitored home to indicate the radius of space normally used by the occupant to interact with an HEA. A regular choice for this parameter would be 50 cm. The distance between two occupant's physical locations is measured through performing a calibration procedure on Kinect sensor (Webb & Ashley, 2012). HEAs occupying a larger space cause larger clusters to be created as clusters in the algorithm can have arbitrary sizes and shapes.

*MinPnts* in line 6 of the algorithm is set to zero in order to label the location of all potential HEAs that operate based on the occupant's interactions. A new cluster is created once a location is visited to interact with HEAs. For example, L01 and L02 are two different groups of locations in the kitchen having a distance of more than $min_r$ between their cluster boundaries. Similarly, L03 and L04 correspond to the groups of locations which the subject mostly visit in order to manipulate a TV and a computer in the living room, respectively.

The output of this grouping is a list called *location_cluster_info*. It contains the cluster ID, boundaries, and the Kinect label associated with each detected cluster of the occupant's locations. An example of *location_cluster_info* is shown in Table 6.4. It is assumed that two clusters of the occupant's locations (labelled L01 and L02) are found for a kitchen area and one cluster labelled L03 is found in a living room area.

Table 6.4 An example of *location_cluster_info* obtained from grouping visited locations

| ***Kinect label*** | ***Cluster ID*** | ***Range*** | |
|---|---|---|---|
| | | ***The x-axis*** | ***The z-axis*** |
| K | L01 | [-0.2378, 0.4522] | [1.4363, 1.7511] |
| K | L02 | [-0.720, -0.1520] | [1.6874, 2.3145] |
| L | L03 | [0.1259, 0.7544] | [0.8232, 1.5332] |

The second operation processes each data point in *power_signature* to include the corresponding cluster ID of the occupant's location using their timestamps. Those data points not associated with any label for the occupant's location are eliminated from the list as they cannot help to associate power signatures with locations of the occupant. The corresponding label for the occupant's location is then added to each of the remaining data points in *power_signature.* After this operation, each record in *power_signature* has a power signature ID, a label for the occupant's location, and a timestamp. This is shown in the example provided in Table 6.5 where it is assumed that four groups of power signatures (*P01, P02, P03,* and *P04*) are identified in the power signal and the three clusters of locations corresponding to those power signatures are labelled L01, L02, and L03.

Table 6.5. An example of a processed *power_signature.* Each data point includes a label for a power signature, a label for the corresponding location of the occupant, and a timestamp.

| ***Timestamp*** | ***Location Cluster ID*** | ***Power signature Cluster ID*** |
|---|---|---|
| 19-Oct-15, 08:47:04 | L01 | P01 |
| 19-Oct-15, 11:35:47 | L01 | P04 |
| 19-Oct-15, 15:25:11 | L03 | P03 |
| 19-Oct-15, 18:42:43 | L02 | P02 |
| 19-Oct-15, 21:11:18 | L03 | P03 |
| 20-Oct-15, 09:23:09 | L02 | P04 |
| 20-Oct-15, 11:40:34 | L01 | P01 |
| 20-Oct-15, 14:47:56 | L03 | P03 |
| 20-Oct-15, 19:31:27 | L01 | P04 |
| 21-Oct-15, 08:46:41 | L02 | P02 |
| 21-Oct-15, 13:29:40 | L03 | P03 |
| 21-Oct-15, 18:26:11 | L01 | P01 |
| 21-Oct-15, 19:24:51 | L02 | P02 |
| 21-Oct-15, 21:01:27 | L01 | P04 |

#### *6.2.1.5 Associating the occupant's locations with power signatures*

This section describes the last step of the training stage as shown in

Figure 6.1. It takes *power_signatures* as input and employs an association rule-mining algorithm (see Section 3.5.5.3) to establish association between the occupant's locations and power signatures. This results in a set of rules which have a location and a power signature as their antecedent and consequent, respectively. This rule set is used to identify the occupant's instrumental ADLs in case the occupant's current location is associated with a detected power signature on the power line. For example, let an association rule for the kitchen to be L01→P01 and at a given time the occupant's location in the kitchen be well within the range of L01. At that time if a detected power signature falls within the boundary of P01, it can be confirmed that the power signature has resulted from the occupant's interaction with an HEA rather than being generated automatically.

The employed association rule-mining algorithm is based on a two-step strategy. A binary transaction table is generated in the first stage. The columns of this table include labels for all groups of locations and power signatures in *power_signatures*. If there are *m* groups of the occupant's locations and *n* groups of power signatures in *power_signatures*, the number of columns in the transaction table is equal to *m*+*n*. The number of rows in this table is equal to the number of records in *power_signatures*. Each row specifies a record in *power_signatures* and has two non-zero values. One value belongs to the column associated with the power signature label and the other value belongs to the column associated with the occupant's location label.

A transaction table for the example of power_signature shown in Table 6.5 is displayed in Table 6.6. Each row in this table relates to seven labels: four labels of power signatures (P01, P02, P03, and P04) in Table 6.5 and three location labels corresponding to those power signatures (L01, L02, and L03). Each row corresponds to a record in power_signature. For example, the first row which has two non-zero values for L01 and P01 corresponds to the first record in Table 6.5 with the combination of L01 and P01.

The association rule-mining algorithm uses the binary transaction table to list frequent items which are combinations of locations and power signatures. The algorithm then outputs rules that reveal frequent co-occurrences of power and location labels, with each rule having a location label and a power signature label respectively as its antecedent and consequent. Each rule has a confidence level to show the level of association between the elements in the rule.

These rules are divided into two categories based on whether a rule has a cluster label for a visited location or a power signature as its antecedent part:

Table 6.6. The transaction table for the example shown in Table 6.5.

| ***Timestamp*** | ***L01*** | ***L02*** | ***L03*** | ***P01*** | ***P02*** | ***P03*** | ***P04*** |
|---|---|---|---|---|---|---|---|
| 19-Oct-15, 08:47:04 | 1 | | | 1 | | | |
| 19-Oct-15, 11:35:47 | 1 | | | | | | 1 |
| 19-Oct-15, 15:25:11 | | | 1 | | | 1 | |
| 19-Oct-15, 18:42:43 | | 1 | | | 1 | | |
| 19-Oct-15, 21:11:18 | | | 1 | | | 1 | |
| 20-Oct-15, 09:23:09 | | 1 | | | | | 1 |
| 20-Oct-15, 11:40:34 | 1 | | | 1 | | | |
| 20-Oct-15, 14:47:56 | | | 1 | | | 1 | |
| 20-Oct-15, 19:31:27 | 1 | | | | | | 1 |
| 21-Oct-15, 08:46:41 | | 1 | | | 1 | | |
| 21-Oct-15, 13:29:40 | | | 1 | | | 1 | |
| 21-Oct-15, 18:26:11 | 1 | | | 1 | | | |
| 21-Oct-15, 19:24:51 | | 1 | | | 1 | | |
| 21-Oct-15, 21:01:27 | 1 | | | | | | 1 |

The first category is called *location_rules* and consisted of those rules associating a location label with a power signature label. Rules in this category are in the form of

"*location Cluster ID → power signature Cluster ID"*

which indicate locations that are linked to specific power signatures. The confidence of such rules is the probability of the power signature in the rule being a result of the occupant's interaction with HEAs given that the occupant is within the location specified by the rule. If during the collection of training dataset, a location is mostly visited for manipulating one particular HEA, the corresponding rule associating the visited location with the power signature of the appliance carries a high degree of confidence. For example, the rule associating a location with the power signature of a refrigerator light, which is only observed when the occupant was in front of the refrigerator, generates almost 100% confidence. This means that when the occupant is in front of the refrigerator and the power signature of the refrigerator light is observed, the approach is 100% confident that the power signature has been resulted from the occupant's interaction.

A location in the house may also be associated with multiple groups of power signatures. For example, some kitchen HEAs may be adjacent, or one device may generate several groups of

power signatures. The confidence of rules associating such locations with their power signatures would not be high because different groups of power signatures are observed when the occupant visited the location. For example, if a toaster and its adjacent kettle share the same group of visited locations, labelled as L01, and the numbers of their interaction events are similar, the confidence of the corresponding rules associating L01 to the power signatures of the toaster and the kettle would be around 50%.

The second category, *power_rules,* involves rules associating the label of a power signature with a label of a location in the form of

*"power signature cluster ID → location cluster ID"*.

The confidence of the rules in this category specifies the confidence with which a power signature observed on the power line can be linked to a specific location. This means that if a power signature is mostly detected when the occupant was visiting a specific location, the corresponding rule associating the power signature with the location would carry a high degree of confidence. If the power signatures of the toaster and the kettle in the abovementioned example were detected only when the occupant's location is labelled as L01, the confidence of the rules for their power signatures would be approximately 100%. If the power signatures of an automatic HEA are detected when the occupant was visiting different locations, the confidence of the corresponding rules associating those power signatures to different locations would be low.

The rules for each category from the transaction matrix shown in Table 6.6 are presented in Table 6.7 (a) and (b), respectively. Note that for each rule in part (a) there is a corresponding rule in part (b) with the antecedent and consequent parts in the reverse order.

Only rules the form of those in *location_rules* are regarded as the final rules because the aim of AIPIA is to identify interactions with HEAs based on the occupant's locations. Rules in *location_rules* with a confidence higher than a threshold can be used to confirm whether based on the occupant's current location, a detected power signature is resulted from the occupant interacting with HEAs.

Table 6.7 (a) *location_rules* and, (b) *power_rules* generated by the association rule-mining algorithm based on the transaction dataset shown in Table 6.6.

| ***Rule*** | ***Confidence*** |
|---|---|
| L3 -> P3 | 100% |
| L2 -> P2 | 75% |
| L1 -> P1 | 50% |
| L1 -> P4 | 50% |
| L2 -> P3 | 50% |
| L2 -> P4 | 25% |

(a)

| ***Rule*** | ***Confidence*** |
|---|---|
| P3 -> L3 | 100% |
| P2 -> L2 | 100% |
| P1 -> L1 | 100% |
| P4 -> L1 | 75% |
| P3 -> L2 | 40% |
| P4 -> L2 | 25% |

(b)

Pruning rules based on a threshold may cause rules associating the location of adjacent HEAs with their groups of power signatures to be eliminated as their confidence is usually low. To prevent this, the confidence of each rule in *location_rules* is compared with that of the corresponding rule in *power_rules* (i.e. the rule with the consequent and antecedent parts in the reverse order) and the higher value is replaced with the confidence of the rule in *location_rules*. For example, assume in the example mentioned above, P01 and P04 are the cluster IDs for the power signatures of the kettle and toaster, respectively. Table 6.7 (a) shows that the confidence of observing P01 and P04 at location L01 (i.e. P01→ L01 and P04→ L01) is 50%. The confidence of these rules is replaced by that of their corresponding rules in *power_rules* (i.e. L01→ P01 and L01→ P04) which are 100% and 75%, respectively. Table 6.8 shows the results of performing this operation on *location_rules* shown in Table 6.7 (a).

A thresholding is performed to remove rules in the processed *location_rules* with a confidence less than an adopted *min_conf*. This is to remove rules which associate locations with the power signatures of the automatically changing state of HEAs (e.g. power signatures resulting from changing from washing to spin drying in a washing machine). The confidence of such rules is low because generation of those power signatures does not require the occupant to be near the appliance and hence the corresponding locations of the occupant are likely to vary.

The remaining rules in *location_rules* are regarded as the final rule set. Each rule is then arbitrarily labelled with an instrumental ADL, a technique typically used by existing approaches (Noury et al., 2011). The contextual information of the room associated with each rule can be used to label the rules (e.g. a feeding activity can be adopted for a rule associated with the kitchen). The name of the monitored room for each rule can be identified based on the Kinect ID in *location_cluster_info*.

Table 6.8. The effects of the post processing operation on the confidence of rules in Table 6.7 (a).

| *Rule* | *Confidence* |
|---|---|
| L3 -> P3 | 100% |
| L2 -> P2 | 100% |
| L1 -> P1 | 100% |
| L1 -> P4 | 75% |
| L2 -> P3 | 50% |
| L2 -> P4 | 25% |

### 6.2.2 Classification stage

The *location_rules*, *location_cluster_info*, and *power_cluster_info* information obtained from the training stage are used to detect the occupant's interactions with HEAs and assign them unique labels. The sensor data in this stage are first processed in a similar method as the training stage in order to extract power signatures and the occupant's locations as shown in Figure 6.1. Each power signature is then checked against the corresponding power ranges of each cluster in *power_cluster_info* to obtain its cluster ID. If no cluster ID is found for the power signature or it falls within power ranges of a cluster ID of *self-regulated* category, the power signature is ignored.

The process described in Section 6.2.1.3 for removal of data points caused by pulses of power of thermostatically controlled HEAs is executed on the rest of the power signatures. The remaining power signatures that do not have a corresponding location of the occupant is eliminated as they cannot help with identification of interactions with HEAs. The occupant's locations for the rest of power signatures are compared against the boundaries of each cluster of locations in *location_cluster_info* and those labelled with a location cluster are paired with the cluster ID of their respective power signature. The approach then checks each pair of cluster IDs to see whether those are associated by a rule in *location_rules*. The power signature in each pair is inferred as the result of an instrumental ADL in case a rule confirms an association for the pair of cluster IDs (performing an instrumental ADL). The occupant's activity is then labelled using the label adopted for the rule.

## 6.3 Experimental results

The collected dataset from the testbed was used to evaluate the effectiveness of the AIPIA

approach in identifying instrumental ADLs. The assignment of the approach parameters in the testbed is first described in this section followed by reporting the results of associating the occupant's locations with the power signatures of HEAs in the training procedure. This section also reports the performance of the approach in identifying instrumental ADLs and compares it with another implementation of AIPIA where only power consumption data was used to identify the occupant's interactions with HEAs.

### 6.3.1 Assignment of the approach parameters

The α parameter described in Section 6.2.1.2 was set to 25 Watts in order to prevent noise on the power line from being detected as a power signature. Figure 6.10 shows an example of noise on the composite active power signal where no HEA changed its operational mode. The example in this figure shows that noise caused variations up to nearly 6 Watts on the signal. Setting α to 25 Watts enabled the approach to robustly detect power signatures generated by HEAs. $w_k$ in Section 0 was set to 180 seconds to account for pause gaps of thermostatically operating HEAs (i.e. the electric cooktop and the microwave) in the testbed. $min_r$ was set to 50 cm.

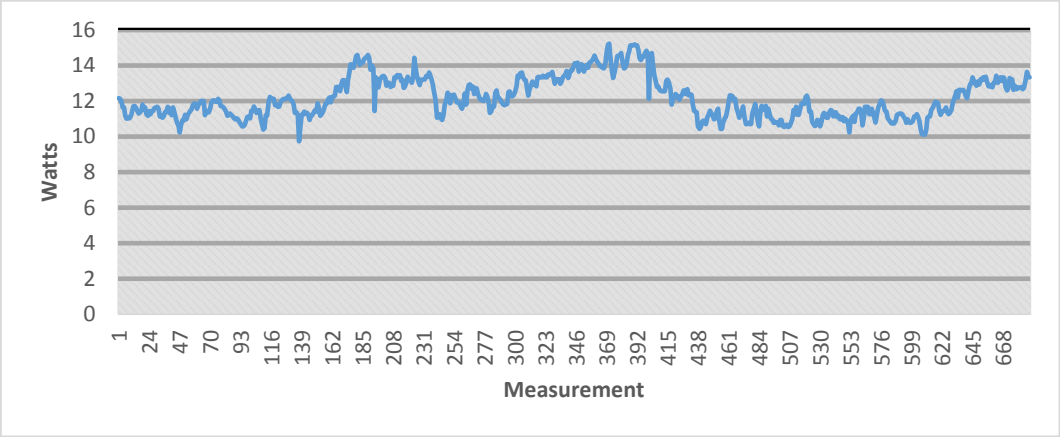


Figure 6.10. An example of noise on the composite active power signal where no HEA changed its operational mode.

### 6.3.2 Training in the experimental setup

The training dataset was processed to obtain information necessary for the classification stage including the rules associating the occupant's locations inside the testbed with power signatures. Power signatures associated with turn-on events in this dataset were detected yielding *power_signatures* to have 1826 entries.

The data points in *power_signatures* were grouped into clusters as shown in Figure 6.11. This figure shows a total of 11 clusters in different colours. Each cluster contains instances of the power signatures it represents. The boundaries of the clusters are shown with black rectangles. Data points surrounded by red rectangles were labelled as noise by the clustering technique and discarded in the subsequent steps.

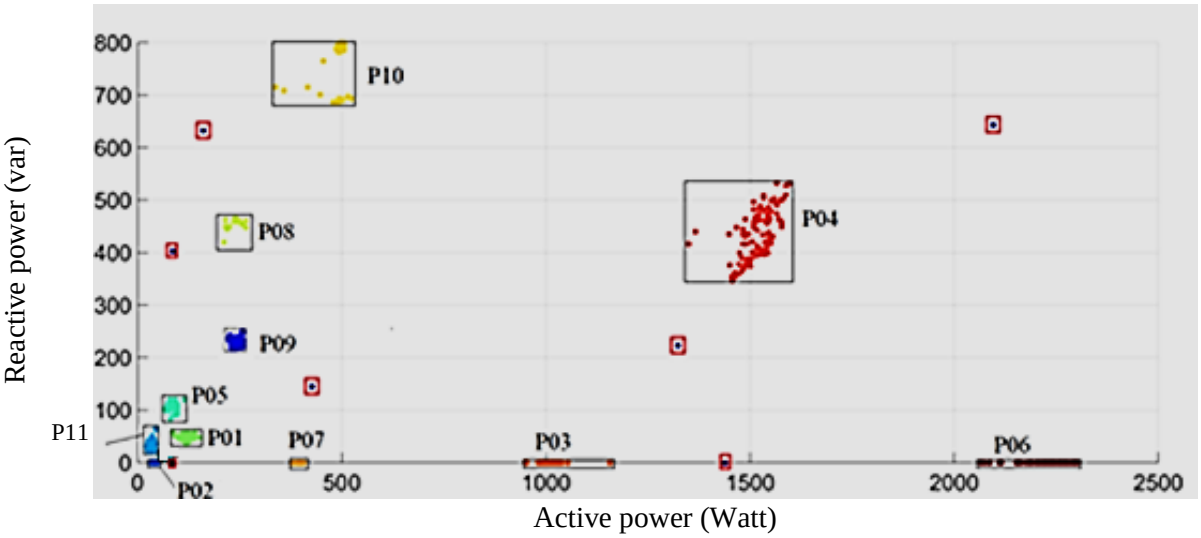


Figure 6.11. P - Q space for the measurement in the experimental place and the detected steady-state clusters shown by their cluster ID

That the region of *P* - *Q* space with *P* and *Q* less than 100 Watts and 200 vars included the groups of power signatures (i.e. P01, P02, P05, P11) positioned close to each other (see Figure 6.11). Using the ground truth, it was verified that except for the refrigerator light and the living room floor lamp that shared the same cluster P02, other HEAs were correctly assigned different cluster labels. HEAs with a relatively high power consumption in this figure were those that consumed more than 100 Watts and 200 vars. It was verified that in terms of high power consumption HEAs, the kettle and one of the operational modes of the electric cooktop shared the same group of power signatures, labelled P03. The reason was that both HEAs performed a heating operation in the kitchen with similar power consumption. This was also the case for the hair dryer and the toaster. The power signatures of both hair dryer and the toaster were thus labelled P07.

The detected cluster IDs were labelled with the name of their corresponding HEAs based on the ground truth for power consumption of HEAs inside the testbed as shown in Table 6.9. This was carried out to evaluate the performance of the AIPIA approach. The implementation of

this approach does not require the name of HEA(s) corresponding to each group of power signature to be known. All the groups of power signatures that occurred based on the occupant's interactions are shown in bold in Table 6.9. Note that since there was no Kinect sensor in the bathroom, none of the cluster IDs for the washing machine is displayed in bold. It is observed that some HEAs generated multiple clusters. For example, the washing machine produced different groups of power signatures because of its components and operation program. Some of these power signatures could not be removed as short pause gaps because of a long period between their occurrences. The electric cooktop produced two groups of power signatures in the data (i.e. P03 and P06) both generated upon the interaction of the occupant.

Table 6.9. The name of HEAs in the testbed along with their associated label of power signatures. Cluster IDs shown in bold are generated upon the interaction of the occupant. The labels are generated arbitrarily.

| ***HEAs*** | ***Group(s) of power signatures*** | | |
|---|---|---|---|
| Washing machine | P08 | P09 | P10 |
| Kettle | **P06** | | |
| Refrigerator (light) | **P02** | | |
| Electric cooktop | **P03** | **P06** | |
| Toaster | **P07** | | |
| Microwave | **P04** | | |
| Computer | **P11** | | |
| TV | **P05** | | |
| Living room light | **P02** | | |
| Hair dryer | **P07** | | |
| Refrigerator (cooling) | P01 | | |

The power signatures were labelled with cluster IDs and the steps outlined in Section 0 were taken to remove data points of self-regulated HEAs (i.e. the refrigerator). Figure 6.12 shows the results of calculating $X^2$ for the PDF associated with each cluster ID. The ground truth of power consumption of the refrigerator showed that the power signature with the value of $X^2$ less than the critical value (i.e. 35.172) was associated with the refrigerator. This resulted in the removal of the refrigerator turn-on events from the dataset. The $X^2$ values for the PDF of cluster IDs associated with the hair dryer and washing machine were relatively high as shown in Figure 6.12. The reason was that these HEAs were only used in specific times during the day and therefore their PDFs were more different from uniform distributions than the rest.

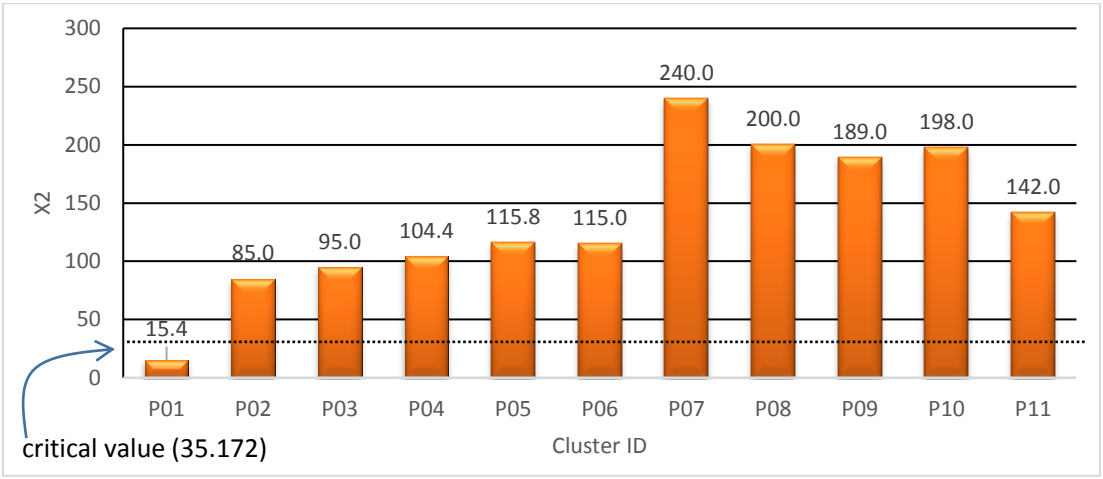


Figure 6.12. Results of the chi-square test on the hourly frequency of turn-on events of HEAs.

Short pause gaps of the remaining HEAs were removed, which resulted in removal of some turn-on events belonging to signature groups P03, P04, P06, P07, and P08. The hair dryer caused pause gaps due to the occupant's behaviour (e.g. turning it on and off) rather than an internal operation. Data for the first interaction in those situations were kept and the rest were eliminated from *power_signatures*. Events of P08 were caused by cyclic reversals of the washing machine tub during the washing cycle. *power_signatures* had 754 entries at the end of this operation.

The occupant's locations during the remaining turn-on events were clustered and each group was assigned an abstract label as shown in Figure 6.13. The physical location of each detected cluster in a room was manually determined based on the ID of the corresponding Kinect and coordinates of the cluster centre. Note that most of the turn-on events of the washing machine took place when the occupant was performing activities elsewhere (e.g. at the dining table or in bed). As a result, the occupant's locations while visiting dining table and bed were associated with a cluster ID. These two detected locations (i.e. L01 and L08) are referred as false locations.

Note that some cluster IDs in Figure 6.13 represent the location of more than one group of power signatures. For example, L03 was the location of interactions with both modes of operation of the electric cooktop. Similarly, L04 included the occupant's locations while interacting with both the kettle and the toaster.

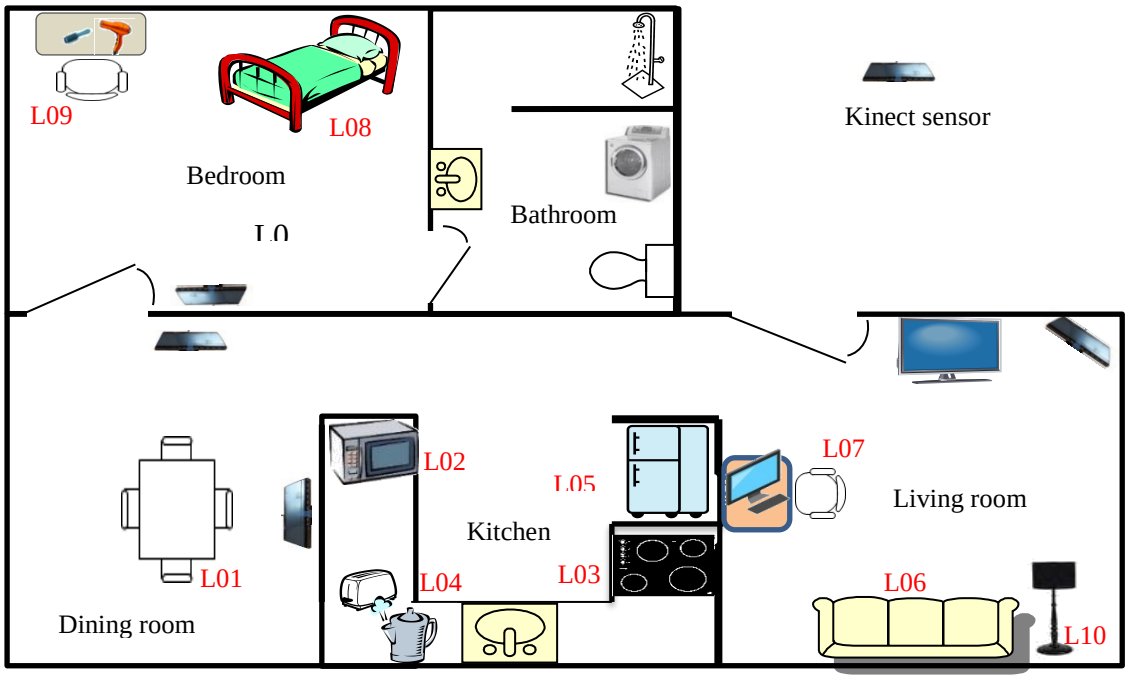


Figure 6.13. Cluster IDs of the occupant's locations inside the testbed.

The initial *location_rules* associating the occupant's locations with their respective power signatures is shown in Table 6.10 (a). The rules associating the power signatures with the occupant's locations (*power_rules*) are shown in Table 6.10 (b). The confidence of rules associating false locations (i.e. L01 and L08) to the groups of power signatures is relatively low in Table 6.10 (a). This is the case for their corresponding rules in Table 6.10 (b) with the consequent and antecedent parts in the reverse order. The confidence of these rules was low because their power signatures were also observed when the occupant visited places other than the location specified by the rule.

The Precision metric in the context of generating rules to associate visited locations with the groups of power signatures was considered to be the ratio of the number of locations correctly associated with their groups of power signatures to the number of all locations associated with the groups of power signatures. The Recall metric was the ratio of the number of locations correctly associated with the groups of power signatures to the number of locations that should have been associated with the groups of power signatures. An accurate set of rules results in a high recall, which means the majority of locations in which HEAs that were interacted with were detected. An accurate set of rules also results in a high precision, meaning false locations were not included in the discovered ones.

Table 6.10. (a) Initial *location_rules* obtained from applying the proposed approach on the training dataset (b) *power_rules* associated with the results.

| ***Location Cluster*** | | ***Power signature cluster*** | ***Confidence*** |
|---|---|---|---|
| L01 | → | P08 | 38.30% |
| L01 | → | P09 | 40.80% |
| L01 | → | P10 | 20.90% |
| L02 | → | P04 | 100% |
| L03 | → | P03 | 45.20% |
| L03 | → | P06 | 33.60% |
| L03 | → | P09 | 21.20% |
| L04 | → | P06 | 78.80% |
| L04 | → | P07 | 21.20% |
| L05 | → | P02 | 98.10% |
| L05 | → | P08 | 1.90% |
| L06 | → | P05 | 88.70% |
| L06 | → | P09 | 11.30% |
| L07 | → | P11 | 100% |
| L08 | → | P08 | 34.20% |
| L08 | → | P09 | 45% |
| L08 | → | P10 | 20.80% |
| L09 | → | P07 | 100% |
| L10 | → | P08 | 6% |
| L10 | → | P02 | 94% |

(a)

| ***Location Cluster*** | | ***Power signature cluster*** | ***Confidence*** |
|---|---|---|---|
| P08 | → | L01 | 32.80% |
| P09 | → | L01 | 39.90% |
| P10 | → | L01 | 52.90% |
| P04 | → | L02 | 100% |
| P03 | → | L03 | 100% |
| P06 | → | L03 | 80% |
| P09 | → | L03 | 10% |
| P06 | → | L04 | 20% |
| P07 | → | L04 | 77.20% |
| P02 | → | L05 | 75.20% |
| P08 | → | L05 | 5.70% |
| P05 | → | L06 | 100% |
| P09 | → | L06 | 8.70% |
| P11 | → | L07 | 100% |
| P08 | → | L08 | 31.50% |
| P09 | → | L08 | 41.30% |
| P10 | → | L08 | 47.30% |
| P07 | → | L09 | 22.80% |
| P08 | → | L10 | 30% |
| P02 | → | L10 | 24% |

(b)

It was observed that when *min_conf* is low, rules associating false locations with power signatures are selected (see Table 6.10). This decreased the precision of the output rule set. Increasing *min_conf,* on the other hand, caused rules associating locations with less frequently observed power signatures to be ignored and a lower level of recall. This parameter was experimentally set to 75% which was considered as a good compromise between a high precision and a high recall.

The final set of association rules obtained from the training stage is shown in Table 6.11. This table shows that the occupant's locations during interactions with all the monitored HEAs have been associated with the power signatures of the respective HEAs. HEAs that had more than one mode of operation (e.g. the electric cooktop) caused multiple rules to be generated with each rule associating the location of those HEAs with one of their power signatures. For

example, rules L03 → P03 and L03 → P06 associated the location of the occupant in front of the electric cooktop with each of its modes of operation.

Two different rules were generated to associate the location L04 to the power signatures generated by the kettle and the toaster as shown in Table 6.11. This was because the occupant was in the same location in the kitchen while interacting with them.

Each rule in the final rule set was labelled with an activity based on the ground truth information. This means that the location and the name of the HEA for each rule were obtained from the ground truth and then the occupant's activity associated with the use of that HEA was assigned to the rule. The labels assigned to rules are shown in Table 6.11.

Table 6.11. The output rule set of the training phase associating locations in the house to power signatures.

| ***Location*** | | ***Power signature*** | ***Confidence*** | ***Activity label*** |
|---|---|---|---|---|
| L02 | → | P04 | 100% | Using microwave |
| L03 | → | P03 | 100% | Using the cooktop mode #1 |
| L03 | → | P06 | 80% | Using the cooktop mode #2 |
| L04 | → | P06 | 78.80% | Using the kettle |
| L04 | → | P07 | 77.20% | Using the toaster |
| L05 | → | P02 | 98.10% | Using the refrigerator |
| L06 | → | P05 | 100% | Watching TV |
| L07 | → | P11 | 100% | Working at the computer |
| L09 | → | P07 | 100% | Using the hair dryer |
| L10 | → | P02 | 94% | Using the floor lamp |

### 6.3.3 Results of identifying instrumental ADLs

*Testing_Data 2* from the collected dataset (See Section 3.5.3.2) was used to evaluate the performance of AIPIA in identifying activities from sensor data. This dataset represents instrumental ADLs of an occupant collected from a combination of a single power meter and Kinect cameras for a total period of 18 days. The AIPIA approach labelled the detected interactions with HEAs as instrumental ADLs based on the labels given to the learned rules in Table 6.11. The label given to each detected interaction was verified by comparing it with the

ground truth provided by the occupant. The confusion matrix for all labelled activities (percentage values) is shown in Table 6.12. There are two extra columns in the tables as follows:

- 'Missed' corresponding to cases where interactions with HEAs mentioned in the ground truth were not identified. This may happen when the occupant's location or the power signature of the HEA during an interaction with the HEA was not within the boundaries of their respective clusters.

- 'False detection' for situations where an automatically generated power signature was detected as the occupant's interaction with an HEA and labelled with an instrumental ADL.

Each value in the diagonal elements of Table 6.12 shows the accuracy of the approach in identifying the occupant's interaction events associated with a specific ADL. These values are calculated using Equation 6.3.

$$Accuracy = \frac{correctly\ identified\ event}{correctly\ identified\ event + \ missed\ events + false\ detections} \tag{6.3}$$

Many missed interaction events were associated with interactions of the cooktop and the electrical kettle as indicated in Table 6.12. The table also shows that most misclassified activities were 'making tea' and 'using the cooktop mode #2' which have been misclassified as each other. This was due to the variations in the occupant's locations during interactions with HEAs associated with these activities. The power signatures generated by these two activities shared the same cluster ID. Since the locations of these activities were close to each other, the AIPIA approach confused these two activities in cases where the occupant was making tea but was located within the boundary of 'using the cooktop mode #2' or vice versa. The diagonal elements showed a classification accuracy of more than 85% for six out of the nine activities, with two classes having a rate of 100% as shown in Table 6.12.

The AIPIA approach was modified in another experiment to use only the data captured from the power sensor and the accuracy in identifying instrumental ADLs was re-calculated. This was carried out to evaluate the impact of combining the occupant's locations with power consumption data on the accuracy of AIPIA in identifying instrumental ADLs. The occupant's

activities were identified in this experiment based on observing specific power signatures on the power line. The training stage of AIPIA assigned activity labels to the groups of power signatures associated with the category of *interaction-generated*. The classification stage then checked whether a detected power signature falls within the boundaries of a cluster in '*interaction-generated'* category. In this case the activity label associated with the cluster was assigned to the power signature, hence the identification of instrumental ADLs.

Table 6.12. Confusion matrix for activities (percentage values). The rows represent actual activities, and the columns represent the identified activities.

| | Using the microwave | Using the cooktop mode #1 | Using the cooktop mode #2 | Using the kettle | Using the toaster | Watching TV | working at the computer | Using the floor lamp | Using the hair dryer | Missed | False detection |
|---|---|---|---|---|---|---|---|---|---|---|---|
| Using the microwave | 94% | 0 | 0 | 0 | 0 | 0 | 0 | 0 | 0 | 0 | %6 |
| Using the cooktop mode #1 | 0 | 80% | 0 | 0 | 0 | 0 | 0 | 0 | 0 | 17% | 3% |
| Using the cooktop mode #2 | 0 | 0 | 75% | 10% | 0 | 0 | 0 | 0 | 0 | 9% | %6 |
| Using the toaster | 0 | 0 | 10% | 78% | 0 | 0 | 0 | 0 | 0 | 12% | 0% |
| Using the kettle | 0 | 0 | 0 | 0 | 95% | 0 | 0 | 0 | 0 | 5% | 0% |
| Watching TV | 0 | 0 | 0 | 0 | 0 | 89% | 0 | 0 | 0 | 5% | 0 |
| working at the computer | 0 | 0 | 0 | 0 | 0 | 0 | 100% | 0 | 0 | 0 | 0 |
| Using the floor lamp | 0 | 0 | 0 | 0 | 0 | 0 | 0 | 89% | 0 | 8% | 0 |
| Using the hair dryer | 0 | 0 | 0 | 0 | 0 | 0 | 0 | 0 | 100% | 0 | 0 |

Equation 6.3 was used to measure the accuracy of this version of the AIPIA. The evaluations showed that this version of the approach had a classification accuracy of 75.1%. It was observed that it could successfully filter out many of the power signatures generated automatically by the thermostatically controlled HEAs as well as the only self-regulating appliance in the testbed which was the refrigerator. All power signatures belonging to the washing machine (i.e. those belonging to clusters P08, P09, and P10) were mistakenly identified as the result of the occupant interacting with HEAs. This was because the approach did not have the occupant's locations during his interactions with the HEAs. This approach also could not correctly distinguish activities involving different HEAs which shared the same group of power signatures. For example, interactions with the hair dryer were labelled as "using the toaster" since the hair dryer and the toaster had similar power signatures and shared the same cluster ID. This was also the case for the kettle and the electric cooktop.

The classification accuracy of AIPIA when used only power consumption data was much lower than the average accuracy of 85.3% obtained when the occupant's locations were combined with power consumption data (the average of diagonal elements in Table 6.12). This combination of data enabled AIPIA to distinguish between the usage events of HEAs with similar power signatures in the same room. It could correctly label most interactions with the kettle and the electric cooktop in the kitchen. None of the power signatures from the washing machine were detected by AIPIA as the result of an activity of the occupant since no rule associated those power signatures with a location. Most misclassifications were due to the fact that the occupant's locations and/or the detected power signatures were outside of their respective cluster boundaries. The combinations of the occupant's location and the detected power signature in those situations did not trigger any rule in the set of learned rules and as such the approach did not identify those events as instrumental ADLs.

## 6.4 Discussion

The *MinPnts* parameter in the algorithm for grouping visited locations was set to zero so every visited location that has co-occurred with a power signature (in '*interaction-generated*' category) has the potential to become a cluster. This parameter can be automatically calculated from the training dataset according to its size. For example, it can be obtained using

$$\text{MinPnts} = NoM \times 25\%$$

where *NoM* indicates the number of months in the training dataset. This choice guarantees that a cluster of the occupant's locations has to have instances in at least 4 days in each month in the dataset.

In the results presented in this chapter, the name of HEAs and the occupant's location for each rule were known from the ground truth. In the implementation of the approach only the contextual information can be used for the room associated with each rule to select more general activity labels. For example, each rule associating a location in the kitchen with a power signature can be labelled as a feeding activity because the kitchen is usually visited for preparing meals. In this case, each interaction with an HEA in the kitchen is identified as a feeding activity.

## 6.5 Summary

A generic approach was presented to automatically identify instrumental ADLs through detecting an occupant's interactions with HEAs. This approach used an association rule-mining algorithm to find mappings between the power signatures of HEAs and the occupant's physical locations. The approach then identified instrumental ADL using the set of association rules. This is the first known system that combines data from a power sensor with Kinect depth maps to identify instrumental ADLs inside a house.

Evaluations of the approach using the data captured from a real-life setting have shown the effectiveness of this approach in terms of detecting interactions with HEAs and identifying them as instrumental ADLs. Evaluation results have also verified the improved performance of the approach when combining data from Kinect sensors with a power meter.

The next chapter presents an approach for monitoring instrumental ADLs of an elderly person living alone. AIPA is employed in the first stage of this approach to generate representations of instrumental ADLs based on the occupant's interactions with HEAs.

# CHAPTER 7: MONITORING INSTRUMENTAL ADLS USING KINECT DEPTH MAPS AND POWER CONSUMPTION DATA

This chapter presents an approach for monitoring instrumental ADLs of an elderly person living alone. Stages of this approach are undertaken to answer the research questions regarding monitoring of instrumental ADLs. The chapter first introduces the problem of monitoring instrumental ADLs and provides a review of the limitations of existing approaches (Section 7.1). It then presents the stages of the proposed approach in Section 7.2. This is followed by the experimental results of evaluation of the approach in Section 7.3 and a discussion and summary in Sections 7.4 and 7.5 respectively.

## 7.1 Introduction

Monitoring instrumental ADLs and identifying long-term deviations from their regular patterns are important in the evaluation of an elderly person's ability to live independently and early detection of deteriorating health. Elderly people tend to have stable lifestyles, enabling the detection of abnormalities in their rhythm of daily living. Some ADL scales have been developed in clinical research to assess the rhythm of daily living of elderly individuals (Xiang et al., 2015). These traditional assessment methods depend on filling out questionnaires and self-reports and consequently fail to elicit precise answers as the elderly person might have difficulty remembering their ADLs or perceive the questionnaire as intrusive.

Advances in telecommunication and sensor technology have led many researchers to propose continuous monitoring of elderly people's interactions with HEAs to assist ADL measurements. The proposed approaches involve fitting sensors into the house and acquiring data about the subject's interactions with domestic objects. The performance of instrumental ADLs is usually identified from sensor data, and the normal patterns of these activities are modelled using machine learning techniques. The model is used to identify long-term deviations of the subject's behaviours from the learned regular patterns. This can allow timely intervention of care givers and early detection of diseases such as dementia and Alzheimer's.

Most existing instrumental ADL monitoring approaches aim at recognising the exact type of subject's activities in order to model their normal behaviour patterns (Peetoom et al., 2015). This poses a limitation on real-life implementation of these approaches as individuals can

perform a wide range of ADLs in various ways in real-life settings.

Another drawback of approaches that involve recognising ADLs is that the subject is required to provide information about the objects in the monitored environment (e.g. the name and application of HEAs), which may not be possible for all situations. For example, a set of fuzzy rules was developed by Banerjee, Keller, Popescu, and Skubic (2015) to recognise instrumental ADLs based on a person's interactions with domestic objects. A single Kinect sensor was installed in the monitored room to provide the depth map of ADLs. The user was required to label objects in the Kinect's field of view and provide information about the room. The set of fuzzy rules was then able to recognise only few instrumental ADLs in new data based on the information provided by the user.

The choice of sensors deployed by an instrumental ADL monitoring approach along with the adopted machine-learning technique is important. The cost, ease of use, and privacy are key aspects of choosing sensors. The most practical and successful approach is considered to be one which involves the use of a machine learning technique for ADL monitoring that is robust to fine variations in ADLs of an individual and requires little training or configuration effort in a household.

This chapter presents a person-tailored unsupervised approach, called AMI-ADLs, for monitoring the pattern of performing instrumental ADLs without a need for recognising the exact type of ongoing ADLs. AMI-ADLs measures a set of activity features, from an unlabelled dataset of Kinect depth maps and house power consumption, to quantify important aspects of the occupant's normal behaviours. The training values of these features are automatically modelled by fuzzy rules in order to characterise the daily activity level of the occupant. Sensor data for each new day are then similarly processed and the long-term deviations of activity level from the occupant's learned profile are reported to a caregiver.

## 7.2 The proposed approach

An unsupervised fuzzy approach, called AMI-ADLs, is proposed to monitor the habitual performance of instrumental ADLs based on simple features extracted from the occupant's daily interactions with HEAs. The layout of this approach which consists of three stages is shown in Figure 7.1. An unlabeled training dataset of the home overall power consumption

(obtained from the power sensor) and the occupant's skeleton data during ADLs (obtained from the Kinect sensors) is used in the first stage to identify the occupant's interactions with HEAs. The detected appliance usage events form representations of the occupant's instrumental ADLs. Each representation includes a unique arbitrary label given to the activity of using the HEA and the time of the usage event. An example of this representation is

$$\text{Activity: Using } HEA_1 \quad time-stamp\text{: } 10\text{:}33\text{:}14 \text{ 11-11-2015}$$

where *Using* $HEA_1$ is an arbitrary label given to the activity of using a specific HEA inside the home and $10\text{:}33\text{:}14$ is the time of the occupant's interaction with $HEA_1$.

The second stage is to automatically generate a model of instrumental ADLs. It first calculates simple features from the habitual performance of instrumental ADLs. A fuzzy rule set is then learned in this stage to model these features. This rule set is used in a fuzzy inference system at Stage 3 to detect deviations in the habitual performance of instrumental ADLs in new data. The output of Stage 3 is daily reports about deviations of instrumental ADLs from the learned normal behaviours of the occupant. By observing drifts from normal behaviour throughout time, caregivers can identify significant changes in the person's wellbeing. Details of these stages are described in the following sections.

### 7.2.1 Stage 1: Generating representations of instrumental ADLs

This stage addresses the first research sub-question in monitoring instrumental ADLs. The input to this stage is a training dataset supplied by a combination of Kinect cameras and a power sensor. The training dataset is processed by AIPIA (see Chapter 6) to generate a timestamped list of detected interactions with HEAs as the representations of instrumental ADLs.

AIPIA generates rules to associate the occupant's locations inside the house with the power signatures of specific HEAs. Each rule in the association rule set is then given an arbitrary label (e.g. *Using HEA1*, *Using HEA2*,…) to indicate the usage of different HEAs. This is to differentiate the usage events of different HEAs. Note that AMI-ADLs does not require the actual name of the monitored HEAs. Given the occupant's current location and a detected power signature, the rule set determines whether the power signature is the result of the occupant's interaction with an HEA and the label of the rule is assigned to that usage event.

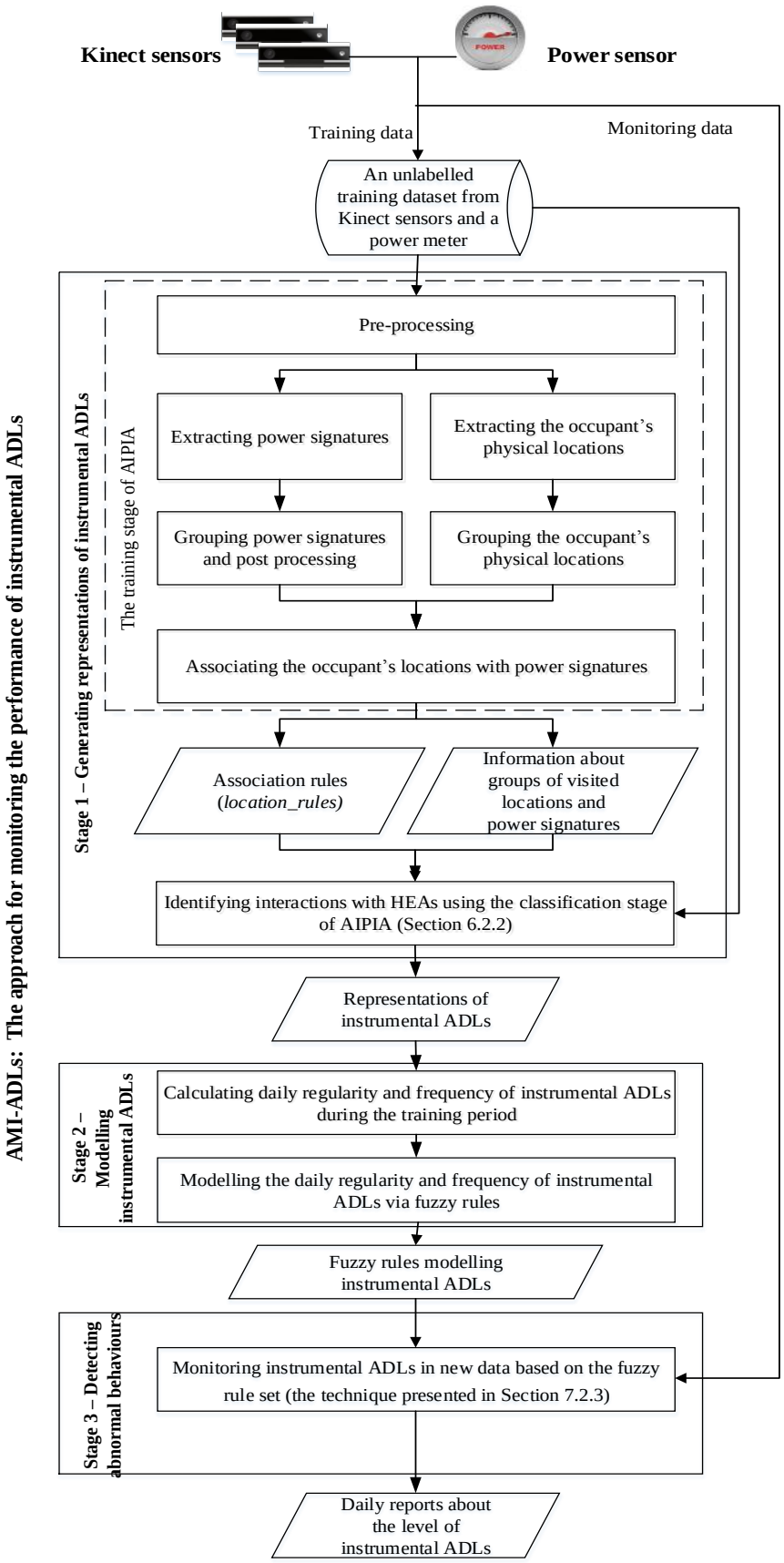


Figure 7.1. The workflow of AMI-ADLs.

This rule set is employed by the procedure described in the classification stage of AIPIA (see Section 6.2.2) to identify and to label the occupant's interactions with HEAs in the training dataset. The output of this operation is a list of the usage events of HEAs along with their timestamps. Table 7.1 shows an example of this list. Column "Activity" in this table indicates the label of the rule that associates the occupant's location with the power signature of the respective HEA. Note that the timestamps of the first four appliance usage events are very close, indicating that they may belong to the same activity (e.g. preparing breakfast in the morning). Activity "*Using $HEA_1$*" has been repeated multiple times across the day indicating that the HEA associated with this activity plays a significant role in the occupant's daily routine.

Table 7.1. An example of the representations of instrumental ADLs

| **Activity** | **Timestamp** |
|---|---|
| *Using $HEA_1$* | 10-Oct-15, 07:34:47 |
| *Using $HEA_1$* | 10-Oct-15, 07:25:14 |
| *Using $HEA_2$* | 10-Oct-15, 07:42:43 |
| *Using $HEA_3$* | 10-Oct-15, 07:42:55 |
| *Using $HEA_1$* | 10-Oct-15, 08:52:41 |
| *Using $HEA_4$* | 10-Oct-15, 09:23:10 |
| *Using $HEA_2$* | 10-Oct-15, 11:23:08 |
| *Using $HEA_1$* | 10-Oct-15, 12:23:14 |
| *Using $HEA_1$* | 10-Oct-15, 16:08:39 |

### 7.2.2 Stage 2: Modelling the performance of instrumental ADLs

This stage addresses the second research sub-question in monitoring instrumental ADLs. It takes the representations of activities from the previous stage and models important aspects of instrumental ADLs. This stage involves two steps. In the first stage, two simple activity features are estimated based on the training representations of instrumental ADLs, and the normal variation ranges of these activity features are calculated. In the second stage, fuzzy rules are generated to model the normal variation ranges of the activity features.

***Calculating activity features from representations of instrumental ADLs*:** Two simple activity features are calculated to quantify the daily instrumental ADLs with regards to their

regularity and frequency. These features which are (1) *regularity* and (2) *frequency* are explained below.

***(1) Regularity*:** Instrumental ADLs are carried out in different times throughout the day. Considering that elderly people usually follow a constant daily routine, the ratio of the length of time the elderly take to perform instrumental ADLs to the overall duration they spend at home is almost constant. A study by Ranjan and Whitehouse (2015) suggested that a substantial change in the regularity of instrumental ADLs lasting for several days can feature a potential warning for a decline in the functional and cognitive abilities of the person.

*Regularity* characterises how regularly the occupant interacts with HEAs (performs instrumental ADLs) on a daily basis. Each day is divided into 24 hourly periods. Let $I_i$ show the number of interactions with HEAs detected for each period $i$ $(1 \leq i \leq 24)$ and let Boolean $O_i$ show whether the occupant is observed by any Kinect sensor inside the home during that period. Each period *i* with $I_i$ greater than zero is called a *period of activity* and each period with $O_i = 1$ is called a *period of presence*. *Regularity* for each day is defined by the ratio of *periods of activity* to *periods of presence*, as shown in Equation 7.1.

$$regularity = \frac{periods\ of\ activity}{periods\ of\ presence} \tag{7.1}$$

The reason why '*periods of presence'* are taken into account instead of 24 periods of the day is to ensure that periods in which the occupant is not inside the house (e.g. during weekends) do not affect the estimation of this feature. The regularity of instrumental ADLs in this case is measured based on only those time periods when the occupant is present in the house.

*The regularity* factor is calculated for every day in the representations of instrumental ADLs. This results in a series named $REG_{training} = \{regularity_1, \cdots, regularity_D\}$ in which $regularity_j$ indicates *regularity* for day $j$ $(1 \leq j \leq D)$ and is calculated via Equation 7.1. $D$ is the total number of days in the training dataset.

***(2) Frequency***: In addition to the regularity of interactions with HEAs, it is important to monitor their frequency. This is because a decline in the frequency of instrumental ADLs can

be attributed to a decline in the occupant's functional ability and health (Ranjan & Whitehouse, 2015). *Frequency* for a given day quantifies how similar the pattern of using important HEAs is to the occupant's daily routine. Important HEAs are those that have been used during most days of capturing the training dataset and thus play an important role in the occupant's daily routine.

The example of representations of instrumental ADLs in Table 7.1 shows that the activity label in each record characterises the usage of a specific HEA. The level of importance of using each HEA in these records is calculated as the ratio of how many days the HEA has been used to the total number of days in the training dataset.

Assume that the occupant's interactions with HEAs during the training period have resulted in a set of $A$ different association rules each having a unique activity label. A choice for these labels can be "*using HEA*$_1$,…, *using HEA*$_A$". A binary variable $B_{i,j}$ is defined such that $i$ ($1 \leq i \leq A$) and $j$ ($1 \leq j \leq D$) indicate the index of an activity and a day in the training dataset, respectively. $B_{i,j}$ is equal to one only if activity label $i$ has been observed during day $j$ in the training dataset (see Equation 7.2).

$$B_{i,j} = \begin{cases} 1, & if\ the\ activity\ label\ 'i'\ is\ observed\ during\ day\ 'j' \\ 0, & otherwise \end{cases} \tag{7.2}$$

The level of importance for each activity label $i$ is calculated using Equation 7.3.

$$Importance_{\mathrm{i}} = \frac{\sum_{j=1}^{D} B_{i,j}}{D} \tag{7.3}$$

Let the number of times an activity $i$ is observed during a given day be denoted by $CoA_i$. The *frequency* for that day is obtained by Equation 7.4.

$$frequency = \sum_{i=1}^{A} \mathrm{CoA_i} \,.\, Importance_i \tag{7.4}$$

where *A* is the number of different activity labels in the representations of instrumental ADLs. *frequency* is calculated for each day in the training dataset to obtain a normal variation range for this feature. This operation results in a series named $FREQ_{training} = \{frequency_1, \cdots, frequency_D\}$ in which *D* indicates the total number of days in the training dataset and $frequency_j$ $(1 \leq j \leq D)$ denotes denoted *frequency* calculated for day $j$. For example, assume that representations of instrumental ADLs from Stage 1 involve instances of four different activities labelled *using HEA1*, *using HEA2*, *using HEA3*, and *using HEA4*. Also, let the count of these activities for each day to be those in Table 7.2. Note that in this example *D* is 5.

Table 7.2. An example of the daily number of activities involving interaction with HEAs

| Activity / Day | *Using HEA1 (i=1)* | *Using HEA2 (i=2)* | *Using HEA3 (i=3)* | *Using HEA4 (i=4)* |
|---|---|---|---|---|
| 1 | $CoA_1$=15 | $CoA_2$=4 | $CoA_3$=1 | $CoA_4$=2 |
| 2 | $CoA_1$=16 | $CoA_2$=7 | $CoA_3$=0 | $CoA_4$=4 |
| 3 | $CoA_1$=11 | $CoA_2$=6 | $CoA_3$=2 | $CoA_4$=1 |
| 4 | $CoA_1$=10 | $CoA_2$=2 | $CoA_3$=0 | $CoA_4$=0 |
| 5 | $CoA_1$=8 | $CoA_2$=0 | $CoA_3$=2 | $CoA_4$=2 |

The values of *frequency* for these five days in this example are calculated as shown in Figure 7.2. It can be seen that '$Using\ HEA_1$' has been carried out every day and thus received an importance of 100%. '$Using\ HEA_3$' was observed only on 50% of days, hence a lower importance. Day 2 has the highest *frequency* of instrumental ADLs whereas Day 5 has the lowest as shown in Figure 7.2. During day 5 '$Using\ HEA_1$has been carried out much less than on day 2. This highly affected *frequency* for day 5, since $Using\ HEA_1$ has an importance of 100%.

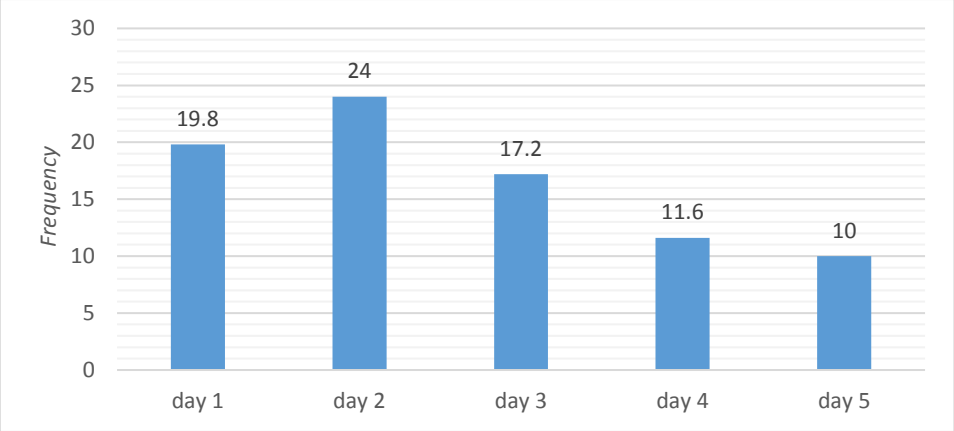


Figure 7.2. An example of *frequency* of four activities shown in Table 7.2.

***Modelling activity features via fuzzy rules***: In this step a set of fuzzy rules is developed to map the activity features into different levels of performing instrumental ADLs. Table 7.3 shows an example where each rule is in the form of:

Rule $R_i$: IF *regularity* is $A_m^1$ AND $frequency$ is $A_n^2$ THEN *Activity_level* is $B_k$"

$R_i$ is the $i$-th rule, *regularity* and $frequency$ are the inputs to the fuzzy rule, *Activity_level* is the output variable which describes how similar the *regularity* and $frequency$ are to those of the occupant's normal behaviour. $A_m^1$ and $A_n^2$ are the fuzzy sets describing *regularity* and $frequency$, respectively. Parameters of these fuzzy sets are learned from the training dataset. $B_k$ is the fuzzy set for the output variable.

Table 7.3. An example of a fuzzy rule set modelling the variation range of *regularity* and *frequency*.

| | **Antecedent** | | **Consequent** |
|---|---|---|---|
| **Index** | ***Regularity*** | ***Frequency*** | ***Activity level*** |
| $R_1$ | *Low* | *Low* | *VeryLow* |
| $R_2$ | *Normal* | *Low* | *Low* |
| $R_3$ | *Normal* | *Normal* | *Normal* |
| ⋮ | ⋮ | ⋮ | ⋮ |

Determining these rules involves two operations. The first operation is *defining fuzzy sets for activity features* (i.e. *regularity* and *frequency)* where a data-driven technique is used to determine the mapping of features values to membership of linguistically labelled fuzzy sets. A number of fuzzy sets are also defined over the output variable. The second operation is

*determining the relation between fuzzy sets of input and output variables* where the fuzzy rule set is generated.

#### *7.2.2.1 Defining fuzzy sets for activity features*

Fuzzy sets are defined over activity features to convert their crisp values into fuzzy labels. These labels quantify the occupant's performance of instrumental ADLs. For example, the value of *frequency* might be mapped to the linguistic label "*high*" if the occupant uses too many HEAs during the day. Three fuzzy sets are defined over each activity features, namely "*low*", "*medium*", and "*high*". These fuzzy sets for *regularity* are obtained by calculating the mean and standard deviation of the training samples in $REG_{training}$. The mean value is denoted by $m_{regularity}$ and the standard deviation value is shown as $\sigma_{regularity}$.

The associated membership functions for "$low$", "$normal$", and "$high$" are defined as equations 7.5, 7.6, and 7.7, respectively. All of these fuzzy sets have Gaussian membership functions. The left horizontal side of the function for "*low*" starts from $m_{regularity\ -}4\sigma_{regularity}$ and the right horizontal side of the function for "*high*" starts from $m_{regularity+}4\sigma_{regularity}$ of the input domain. This is to make sure that input values lying outside the domain interval receive a degree of membership in a fuzzy set.

$$\mu^{1}_{\text{low}}(\text{x}) = \begin{cases} \text{e}^{\frac{-\left(\text{x}-\left(\text{m}_{\text{regularity}-}4\sigma_{\text{regularity}}\right)\right)^{2}}{2\,(\sigma_{\text{regularity}})^{2}}}, & \text{x} \geq \left(\text{m}_{\text{regularity}-}4\sigma_{\text{regularity}}\right) \\ 1, & \text{otherwise} \end{cases} \tag{7.5}$$

$$\mu^{1}_{\text{normal}}(\text{x}) = \text{e}^{\frac{-\left(\text{x}-\text{m}_{\text{regularity}}\right)^{2}}{2\,(\sigma_{\text{regularity}})^{2}}} \tag{7.6}$$

$$\mu^{1}_{\text{high}}(x) = \begin{cases} e^{\frac{-\left(x-\left(m_{\text{regularity}+4\sigma_{\text{regularity}}}\right)\right)^{2}}{2\,(\sigma_{\text{regularity}})^{2}}} & , x \geq \left(m_{\text{regularity}+4\sigma_{\text{regularity}}}\right) \\ 1 & , \text{otherwise} \end{cases}$$

(7.7)

An example of these fuzzy sets defined over *regularity* is shown in Figure 7.3. Note that in this example $m_{regularity}$ and $\sigma_{regularity}$ are 0.4 and 0.07 respectively. *regularity* receives a higher membership degree from "*normal*" if it falls within the range of $[m_{frequency} - 2\sigma_{frequency}, m_{frequency} + 2\sigma_{frequency}]$.

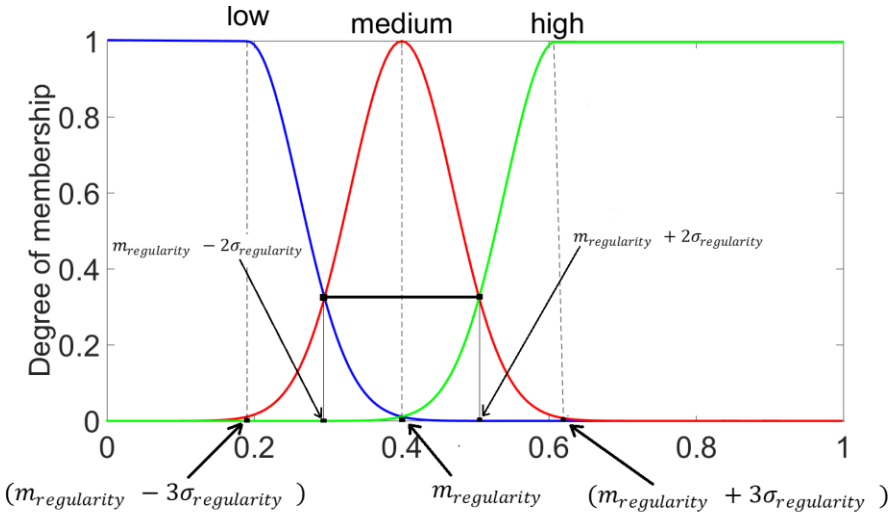


Figure 7.3. An example of fuzzy sets defined over *regularity*.

Three fuzzy sets are similarly defined over *frequency* by using the mean and standard deviation of training samples in $FREQ_{training}$. The mean value is denoted as $m_{frequency}$ and the standard deviation is shown as $\sigma_{frequency}$. The membership functions associated with fuzzy sets "*low*", "*normal*", and "*high*" are defined as equations 7.8, 7.9, and 7.10 respectively.

$$\mu^{2}_{\text{low}}(x) = \begin{cases} e^{\frac{-\left(x-\left(m_{\text{frequency}-4\sigma_{\text{frequency}}}\right)\right)^{2}}{2\,(\sigma_{\text{frequency}})^{2}}} & , x \geq \left(m_{\text{frequency}-4\sigma_{\text{frequency}}}\right) \\ 1 & , \text{otherwise} \end{cases}$$

(7.8)

$$\mu^2_{normal}(x) = e^{\frac{-(x-m_{frequency})^2}{2\,(\sigma_{frequency})^2}} \tag{7.9}$$

$$\mu^2_{high}(x) = \begin{cases} e^{\frac{-\left(x-(m_{frequency+}4\sigma_{frequency})\right)^2}{2\,(\sigma\ frequency)^2}} & , x \geq \left(m_{frequency+}4\sigma_{frequency}\right) \\ 1 & , otherwise \end{cases} \tag{7.10}$$

The space of the output variable *activity_level* is limited to [-1 +1]; a value near -1 means that the occupant's instrumental ADLs showed a high downward drift from the normal routine in terms of their frequency and regularity. A value of around +1 indicates the opposite. A value of around zero shows normal regularity and frequency of instrumental ADLs during the day. The range of this variable is composed of five fuzzy sets "*VeryLow*", "*Low*", "*Normal*", *High*" and "*VeryHigh*". Figure 7.4 shows the fuzzy partition of this range into the fuzzy sets.

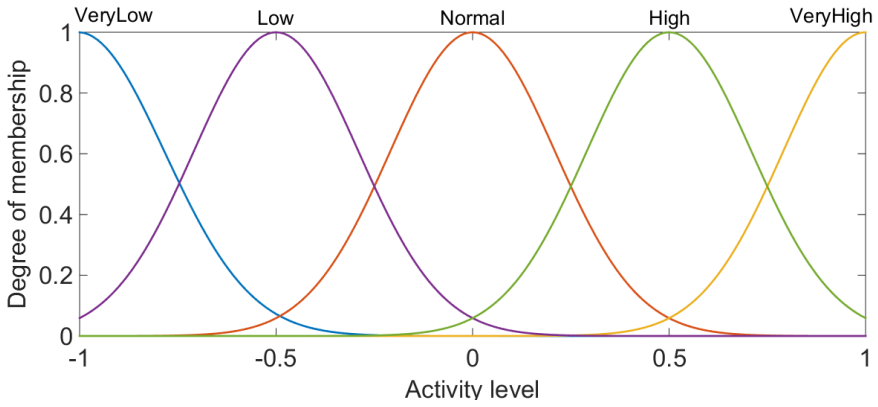


Figure 7.4. Fuzzy sets defined over *activity_level*.

### *7.2.2.2 Determining fuzzy rules*

Nine fuzzy rules are defined to characterise the relationship between the input fuzzy variables (i.e. *regularity* and *frequency*) and *activity_level*. A simple way to demonstrate these rules is through an IF-THEN table that captures the relationship between fuzzy variables in the antecedent and consequent of the rules. This is illustrated in Table 7.4. Each rule in this table indicates the activity level of the occupant given the regularity and frequency of instrumental ADLs.

Table 7.4. Table of fuzzy rules to monitor instrumental ADLs

| ***Rule*** | ***If*** | | ***Then*** |
|---|---|---|---|
| | ***Frequency*** | ***Regularity*** | ***Activity_level*** |
| $R_1$ | *low* | *Low* | *very_low* |
| $R_2$ | *low* | *Normal* | *Low* |
| $R_3$ | *low* | *High* | *High* |
| $R_4$ | *normal* | *Low* | *Low* |
| $R_5$ | *normal* | *Normal* | *Normal* |
| $R_6$ | *normal* | *High* | *High* |
| $R_7$ | *high* | *Low* | *Low* |
| $R_8$ | *high* | *Normal* | *High* |
| $R_9$ | *high* | *High* | *very_high* |

Note that when *frequency* is low and *regularity* is high, the *activity_level* is determined to be high. This situation suggests that although there are fewer instrumental ADLs than in the normal profile, the occupant has been active for an extended duration of time. On the contrary, high *frequency* and low *regularity* lead *activity_level* to be low, which suggests that the subject has spent less time to perform instrumental ADLs. For example, they might have skipped preparing a meal in the kitchen.

### 7.2.3 Stage 3: Detecting abnormal behaviours

This stage addresses the third research sub-question in monitoring instrumental ADLs. The fuzzy rule set developed in the previous stage is used by a fuzzy inference system to monitor the performance of instrumental ADLs in new data. The outputs of this stage are customised reports showing the trends of the subject's activity level over a long-term period (e.g. days or weeks). These outputs can be interpreted intuitively by care givers to identify deviations from normal behaviours.

Sensor data of each new day are similarly processed using the procedure described in Section 6.2.2 to identify appliance usage events. This results in a list of instrumental ADLs in the form shown in Table 7.1. The daily values of *regularity* and *frequency* are then calculated using equations 7.1, and 7.4 respectively. These values are converted into their respective fuzzy labels and evaluated by the FIS to determine the occupant's activity level for the day.

Among different types of FIS, Mamdani is implemented because it is robust and involves simplified calculations. This type of FIS consists of a fuzzifier, a fuzzy rule set, a fuzzy inference engine, and a defuzzifier. For each input variable, the fuzzifier determines the

degrees of membership of a crisp value in the fuzzy sets defined over the variable. The degrees of membership of the input in the fuzzy sets over variables are employed by the inference engine to evaluate the fuzzy rules and to generate the fuzzy output of the system.

The '*min'* operator is used to calculate both "AND" and "THEN" parts of the fuzzy rules. Since fuzzy sets in the input variables might have overlapping ranges, an input crisp value can be a member of multiple fuzzy sets. This causes the membership degree of a fuzzy set at the consequent of multiple rules to be nonzero which means multiple rules are triggered. The fuzzy sets that represent the outputs of the triggered rules are combined to generate the fuzzy output of FIS. This is carried out through a process called aggregation. The input of the aggregation process is the list of truncated membership functions returned by the consequent of the triggered rules. The output of the aggregation process is a fuzzy set for the output variable.

The aggregation operator '*max'* is used here. The fuzzy set for the output variable is therefore the maximum of the output fuzzy sets in the consequent of the triggered rules (Equation 7.11).

$$f_{activity\_level} = max\left(B_{k_{R_1}}, B_{k_{R_2}}, \ldots, B_{k_{R_n}}\right) \tag{7.11}$$

$B_{k_{R_i}}$ in the above equation represents the degree of membership in the fuzzy set in the consequent of the *i*-th triggered rule.

The defuzzification step of the FIS converts the fuzzy set for the output variable into a crisp value, i.e. *activity_level*. The centre of gravity method is used here as the defuzzifier which outputs the centre of the gravity of the combined fuzzy set of the output variable (see Equation 7.12).

$$activity_{level} = \frac{\int activity_{level} \times d\left(f_{activity_{level}}\right)}{\int activity_{level} \times d\left(f_{activity_{level}}\right)} \tag{7.12}$$

For each day in the new data, the occupant's activity level is reported to the caregiver via a notice generated in the form of:

"The activity level of the occupant was X on dd/mm/yy"

(7.13)

*X* represents the fuzzy set with the maximum matching measure for *activity_level* of that day and is obtained from Equation 7.14.

$$X = \arg max_{k=1}^{5} \left( \mu_{B_k}(activity_{level}) \right)$$

(7.14)

$\mu_{B_k}(x)$ in Equation 7.14 represents the membership function of fuzzy set $B_k$. *dd/mm/yy* indicates the date at which instrumental ADLs are monitored. One example of the generated notice can be:

"*The activity level of the occupant was normal on 02/04/15*"

The interpretation of *activity_level* for a given day is simple. This figure would be around zero if the frequency and the regularity of instrumental ADLs for the day are close to those associated with the occupant's normal behaviour. This indicates that the occupant maintained the normal routine throughout the day. If this index is below zero, it means that the occupant performed instrumental ADLs either less frequently or less regularly than they normally do. If this situation persists for consecutive days, it indicates a need for medical help. If this index is around one, it shows a major upward drift from the normal daily routine. For example, this situation may occur if the occupant is awake most of the night (as a result of an illness) and hence more usage events of HEAs.

The daily values of *activity_level* along with their respective fuzzy terms are stored in a database for the purpose of generating visual representations for a given long-term period. Plotting values of *activity_level* across this period allows long-term trend analyses of the occupant's behaviours. The *x* axis in this plot shows the days during which monitoring happens and the *y* axis indicates *activity_level* whose value ranges between -1 to 1. Observing trends of changes in *activity_level* can help caregivers to identify persisting drifts from the daily routine as warning signs (Noury et al., 2011).

A Gantt chart is also generated for a given period to represent the time span of each activity level. On the vertical axis of this chart there is a list of linguistic labels associated with

*activity_level* (i.e. "*very low*", "*low*", "*normal*", "*high*", and "*very high*") and the horizontal axis represents the time span of the monitoring period broken down into days. Activity levels are represented by horizontal bars of varying lengths; the position and length of each bar reflects the start date, duration and end date for the respective period during which the activity level has been detected. This chart facilitates interpretation of activity levels of instrumental ADLs, identification of when each deviation from normal behaviour begins and ends, and estimation of how long each period of deviation is.

The Gantt chart of an imaginary two-week period is shown in Figure 7.5. The occupant's behaviour is shown as normal for the first four days followed by a drift to a state of being overactive during the next two days. This upward trend continues as the occupant is detected to be highly overactive during the following four days. The occupant is again normally active during the last three days of the period.

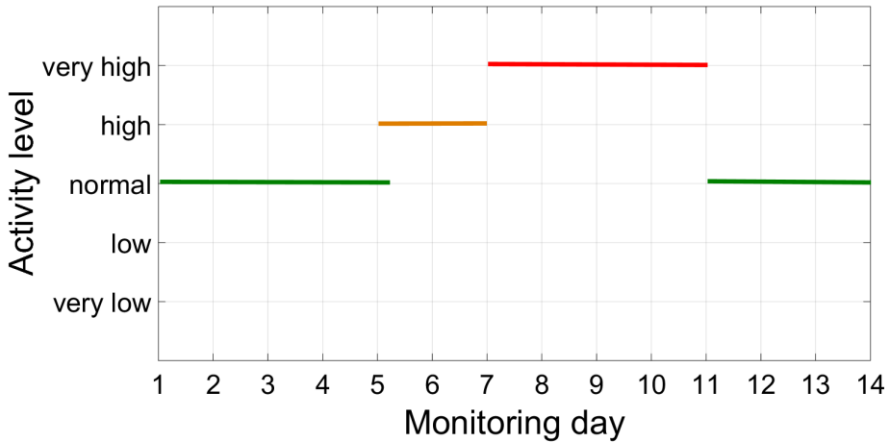


Figure 7.5. Example of a Gantt chart for a two-week period of monitoring. The horizontal axis shows the days and the vertical axis indicates the activity level during each day.

## 7.3 Experimental results

The dataset captured from the testbed (see Section 3.4.3.2) was used to evaluate the effectiveness and robustness of AMI-ADLs. Section 7.3.1 provides a validation of the effectiveness of this approach and Section 7.3.2 evaluates its robustness in regards to errors in the identification of the occupant's instrumental ADLs.

### 7.3.1 Evaluating the performance of AMI-ADLs

The training dataset captured from the testbed was used to develop the stages of AMI-ADLs.

Daily data in this dataset simulated a normal routine of ADLs associated with an elderly person living alone. A rule set was obtained from the first stage of AMI-ADLs to associate the occupant's locations with the power signatures. This rule set was shown in the previous chapter (see Table 6.11). The rules were labelled with the names of their respective HEAs (see "Activity labels" in Table 6.11) for the sake of presenting results to readers. In an implementation of AMI-ADLs, these rules can be assigned arbitrary labels and there is no need for the names of their respective HEAs to be stipulated.

Using this rule set the occupant's interactions with HEAs were detected in the training dataset. These interaction events were then labelled based on labels that were given to the rules which resulted in obtaining the representations of instrumental ADLs in the form of those shown in Table 7.1. The representations of instrumental ADLs were then used to perform steps if Stage 2. *Regularity* of instrumental ADLs was measured for each day in the training dataset as shown in Figure 7.6.

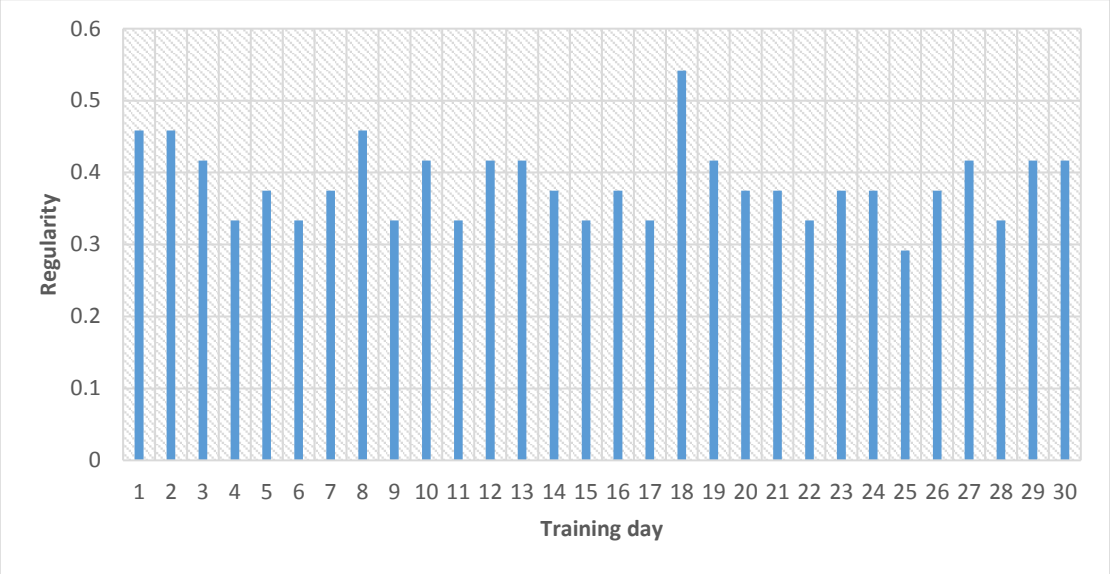


Figure 7.6. *Regularity* values obtained for 30 days of the training period.

The indices $m_{regularity}$ and $\sigma_{regularity}$ were estimated based on the *regularity* values. The former was estimated to be 0.39 while $\sigma_{regularity}$ was 0.066. Three fuzzy sets were then defined to represent *regularity* (see Figure 7.7).

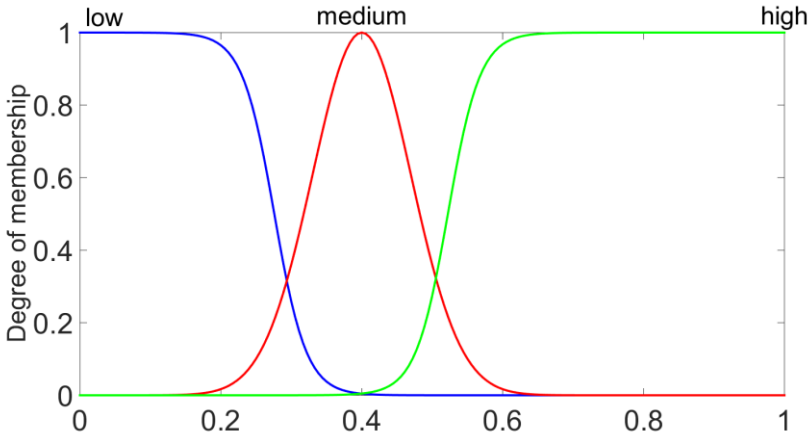


Figure 7.7. Fuzzy sets learned from the training dataset for *regularity*.

The importance of different activities was calculated, as shown in Figure 7.8. The refrigerator and kettle received an importance of 100% because they had been used every day while capturing the training dataset. The hair dryer had been used 82% of the days, the computer 48% of the period, and "using cooktop mode #2" occurred 27% of the period, which was the least frequent. The other HEAs had been employed almost every day resulting in an importance of over 85%.

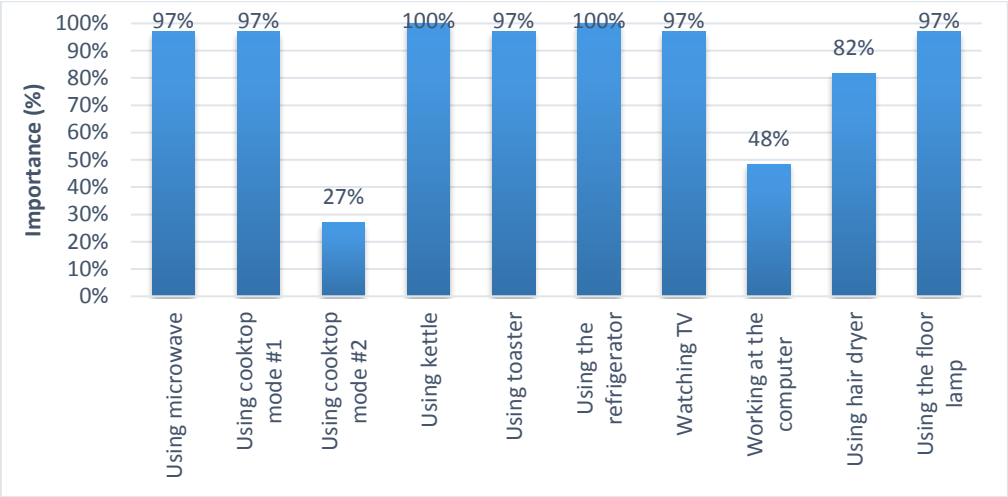


Figure 7.8. The importance of different activity labels calculated from Stage 2.

The value of *frequency* was calculated for each day in the training dataset based on the importance of using different HEAs (see Figure 7.9).

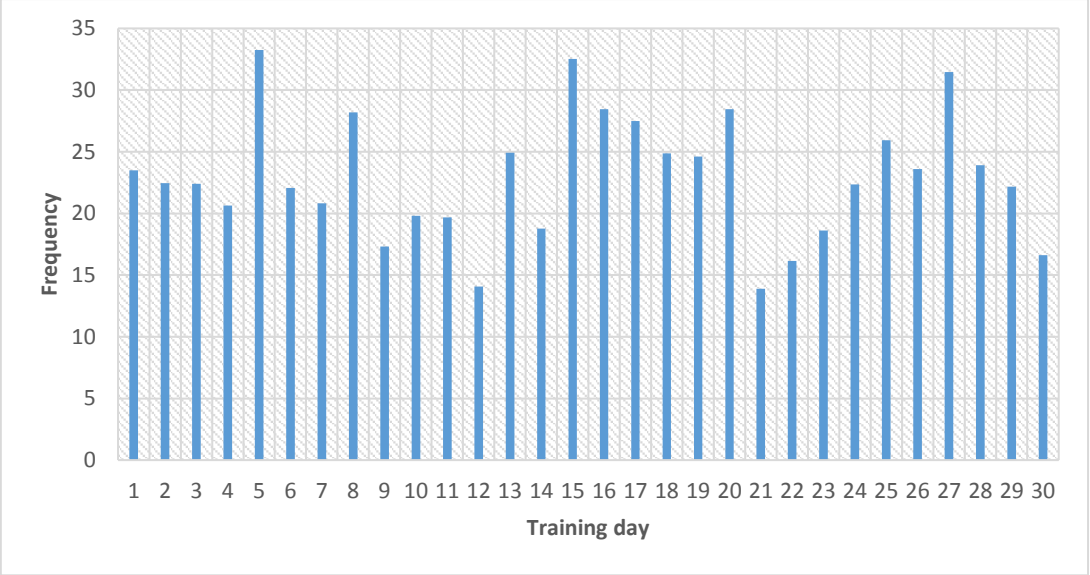


Figure 7.9. *Frequency* values calculated based on the training data.

The indices $m_{frequency}$ and $\sigma_{frequency}$ were estimated based on these values to be 23.46 and 5.266, respectively. Three fuzzy sets shown in Figure 7.10 were accordingly defined to represent *frequency*.

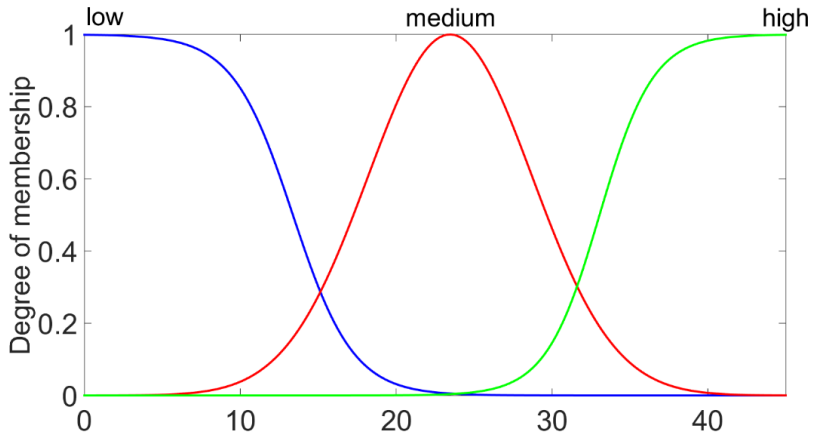


Figure 7.10. Fuzzy sets learned from the training dataset to represent *frequency*.

Figure 7.11 shows the input–output surface plot of the developed FIS based on fuzzy sets defined over *regularity* and *frequency*. This figure indicates that the use of the centre of gravity method for defuzzification provides smooth transitions between different levels of activity.

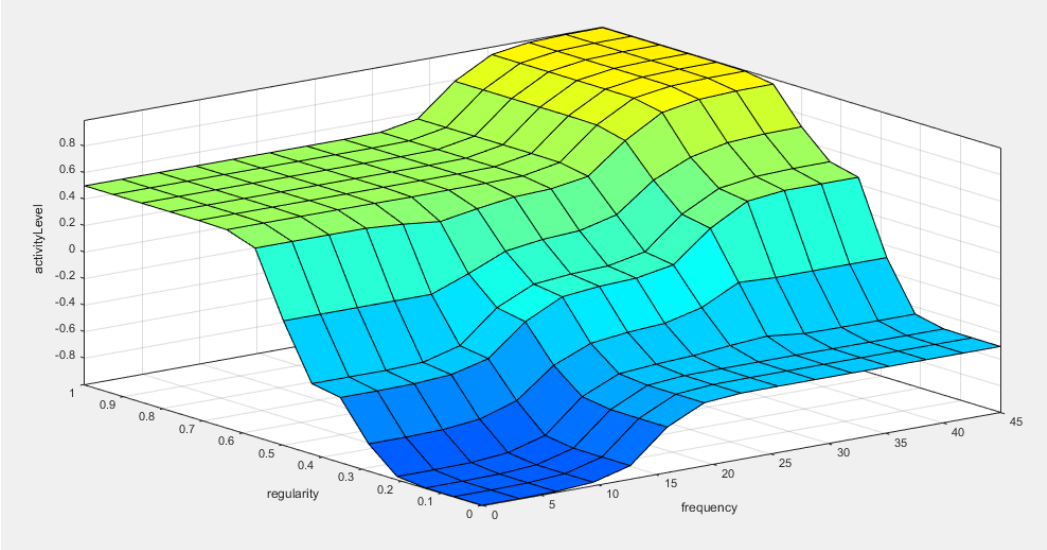


Figure 7.11. The surface plot of the developed FIS.

*Testing_data 2* from the collected dataset was used to validate the ability of the system to identify changes in the daily routine of the monitored person. The data involved two 9-day recordings each featuring a scenario of deviation from routine instrumental ADLs. Each recording showed three periods: normal behaviour (the first three days), slight deviation (the second three days) and major deviation (the last three days). The deviation from the normal behaviour in the first recording was upward which means the occupant became more active throughout the day and used more HEAs. The deviation in the second recording was downward, showing that the occupant used fewer HEAs during shorter periods of the day. These scenarios were defined according to cognitive impairments that might affect the elderly people's activities in real-life settings (Gustafson, Brun, Johanson, Passant, & Risberg, 1995).

The *activity_level* and its respective linguistic label were obtained for each day in these recordings. The linguistic labels were compared with the ground truth of the scenarios to see whether they reflect the correct level of deviation from the normal daily routine. It was observed that the system associated *normal* to the three normal days at the beginning of each recording and generated a different output for the subsequent days in which instrumental ADLs were carried out differently from the normal routine. Details of the two testing scenarios with the outputs obtained from the system are explained below.

***A downward deviation from the normal routine of instrumental ADLs*:** This scenario was devised to test how effectively AMI-ADLs detects a downward deviation from the normal

profile of instrumental ADLs. This decline usually happens as a result of deteriorating health, such as cognitive impairment and fatigue (Noury et al., 2011).

This scenario was carried out over a period of nine days. The occupant performed instrumental ADLs according to his daily routine during the first third. He started to skip breakfast and performed fewer instrumental ADLs (e.g. using the refrigerator) during the second third. During the last three days, he spent most of daytime in the living room and skipped two major meals (i.e. breakfast and lunch).

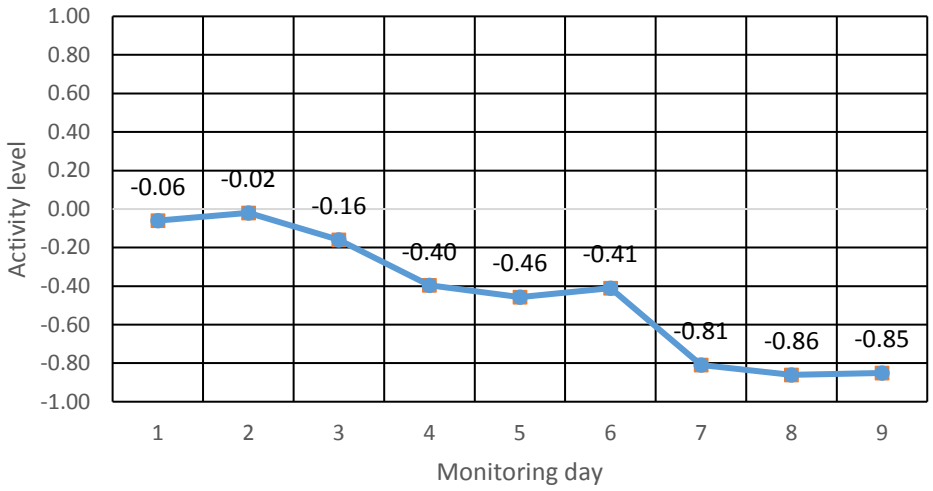


(a)

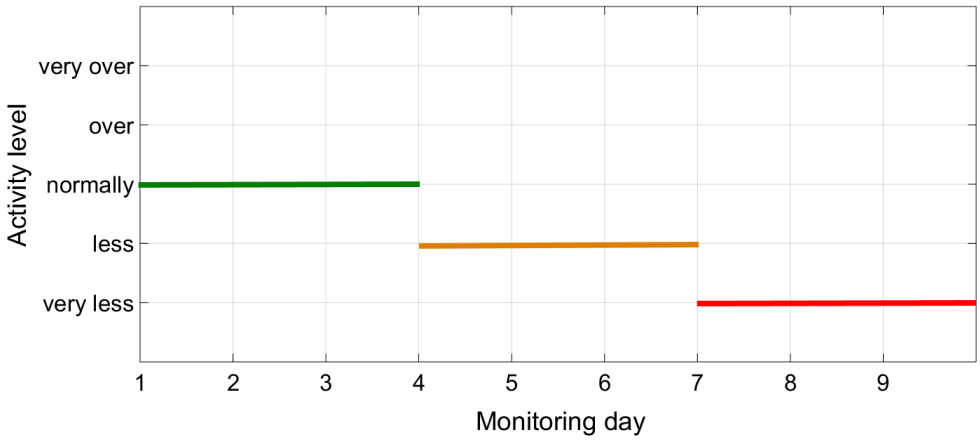


(b)

Figure 7.12. (a) The plot for *activity_level* and (b) the respective Gantt chart for a test scenario featuring a downward deviation from the normal routine of instrumental ADLs.

The plot for values of *activity_level* and the Gantt chart for their respective linguistic label Parts

(a) and (b) is shown in Figure 7.12. Figure 7.12 (a) clearly shows a noticeable downward trend in *activity_level*. The activity level fluctuated around zero for the first three days indicating a normal behaviour. The system correctly labelled this period as "*normal*". *regularity* and *frequency* decreased during the second three days and thus the values of *activity_level* dropped to around -0.40. The activity levels during those days were labelled "*low"*. *activity_level* for days 7 to 9 fell down substantially to around -0.85, hence "*very less"* in the figure.

***An upward deviation from the normal routine of instrumental ADLs*:** This scenario was devised to evaluate how effectively AMI_ADLs could detect a rising level of instrumental ADLs. This increase may occur when an elderly person becomes insomniac and stays active around the house for a longer period which in turn increases night-time or early morning activities. Another possible situation where this may occur is when a wandering or agitated elderly person with cognitive deterioration stays active for an extended duration and repeats some instrumental ADLs several times during the day (e.g. making the afternoon tea multiple times) (G. C. Franco et al., 2008).

The recording for this scenario also involved a period of nine days. The occupant performed instrumental ADLs according to his daily routine during the first three days. This was changed during the second three days as he simulated the behaviour associated with insomniac elderly people. He stayed awake for a longer period and interacted with more HEAs. For example, he prepared a snack late at night in the kitchen or interacted with computer and TV more than usual in the evening. The occupant simulated a higher deviation from the daily routine during the last three days. He woke up earlier than usual (5:30 AM instead of 7 AM), went to bed late, and carried out instrumental ADLs multiple times during the day. Parts (a) and (b) in Figure 7.13 respectively show the plot of *activity_level* values and the Gantt chart of their corresponding linguistic labels.

The values of *activity_level* show an overall upward trend in Figure 7.13 (a) due to an increase in the regularity and frequency of instrumental ADLs across the three periods. The first three days were labelled as *normal* since their *activity_level* values were around zero (see Figure 7.13 (b)).

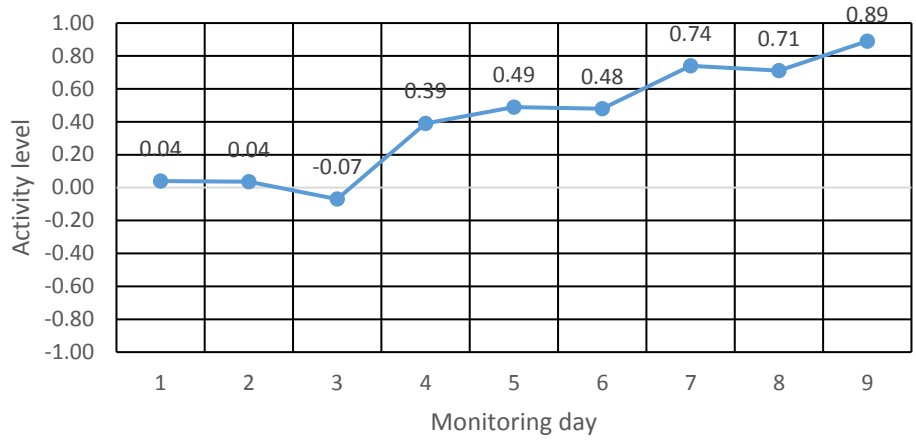


(a)

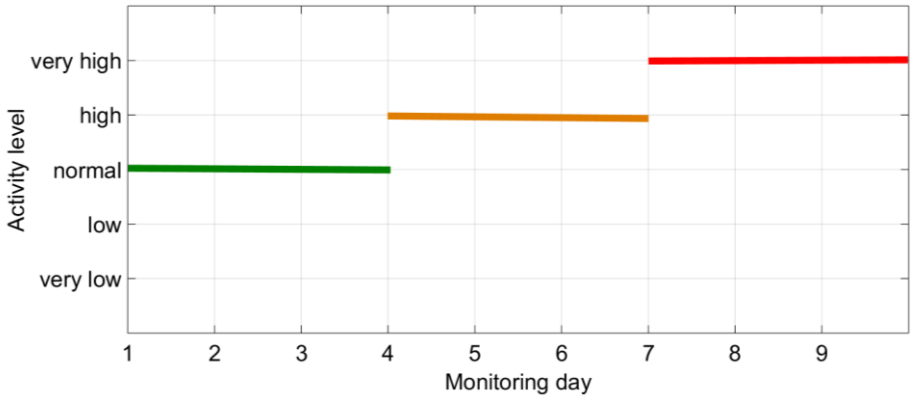


(b)

Figure 7.13. (a) The plot of *activity_level* values and (b) the respective Gantt chart obtained from monitoring a testing scenario of being over active.

The *activity_level* during the second three days increased and therefore was labelled as *high* as shown in Figure 7.13 (a). This was because unusual numbers of electrical events were identified in the early morning and late night of these days which resulted in the daily values of *regularity* and *frequency* to fall outside their normal variation range.

The *activity_level* was correctly flagged as *very high* for the last third of the recording (see Figure 7.13 (b)). The reason was that the number of appliance usage events almost doubled and the duration in which the occupant was active in the house was also longer than usual duration. As a result, *activity_level* went beyond 0.7 for the last period of the recording (see Figure 7.13 (a)).

### 7.3.2 Robustness of AMI-ADLs in regards to errors in identifying instrumental ADLs

The experimental evaluations in Chapter 6 suggested that the labels given to the occupant's interactions with HEAs are not always accurate. Evaluating the performance of AIPIA showed an error rate of approximately 15%. This error in identifying instrumental ADLs occurred in the following situations:

1. Misclassification of instrumental ADLs: this happens when AIPIA assigns wrong labels to the occupant's interactions with HEAs.

2. Missing instrumental ADLs: this happens in case the occupant interacts with a monitored HEA and the approach cannot identify this event.

3. Identifying automatically generated power signatures as a result of the occupant's interactions with HEAs: although AIPIA performs post-processing operations to eliminate automatically generated power signatures, some may remain in the processed data. Depending on the occupant's location when those power signatures occur, association rules might fire and identify the power signatures as instrumental ADLs.

This section demonstrates the impact of these errors on the performance of the FIS developed in Stage 3 to monitor instrumental ADLs. *Testing_Data 2* which involved sensor data for 18 days (two nine-day recordings) with different levels of instrumental ADLs was used. Based on the ground truth information for the usage of HEAs, all of the occupant's interactions with HEAs were manually assigned labels. This resulted in a list of instrumental ADLs with their timestamps in the form of those shown in Table 7.1. The FIS developed in Stage 3 of AMI-ADLs was then used to assign a linguistic label to the activity level of each day. These linguistic labels were used as the ground truth of the activity level for these 18 days.

To simulate a specific error rate in identifying instrumental ADLs of each day in the list, the labels of instrumental ADLs were modified according to three situations mentioned above. Given an error rate $e$, $e/3$ of instrumental ADLs of the day were randomly selected and deleted. Another $e/3$ were randomly selected and their labels were replaced by randomly chosen labels, and the other $e/3$ were added to the day with a randomly chosen label and a random time of the day. The resulting list of instrumental ADLs was then processed by the FIS to obtain labels

for the activity levels of different days. The ratio of days that received a label different from their ground truth to the total number of days in the list was then calculated.

The process described above was repeated for values of *e* from 0 to 1 with steps of 0.05. The results in Figure 7.14 show the error rate in identifying instrumental ADLs on the horizontal axis and the percentage of days labelled differently from their ground truth on the vertical axis. Results in this figure suggest that the developed FIS possess a high level of robustness in regards to errors in the detection of instrumental ADLs. From Chapter 6 the error rate of identifying instrumental ADLs was estimated to be around 15%. The results in this figure show that only 6% of the days may be labelled incorrectly by AMI-ADLs because of this error rate, hence the robustness of this approach in regards to errors in the detection of instrumental ADLs.

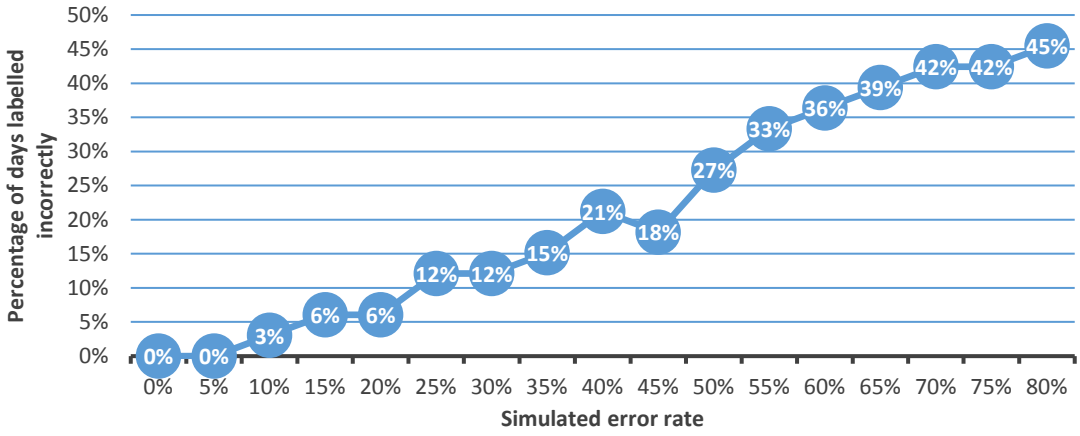


Figure 7.14. Results of evaluating the robustness of the developed FIS in regards to error in the detection of instrumental ADLs. *x* axis shows the error rate in detecting instrumental ADLs and *y* axis represents the percentage of inaccurately categorised days.

## 7.4 Discussion

This chapter examined the use of an unsupervised fuzzy approach to monitor instrumental ADLs of an elderly person living alone. For each monitoring day, the index of the occupant's activity level was reported to caregivers in the form of a number and its corresponding linguistic label. This output is more intuitive to caregivers in comparison with the output from the ADL monitoring approach in Belley et al. (2014) where a list of events in which an appliance is switched on and off is reported to caregivers.

Noury et al. (2011) used a similar index to report the daily activity level of an elderly to caregivers and reported that this index is intuitive and informative to professionals working in

the field. The index of activity level reported by Noury et al. (2011) ranged from 0 to 1 and decreased in both cases of the occupant being less active than usual or over active. This is different from the output of AMI-ADLs as it ranges from -1 to 1 and thereby provides the direction of deviation from the normal activity level.

Although the index of activity level has no dimension, its trend can be monitored for the same occupant during a given period. This is because the normal variation ranges of activity features are tailored to the daily routine of the monitored person. Obtaining similar values of this index during a monitoring period for a person indicates that similar patterns of instrumental ADLs have been followed by that person. Obtaining similar values of this index from another individual does not necessarily mean that the second person performed patterns of ADLs similar to the first person's.

The comparison of AMI-ADLs with existing approaches for monitoring instrumental ADLs was challenging. No existing approach has been described which uses unlabelled data from a combination of Kinect depth maps and power consumption of the house to monitor instrumental ADLs of the elderly. Defining comparison standards between AMI-ADLs and existing approaches was not possible. Yet it can be argued that an advantage of AMI-ADLs over other approaches is that it involves a single power sensor and a few Kinect sensors which can be retrofitted to existing houses. Unlike other approaches such as the one presented in Debes et al. (2016) which involves attaching numerous sensors to household objects.

Another advantage of the AMI-ADLs approach was that it does not require labelling a training dataset of the occupant's activities to identify the performance of instrumental ADLs. This is in contrast to many existing approaches (e.g. approaches in Belley et al. (2014), Rahimi et al. (2011) and Wilson et al. (2015)). For example, the approach in Clement et al. (2014) involved an initialising phase in which individual sensors were attached to each appliance to gather information about their consumption pattern.

The use of simple activity features in AMI-ADLs which does not require the name of HEAs to be known is also an improvement on other approaches. Many other approaches that monitor instrumental ADLs are based on the usage of HEAs. For example, the approaches in Cho et al. (2010) and Noury et al. (2011) involved a learning phase in which the name and function of the detected HEAs are acquired. These approaches then used this information to associate

importance levels to the occupant's interactions with different HEAs.

The AMI-ADLs approach was evaluated only in one real-life experimental setting. It is proposed that it could also be applied to different dwelling situations. Each room in the testbed was monitored by one Kinect camera. Multiple Kinect sensors could be used in the same room to obtain richer training data for monitoring the same area from different angles.

## 7.5 Summary

This chapter examined the use of an unsupervised fuzzy approach to monitor instrumental ADLs of an elderly person living alone. AIPA was employed in the first stage of this approach to generate representations of instrumental ADLs based on the occupant's interactions with HEAs. Two activity features were employed to quantitatively describe key aspects of the occupant's daily routine of instrumental ADLs. Normal variations in the training samples of these features were modelled via fuzzy sets to address real-life variations in the occupant's habit of performing instrumental ADLs. A set of fuzzy rules was defined to classify these fuzzy sets into levels of daily activities. The occupant's activity level for each monitoring day was reported to caregivers both in the form of an index ranging from -1 to 1 and a linguistic label.

The validation results using scenarios from real-life settings have shown the effectiveness of AMI-ADLs in identifying upward and downward drifts from the daily routine of instrumental ADLs. The results also confirmed the robustness of this approach as its output remained stable around the normal range during periods in which the occupant displayed normal behaviour and accurately represented the days when the occupant became less or more active in the form of downward and upward deviations, respectively.

The next chapter presents a general discussion, conclusions and future directions of this study.

# CHAPTER 8:
# GENERAL DISCUSSION

This chapter presents general discussions and conclusions of the research reported in the earlier chapters. It starts with a general discussion of the research methodology and the overview of the adopted ADL monitoring framework (Section 8.1). This section also focuses on how the research questions were answered through the development of the monitoring framework. This is followed by conclusions derived from the findings and validation of the approaches involved in the framework (Section 8.2). The chapter then outlines the limitations of the study in Section 8.3 and future research directions in Section 8.4.

## 8.1 General discussion and overview of the research

The primary aim of this research was to investigate a hybrid framework for the unsupervised monitoring of both physical and instrumental ADLs of elderly people living alone via inexpensive and minimally-intrusive sensors. This research aimed to address existing gaps in the research related to monitoring ADLs of the elderly which have not been answered adequately. The methodology was developed in light of a critical examination of existing monitoring approaches which was conducted in Chapter 2.

The review of the literature concluded that detecting abnormal behaviour in both physical and instrumental ADLs is crucial when monitoring elderly people's well-being and their ability to live independently. Different approaches have been proposed to detect abnormal physical and instrumental activities. To date, however, no well-established framework has been proposed to monitor both types of activities concurrently.

The literature review in the present study also indicated that for monitoring physical ADLs, most studies have used either intrusive video cameras or have asked the subject to wear sensors which might easily forget to put on. The Microsoft Kinect depth sensor is a low-intrusive alternative to video cameras which can provide the 3D structure of ADLs. The application of Kinect depth sensors for monitoring elderly people's activities is in its infancy. Most current approaches consist of simple thresholding techniques that detect only falls amongst a wide range of abnormal behaviours (e.g., Banerjee et al., 2014).

The literature indicates that most approaches for monitoring instrumental ADLs involve either using a network of environmental sensors or installing a power sensor in the electricity box of the house. The use of environmental sensors requires a costly maintenance and the incorporation of sensors into a house during its construction. Although a power sensor installed in the electricity box can help to non-intrusively identify instrumental ADLs based on the use of HEAs, this approach needs a prior knowledge about HEAs in use or a labelled dataset of home power consumption.

The literature review also revealed that most techniques adopted for monitoring physical ADLs were based on simple thresholding or supervised machine learning algorithms. The former cannot be generalised to fit across different environments while the latter entails the laborious generation of a labelled training dataset of activities. These approaches are limited as they confine emergency situations to only fall incidents and have a pre-assumed model of body motion. Many of the approaches proposed for monitoring instrumental ADLs involve a supervised machine learning technique to map sensor data into a limited list of activities carried out by most elderly people.

Sensory data captured from real life settings are noisy and there are inherent variations in ADLs. Monitoring approaches based on fuzzy logic have addressed noisy sensory data and variations in ADLs since they incorporate fuzzy sets to represent attributes describing ADLs. Most existing fuzzy ADL monitoring approaches focus on using a fixed number of pre-defined fuzzy sets over attributes (e.g., the approach presented by Kepski et al. (2012)). Fuzzy sets in these approaches do not accurately represent the subject's activities and incorporate outliers in sensor data.

The research questions in this study aimed to address drawbacks mentioned above. The main research question directing this research was

> *How can a framework incorporating unlabelled data from inexpensive and non-intrusive sensors (i.e., Kinect sensors and a power meter) be developed for unsupervised monitoring of both physical and instrumental ADLs of elderly people living alone?*

This question was answered through developing the hybrid monitoring framework, which used unlabelled data from a combination of Kinect sensors and a power meter to concurrently

monitor physical and instrumental ADLs. While Kinect depth maps provided 3D information on physical ADLs, the instrumental ADLs were monitored through the fusion of power consumption data with the occupant's locations, the latter obtained from the Kinect depth maps. This hybrid framework represented the general approach taken in this study (i.e., continuous monitoring of physical and instrumental ADLs), and its overview is shown in Figure .8.1

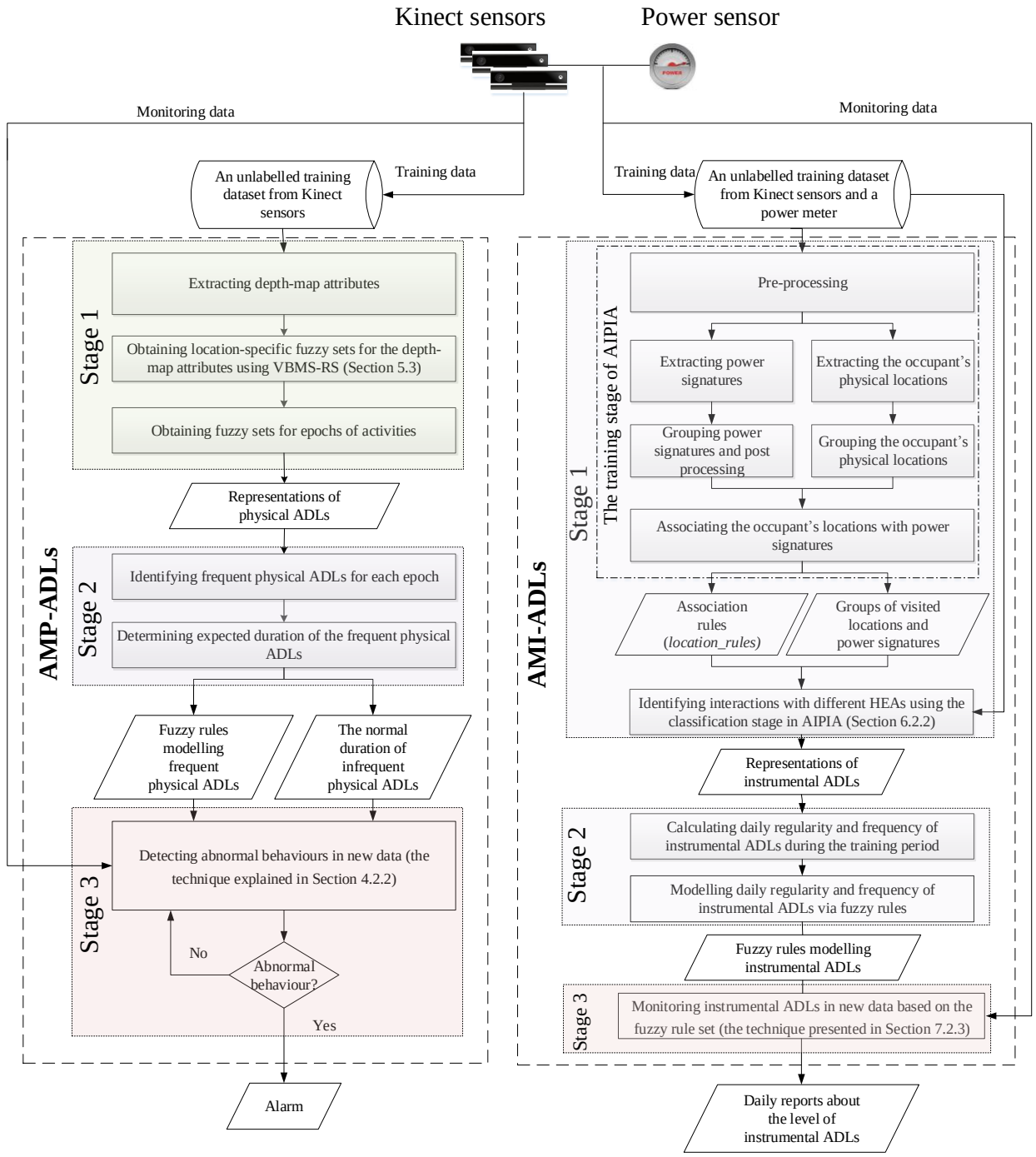


Figure 8.1. The overall approach taken for monitoring the physical and instrumental ADLs of an elderly person.

The framework involved two unsupervised approaches, named AMP-ADLs and AMI-ADLs, for monitoring physical and instrumental ADLs, respectively. Each approach took an unlabelled training dataset of the subject's ADLs and generated important information for caregivers.

The procedure of AMP-ADLs was described in Chapter 4. This approach took the depth maps of ADLs from Kinect sensors and notified caregivers when a potential emergency situation was detected. The details of AMI-ADLs were explained in Chapter 7. This approach used the occupant's physical locations from Kinect depth maps together with the aggregated power consumption of the house and generated daily reports showing the deviations of the occupant's behaviours from their normal routine.

Each of the monitoring approaches involved three stages as shown in
Figure 8.1, with each stage answering one research sub-question. These questions are reiterated and how each has been addressed is explained below.

**Research sub-question 1:** Since elderly people may perform ADLs differently, the two monitoring approaches in
Figure 8.1 needed to be adequately tailored to the behaviours of the monitored elderly person. The first step in tailoring the monitoring approaches to a specific person was to convert raw sensory data captured from their activities into representations of ADLs. The first research sub-question was therefore to investigate:

> *How can data from multiple sensors (i.e., Kinect sensors and a power meter) be used to represent physical and instrumental ADLs of the monitored elderly person?*

This question was answered through steps included in Stage 1 of each monitoring approach. In Stage 1 of AMP-ADLs the occupant's location and 3D body posture during physical ADLs were described through a set of attributes extracted from Kinect depth maps. These attributes were called depth map attributes, examples of which were shown in Table 4.1. The crisp values of the depth map attributes were converted into fuzzy labels based on the location-specific fuzzy sets defined for each attribute. Equation 5.1 was used for this conversion. Examples of fuzzy labels for attributes were shown in Table 4.3 where each combination of fuzzy labels

represented a specific body posture of the occupant observed at a specific location.

The time of physical activities associated with each monitored location was also converted into fuzzy labels. Equation 4.2 was used for this conversion. The physical ADLs of the subject were then represented through combinations of fuzzy labels describing the depth map attributes and time of the activities. An example of this representation was provided in Table 4.4.

In Stage 1 of AMI-ADLs, the instrumental ADLs during each day were represented as a timestamped list of the occupant's interactions with different HEAs (see Table 7.1 for an example). The AIPIA approach presented in Chapter 6 was used to generate this list based on an unlabelled training dataset captured from a combination of Kinect sensors and a power meter. The occupant's visited locations were associated with power signatures to identify instrumental ADLs based on the occupant's interactions with HEAs. Each association between the occupant's location and a power signature was represented by an association rule and was given an arbitrary label to differentiate the usage of different HEAs. These rules were then employed to obtain a timestamped list of interactions with different HEAs during the training period. This list represented instrumental ADLs.

**Research sub-question 2:** In order to learn the normal behaviour patterns of a monitored elderly person, it was necessary to build profiles of their physical and instrumental ADLs. The second research sub-question investigated achieving this goal without a need for labelling training data:

> *How can techniques be developed that automatically learn from the proposed data representation to generate models of physical and instrumental ADLs?*

This was addressed through the steps shown in Stage 2 of the two monitoring approaches in Figure 8.1. An unsupervised technique was presented in Stage 2 of AMP-ADLs to generate a model of physical ADLs (see Chapter 4). For each epoch of activity, frequent combinations of fuzzy attributes were obtained using a fuzzy association rule mining algorithm. These patterns represented frequent physical ADLs of the occupant. These were modelled along with their location and time in the antecedent of fuzzy rules. The normal duration of each frequent physical ADL was determined and modelled as the consequent of the respective rule. A z-shaped membership function was generated (using Equation 4.3) to model the duration of each

frequent physical ADL. Table 4.5 showed an example of these fuzzy rules. The duration of infrequent physical ADLs was automatically modelled using a statistical technique. This duration for each monitored location $r$ was shown as $EA_r$.

A technique was presented in Stage 2 of AMI-ADLs to automatically model the occupant's instrumental ADLs (see Chapter 7). The technique calculated two attributes based on the training representations of instrumental ADLs. These attributes were: the daily regularity of the occupant's interactions with HEAs, calculated using Equation 7.1, and the daily frequency of using important devices, obtained from Equation 7.4. The values of these attributes were determined for all days in the training dataset. Fuzzy sets were defined to model the normal variation range of these attributes based on the statistics of the training values. Equations 7.5 to 7.7 were used to generate fuzzy sets modelling the daily regularity of instrumental ADLs. Equations 7.8 to 7.10 were used to generate fuzzy sets modelling the daily frequency of instrumental ADLs. A set of fuzzy rules then mapped fuzzy values of these attributes to different levels of instrumental ADLs. Examples of these fuzzy rules were shown in Table 7.3.

**Research sub-question 3:** The last research sub-question focused on detecting abnormalities in new data captured from an elderly person's activities. It aimed to address the question:

> *How can techniques be developed that detect unexpected patterns and abnormal behaviours using the models of physical and instrumental ADLs?*

This question was answered by developing the techniques in Stage 3 of the monitoring approaches, as shown in
Figure 8.1. These techniques categorised the similarity of new data related to the monitored person's physical and instrumental ADLs to their respective models of normal behaviours.

The technique in Stage 3 of AMP-ADLs calculated the representation of physical ADLs for each new Kinect observation from the occupant's activities (see Section 4.2.2). If the representation corresponded to a frequent physical ADL described by a fuzzy rule, the duration of the activity during consecutive observations was evaluated against the consequent of that fuzzy rule. An alarm was raised when the occupant's activity lasted longer than usual duration. In case the representation did not correspond to any fuzzy rules, an alarm was raised when this

situation lasted longer than a data-driven value.

The technique in Stage 3 of AMI-ADLs incorporated the fuzzy rule set from Stage 2 into a fuzzy inference system to categorise the daily level of instrumental ADLs in new data into abstract labels such as ’*low* ‘, ’*normal* ‘, and ’*high* ‘. These labels were determined by comparing the daily regularity and frequency of the occupant’s interactions with HEAs in new data to the developed model of normal behaviours. For each monitoring day, a report was generated to inform caregivers about the daily level of instrumental ADLs (see Equation 7.13). Detecting abnormalities in instrumental ADLs resulted in labelling days when these were observed as ’*abnormal*’.

No public dataset which supplies continuous power consumption and Kinect data for ADLs inside a residential home was available. A continuous dataset of physical and instrumental ADLs was collected from a real-life setting to test the effectiveness of the proposed approaches. This served as proof of the concept in that it enabled the researcher to evaluate the developed techniques using data captured from a real-life setting.

The proposed framework was evaluated in a one-bedroom-apartment as a testbed. This could be scaled to monitor larger houses using additional Kinect sensors. In this case each of the additional sensors would add its training observations to the training dataset.

## 8.2 Conclusions

This section presents the findings in regards to the approaches developed for monitoring physical and instrumental ADLs.

### 8.2.1 Findings for monitoring physical ADLs

Monitoring physical activities can help identify emergency situations that elderly people living alone may experience. The literature review in the present study showed that if existing approaches are used, labelling training data is inevitable in most of the cases (e.g., S. H. Liu & Cheng, 2012). Current research has also shown that these approaches are not robust enough to handle fine variations in physical ADLs conducted in real-life settings (e.g., Banerjee et al. (2014). Existing fuzzy approaches choose predefined fuzzy sets, use prior knowledge to develop fuzzy rules and incorporate outliers in the range of fuzzy attributes. An unsupervised

data-driven fuzzy approach, called AMP-ADLs, was presented in Chapter 4. This improved on existing fuzzy monitoring approaches as it could handle fine variations and outliers when monitoring physical ADLs. This approach monitored the key aspects of physical ADLs of elderly people using depth maps captured from Kinect sensors.

The AMP-ADLs approach learned the subject's normal behaviour patterns from an unlabelled dataset of their physical ADLs. The epochs of activity associated with each monitored location were obtained using the mean shift algorithm. Evaluation results verified the higher accuracy of this technique in identifying the epochs of activities compared to other techniques (see Appendix B). For example, Hsu et al. (2010) and Hoque and Stankovic (2012) proposed using Fuzzy C-Means and DBSCAN algorithms to model the time of ADLs when monitoring the elderly. When these techniques were applied to the collected dataset, the accuracies obtained for Fuzzy C-Means and DBSCAN algorithms were 24% and 31% respectively lower than that of the technique used in AMP-ADLs.

For each epoch, the fuzzy rules that modelled the elderly person's frequent behaviour patterns and the normal durations of those patterns were learned based on a fuzzy association rule mining algorithm. A situation was identified as an emergency when the occupant's behaviour in new data was recognised as frequent with a longer than usual duration or infrequent with a duration exceeding a data-driven value.

Fine variations in the subject's physical ADLs were handled using fuzzy sets that were defined over the depth map attributes. In the prototype version of AMP-ADLs (discussed in Chapter 4) a specific number of fuzzy sets were defined over each attribute. This was achieved by applying the FCM algorithm on the combined dataset of the attribute from all monitored locations. The performance of this technique for defining different numbers of fuzzy sets over each attribute was evaluated. It was observed that while this number should be chosen empirically, it has a major impact on the sensitivity and specificity of the approach. Increasing this number improved the ability of the system to accurately classify more testing scenarios of abnormal behaviours while negatively impacting its ability to tolerate fine variations during ADLs. The best overall performance was achieved when three fuzzy sets were defined over each attribute as the resulting fuzzy rule could correctly classify more testing scenarios of normal and abnormal behaviours.

Evaluating the performance of AMP-ADLs when using this technique to define fuzzy sets also showed that not all frequent behaviour patterns could be modelled accurately by the rule set since the fuzzy sets were unable to represent some of the ADLs of the subject. Outliers and noisy measurements in data were also included in the range of generated membership functions associated with the fuzzy sets. The evaluation also highlighted the effect of the number of membership functions, defined over the depth map attributes, on the number of learned fuzzy rules.

The study addressed these limitations and refined AMP-ADLs through introducing a novel unsupervised membership function generation method called VBMS-RS in Chapter 5. VBMS-RS automatically learned the number of representative membership functions for an attribute from its underlying data distribution and set up parameters associated with each membership function excluding outliers in the data. AMP-ADLs was modified to employ VBMS-RS for defining fuzzy sets over depth map attributes. For each attribute, the captured dataset from each location was processed separately to generate location-specific membership functions. The resulting location-specific membership functions were used in the antecedent of fuzzy rules to model frequent ADLs in that location. AMP-ADLs shifted from using the combined dataset of all monitored locations for parameterising attributes to processing the dataset of each location separately.

Evaluations in Chapter 5 showed that the application of VBMS-RS improved AMP-ADLs. The rule set obtained from the output of this technique could accurately classify more scenarios of normal and abnormal behaviours with fewer rules when compared to the rule sets obtained from other membership function generating techniques including the one used in the prototype version of AMP-ADLs. It was observed that membership functions generated by other techniques to parameterise an attribute supported a wider range outside the boundary of component distributions. This resulted in the sensor data of abnormal situations receiving a positive membership degree from those MFs and being classified as normal.

Location-specific triangular and trapezoidal membership functions were generated by all membership function generating techniques. Evaluating the accuracy of the resulting rule sets showed that the rule set resulting from using triangular membership functions via VBMS-RS could better represent ADLs performed in each location and could tolerate slight posture variations during ADLs.

Evaluations in Chapter 5 also compared the performance of AMP-ADLs for monitoring physical ADLs with the performance of two other unsupervised fuzzy approaches presented by Seki (2009) and Brulin et al. (2012). The results of this comparison indicated that the AMP-ADLs method significantly outperforms these approaches.

### 8.2.2 Findings for monitoring instrumental ADLs

Instrumental ADLs can also be monitored to identify long-term changes in elderly people's health. Many approaches have proposed the monitoring of instrumental ADLs based on elderly people's usage of HEAs. Most of these approaches need a network of power sensors, a labelled dataset or prior knowledge about the characteristics of HEAs to estimate their usage (e.g., Wilson et al. (2015). The approach presented in this study was named AMI-ADLs. It could monitor the usage events of HEAs based on an unlabelled training dataset of the house composite power signals and the occupant's physical locations without any prior knowledge of the HEAs. The house composite power consumption was captured by one power sensor and the occupant's locations were obtained by a few Kinect sensors.

AMI-ADLs involved three stages. In the first stage the time of the subject's interactions with each appliance was identified in the training dataset. An approach called AIPIA was introduced for this aim. This approach used several pre-processing operations to initially remove noise from the Kinect depth maps and the house power consumption signals. Figures 6.2 and 6.4 showed the examples of the pre-processed data. The occupant's physical locations and power signatures were then extracted from the training dataset. The examples of these were shown in Tables 6.1 and 6.2, respectively. A novel clustering technique was introduced to separately group the occupant's locations and specific power signatures (see Figure 6.5). Post-processing operations were then carried out to remove power signatures automatically generated by HEAs. AIPIA then associated the groups of power signatures with the groups of the occupant's physical locations to obtain an association rule set. This rule set was used to identify the occupant's interactions with each appliance in the new data and label them with activity labels.

The collected dataset from the testbed was used to evaluate AIPIA. The results confirmed the effectiveness of its clustering techniques which could accurately identify the groups of the occupant's physical locations and power signatures belonging to most of HEAs. The evaluation

results also demonstrated the effectiveness of AIPIA in distinguishing power signatures generated automatically by self-regulated devices from those generated as a result of the occupant's instrumental ADLs. Evaluating the overall performance of AIPIA showed an average classification accuracy of more than 85.3% for correctly identifying an elderly person's interactions with different HEAs. It was observed that when the occupant's interactions with HEAs were identified based on using only power consumption data, the accuracy reduced to 75.1%.

The daily frequency and regularity of the identified interactions with important HEAs were modelled in the second stage of AMI-ADLs. This was achieved through developing a set of fuzzy rules, the parameters of which were learned from the training data. In the third stage of AMI-ADLs, a fuzzy inference system employed the set of fuzzy rules to determine the frequency and regularity of appliance usage during a monitoring day. These were used to label the activity level of the occupant as '*veryLow*', '*low*', '*normal*', '*high*', and '*veryHigh*'.

The results of validating AMI-ADLs in Chapter 7 demonstrated the ability of this approach to identify simulated upward and downward deviations from normal behaviours. The experiments in that chapter further demonstrated the robustness of AMI-ADLs in regards to errors in identifying instrumental ADLs as it could effectively classify normal and abnormal behaviour patterns despite errors in the list of the used HEAs.

Contrary to other monitoring approaches that work with the installation of many sensors (e.g., the approach in Cho et al. (2010)), the AMI-ADLs method monitors the performance of instrumental ADLs using a power meter in the main electrical panel and a few Kinect depth sensors. The AMI-ADLs approach is also an improvement on those proposed by Noury et al. (2011) and Wilson et al. (2015) as it does not need a labelled dataset of home power consumption or prior knowledge about the characteristics of HEAs to estimate their usage.

To the best of the researcher's knowledge, no existing approach has used unlabelled data from a combination of Kinect sensors and a single power meter to automatically monitor the instrumental ADLs of the elderly. Section 7.4 discussed the fact that this presents a challenge in making quantitative performance comparisons between AMI-ADLs and other approaches for monitoring instrumental ADLs. The promising results reported in this study will serve as an impetus for further research on the use of a power sensor together with Kinect depth cameras

to monitor ADLs in an unsupervised manner. A direct quantitative comparison of the performance of different approaches will then be possible.

## 8.3 Limitations

There are a number of limitations associated with the work presented in this study:

- The system can only monitor an individual, as it assumes that there is a single occupant in the home and stops monitoring if multiple persons are detected.

- In case the monitored individual changes their behaviour patterns after the training dataset is recorded (e.g. if there is a change in the locations of furniture and the addition or removal of HEAs), the current version of the system cannot automatically re-train itself to incorporate new modifications; thus, a new training dataset must be collected and the system must be re-trained.

- The system is not able to identify any abnormal behaviour when the individual is not detected by any Kinect sensors. This is due to the system's inability to monitor the duration of the individual's absence. Therefore, on such occasions no alarm is raised.

- The current version of the system does not take into account normal changes of the behaviour patterns on weekends in comparison with those during weekdays. The monitored individual may also change the pattern and times of ADLs due to circumstances such as climate and seasons. Addressing these would require the development of separate models of normal behaviours for different times of the week and year.

## 8.4 Future directions

- A relevant focus for future research is the techniques to update an existing monitoring rule set in an incremental fashion to accommodate new normal behaviour patterns and modifications in the monitored home. It is not uncommon for a person to change the placement of furniture in their home or the location where they perform ADLs. Data relevant to new behaviour patterns might become available well after the training

period. An incremental learning technique can be investigated to update an existing fuzzy rule set which is used to monitor activities with new data. In this way, the system will adapt itself once a new normal behaviour pattern was identified.

- The proposed monitoring framework could be extended to make it applicable in dwellings occupied by more than one person through identifying them from Kinect data. An example of such a technique is presented in P. Das, Sadhu, Konar, Lekova, and Nagar (2015).

- Techniques to automatically determine the thresholds associated with the data mining approaches in Chapters 4 and 6 could be further investigated. The threshold values for *minsup* in Chapter 4 and *min_conf in Chapter 6 are determined experimentally.* A data-driven approach could be investigated to derive these values automatically from the frequency distribution of behaviour patterns.

# REFERENCES


Agrawal, R., Imieliński, T., & Swami, A. (1993). Mining association rules between sets of items in large databases. *ACM SIGMOD Record*, *22*(2), 207-216. doi: 10.1145/170036.170072

Agrawal, R., & Srikant, R. (1995). Mining sequential patterns. In *Proceedings of the Eleventh International Conference on Data Engineering.* (pp: 3-14) doi:10.1109/ICDE.1995.380415

Akhlaghinia, M. J., Lotfi, A., Langensiepen, C., & Sherkat, N. (2008). Occupant Behaviour Prediction in Ambient Intelligence Computing Environment. *International Journal of Uncertain Systems, 2*(2) doi: citeulike-article-id:10160708

Alam, M., Reaz, M., & Husain, H. (2011). Temporal modeling and its application for anomaly detection in smart homes. *Int. J. Phys. Sci*, *6*(31), 7233-7241. doi: 10.5897/IJPS11.1410

Allen, J. F., & Ferguson, G. (1994). Actions and events in interval temporal logic. *Journal of logic and computation, 4*(5), 531-579. doi: 10.1007/978-0-585-28322-7_7

Alwan, M., Kell, S., Dalal, S., Turner, B., Mack, D., & Felder, R. (2003). In-home monitoring system and objective ADL assessment: Validation study. Paper presented at the *International Conference on Independence, Aging and Disability, Washington, DC.*

Amiribesheli, M., Benmansour, A., & Bouchachia, A. (2015). A review of smart homes in healthcare. *Journal of Ambient Intelligence and Humanized Computing*, *6*(4), 495-517. doi: 10.1007/s12652-015-0270-2

Amirjavid, F., Bouzouane, A., & Bouchard, B. (2014). Data driven modeling of the simultaneous activities in ambient environments. *Journal of Ambient Intelligence and Humanized Computing, 5*(5), 717-740. doi: 10.1007/s12652-013-0185-8

Anderson, D., Luke, R. H., Keller, J. M., & Skubic, M. (2008). Extension of a soft-computing framework for activity analysis from linguistic summarizations of video. In *Proceedings of IEEE International Conference on Fuzzy Systems.* (pp: 1404-1410) doi:10.1109/FUZZY.2008.4630555

Andr, A., Chaaraoui, Climent-P, P., rez, Fl, F., & rez-Revuelta. (2012). A review on vision techniques applied to Human Behaviour Analysis for Ambient-Assisted Living. *Expert Syst. Appl., 39*(12), 10873-10888. doi: 10.1016/j.eswa.2012.03.005

Ariani, A., Redmond, S. J., Chang, D., & Lovell, N. H. (2012). Simulated unobtrusive falls detection with multiple persons. *IEEE Transactions on Biomedical Engineering, 59*(11), 3185-3196. doi: 10.1109/TBME.2012.2209645

Aritoni, O., & Negru, V. (2011). A Methodology for Household Appliances Behaviour Recognition in AmI Systems Proceedings of the 7th International Conference on Autonomic and Autonomous Systems (ICAS'11), (pp: 175-178)

Arrillaga, J., Watson, N. R., & Chen, S. (2000). *Power system quality assessment*: Wiley.

Ashley, J. (2015). *Beginning Kinect Programming: With the Kinect for Windows V2 SDK*. Berkely, CA, USA: Apress.

Atallah, L., Lo, B., Ali, R., King, R., & Yang, G.-Z. (2009). Real-time activity classification using ambient and wearable sensors. *IEEE Transactions on Information Technology in Biomedicine, 13*(6), 1031-1039. doi: 10.1109/TITB.2009.2028575

Bamis, A., Lymberopoulos, D., Teixeira, T., & Savvides, A. (2008). Towards Precision Monitoring of Elders for Providing Assistive Services. In *Proceedings of the 1st International Conference on Pervasive Technologies Related to Assistive Environments.* (pp: 49-57) doi:10.1145/1389586.1389645

Bamnett, V., & Lewis, T. (1978). Outliers in statistical data. *Journal of the Royal Statistical*

*Society. Series B (Methodological), 141*(4) Retrieved from http://www.jstor.org/stable/2344513

Banerjee, T., Keller, J. M., Popescu, M., & Skubic, M. (2015). Recognizing complex instrumental activities of daily living using scene information and fuzzy logic. *Computer Vision and Image Understanding, 140*, 68-82. Retrieved from http://dx.doi.org/10.1016/j.cviu.2015.04.005

Banerjee, T., Keller, J. M., Skubic, M., & Stone, E. E. (2014). Day or night activity recognition from video using fuzzy clustering techniques. *IEEE Transactions on Fuzzy Systems, 42*(3), 483-493. doi: 10.1109/TFUZZ.2013.2260756

Bang, S., Kim, M., Song, S.-K., & Park, S.-J. (2008). Toward real time detection of the basic living activity in home using a wearable sensor and smart home sensors. In *Proceedings of 30th Annual International Conference of the IEEE Engineering in Medicine and Biology Society.* (pp: 5200-5203) doi:10.1109/IEMBS.2008.4650386

Bao, L., & Intille, S. (2004). Activity Recognition from User-Annotated Acceleration Data. In A. Ferscha & F. Mattern (Eds.), *Pervasive Computing* (Vol. 3001, pp. 1-17): Springer Berlin Heidelberg. doi: 10.1007/978-3-540-24646-6_1

Barnes, N. M., Edwards, N. H., Rose, D. A. D., & Garner, P. (1998). Lifestyle monitoring-technology for supported independence. *Computing & Control Engineering Journal, 9*(4), 169-174. doi: 10.1049/cce:19980404

Basili, V. R. (1993). *The experimental paradigm in software engineering*: Springer.

Belley, C., Gaboury, S., Bouchard, B., & Bouzouane, A. (2014). An efficient and inexpensive method for activity recognition within a smart home based on load signatures of appliances. *Pervasive and Mobile Computing, 12*, 58-78. Retrieved from http://dx.doi.org/10.1016/j.pmcj.2013.02.002

Bennett, T. R., Wu, J., Kehtarnavaz, N., & Jafari, R. (2016). Inertial Measurement Unit-Based Wearable Computers for Assisted Living Applications: A signal processing perspective. *IEEE Signal Processing Magazine, 33*(2), 28-35.

Berkan, R. C., & Trubatch, S. (1997). *Fuzzy System Design Principles*: Wiley-IEEE Press.

Berry, M. J., & Linoff, G. (1997). *Data mining techniques: for marketing, sales, and customer support*: Wiley.

Bian, Z. P., Hou, J., Chau, L. P., & Magnenat-Thalmann, N. (2015). Fall Detection Based on Body Part Tracking Using a Depth Camera. *IEEE Journal of Biomedical and Health Informatics, 19*(2), 430-439. doi: 10.1109/JBHI.2014.2319372

Bidargaddi, N., & Sarela, A. (2008). Activity and heart rate-based measures for outpatient cardiac rehabilitation. *Methods of information in medicine, 47*(3), 208-216.

Bilmes, J. A. (1998). A gentle tutorial of the EM algorithm and its application to parameter estimation for Gaussian mixture and hidden Markov models. *International Computer Science Institute, 4*(510), 126.

Biswas, J., Tolstikov, A., Jayachandran, M., Foo, V., Wai, A. A. P., Phua, C., . . . Lee, J.-E. (2010). Health and wellness monitoring through wearable and ambient sensors: exemplars from home-based care of elderly with mild dementia. *Ann. Telecommun, 65*(9), 505-521. doi: 10.1007/s12243-010-0176-0

Bourke, A. K., & Lyons, G. M. (2008). A threshold-based fall-detection algorithm using a bi-axial gyroscope sensor. *Medical engineering & physics, 30*(1), 84-90. Retrieved from http://dx.doi.org/10.1016/j.medengphy.2006.12.001

Brdiczka, O., Langet, M., Maisonnasse, J., & Crowley, J. L. (2009). Detecting Human Behavior Models From Multimodal Observation in a Smart Home. *IEEE Transactions on Automation Science and Engineering, 6*(4), 588-597. doi: 10.1109/TASE.2008.2004965

Brdiczka, O., Reignier, P., & Crowley, J. L. (2007). Detecting Individual Activities from Video

in a Smart Home. In B. Apolloni, R. J. Howlett & L. Jain (Eds.), *11th International Conference on Knowledge-Based Intelligent Information and Engineering Systems* (pp. 363-370): Springer Berlin Heidelberg. doi: 10.1007/978-3-540-74819-9_45

Brockmann, M., Gasser, T., & Herrmann, E. (1993). Locally adaptive bandwidth choice for kernel regression estimators. *Journal of the American Statistical Association, 88*(424), 1302-1309.

Brownsell, S., Bradley, D., Blackburn, S., Cardinaux, F., & Hawley, M. S. (2011). A systematic review of lifestyle monitoring technologies. *Journal of telemedicine and telecare, 17*(4), 185-189.

Brulin, D., Benezeth, Y., & Courtial, E. (2012). Posture recognition based on fuzzy logic for home monitoring of the elderly. *IEEE Transactions on Information Technology in Biomedicine, 16*(5), 974-982. doi: 10.1109/TITB.2012.2208757

Brys, G., Hubert, M., & Struyf, A. (2004). A Robust Measure of Skewness. *Journal of Computational and Graphical Statistics, 13*(4), 996-1017. Retrieved from http://www.jstor.org/stable/27594089

Buettner, M., Prasad, R., Philipose, M., & Wetherall, D. (2009). Recognizing daily activities with RFID-based sensors. In *Proceedings of the 11th international conference on Ubiquitous computin.* (pp: 51-60) doi:10.1145/1620545.1620553

Bui, H. H., Venkatesh, Svetha,West, Geoff. (2002). Policy recognition in the Abstract Hidden Markov Model. *Journal of artificial intelligence research, 17*, 451-499.

Cardinaux, F., Brownsell, S., Hawley, M., & Bradley, D. (2008). Modelling of behavioural patterns for abnormality detection in the context of lifestyle reassurance. *Progress in Pattern Recognition, Image Analysis and Applications* (pp. 243-251): Springer.

Celler, B., Earnshaw, W., Ilsar, E., Betbeder-Matibet, L., Harris, M., Clark, R., . . . Lovell, N. (1995). Remote monitoring of health status of the elderly at home. A multidisciplinary project on aging at the University of New South Wales. *International journal of bio-medical computing, 40*(2), 147-155.

Chakraborty, A., Chakraborty, A., & Mukherjee, B. (2016). Detection of Parkinson's Disease Using Fuzzy Inference System. *Intelligent Systems Technologies and Applications* (Vol. 384, pp. 79-90): Springer. doi: 10.1007/978-3-319-23036-8_7

Chandola, V., Banerjee, A., & Kumar, V. (2009). Anomaly detection: A survey. *ACM computing surveys (CSUR), 41*(3), 15.

Chandra, C., Moore, M. S., & Mitra, S. K. (1998, 31 May). An efficient method for the removal of impulse noise from speech and audio signals. In *Proceedings of IEEE International Symposium on Circuits and Systems.* (pp: 206-208) doi:10.1109/ISCAS.1998.698795

Charriere, K., Quelled, G., Lamard, M., Martiano, D., Cazuguel, G., Coatrieux, G., & Cochener, B. (2016). Real-time multilevel sequencing of cataract surgery videos. In *Proceedings of 14th International Workshop on Content-Based Multimedia Indexing (CBMI).* (pp: 1-6) doi:10.1109/CBMI.2016.7500245

Chen, J., Kam, A. H., Zhang, J., Liu, N., & Shue, L. (2005). Bathroom activity monitoring based on sound. *Pervasive Computing* (pp. 47-61): Springer. doi: 10.1007/11428572_4

Chen, J., Kwong, K., Chang, D., Luk, J., & Bajcsy, R. (2005). Wearable sensors for reliable fall detection. In *Proceedings of 27th Annual International Conference of the Engineering in Medicine and Biology Society.* (pp: 3551-3554) doi:10.1109/IEMBS.2005.1617246

Chikhaoui, B., Wang, S., & Pigot, H. (2011). A frequent pattern mining approach for ADLs recognition in smart environments. In *Proceedings of 2011 IEEE International Conference on Advanced Information Networking and Applications.* (pp: 248-255) doi:10.1109/AINA.2011.13

Cho, H. S., Yamazaki, T., & Hahn, M. (2010). AERO: extraction of user's activities from

electric power consumption data. *IEEE Transactions on Consumer Electronics, 56*(3), 2011-2018. doi: 10.1109/TCE.2010.5606359

Chung, P.-C., & Liu, C.-D. (2008). A daily behavior enabled hidden Markov model for human behavior understanding. *Pattern Recognition, 41*(5), 1572-1580. doi: http://doi.org/10.1016/j.patcog.2007.10.022

Claes, V., Devriendt, E., Tournoy, J., & Milisen, K. (2015). Attitudes and perceptions of adults of 60 years and older towards in-home monitoring of the activities of daily living with contactless sensors: An explorative study. *International journal of nursing studies, 52*(1), 134-148.

Clement, J., Ploennigs, J., & Kabitzsch, K. (2012). Smart Meter: Detect and Individualize ADLs. In R. Wichert & B. Eberhardt (Eds.), *Ambient Assisted Living* (pp. 107-122): Springer Berlin Heidelberg. doi: 10.1007/978-3-642-27491-6_8

Clement, J., Ploennigs, J., & Kabitzsch, K. (2014). Detecting Activities of Daily Living with Smart Meters. *Ambient Assisted Living* (pp. 143-160): Springer.

Clifton, D. A., Bannister, P. R., & Tarassenko, L. (2007). A framework for novelty detection in jet engine vibration data. In *Proceedings of Trans Tech Publ.* Key engineering materials, (pp: 305-310)

Clifton, L. A., Yin, H., & Zhang, Y. (2006). Support vector machine in novelty detection for multi-channel combustion data. *Advances in Neural Networks* (pp. 836-843): Springer.

Cochran, W. G. (1952). The $\chi 2$ test of goodness of fit. *The Annals of Mathematical Statistics, 23*(3), 315-345. Retrieved from http://www.jstor.org/stable/2236678

Cohen, M., & Miller, J. (2000). The use of nursing home and assisted living facilities among privately insured and non-privately insured disabled elders. *Washington, DC: Office of the Assistant Secretary for Planning and Evaluation, US Department of Health and Human Services. Retrieved December, 4*, 2009.

Comaniciu, D., & Meer, P. (2002). Mean shift: A robust approach toward feature space analysis. *IEEE Transactions on Pattern Analysis and Machine Intelligence, 24*(5), 603-619. doi: 10.1109/34.1000236

Comaniciu, D., Ramesh, V., & Meer, P. (2001, 2001). The variable bandwidth mean shift and data-driven scale selection. In *Proceedings of Eighth IEEE International Conference on Computer Vision.* (pp: 438-445) doi:10.1109/ICCV.2001.937550

Cook, D. J., & Holder, L. B. (2011). Sensor selection to support practical use of health-monitoring smart environments. *Wiley Interdisciplinary Reviews: Data Mining and Knowledge Discovery, 1*(4), 339-351. doi: 10.1002/widm.20

Cook, D. J., & Krishnan, N. (2014). Mining the home environment. *Journal of intelligent information systems, 43*(3), 503-519.

Cook, D. J., & Schmitter-Edgecombe, M. (2009). Assessing the quality of activities in a smart environment. *Methods of information in medicine, 48*(5), 480.

Cucchiara, R., Prati, A., & Vezzani, R. (2007). A multi-camera vision system for fall detection and alarm generation. *Expert Systems, 24*(5), 334-345. doi: 10.1111/j.1468-0394.2007.00438.x

Dal Mutto, C., Zanuttigh, P., & Cortelazzo, G. M. (2012). *Time-of-flight cameras and microsoft Kinect™*: Springer Science & Business Media.

Das, B., Chen, C., Dasgupta, N., Cook, D. J., & Seelye, A. M. (2010). Automated prompting in a smart home environment. In *Proceedings of IEEE International Conference on Data Mining* (pp: 1045-1052)

Das, P., Sadhu, A. K., Konar, A., Lekova, A., & Nagar, A. K. (2015). Type 2 fuzzy induced person identification using Kinect sensor. In *Proceedings of IEEE International Conference on Fuzzy Systems (FUZZ-IEEE).* (pp: 1-8) doi:10.1109/FUZZ-IEEE.2015.7338107

Debes, C., Merentitis, A., Sukhanov, S., Niessen, M., Frangiadakis, N., & Bauer, A. (2016). Monitoring Activities of Daily Living in Smart Homes: Understanding human behavior. *IEEE Signal Processing Magazine, 33*(2), 81-94. doi: 10.1109/MSP.2015.2503881

Doctor, F., Iqbal, R., & Naguib, R. N. (2014). A fuzzy ambient intelligent agents approach for monitoring disease progression of dementia patients. *Journal of Ambient Intelligence and Humanized Computing, 5*(1), 147-158.

Dubey, R., Ni, B., & Moulin, P. (2012). A depth camera based fall recognition system for the elderly. In A. Campilho & M. Kamel (Eds.), *Image analysis and recognition* (Vol. 7325, pp. 106-113): Springer. doi: 10.1007/978-3-642-31298-4_13

Duda, R. O., Hart, P. E., & Stork, D. G. (2012). *Pattern classification*: John Wiley & Sons.

Duong, T. V., Bui, H. H., Phung, D. Q., & Venkatesh, S. (2005). Activity recognition and abnormality detection with the switching hidden semi-Markov model. In *Proceedings of 2005 IEEE Computer Society Conference on Computer Vision and Pattern Recognition (CVPR'05).* (pp: 838-845) doi:10.1109/CVPR.2005.61

Durant, J., Leger, G. C., Banks, S. J., & Miller, J. B. (2016). Relationship between the Activities of Daily Living Questionnaire and the Montreal Cognitive Assessment. *Alzheimer's & Dementia: Diagnosis, Assessment & Disease Monitoring, 4*, 43-46.

Easterbrook, S., Singer, J., Storey, M.-A., & Damian, D. (2008). Selecting empirical methods for software engineering research. *Guide to advanced empirical software engineering* (pp. 285-311): Springer.

Elbert, D., Storf, H., Eisenbarth, M., Ünalan, Ö., & Schmitt, M. (2011). An approach for detecting deviations in daily routine for long-term behavior analysis. In *Proceedings of 5th International Conference on Pervasive Computing Technologies for Healthcare (PervasiveHealth).* (pp: 426-433)

Fernandez-Luque, F. J., Martínez, F., Domènech, G., Zapata, J., & Ruiz, R. (2013). EMFi-based low-power occupancy sensor. *Sensors and Actuators A: Physical, 191*, 78-88.

Fillenbaum, G. G. (1984). The wellbeing of the elderly: approaches to multidimensional assessment. *WHO Offset Publ, 84*, 1-99.

Fink, O., Zio, E., & Weidmann, U. (2015). Novelty detection by multivariate kernel density estimation and growing neural gas algorithm. *Mechanical Systems and Signal Processing, 50*, 427-436. Retrieved from http://dx.doi.org/10.1016/j.ymssp.2014.04.022

Fogarty, J., Au, C., & Hudson, S. E. (2006). Sensing from the basement: a feasibility study of unobtrusive and low-cost home activity recognition. In *Proceedings of 19th annual ACM symposium on User interface software and technology*. (pp: 91-100) doi:10.1145/1166253.1166269

Fouquet, Y., Franco, C., Villemazet, C., Demongeot, J., & Vuillerme, N. (2010). Telemonitoring of the elderly at home: Real-time pervasive follow-up of daily routine, automatic detection of outliers and drifts. In M. A. Al-Qutayri (Ed.), *Smart Home Systems*: InTech. doi: 10.5772/8414

Franco, C., Demongeot, J., Villemazet, C., & Vuillerme, N. (2010). Behavioral Telemonitoring of the Elderly at Home: Detection of Nycthemeral Rhythms Drifts from Location Data. In *Proceedings of 24th International Conference on Advanced Information Networking and Applications Workshops.* (pp: 759-766) doi:10.1109/WAINA.2010.81

Franco, G. C., Gallay, F., Berenguer, M., Mourrain, C., & Couturier, P. (2008). Non-invasive monitoring of the activities of daily living of elderly people at home–a pilot study of the usage of domestic appliances. *Journal of telemedicine and telecare, 14*(5), 231-235.

Gaddam, A., Mukhopadhyay, S. C., & Sen Gupta, G. (2011). Elder care based on cognitive sensor network. *Sensors Journal, IEEE, 11*(3), 574-581.

Gardner, A. B., Krieger, A. M., Vachtsevanos, G., & Litt, B. (2006). One-class novelty detection for seizure analysis from intracranial EEG. *The Journal of Machine Learning Research, 7*, 1025-1044.

Geng, Y., Chen, J., Fu, R., Bao, G., & Pahlavan, K. (2016). Enlighten Wearable Physiological Monitoring Systems: On-Body RF Characteristics Based Human Motion Classification Using a Support Vector Machine. *IEEE Transactions on Mobile Computing, 15*(3), 656-671. doi: 10.1109/TMC.2015.2416186

Ghassemian, M., Auckburaully, S. F., Pretorius, M., & Jai-Persad, D. (2011). Remote Elderly Assisted Living System-A preliminary research, development and evaluation. In *Proceedings of IEEE 22nd International Symposium on Personal Indoor and Mobile Radio Communications (PIMRC).* (pp: 2219-2223) doi:10.1109/PIMRC.2011.6139911

Gokalp, H., & Clarke, M. (2013). Monitoring activities of daily living of the elderly and the potential for its use in telecare and telehealth: A review. *Telemedicine and e-Health, 19*(12), 910-923.

Grubbs, F. E. (1969). Procedures for detecting outlying observations in samples. *Technometrics, 11*(1), 1-21.

Gu, T., Chen, S., Tao, X., & Lu, J. (2010). An unsupervised approach to activity recognition and segmentation based on object-use fingerprints. *Data & Knowledge Engineering, 69*(6), 533-544.

Gu, T., Wu, Z., Tao, X., Pung, H. K., & Lu, J. (2009). EPSICAR: An Emerging Patterns based approach to sequential, interleaved and Concurrent Activity Recognition. In *Proceedings of IEEE International Conference on Pervasive Computing and Communications.* (pp: 1-9) doi:10.1109/PERCOM.2009.4912776

Guesgen, H. W., & Marsland, S. (2010). Spatio-temporal reasoning and context awareness. *Handbook of Ambient Intelligence and Smart Environments* (pp. 609-634): Springer.

Gustafson, L., Brun, A., Johanson, A., Passant, U., & Risberg, J. (1995). Early clinical manifestations and the course of Alzheimer's disease related to regional cerebral blood flow and neuropathology. *Research advances in Alzheimer's diesease and related disorders*, 209-218.

Hamid, R., Maddi, S., Johnson, A., Bobick, A., Essa, I., & Isbell, C. (2009). A novel sequence representation for unsupervised analysis of human activities. *Artificial Intelligence, 173*(14), 1221-1244.

Hanson, M. A., Barth, A. T., & Silverman, C. (2011). In home assessment and management of health and wellness with BeClose™ ambient, artificial intelligence. In *Proceedings of Proceedings of the 2nd Conference on Wireless Health.* (pp: 25) doi:10.1145/2077546.2077574

Harmankaya, O., Okuturlar, Y., Kocoglu, H., Kaptanogullari, H., Yucel, S. K., Ozkan, H., . . . Hursitoglu, M. (2015). Renal biopsy in the elderly: a single-center experience. *International urology and nephrology, 47*(8), 1397-1401.

Harper, S. (2014). Economic and social implications of aging societies. *Science, 346*(6209), 587-591.

Hart, G. W. (1992). Nonintrusive appliance load monitoring. *Proceedings of the IEEE, 80*(12), 1870-1891.

Hawkins, D. M. (1980). *Identification of outliers* (Vol. 11): Chapman and Hall London.

Hayes, T. L., Pavel, M., Larimer, N., Tsay, I. A., Nutt, J., & Adami, A. G. (2007). Distributed healthcare: Simultaneous assessment of multiple individuals. *IEEE Pervasive Computing,*(1), 36-43. doi: 10.1109/MPRV.2007.9

He, Z., Xu, X., Huang, J. Z., & Deng, S. (2004). A frequent pattern discovery method for outlier detection. *Advances in Web-Age Information Management* (pp. 726-732): Springer.

Hein, A., Winkelbach, S., Martens, B., Wilken, O., Eichelberg, M., Spehr, J., . . . Hülsken-

Giesler, M. (2010). Monitoring systems for the support of home care. *Informatics for Health and Social Care, 35*(3-4), 157-176.

Helal, S., Chen, C., Kim, E., Bose, R., & Lee, C. (2012). Toward an ecosystem for developing and programming assistive environments. *Proceedings of the IEEE, 100*(8), 2489-2504. doi: 10.1109/JPROC.2012.2200548

Hoque, E., & Stankovic, J. (2012). AALO: Activity recognition in smart homes using Active Learning in the presence of Overlapped activities. In *Proceedings of IEEE 6th International Conference on Pervasive Computing Technologies for Healthcare (PervasiveHealth).* (pp: 139-146) doi:10.4108/icst.pervasivehealth.2012.248600

Hsu, H.-H., Lu, K.-C., & Takizawa, X. (2010). Abnormal behavior detection with fuzzy clustering for elderly care. In *Proceedings of International Computer Symposium (ICS).* (pp: 6-11) doi:10.1109/COMPSYM.2010.5685422

Hsueh, Y.-L., Lin, N.-H., Chang, C.-C., Chen, O. T.-C., & Lie, W.-N. (2015). Abnormal event detection using Bayesian networks at a smart home. In *Proceedings of 8th International Conference on Ubi-Media Computing (UMEDIA).* (pp: 273-277) doi:10.1109/UMEDIA.2015.7297468

Hughes, B. M., Chan, J. S., & Koval, D. O. (1993). Distribution customer power quality experience. *Industry Applications, IEEE Transactions on, 29*(6), 1204-1211.

Intille, S. S., Larson, K., Tapia, E. M., Beaudin, J. S., Kaushik, P., Nawyn, J., & Rockinson, R. (2006). Using a live-in laboratory for ubiquitous computing researchPaper presented at the *Proceedings of the 4th international conference on Pervasive Computing, Dublin, Ireland.* (pp. 349-365). 2094967: Springer-Verlag. doi: 10.1007/11748625_22

Jakkula, V., & Cook, D. (2008). Anomaly detection using temporal data mining in a smart home environment. *Methods Inf Med, 47*(1), 70-75.

Jianxin, W., Osuntogun, A., Choudhury, T., Philipose, M., & Rehg, J. M. (2007, 14-21 Oct. 2007). A Scalable Approach to Activity Recognition based on Object Use Computer Vision, 2007. ICCV 2007. IEEE 11th International Conference on, (pp: 1-8) doi:10.1109/iccv.2007.4408865

Kadouche, R., Pigot, H., Abdulrazak, B., & Giroux, S. (2011). User's Behavior Classification Model for Smart Houses Occupant Prediction. In L. Chen, C. D. Nugent, J. Biswas & J. Hoey (Eds.), *Activity Recognition in Pervasive Intelligent Environments* (Vol. 4, pp. 149-164): Atlantis Press. doi: 10.2991/978-94-91216-05-3_7

Kalekar, P. S. (2004). Time series forecasting using Holt-Winters exponential smoothing. *Kanwal Rekhi School of Information Technology, 4329008*, 1-13.

Karg, M., & Kirsch, A. (2013). Simultaneous Plan Recognition and Monitoring (SPRAM) for Robot Assistants. In *Proceedings of Human Robot Collaboration Workshop at Robotics Science and Systems Conference*

Kepski, M., Kwolek, B., & Austvoll, I. (2012). Fuzzy inference-based reliable fall detection using Kinect and accelerometer. In *Proceedings of Artificial Intelligence and Soft Computing.* (pp: 266-273) doi:10.1007/978-3-642-29347-4_31

Khan, S. S., & Hoey, J. (2016). Review of Fall Detection Techniques: A Data Availability Perspective. *arXiv preprint arXiv:1605.09351*,

Kim, E., Helal, S., & Cook, D. (2010). Human activity recognition and pattern discovery. *IEEE Pervasive Computing, 9*(1), 48-53. doi: 10.1109/MPRV.2010.7

Kinect. (2013). Retrieved from http://www.xbox.com/en-US/kinect?xr=shellnav

Kinect for Windows SDK 2.0. (2015). Retrieved from http://www.microsoft.com/en-au/download/details.aspx?id=44561

Kinect v2. (2015). Retrieved from https://vvvv.org/documentation/kinect

König, A., Crispim Junior, C. F., Derreumaux, A., Bensadoun, G., Petit, P.-D., Bremond, F., . . . Robert, P. (2015). Validation of an automatic video monitoring system for the

detection of instrumental activities of daily living in dementia patients. *Journal of Alzheimer's Disease, 44*(2), 675-685.
Krishnan, N. C., & Cook, D. J. (2014). Activity recognition on streaming sensor data. *Pervasive and mobile computing, 10*(B), 138-154. Retrieved from http://dx.doi.org/10.1016/j.pmcj.2012.07.003
Kukolj, D. (2002). Design of adaptive Takagi–Sugeno–Kang fuzzy models. *Applied Soft Computing, 2*(2), 89-103.
Kuok, C. M., Fu, A., & Wong, M. H. (1998). Mining fuzzy association rules in databases. *ACM Sigmod Record, 27*(1), 41-46.
Kwolek, B., & Kepski, M. (2016). Fuzzy inference-based fall detection using kinect and body-worn accelerometer. *Applied Soft Computing, 40*, 305-318. Retrieved from http://dx.doi.org/10.1016/j.asoc.2015.11.031
Labonnote, N., & Høyland, K. (2015). Smart home technologies that support independent living: challenges and opportunities for the building industry – a systematic mapping study. *Intelligent Buildings International*, 1-24. doi: 10.1080/17508975.2015.1048767
Lancaster, H. O., & Seneta, E. (2005). *Chi-Square Distribution*: Wiley Online Library.
Laurikkala, J., Juhola, M., Kentala, E., Lavrac, N., Miksch, S., & Kavsek, B. (2000). Informal identification of outliers in medical data. In *Proceedings of Fifth International Workshop on Intelligent Data Analysis in Medicine and Pharmacology*. (pp: 20-24)
Lauterbach, C., Steinhage, A., & Techmer, A. (2012). Large-area wireless sensor system based on smart textiles. In *Proceedings of International Multi-Conference on Systems, Sygnals & Devices*.
Lee, Y. S., & Chung, W. Y. (2012, 5-7 Jan. 2012). Automated abnormal behavior detection for ubiquitous healthcare application in daytime and nighttime. In *Proceedings of 2012 IEEE-EMBS International Conference on Biomedical and Health Informatics*. (pp: 204-207) doi:10.1109/BHI.2012.6211545
Li, H., Zhang, Q., & Duan, P. (2008). A novel one-pass neural network approach for activities recognition in intelligent environments. In *Proceedings of 7th World Congress on Intelligent Control and Automation*. (pp: 50-54) doi:10.1109/WCICA.2008.4592901
Li, L., Song, G., & Ou, J. (2011). Hybrid active mass damper (AMD) vibration suppression of nonlinear high-rise structure using fuzzy logic control algorithm under earthquake excitations. *Structural Control and Health Monitoring, 18*(6), 698-709.
Li, Q., Stankovic, J. A., Hanson, M. A., Barth, A. T., Lach, J., & Zhou, G. (2009). Accurate, fast fall detection using gyroscopes and accelerometer-derived posture information. In *Proceedings of Sixth International Workshop on Wearable and Implantable Body Sensor Networks*. (pp: 138-143) doi:10.1145/2559636.2559790
Liu, S. H., & Cheng, W.-C. (2012). Fall detection with the support vector machine during scripted and continuous unscripted activities. *Sensors, 12*(9), 12301-12316.
Liu, Y., Zhao, Y., Chen, L., Pei, J., & Han, J. (2012). Mining frequent trajectory patterns for activity monitoring using radio frequency tag arrays. *IEEE Transactions on Parallel and Distributed Systems, 23*(11), 2138-2149.
Lotfi, A., Langensiepen, C., Mahmoud, S. M., & Akhlaghinia, M. J. (2012). Smart homes for the elderly dementia sufferers: identification and prediction of abnormal behaviour. *Journal of ambient intelligence and humanized computing, 3*(3), 205-218.
Lühr, S., West, G., & Venkatesh, S. (2007). Recognition of emergent human behaviour in a smart home: A data mining approach. *Pervasive and Mobile Computing, 3*(2), 95-116.
Lundström, J., Järpe, E., & Verikas, A. (2016). Detecting and exploring deviating behaviour of smart home residents. *Expert Systems with Applications, 55*, 429-440. Retrieved from http://dx.doi.org/10.1016/j.eswa.2016.02.030
Lustrek, M., Gjoreski, H., Gonzalez Vega, N., Kozina, S., Cvetkovic, B., Mirchevska, V., &

Gams, M. (2015). Fall Detection Using Location Sensors and Accelerometers. *IEEE Pervasive Computing, 14*(4), 72-79. doi: 10.1109/MPRV.2015.84

Mahmoud, S. M., Lotfi, A., & Langensiepen, C. (2012). User activities outlier detection system using principal component analysis and fuzzy rule-based system. In *Proceedings of the 5th International Conference on PErvasive Technologies Related to Assistive Environments.* (pp: 1-8) Heraklion, Crete, Greece.doi:10.1145/2413097.2413130

Makantasis, K., Protopapadakis, E., Doulamis, A., Grammatikopoulos, L., & Stentoumis, C. (2012). Monocular camera fall detection system exploiting 3d measures: a semi-supervised learning approach. In *Proceedings of Springer*. Computer Vision–ECCV 2012. Workshops and Demonstrations, (pp: 81-90)

Makonin, S., Popowich, F., Bartram, L., Gill, B., & Bajić, I. V. (2013, 21-23 Aug. 2013). AMPds: A public dataset for load disaggregation and eco-feedback research. In *Proceedings of 2013 IEEE Electrical Power & Energy Conference.* (pp: 1-6) doi:10.1109/EPEC.2013.6802949

Manku, G. S. (2016). Frequent Itemset Mining over Data Streams. *Data Stream Management* (pp. 209-219): Springer.

Marchiori, A., Hakkarinen, D., Han, Q., & Earle, L. (2011). Circuit-level load monitoring for household energy management. *Pervasive Computing, IEEE, 10*(1), 40-48.

Martin, T., Majeed, B., Lee, B.-S., & Clarke, N. (2006). Fuzzy ambient intelligence for next generation telecare. In *Proceedings of IEEE.* Fuzzy Systems, 2006 IEEE International Conference on, (pp: 894-901)

Martin, T., Majeed, B., Lee, B.-S., & Clarke, N. (2007). A Third-Generation Telecare System using Fuzzy Ambient Intelligence *Computational Intelligence for Agent-based Systems* (pp. 155-175): Springer.

Mastorakis, G., & Makris, D. (2014). Fall detection system using Kinect's infrared sensor. *Journal of Real-Time Image Processing, 9*(4), 635-646.

Mathie, M. J., Coster, A. C., Lovell, N. H., Celler, B. G., Lord, S. R., & Tiedemann, A. (2004). A pilot study of long-term monitoring of human movements in the home using accelerometry. *Journal of telemedicine and telecare, 10*(3), 144-151.

Medjahed, H., Istrate, D., Boudy, J., & Dorizzi, B. (2009, 20-24 Aug. 2009). Human activities of daily living recognition using fuzzy logic for elderly home monitoring. In *Proceedings of IEEE International Conference on Fuzzy Systems.* (pp: 2001-2006) doi:10.1109/FUZZY.2009.5277257

Mehr, H. D., Polat, H., & Cetin, A. (2016, 20-21 April 2016). Resident activity recognition in smart homes by using artificial neural networks. In *Proceedings of 4th International Istanbul Smart Grid Congress and Fair (ICSG).* (pp: 1-5) doi:10.1109/SGCF.2016.7492428

Messing, R., Pal, C., & Kautz, H. (2009). Activity recognition using the velocity histories of tracked keypoints. In *Proceedings of 12th International Conference on Computer Vision.* (pp: 104-111) doi:10.1109/ICCV.2009.5459154

Mlinac, M. E., & Feng, M. C. (2016). Assessment of Activities of Daily Living, Self-Care, and Independence. *Archives of Clinical Neuropsychology, 31*(6), 506-516.

Moeinzadeh, H., Nasersharif, B., Rezaee, A., & Pazhoumand-dar, H. (2009). Improving classification accuracy using evolutionary fuzzy transformationPaper presented at the *Proceedings of the 11th Annual Conference Companion on Genetic and Evolutionary Computation Conference: Late Breaking Papers, Montreal, Québec, Canada.* (pp. 2103-2108). 1570284: ACM. doi: 10.1145/1570256.1570284

Munstermann, M., Stevens, T., & Luther, W. (2012). A novel human autonomy assessment system. *Sensors, 12*(6), 7828-7854.

Nag, A., & Mukhopadhyay, S. C. (2014). Smart Home: Recognition of activities of elderly for

24/7; Coverage issues. In *Proceedings of Proceedings of the 2014 International Conference on Sensing Technology*. (pp: 480-489) Liverpool, UK.

Nguyen, N. T., Phung, D. Q., Venkatesh, S., & Bui, H. (2005, 20-25 June 2005). Learning and detecting activities from movement trajectories using the hierarchical hidden Markov model. In *Proceedings of IEEE Computer Society Conference on Computer Vision and Pattern Recognition (CVPR'05)*. (pp: 955-960 vol. 952) doi:10.1109/CVPR.2005.203

Noury, N., Berenguer, M., Teyssier, H., Bouzid, M. J., & Giordani, M. (2011). Building an index of activity of inhabitants from their activity on the residential electrical power line. *IEEE Transactions on Information Technology in Biomedicine, 15*(5), 758-766. doi: 10.1109/TITB.2011.2138149

OpenNI. (2013). Retrieved from http://www.openni.org/

Outram Research Ltd. (2014). PM1000 Power Quality Analyser. Retrieved from http://www.outramresearch.co.uk/pages/product_pm1000.shtml

Özdemir, A. T., & Barshan, B. (2014). Detecting falls with wearable sensors using machine learning techniques. *Sensors, 14*(6), 10691-10708.

Papamatthaiakis, G., Polyzos, G. C., & Xylomenos, G. (2010, 9-12 Jan. 2010). Monitoring and Modeling Simple Everyday Activities of the Elderly at Home Consumer Communications and Networking Conference (CCNC), 2010 7th IEEE, (pp: 1-5) doi:10.1109/ccnc.2010.5421717

Pazhoumand-Dar, H., & Yaghobi, M. (2010, 28-30 July 2010). DTBSVMs: A New Approach for Road Sign Recognition 2010 2nd International Conference on Computational Intelligence, Communication Systems and Networks, (pp: 314-319) doi:10.1109/CICSyN.2010.17

Pazhoumand-dar, H., & Yaghoobi, M. (2013). A new approach in road sign recognition based on fast fractal coding. *Neural Computing and Applications, 22*(3), 615-625. doi: 10.1007/s00521-011-0718-z

Pedrycz, W. (1994). Why triangular membership functions? *Fuzzy Sets Syst., 64*(1), 21-30. doi: 10.1016/0165-0114(94)90003-5

Peetoom, K. K., Lexis, M. A., Joore, M., Dirksen, C. D., & De Witte, L. P. (2015). Literature review on monitoring technologies and their outcomes in independently living elderly people. *Disability and Rehabilitation: Assistive Technology, 10*(4), 271-294.

Pierleoni, P., Belli, A., Palma, L., Pellegrini, M., Pernini, L., & Valenti, S. (2015). A High Reliability Wearable Device for Elderly Fall Detection. *IEEE Sensors Journal, 15*(8), 4544-4553. doi: 10.1109/JSEN.2015.2423562

Pierleoni, P., Pernini, L., Belli, A., Palma, L., Valenti, S., & Paniccia, M. (2015). SVM-based fall detection method for elderly people using Android low-cost smartphones. In *Proceedings of Sensors Applications Symposium (SAS)*. (pp: 1-5) doi:10.1109/SAS.2015.7133642

Pihala, H. (1998). *Non-intrusive appliance load monitoring system based on a modern kWh-meter*: Technical Research Centre of Finland.

Pimentel, M. A., Clifton, D. A., Clifton, L., & Tarassenko, L. (2014). A review of novelty detection. *Signal Processing, 99*, 215-249. Retrieved from http://dx.doi.org/10.1016/j.sigpro.2013.12.026

Planinc, R., & Kampel, M. (2012). Robust fall detection by combining 3D data and fuzzy logic. In *Proceedings of Computer Vision-ACCV 2012 Workshops*. (pp: 121-132)

Planinc, R., & Kampel, M. (2013). Introducing the use of depth data for fall detection. *Personal and ubiquitous computing, 17*(6), 1063-1072.

Power-Mate 10AHD Serial. (2016). POWER-MATE™ 10A Power Meter Serial. Retrieved from http://www.cabac.com.au/products/electrical-test-and-measurement/power-meters/PM10AHDS

Prakash, A., Kemp, C. C., & Rogers, W. A. (2014). Older adults' reactions to a robot's appearance in the context of home use. In *Proceedings of Proceedings of the 2014 ACM/IEEE international conference on Human-robot interaction.* (pp: 268-269) doi:10.1145/2559636.2559790

Putchana, W., Chivapreecha, S., & Limpiti, T. (2012). Wireless intelligent fall detection and movement classification using fuzzy logic. In *Proceedings of Biomedical Engineering International Conference (BMEiCON).* (pp: 1-5) doi:10.1109/BMEiCon.2012.6465472

Raheja, J. L., Minhas, M., Prashanth, D., Shah, T., & Chaudhary, A. (2015). Robust gesture recognition using Kinect: A comparison between DTW and HMM. *Optik - International Journal for Light and Electron Optics, 126*(11–12), 1098-1104. doi: http://dx.doi.org/10.1016/j.ijleo.2015.02.043

Rahimi, S., Chan, A. D., & Goubran, R. A. (2011). Usage monitoring of electrical devices in a smart home. In *Proceedings of Annual International Conference of the IEEE Engineering in Medicine and Biology Society.* (pp: 5307-5310) doi:10.1109/IEMBS.2011.6091313

Ranjan, J., & Whitehouse, K. (2015). Rethinking the fusion of technology and clinical practices in functional behavior analysis for the elderly. *Human Behavior Understanding* (pp. 52-65): Springer.

Rashidi, P., & Cook, D. J. (2010). Mining and monitoring patterns of daily routines for assisted living in real world settings. In *Proceedings of 1st ACM International Health Informatics Symposium.* (pp: 336-345) doi:10.1145/1882992.1883040

Rashidi, P., Cook, D. J., Holder, L. B., & Schmitter-Edgecombe, M. (2011). Discovering activities to recognize and track in a smart environment. *IEEE Transactions on Knowledge and Data Engineering, 23*(4), 527-539. doi: 10.1109/TKDE.2010.148

Ravishankar, V. K., Burleson, W., & Mahoney, D. (2015). Smart Home Strategies for User-Centered Functional Assessment of Older Adults. *International Journal of Automation and Smart Technology, 5*(4), 233-242.

Reinhardt, A., Baumann, P., Burgstahler, D., Hollick, M., Chonov, H., Werner, M., & Steinmetz, R. (2012). On the accuracy of appliance identification based on distributed load metering data. In *Proceedings of IEEE.* Sustainable Internet and ICT for Sustainability (SustainIT), 2012, (pp: 1-9)

Ribeiro, P. C., & Santos-Victor, J. (2005). Human activity recognition from video: modeling, feature selection and classification architecture. In *Proceedings of Citeseer.* Proceedings of International Workshop on Human Activity Recognition and Modelling, (pp: 61-78)

Riboni, D., Bettini, C., Civitarese, G., Janjua, Z. H., & Helaoui, R. (2015). Fine-grained recognition of abnormal behaviors for early detection of mild cognitive impairment. In *Proceedings of IEEE International Conference on Pervasive Computing and Communications (PerCom).* (pp: 149-154) doi:10.1109/PERCOM.2015.7146521

Rivera-Illingworth, F., Callaghan, V., & Hagras, H. (2010). Detection of normal and novel behaviours in ubiquitous domestic environments. *The Computer Journal, 53*(2), 142-151.

Rob, K. (2013). Collaboration, expertise produce enhanced sensing in Xbox One. Retrieved from http://blogs.microsoft.com/blog/2013/10/02/collaboration-expertise-produce-enhanced-sensing-in-xbox-one/

Rougier, C., Auvinet, E., Rousseau, J., Mignotte, M., & Meunier, J. (2011). Fall detection from depth map video sequences *Toward Useful Services for Elderly and People with Disabilities* (pp. 121-128): Springer.

Rougier, C., Meunier, J., St-Arnaud, A., & Rousseau, J. (2011). Robust video surveillance for fall detection based on human shape deformation. *IEEE Transactions on Circuits and*

*Systems for Video Technology, 21*(5), 611-622. doi: 10.1109/TCSVT.2011.2129370
Rousseeuw, P. J., & Hubert, M. (2011). Robust statistics for outlier detection. *Wiley Interdisciplinary Reviews: Data Mining and Knowledge Discovery, 1*(1), 73-79.
Rowe, A., Berges, M., & Rajkumar, R. (2010). Contactless sensing of appliance state transitions through variations in electromagnetic fields. In *Proceedings of ACM*. Proceedings of the 2nd ACM Workshop on Embedded Sensing Systems for Energy-Efficiency in Building, (pp: 19-24)
Roy, P. C., Bouzouane, A., Giroux, S., & Bouchard, B. (2011). Possibilistic activity recognition in smart homes for cognitively impaired people. *Applied Artificial Intelligence, 25*(10), 883-926.
Sarabadani Tafreshi, A., Klamroth-Marganska, V., Nussbaumer, S., & Riener, R. (2015). Real-time closed-loop control of human heart rate and blood pressure. *IEEE Transactions on Biomedical Engineering, 62*(5), 1434-1442. doi: 10.1109/TBME.2015.2391234
Scholz, F. (1985). Maximum likelihood estimation. *Encyclopedia of statistical sciences*, doi: 10.1002/0471667196.ess1571.pub2
Scott, D. W. (2015). *Multivariate density estimation: theory, practice, and visualization*: John Wiley & Sons.
Seki, H. (2009). Fuzzy inference based non-daily behavior pattern detection for elderly people monitoring system. In *Proceedings of Annual International Conference of the IEEE Engineering in Medicine and Biology Society.* (pp: 6187-6192) doi:10.1109/IEMBS.2009.5334614
Sheather, S. J., & Jones, M. C. (1991). A reliable data-based bandwidth selection method for kernel density estimation. *Journal of the Royal Statistical Society. Series B (Methodological)*, 683-690.
Shieh, J.-S., Chuang, C.-T., Wang, X., & Kuo, P.-Y. (2006). Remote monitoring of mobility changes of the elderly at home using frequency rank order statistics. *Journal of Medical and Biological Engineering, 26*(2), 81.
Shin, J. H., Lee, B., & Park, K. S. (2011). Detection of abnormal living patterns for elderly living alone using support vector data description. *IEEE Transactions on Information Technology in Biomedicine, 15*(3), 438-448. doi: 10.1109/TITB.2011.2113352
Sim, K., Phua, C., Yap, G.-E., Biswas, J., & Mokhtari, M. (2011). Activity recognition using correlated pattern mining for people with dementia. In *Proceedings of Annual International Conference of the IEEE Engineering in Medicine and Biology Society.* (pp: 7593-7597) doi:10.1109/IEMBS.2011.6091872
Srinivasan, V., Stankovic, J., & Whitehouse, K. (2011). Watersense: Water flow disaggregation using motion sensors. In *Proceedings of ACM*. Proceedings of the Third ACM Workshop on Embedded Sensing Systems for Energy-Efficiency in Buildings, (pp: 19-24)
Steinhauer, H. J., Chua, S.-L., Guesgen, H. W., & Marsland, S. (2010). Utilising Temporal Information in Behaviour Recognition AAAI Spring Symposium: It's All in the Timing
Stone, E. E., & Skubic, M. (2015). Fall detection in homes of older adults using the Microsoft Kinect. *IEEE Journal of Biomedical and Health Informatics, 19*(1), 290-301. doi: 10.1109/JBHI.2014.2312180
Suryadevara, N. K., & Mukhopadhyay, S. C. (2015). Sensor Activity Pattern (SAP) Matching Process and Outlier Detection. *Smart Homes* (pp. 159-175): Springer.
Suryadevara, N. K., Quazi, M., & Mukhopadhyay, S. C. (2012). Intelligent sensing systems for measuring wellness indices of the daily activities for the elderly. In *Proceedings of 8th International Conference on Intelligent Environments (IE).* (pp: 347-350) doi:10.1109/IE.2012.49
Tajbakhsh, A., Rahmati, M., & Mirzaei, A. (2009). Intrusion detection using fuzzy association

rules. *Applied Soft Computing, 9*(2), 462-469.
Tan, K. K., He, H. G., Chan, S. C., & Vehviläinen-Julkunen, K. (2015). The experience of older people living independently in Singapore. *International nursing review, 62*(4), 525-535.
Tang, D., Yoshihara, Y., Takeda, T., Botzheim, J., & Kubota, N. (2015). Informationally Structured Space for Life Log Monitoring in Elderly Care. In *Proceedings of IEEE International Conference on Systems, Man, and Cybernetics (SMC).* (pp: 1421-1426) doi:10.1109/SMC.2015.252
Tarassenko, L., Hann, A., & Young, D. (2006). Integrated monitoring and analysis for early warning of patient deterioration. *British journal of anaesthesia, 97*(1), 64-68.
Teh, C. H., & Chin, R. T. (1988). On image analysis by the methods of moments. *IEEE Transactions on Pattern Analysis and Machine Intelligence, 10*(4), 496-513. doi: 10.1109/34.3913
Tong, Y., Chen, R., & Gao, J. (2015). Hidden State Conditional Random Field for Abnormal Activity Recognition in Smart Homes. *Entropy, 17*(3), 1358. Retrieved from http://www.mdpi.com/1099-4300/17/3/1358
van Kasteren, T. L., Englebienne, G., & Kröse, B. J. (2011). Human activity recognition from wireless sensor network data: Benchmark and software. In L. Chen, C. D. Nugent, J. Biswas & J. Hoey (Eds.), *Activity recognition in pervasive intelligent environments* (pp. 165-186): Springer. doi: 10.2991/978-94-91216-05-3_8
Velayudhan, A., & Gireeshkumar, T. (2015). An Autonomous Obstacle Avoiding and Target Recognition Robotic System Using Kinect. *Intelligent Computing, Communication and Devices* (pp. 643-649): Springer.
Virone, G., Alwan, M., Dalal, S., Kell, S. W., Turner, B., Stankovic, J. A., & Felder, R. (2008). Behavioral patterns of older adults in assisted living. *IEEE Transactions on Information Technology in Biomedicine, 12*(3), 387-398. doi: 10.1109/TITB.2007.904157
Virone, G., Noury, N., & Demongeot, J. (2002). A system for automatic measurement of circadian activity deviations in telemedicine. *IEEE Transactions on Biomedical Engineering, 49*(12), 1463-1469. doi: 10.1109/TBME.2002.805452
Vrotsou, K., Ellegard, K., & Cooper, M. (2007, 4-6 July 2007). Everyday Life Discoveries: Mining and Visualizing Activity Patterns in Social Science Diary Data Information Visualization, 2007. IV '07. 11th International Conference, (pp: 130-138) doi:10.1109/iv.2007.48
Vuegen, L., Van Den Broeck, B., Karsmakers, P., Van Hamme, H., & Vanrumste, B. (2015). Monitoring activities of daily living using Wireless Acoustic Sensor Networks in clean and noisy conditions. In *Proceedings of 37th Annual International Conference of the IEEE Engineering in Medicine and Biology Society (EMBC).* (pp: 4966-4969) doi:10.1109/EMBC.2015.7319506
Wand, M. P., & Jones, M. C. (1994). *Kernel smoothing*: Crc Press.
Wang, C., Pastore, F., Goknil, A., Briand, L., & Iqbal, Z. (2015). Automatic generation of system test cases from use case specifications. In *Proceedings of the 2015 International Symposium on Software Testing and Analysis.* (pp: 385-396) doi:10.1145/2771783.2771812
Webb, J., & Ashley, J. (2012). *Beginning Kinect Programming with the Microsoft Kinect SDK*: Apress.
Wen-Chih, P., Wangling, H., YiLing, C., & PeiChing, L. (2007, 7-10 Oct. 2007). TagFree: Identifying users without tags in smart home environments Systems, Man and Cybernetics, 2007. ISIC. IEEE International Conference on, (pp: 3690-3697) doi:10.1109/icsmc.2007.4413826
Wilson, C., Lina, S., Stankovic, V., Liao, J., Coleman, M., Hauxwell-Baldwin, R., . . . Hassan,

T. (2015). Identifying the time profile of everyday activities in the home using smart meter data. Paper presented at the *the European Council for an Energy Efficient Economy (ECEEE), Toulon/Hyères, France.* Retrieved from http://www.refitsmarthomes.org/?p=787

Wohlin, C., Höst, M., & Henningsson, K. (2003). Empirical research methods in software engineering. *Empirical methods and studies in software engineering* (pp. 7-23): Springer.

World Health Organization. (2015). *World report on ageing and health*. Retrieved from Ageing and life-course website: http://www.who.int/ageing/publications/world-report-2015/en/

Wu, Chen, Y. H., Yeh, C. H., & Li, Y. F. (2013). Reasoning-Based Framework for Driving Safety Monitoring Using Driving Event Recognition. *Intelligent Transportation Systems, IEEE Transactions on, PP*(99), 1-11. doi: 10.1109/TITS.2013.2257759

Xavier, A. J., Sigulem, D., & Ramos, L. R. (2010). Time orientation and executive functions in the prediction of mortality in the elderly: Epidoso study. *Revista de Saúde Pública, 44*(1), 148-158.

Xiang, Y., Tang, Y.-p., Ma, B.-q., Yan, H.-c., Jiang, J., & Tian, X.-y. (2015). Remote Safety Monitoring for Elderly Persons Based on Omni-Vision Analysis. *PloS one, 10*(5), e0124068.

Yang, L., Ren, Y., & Zhang, W. (2016). 3D depth image analysis for indoor fall detection of elderly people. *Digital Communications and Networks, 2*(1), 24-34.

Yu, M., Rhuma, A., Naqvi, S. M., Wang, L., & Chambers, J. (2012). A posture recognition-based fall detection system for monitoring an elderly person in a smart home environment. *Information Technology in Biomedicine, IEEE Transactions on, 16*(6), 1274-1286.

Yu, M., Yu, Y., Rhuma, A., Naqvi, S. M. R., Wang, L., & Chambers, J. A. (2013). An online one class support vector machine-based person-specific fall detection system for monitoring an elderly individual in a room environment. *Biomedical and Health Informatics, IEEE Journal of, 17*(6), 1002-1014.

Yuan, X., Yu, S., Dan, Q., Wang, G., & Liu, S. (2015). Fall detection analysis with wearable MEMS-based sensors. In *Proceedings of 16th International Conference on Electronic Packaging Technology (ICEPT).* (pp: 1184-1187) doi:10.1109/ICEPT.2015.7236791

Zadeh, L. A. (1965). Information and control. *Fuzzy sets, 8*(3), 338-353.

Zadeh, L. A. (1973). Outline of a New Approach to the Analysis of Complex Systems and Decision Processes. *IEEE Transactions on Systems, Man, and Cybernetics, SMC-3*(1), 28-44. doi: 10.1109/TSMC.1973.5408575

Zadeh, L. A. (1978). Fuzzy sets as a basis for a theory of possibility. *Fuzzy sets and systems, 1*(1), 3-28.

Zambanini, S., Machajdik, J., & Kampel, M. (2010a). Detecting falls at homes using a network of low-resolution cameras. In *Proceedings of IEEE.* Information Technology and Applications in Biomedicine (ITAB), 2010 10th IEEE International Conference on, (pp: 1-4)

Zambanini, S., Machajdik, J., & Kampel, M. (2010b). Early versus late fusion in a multiple camera network for fall detection. In *Proceedings of 34th annual workshop of the Austrian Association for Pattern Recognition (AAPR).* (pp: 15-22)

Zerrouki, N., Harrou, F., Sun, Y., & Houacine, A. (2016). Accelerometer and Camera-Based Strategy for Improved Human Fall Detection. *Journal of Medical Systems, 40*(12), 284. doi: 10.1007/s10916-016-0639-6

Zhan, K., Faux, S., & Ramos, F. (2015). Multi-scale Conditional Random Fields for first-person activity recognition on elders and disabled patients. *Pervasive and Mobile*

*Computing, 16, Part B*, 251-267. doi: http://dx.doi.org/10.1016/j.pmcj.2014.11.004
Zhang, C., Tian, Y., & Capezuti, E. (2012). *Privacy preserving automatic fall detection for elderly using RGBD cameras*: Springer.
Zhang, S., McCullagh, P., Nugent, C., Zheng, H., & Black, N. (2011). A subarea mapping approach for indoor localization. *Toward Useful Services for Elderly and People with Disabilities* (pp. 80-87): Springer.
Zhongna, Z., Xi, C., Yu-Chia, C., Zhihai, H., Han, T. X., & Keller, J. M. (2008). Activity Analysis, Summarization, and Visualization for Indoor Human Activity Monitoring. *Circuits and Systems for Video Technology, IEEE Transactions on, 18*(11), 1489-1498. doi: 10.1109/tcsvt.2008.2005612

# APPENDIX A – EXTRACTING DEPTH MAP ATTRIBUTES AND SELECTING FEATURES

This appendix first explores different types of image features used by existing studies for describing the posture of people during ADLs. This is followed an explanation of the calculation of commonly used features. The process of feature selection procedure to find the most suitable feature subset is also presented. The appendix is concluded by showing the results.

**Image features for describing ADLs**

The first step of camera-based approaches for monitoring and classification of activities the binary mask of the person (i.e. silhouette) is the segmented from video images or depth maps. Several features are used subsequently to describe body postures related to ADLs. A list of such features is shown in Table A.1. Most approaches have used the horizontal and vertical coordinates of the person's centre of gravity, denoted by $C_x$ and $C_y$ respectively. The aspect ratio (denoted as $AR$) of the minimum bounding rectangle (MBR) for the detected person and the orientation of the body ($\theta$) are amongst other prominent features.

A number of proposed approaches have employed other types of features as shown in Table A.1. Some techniques have estimated the 3D location of specific skeleton joints of the subject to model and monitor ADLs. Eccentricity of the segmented silhouette has been also used which is calculated as the ratio of the major and minor axis of the ellipse fitting the silhouette (Y. Liu et al., 2012).

A study by Brulin et al. (2012) employed the ratio of the distance between the centre of gravity of the person and the bottom side of the MBR to detect falls. Another technique by Seki (2009) used the area of the detected silhouette in the image for describing ADLs. Banerjee et al. (2014) developed a 3-D model of the person, named "voxel person", and employed Zernike moments (with order m = 2, 3, and 4 and angular dependence n = 0, 1 and 2, respectively) to describe ADLs. Projection histograms, as the total numbers of foreground pixels projected along horizontal and vertical directions were also taken into account for the classification of different postures (e.g. sitting, lying down, and standing) as shown in Table A.1 (Cucchiara, Prati, & Vezzani, 2007). The procedure for calculation of the most commonly used features is explained

in more detail in the following section.

Table A.1. Feature extracted from the silhouette of a detected body (Brulin et al., 2012)

| Method | Image descriptors used | | | |
|---|---|---|---|---|
| | ***AR* of MBR or axes ration of the fitted ellipse** | $\theta$ | **Centre of gravity** | **Other descriptors** |
| Banerjee et al. (2014) | | | | Zernike Moments |
| Brulin et al. (2012) | * | * | * | |
| Yu, Rhuma, Naqvi, Wang, and Chambers (2012) | * | | | Projection histogram |
| Lee and Chung (2012) | * | * | * | |
| Seki (2009) | | * | * | Area of the silhouette in the image |
| Zambanini, Machajdik, and Kampel (2010a) | * | * | | Motion Speed during consecutive frames |
| Mastorakis and Makris (2014) | * | | | Deviation of MBR during consecutive frames |
| Makantasis, Protopapadakis, Doulamis, Grammatikopoulos, and Stentoumis (2012) | * | * | | |
| Xiang et al. (2015) | * | | | |
| Y. Liu et al. (2012) | | | | Locations of skeleton joints |
| Bian, Hou, Chau, and Magnenat-Thalmann (2015) | | | | Locations of skeleton joints |

**Calculating features**

Given the MBR obtained for the segmented silhouette of a person, *AR* of the MBR is obtained as:

$$AR = \frac{height\ of\ the\ MBR}{width\ of\ \text{the}\ MBR}$$

$C_x$, $C_y$ and $\theta$ are obtained via the calculation of geometric moments for the silhouette of the person. Geometric moments are used in image processing to describe the shape of objects (Teh & Chin, 1988). The $(p\ +\ q)^{th}$ order of geometric moments, denoted as $m_{pq}$, for a grey-level image $f(x, y)$ is calculated as Equation A.1.

$$m_{pq} = \iint_{-\infty}^{\infty} x^p y^q\, f(x,y) dx dy \tag{A.1}$$

In the case of calculating geometric moments for a binary image (e.g. the subject's silhouette),

the double integral in Equation A.1 changes to summations, and the grey value function $f(x, y)$ becomes:

$$f(x,y) = \begin{cases} 1, & (x,y) \in \text{the silhouette} \\ 0, & \text{therwise} \end{cases}.$$

Thus, Equation A.1 becomes Equation A.2.

$$m_{pq} = \sum_{i=1}^{N} \sum_{j=1}^{M} i^p j^q \tag{A.2}$$

where N and M are the size of the binary silhouette with respect to the vertical and horizontal axes, respectively. By using the first and zero-order geometrical moments, coordinates for the centre of the gravity of the silhouette are calculated via Equation A.3.

$$C_x = \frac{\mu_{10}}{\mu_{00}} \quad C_y = \frac{\mu_{01}}{\mu_{00}} \tag{A.3}$$

The orientation of the person is obtained as the angle between the major axis of the ellipse fitted to the person' silhouette and the horizontal axis x. This is calculated via using the first- and second-order geometrical moments (see Equation A.4) expressed in degrees, ranging from 0 to 90.

$$\theta = \left| \tan^{-1} \frac{2\mu_{11}}{(\mu_{20} - \mu_{02})} \right| \tag{A.4}$$

The area of the silhouette in an image is obtained as the zero-order geometrical moment (i.e. $\mu_{00}$).

**Feature selection**

A wide range of attributes have been proposed to characterise and model body postures during ADLs as shown in Table A.1. Using the combination of all attributes in order to characterise ADLs has an increasing impact on the complexity of a classification model. Some of these attributes might be either redundant or irrelevant to the task of this study, and can thus be removed without causing much loss of information. A feature selection procedure was performed to evaluate the effectiveness of different subsets of attributes to reduce the

dimensionality of data and the processing complexity of the developed model. The flowchart for this procedure is shown in Figure A.1. It involved two major components: (1) a search technique for generating feature subsets and (2) an evaluation technique which gave a score to each feature subset. The adopted algorithm for the first component was the brute-search approach which outputs all feature subsets to find the one with the highest score. A predictive model was used for the second component to estimate the score of a given subset as the error rate of classifying unseen data.

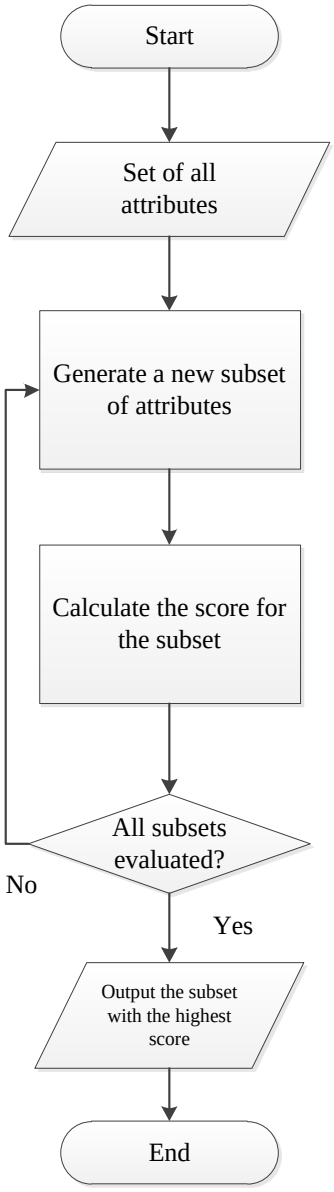


Figure A.1. The flowchart for the feature selection algorithm carried out in this study

Given a labelled dataset of all features, the dataset was first divided into a training set and a test set. Different subsets of features were extracted from the training data and used to train

predictive models. The classification rate of those models were evaluated on the unseen test data to give a classification score to each subset of features.

A Naive Bayes classifier was adopted as the predictive model since it is particularly suited when the dimensionality of the input is high and often outperforms more sophisticated supervised classification techniques (Ribeiro & Santos-Victor, 2005). This classifier models the distribution of the training data as a mixture of Gaussians, estimated using the EM algorithm (Bilmes, 1998). The likelihood for each class of activity to the unseen testing data is calculated using a Bayesian likelihood function and the testing data is then labelled with the activity with maximum likelihood.

A labelled dataset was collected during an experiment in which various activities were performed in the living room area of the testbed and a static Kinect camera captured observations associated with activities. The list of activities performed included (1) standing in a particular location as a habit, (2) sitting on the sofa (3) lying on the sofa, (4) sitting behind the computer desk, (5) sitting on the floor and (6) lying on the floor. Each activity was performed 10 times with slight variations in order to capture the variability in the attributes for each activity. For example, in one instance for sitting on the sofa, the occupant was talking on the phone whereas in the other instance, he was reading a book. Kinect observations captured for this experiment were labelled manually with their respective activities. Each observation in the dataset thereby belonged to one of the six classes of activities. Table A.2 shows the number of observations per activity, and Figure A.2 shows example colour images and their respective binary mask of the person for different activities.

Table A.1. The number of Kinect observations per activity captured for the feature selection experiment

| ***Index*** | ***Activity*** | ***Number of observations*** |
|---|---|---|
| 1 | Standing | 50 |
| 2 | Sitting on the sofa | 62 |
| 3 | Lying on the sofa | 45 |
| 4 | Sitting behind the computer desk | 50 |
| 5 | Sitting on the floor | 42 |
| 6 | Lying on the floor | 49 |

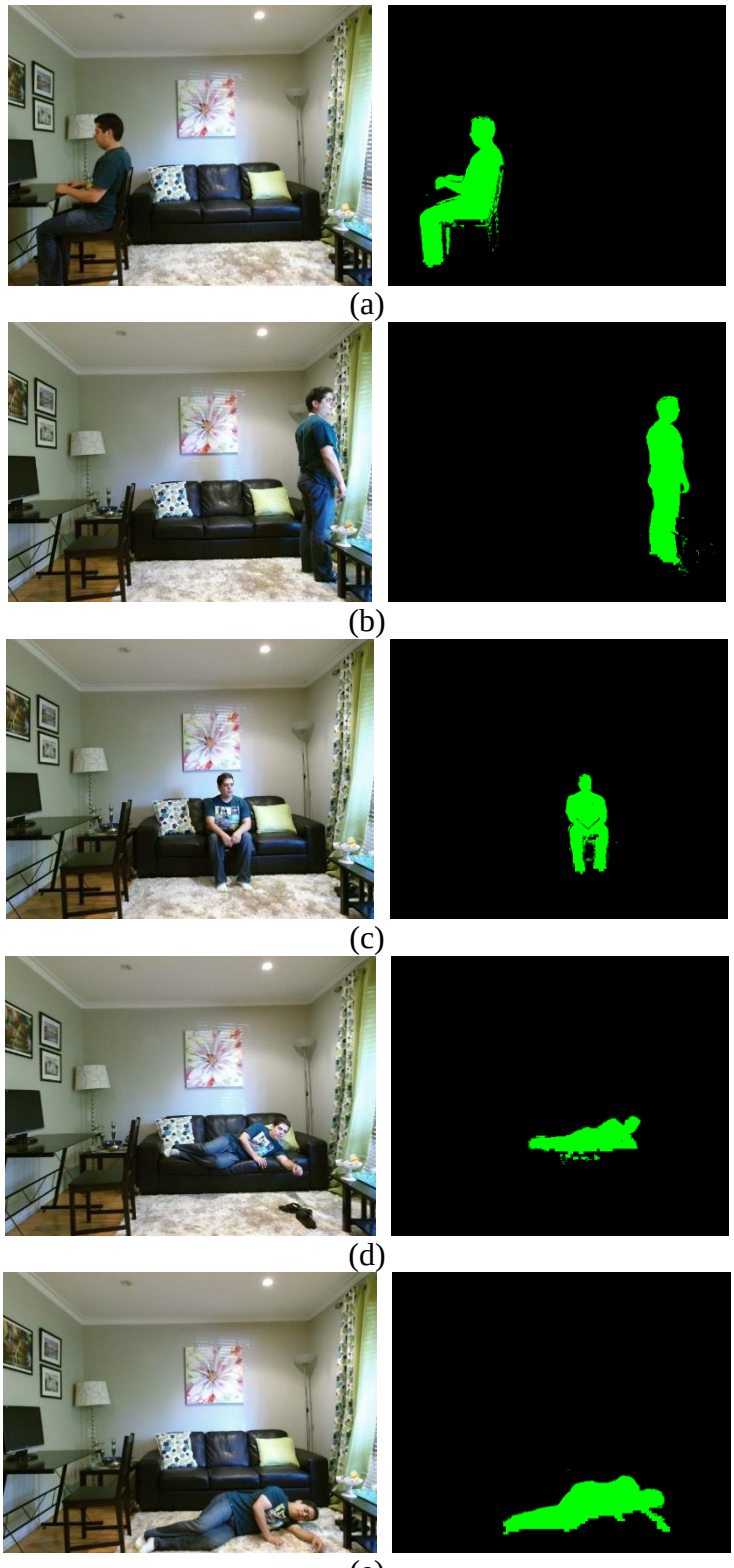

Figure A.2 (a)-(c) Example observations of different postures with their binary mask of the person. (a) Sitting behind a computer desk, (b) standing by the window, (c) sitting on the sofa, (d) sleeping on the sofa, and (e) lying on the floor.

Different attributes from the collected labelled dataset, were extracted and incorporated in the feature selection procedure to find the most informative set as shown in Table A.3.

Table A.3. The list of features extracted for the feature selection procedure

| Index | Attribute | Description |
|---|---|---|
| 1 | Cx | The horizontal coordinate for centre of gravity |
| 2 | Cy | The vertical coordinate for centre of gravity |
| 3 | X | Coordinate of the heap centre joint on the X axis |
| 4 | Y | Coordinate of the heap centre joint on the Y axis |
| 5 | Z | Coordinate of the heap centre joint on the Z axis |
| 6 | AR | Aspect ratio of MBR |
| 7 | $\theta$ | Orientation of the body |
| 8 | Area | Number of pixels in the silhouette |
| 9 | Depth $_{Mean}$ | Mean of depth values associated with the silhouette of the subject |
| 10 | Depth $_{Var}$ | variance of depth values associated with the silhouette of the subject |
| 11 | Solidity | The ratio of the major to the minor axes of the fitted ellipes |
| 12 | Z(2,0) | Zernike moment with m=2 and n=0 in Equation |
| 13 | Z(3,1) | Zernike moment with m=3 and n=1 in Equation |
| 14 | Z(4,2) | Zernike moment with m=4 and n=2 in Equation |
| 15 | Δ AR | Deviation of MBR during consecutive frames |
| 16 | MS | Motion speed during consecutive frames |

A three-fold cross validation was performed to evaluate each subset of features. For each fold two-thirds of the observations in the dataset were used as a training set and the accuracy of the developed model was evaluated based on the remaining one-third of the observations. This process was repeated three times for each feature subset so that a third of the dataset was used once as the test set. The classification accuracy obtained from the three folds were averaged and used as the classification score of the feature subset.

The best score was obtained for feature selection of the subset of {$C_X$, Cy, AR, O} with a classification error rate of 6.25%. The scatter plot matrix for this subset with each row containing the scatter plots of one attribute against the columns of the other is shown in Figure A.3. Data points with different colours represent different class of activities.

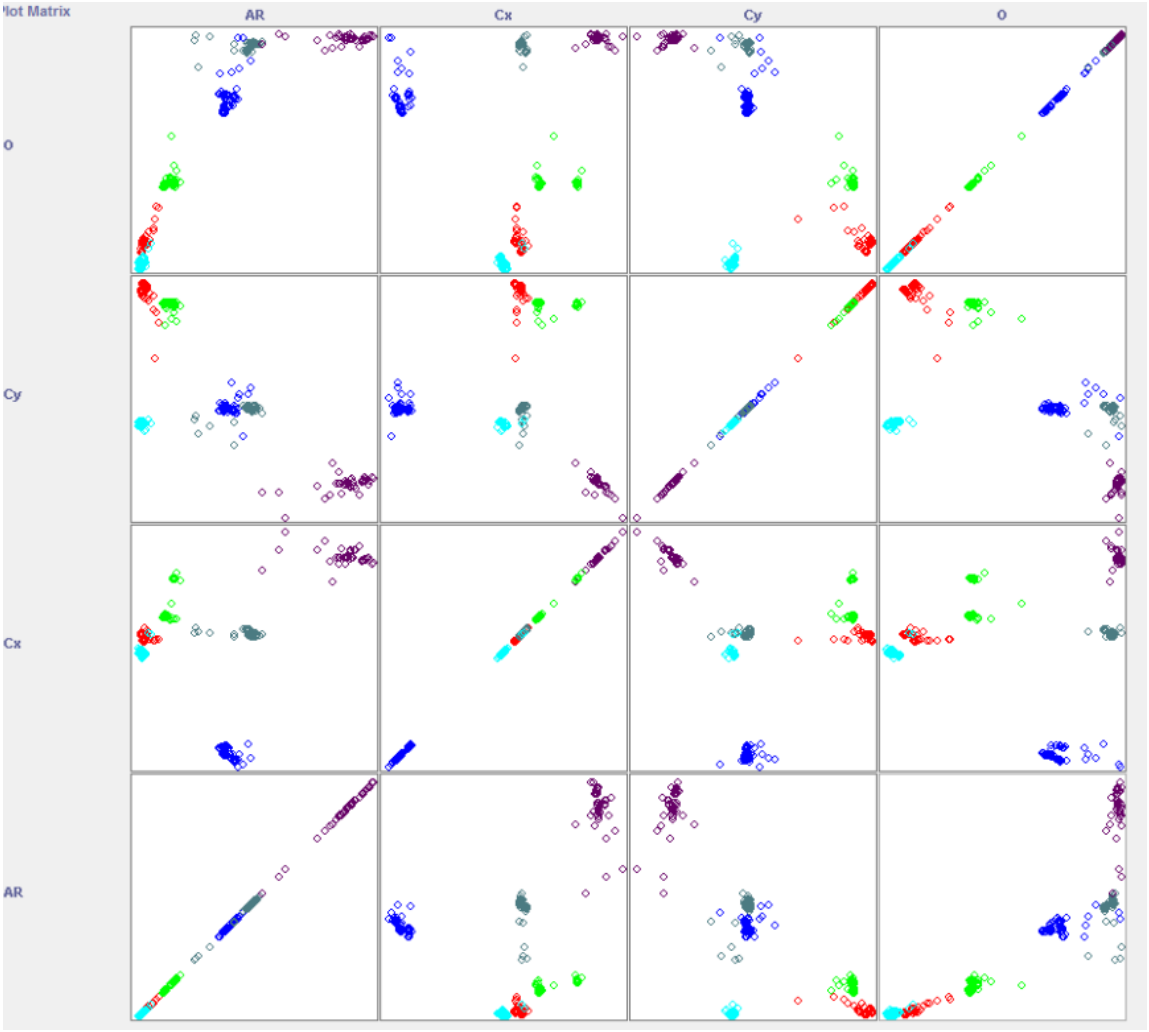


Figure A.3. The scatter plot matrix for the selected subset of attributes

# APPENDIX B – COMPARING THE PERFORMANCE OF CLUSTERING TECHNIQUES IN IDENTIFYING EPOCHS OF ACTIVITIES

Many clustering techniques have been used in different studies to estimate epochs of activities base on the timestamps of sensor data. The use of GMMs was suggested by Cardinaux et al. (2008) to model the time and duration of normal behaviour patterns. GMMs were estimated via using the Expectation Maximization algorithm (Duda et al., 2012). Noury et al. (2011) used the k-means algorithm to estimate epochs of activities via clustering the time of electrical events detected on the power line. The fuzzy c-means clustering algorithm was used by Hsu et al. (2010) to model the time of ADLs for monitoring the elderly. Hoque and Stankovic (2012) employed DBSCAN, which is a density based clustering algorithm to group the starting times of ADLs.

An experiment was conducted to compare the performance of the mean shift algorithm with the abovementioned clustering techniques in identifying epochs of activities. The training Kinect depth maps collected from the testbed were used in this experiment. The ground truth for epochs of activities was obtained based on the daily schedule followed by the researcher to simulate activities. Most of clustering techniques mentioned above needed the number of clusters in advance. This number for the dataset of each monitored location was determined as the number of peaks in the histogram of the time of observations. The bin size of the histogram was determined using the plug-in rule (see Section 3.6.3). The number of peaks in the histogram was detected using the MATLAB *findpeaks* function, which defines a peak as a sample larger than its two neighbours.

The time points associated with the centres of the detected clusters from each clustering technique were arranged in an ascending order, and their temporal order was used to label clusters with epochs (i.e. Epoch 1, Epoch 2, etc.). For example, if two clusters were detected for the living room area with the cluster centres of 08:00 AM and 18:00 PM, observations associated with the first cluster were labelled as belonging to Epoch 1 and those associated with the second cluster were labelled as Epoch 2. The qualitative comparison of the results of the clustering techniques is first described through showing epochs estimated by each technique. This is followed by a quantitative comparison of the accuracy of clustering techniques.

For the kitchen dataset, five peaks were detected using the MATLAB *findpeaks* function. The results of different techniques for this dataset are shown in Figure B.1. In each part of this figure, the same colour rectangles from the ground truth shown in Figure 4.12 (a) are used to label epochs. The distribution of observations for Epoch 1 and Epoch 2 in the kitchen dataset are almost separate (Figure 4.12 (a)). All techniques could identify these two epochs correctly as the black and green rectangles in different parts of Figure B.1 cover almost the same period. Since the distribution of Epoch 3 (shown within the blue rectangle in Figure 4.12 (a)) is immediately followed by the smaller distribution of Epoch 4 (shown within the purple rectangle), techniques other than the mean shift algorithm could not separate Epoch 3 and Epoch 4 accurately. For example, using FCM and GMM, most of the observations for Epoch 4 have been grouped in the same cluster as those for Epoch 3. Note that DBSCAN generated less accurate results, as shown in Figure B.1 (d). While epochs 1 and 2 have been estimated correctly, all activities between 10:00 AM and 20:00 PM have been clustered by DBSCAN as belonging to Epoch 3. The reason is that DBSCNS generally clusters all data points located in a certain proximity to each other as belonging to the same group. As there was no gap in the time of observations between 10:00 AM and 20:00 PM in the kitchen dataset, all the data points belonging to this range were clustered together. The mean shift algorithm yielded better results since the time spans of the estimated epochs are very similar to those shown for the ground truth as shown in Figure B.1 (e).

The results of using different clustering techniques for the living room dataset are shown in Figure B.2. From the ground truth for epochs associated with this location (shown in Figure 4.12 (b)), it is observed that the distribution of this dataset has four distinct peaks each corresponding to an epoch. With the exception of the mean shift algorithm, all other techniques clustered observations for Epoch 1 and Epoch 2 as belonging to the same epoch as shown in Figure B.2. This is because those techniques aim to partition the data into clusters in a way that minimises a distance metric amongst data points assigned to the same cluster. As component distributions belonging to Epoch 1 and Epoch 2 overlap, choosing one cluster centre to represent all data points for Epoch 1 and Epoch 2 optimised the distance criterion for those techniques.

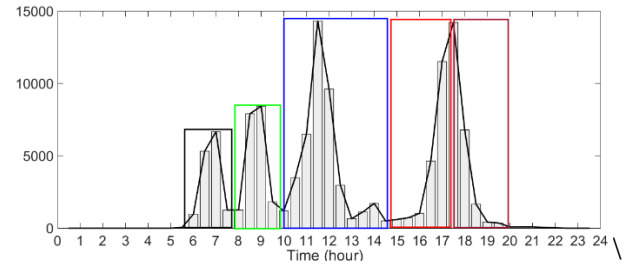


(a)

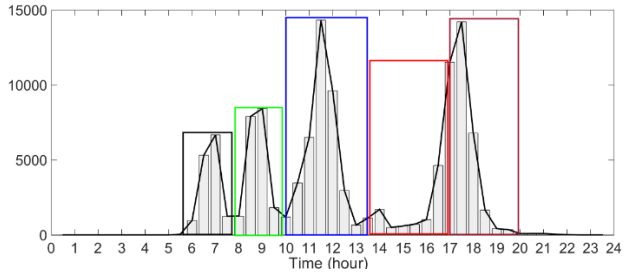


(b)

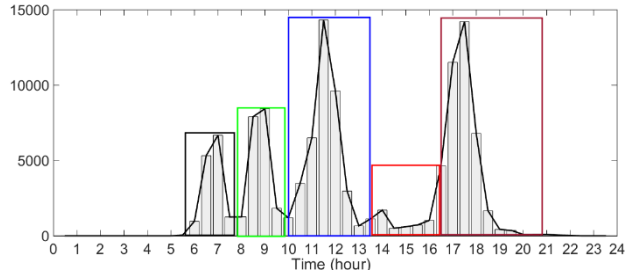


(c)

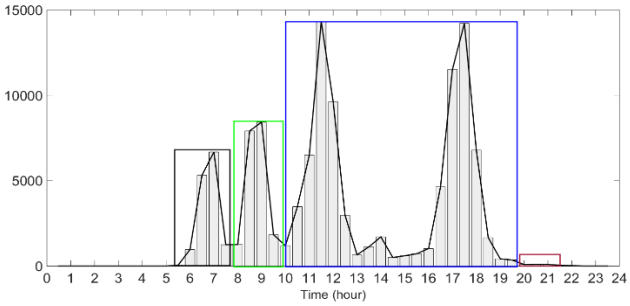


(d)

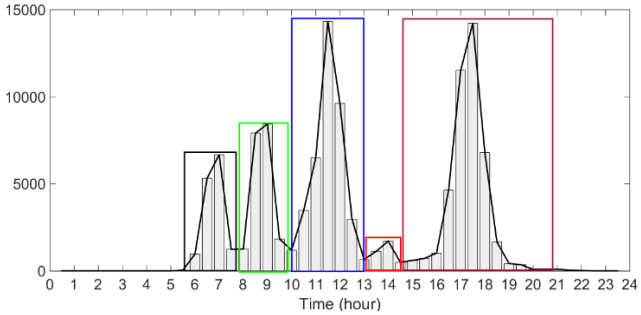


(e)

Figure B.1. Results of applying different clustering techniques for estimating epochs of activities for the kitchen dataset. Results generated by (a) FCM, (b) GMM, (c) k-means, (d) DBSCANS, and (e) mean shift.

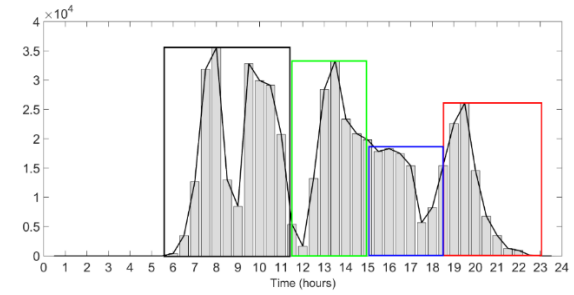


(a)

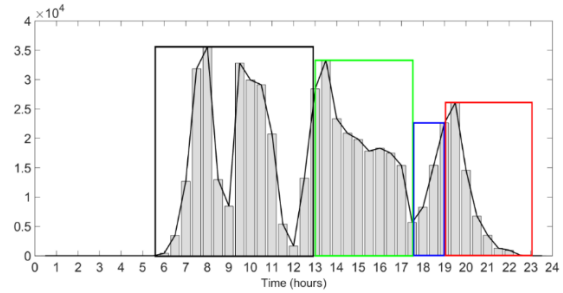


(b)

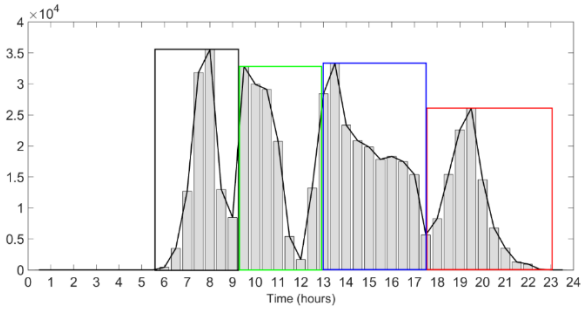


(c)

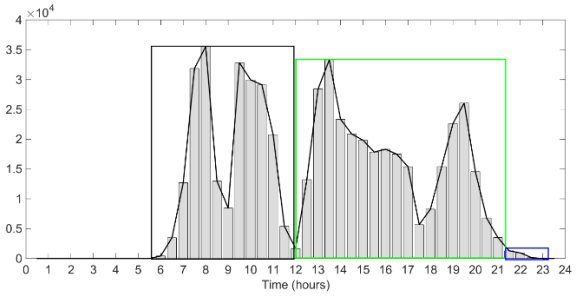


(d)

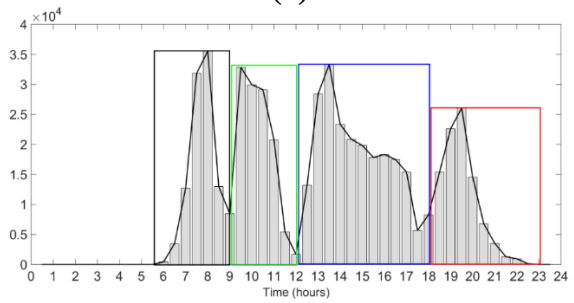


(e)

Figure B.2 Results of applying different clustering techniques for estimating epochs of activities for the living room dataset (a) FCM, (b) GMM, (c) k-means, (d) DBSCANS, and (e) mean shift

One conclusion to draw from the diagrams in Figure B.2 is that, when compared to other techniques, the epochs from the mean shift algorithm are more similar to those obtained from the ground truth. This is logical since mean shift tends to group all observations belonging to the same peak in a mixture of data distribution as belonging to the same cluster. The living room area was occupied during specific periods in a daily routine to perform specific ADLs. The time spent in this area for each ADL caused a peak in the distribution of time of observations, and those peaks were correctly identified as different epochs by the mean shift algorithm.

While the diagrams shown in Figure B.1 and Figure B.2 indicate that the results obtained from the mean shift algorithm are more accurate, they do not present any quantitative evidence of the relative accuracies of the clustering techniques. The observations in the training dataset for each location were labelled with their corresponding epochs, obtained from the ground truth. The mean square error (MSE) of the results from each clustering technique relative to the ground truth was calculated. This measure of error was employed to estimate the classification accuracy of each clustering technique, as shown in Table B.1. For the kitchen dataset, the DBSCANS, FCM and GMM algorithms resulted in average accuracies of 35%, 53% and 72%, respectively. This was mainly because these techniques labelled many observations between 15:00 PM and 17:00 PM as incorrectly belonging to Epoch 4. K-means resulted in a higher performance as it could correctly estimate more epochs. The best result for the kitchen dataset was obtained using Mean Shift algorithm with 99% accuracy, whereas the least accurate results were yielded by DBSCANS which failed to identify epochs 3 and 4. This was due to the fact that Mean Shift aims to identify locations for local maxima of the data distribution as epochs, whereas DBSCANS considers data points as a cluster if located within a certain proximity to each other. GMM resulted in an accuracy of 82%.

It can be observed that the highest accuracy for the living room dataset belongs to the mean shift algorithm followed by k-means. As expected, DBSCANS grouped many observations for different epochs as belonging to the same cluster, resulting in an accuracy of 32%.

For the dining room and bedroom datasets, all techniques achieved a high accuracy rate of around 100%. Data distributions associated with epochs for these datasets were well separated, and thus all techniques could identify the data points associated with an epoch as a separate cluster.

Table B.1 The classification results of clustering techniques for different locations.

| ***Clustering technique*** | ***Kitchen*** | ***Dining room*** | ***Living room*** | ***Bedroom*** | ***Average*** |
|---|---|---|---|---|---|
| K-means | 72% | 100% | 85% | 100% | 89.2% |
| Fuzzy C-means | 53% | 100% | 42% | 100% | 74% |
| GMM | 82% | 99% | 38% | 100% | 80% |
| Mean shift | 99% | 100% | 92% | 100% | 98% |
| DBSCAN | 35% | 100% | 32% | 100% | 66.7% |